United States
Environmental Protection
Agency

EPA/600/R-20/143 | June 2020 | www.epa.gov/research

(Appendices - 1 of 2)
The Influence of Stormwater Management Practices and Wastewater Infiltration on Groundwater Quality: Case Studies

Appendix A. Methods Supporting Information
Appendix B. Louisville Supporting Information
Appendix C. Yakima Supporting Information
Appendix D. Fort Riley Supporting Information

Office of Research and Development
Center for Environmental Solutions & Emergency Response | Groundwater Characterization & Remediation Division

Appendix A. Methods Supporting Information

Table of Contents

1.1 Analytical Methods

Table A-1. Field parameters measured, and method used for the Fort Riley, Louisville, and Yakima studies.

Parameter	Method	Study
Temperature	EPA Method 170.1	F[1], L[2], Y[3]
Alkalinity	Standard Method 2320B; HACH method 8203	F, L
	Standard Method 2320B	Y
pH	EPA Method 150.2	F, L, Y
Oxidation-Reduction Potential	No EPA Method	F, L, Y
Specific Conductivity	EPA Method 120.1	F, L, Y
Dissolved Oxygen	EPA Method 360.1	F, L, Y
Turbidity	EPA Method 180.1	F, L
Total Dissolved Solids[4]	No EPA Method	F, L

[1]Fort Riley.
[2]Louisville.
[3]Yakima.
[4]Calculated value from the YSI multiprobe or calculated by TDS = SPC x 0.65.

Table A-2. Dissolved metal, nutrient, anion, carbon species, and water isotope methods used, preservation and holding times for the Fort Riley, Louisville, and Yakima studies.

Parameter	Analytical Method	Preservation	Holding Time
Dissolved Metals ICP-OES	EPA Method 200.7	HNO_3, pH<2; room temperature	6 months
Dissolved Metals ICP-MS	EPA Method 200.8		
Total Nitrogen (TN)	ASTM D5176-08	HCL; pH<2 refrigerate < 6°C	28 d
Total Kjeldahl Nitrogen (TKN) (Yakima)	K-GCRD-SOP-1151-0	H_2SO_4, pH<2; refrigerate <6°C	
Nitrate + Nitrite	EPA Method 353.1		
Nitrate + Nitrite (Yakima)	K-GCRD-SOP-1151-0		
Ammonia	SM4500-NH3		
Ammonia (Yakima)	K-GCRD-SOP-1151-0		
Phosphate	EPA Method 365.1		
Phosphate	K-GCRD-SOP-1151-0	Refrigerate <6°C	48 h
Bromide	K-GCRD-SOP-3329-0		28 d
Chloride			
Fluoride			
Sulfate			
Iodide	K-GCRD-SOP-1097-2		
DOC	EPA Method 9060A (K-GCRD-SOP-1165-0)		7 d
DIC			14 d
Stable Isotopes of Water	K-GCRD-SOP-1137-0		Stable
Dissolved Carbon Dioxide	Speciation Calculation based on the sample pH and DIC concentration.	NA	NA
Bicarbonate			
Carbonate			
Volatile organic compounds (VOC) (Fort Riley only)	EPA Method 624.1	HCL, pH <2; refrigerate < 4°C (no headspace)	14 d
Organic compounds (Fort Riley only)	SBSE EPA Method 625	refrigerate <4°C	7 d

Table A-3. Volatile organic compounds (VOCs) that were measured as part of the Fort Riley study.

Parameter	Parameter
Acetone	cis-1,3-Dichloropropene
Benzene	trans-1,3-Dichloropropene
Bromodichloromethane	Ethyl benzene
Bromoform	2-Hexanone
Bromomethane	Isopropylbenzene
2-Butanone	Methyl Acetate
Carbon tetrachloride	Methyl Cyclohexane
Carbon disulfide	Methyl tert-butyl ether
Chlorobenzene	Methylene chloride
Chloroethane	4-Methyl-2-pentanone
Chloroform	Naphthalene
Chloromethane	Styrene
Cyclohexane	1,1,2-Trichlorotrifluoroethane
Dichlorodifluoromethane	1,1,2,2-Tetrachloroethane
Dibromochloromethane	Tetrachloroethene
1,2-Dibromo-3-chloropropane	Toluene
1,2-Dibromoethane (EDB)	1,1,1-Trichloroethane
1,2-Dichlorobenzene	1,1,2-Trichloroethane
1,3-Dichlorobenzene	1,2,3-Trichlorobenzene
1,4-Dichlorobenzene	1,2,4-Trichlorobenzene
1,1-Dichloroethane	Trichlorofluoromethane
1,2-Dichloroethane	Trichloroethene
1,1-Dichloroethene	Vinyl chloride
trans-1,2-Dichloroethene	o-Xylene
cis-1,2-Dichloroethene	m/p-Xylene
1,2-Dichloropropane	

Table A-4. Organic compounds that were measured as part of the Fort Riley study.

Parameter	Parameter	Parameter
1,2,4-Trichlorobenzene	Benzo(b)fluoranthene	Fluorene
1,2-Dibromo-3-Chloropropane	Benzo(g,h,i)perylene	γ-BHC (γ-hexachlorocyclohexane)
1,2-Dichlorobenzene	Benzo(k)fluoranthene	Heptachlor
1,3-Dichlorobenzene	Bifenthrin	Heptachlor Epoxide
1,4-Dichlorobenzene	bis(2-Chloroethoxy)methane	Hexachlorobenzene
17α-Ethynyl Estradiol (Ethynyl Estradiol)	bis(2-Ethylhexyl)phthalate	Hexachlorobutadiene
17B-Estradiol	Bromacil	Hexachlorocyclopentadiene
2,4,5-Trichlorophenol	Butylbenzylphthalate	Hexachloroethane
2,4,6-Trichlorophenol	Carbazole	Indeno(1,2,3-cd)pyrene
2,4-Dichlorophenol	Chlordane, technical	Isophorone
2,4-Dimethylphenol	Chlorothalonil	Malathion
2,4-Dinitrotoluene	Chlorpyrifos	Metolachlor
2,6-Dinitrotoluene	Chrysene	Naphthalene
2-Chloronaphthalene	Coprostanol	p,p'-DDD (1-chloro-4-[2,2-dichloro-1-(4-chlorophenyl)ethyl]benzene)
2-Methylnaphthalene	δ-BHC (δ-hexachlorocyclohexane)	p,p'-DDE (1,1-bis-(4-chlorophenyl)-2,2-dichloroethene)
4-Bromophenyl-phenylether	Diazinon	p,p'-DDT (1,1'-(2,2,2-trichloroethane-1,1-diyl)bis(4-chlorobenzene)
4-Chloro-3-methylphenol	Dibenz(a,h)anthracene	p,p'-Methoxychlor (Methoxychlor)
4-Chlorophenyl-phenylether	Dibenzofuran	Pendimethalin
4-n-Nonylphenol	Dieldrin	Pentachlorophenol
4-tert-Octylphenol	Diethylphthalate	Permethrin
4-n-Nonylphenol Diethoxylate	Diethyltoluamide (DEET)	Phenanthrene
4-tert-Octylphenol Diethoxylate	Dimethenamid	Progestrone
4-tert-Octylphenol Monoethoxylate	Dimethylphthalate	Propachlor
α-BHC (α-hexachlorocyclohexane)	Di-n-butylphthalate	Propanil
Acenaphthene	Di-n-octylphthalate	Propazine
Acenaphthylene	Endosulfan I	Pyrene
Acetochlor	Endosulfan II	Pyrethrins
Alachlor	Endosulfan Sulfate	Simazine
Aldrin	Endrin	Terbufos
Anthracene	Endrin Ketone	Testosterone
Atrazine	Estrone	Triclosan
Azobenzene	Ethalfluralin	Trifluralin
ß-BHC (ß-hexachlorocyclohexane)	Ethoprop	Tris (2-butoxyethyl) phosphate (TBEP)
Benzo(a)anthracene	Ethyl Parathion	Tris(2-chloroethyl) phosphate (TCEP)
Benzo(a)pyrene	Fluoranthene	

1.2 Water Quality Sampling Methods

Table A-5. Geochemical parameter stability guidelines.

Parameter	Stabilization Criteria
pH	≤0.02 pH units/min
Oxidation Reduction Potential (ORP)	≤ 1 mV/min
Specific Conductance (SPC)	≤ 1 %/min
Dissolved Oxygen (DO)	≤ 0.25 mg/L/min

1.3 Geochemical Modeling

For speciation modeling the solution data as imported into the SpecE8 application from spreadsheet software containing the solution data using the GSS Application in Geochemist's Workbench and was sent to the SpecE8 application for batch analysis using the launch function in the GSS application. The speciation modeling was performed by the SpecE8 application in Geochemist's Workbench. The thermodynamic database used was the thermo.com.V8.R6+t.dat. The convergence criteria was set to 5×10^{-11} and maximum number of iterations, was set to 999. The ionic strength was calculated using the Debye – Hückel model. The solution data as imported in to the SpecE8 application from spreadsheet software using the GSS Application in Geochemist's Workbench. The resulting output was saved as text files. The text files were then imported into a spreadsheet for manipulation and analysis.

Another use for geochemical modeling was the creation of activity diagrams and Eh – pH diagrams. This was accomplished using the Act2 application in the Geochemist Workbench software. The thermodynamic database used was the thermo.com.V8.R6+t.dat database and the electrical conductivity file used was the conductivity-USGS.dat file. The pH and solution species needed were imputed into the Act2 application and the application was run creating the diagram of interest. The output was saved as a text file.

The final geochemical modeling application was reaction path modeling using the React application in geochemist workbench (Bethke et al., 2018b). The reaction path modeling used the same database and conductivity file as was used in the Act2 app. The maximum number of iterations was again set to 999 for the initial step, but the convergence criterion used in this case 1×10^{-9} because of convergence issues encountered running the model. The step size was set at 0.01 with a maximum of 400 iterations per step. The ionic strength was calculated using the Debye – Hückel model. The solution data was entered into the React application and one variable was selected to change using the slide function from a minimal concentration to the maximum concentration desired. The output was saved as a text file for later use.

1.4 References

Alkalinity: Hach Method 8203. DOC316.53.01166. Hach/Hach Lange GmbH. 2018. 8 p.

ASTM. Standard D 5176-08, *Standard Test Method for Total Chemically Bound Nitrogen in Water by Pyrolysis and Chemiluminescence Detection*. American Society of Testing and Materials International, West Conshohocken, PA, www.astm.org. 2008.

Bethke, C.M.; Farrell, B.; Yeakel, S. *GWB Essentials Guide*. The Geochemist's Workbench Release 12. Aqueous Solutions, LLC. Champaign, IL. 2018a. 198 pp.

Bethke, C.M.; Farrell, B.; Yeakel, S. *GWB Reaction Modeling Guide*. The Geochemist's Workbench Release 12. Aqueous Solutions, LLC. Champaign, IL. 2018b. 208 pp.

EPA Method 120.1 Conductance (Specific Conductance, umhos at 25°C), (Issued 1982). In: Methods for Chemical Analysis of Water and Wastes. U.S. Environmental Protection Agency. EPA/600/4-79-020. 1983. 3 pp.

EPA Method 150.2 pH, Continuous Monitoring (Electrometric), (Issued 1982). In: Methods for Chemical Analysis of Water and Wastes. U.S. Environmental Protection Agency. EPA/600/4-79-020. 1983. 3 pp.

EPA Method 170.1 Temperature, (Issued 1971). U.S. Environmental Protection Agency. In: Methods for Chemical Analysis of Water and Wastes. U.S. Environmental Protection Agency. EPA/600/4-79-020. 1983. 1 pp.

EPA Method 180.1 Determination of Turbidity by Nephelometry, Revision 2. U.S. Environmental Protection Agency. Office of Research and Development. Environmental Monitoring Systems Laboratory. 1993. 10 pp.

EPA Method 200.7 Determination of Metals and Trace Elements in Water and Wastes by Inductively Coupled Plasma-Atomic Emission Spectrometry, Revision 4.4. U.S. Environmental Protection Agency. Office of Research and Development. Environmental Monitoring Systems Laboratory. 1994. 58 pp.

EPA Method 200.8 Determination of Trace Elements in Water and Wastes by Inductively Coupled Plasma-Mass Spectrometry, Revision 5.4. U.S. Environmental Protection Agency. Office of Research and Development. Environmental Monitoring Systems Laboratory. 1994. 57 pp.

EPA Method 353.1 Nitrogen, Nitrate-Nitrite (Colorimetric, Automated, Hydrozine Reduction), (Issued 1978). In: Methods for Chemical Analysis of Water and Wastes. U.S. Environmental Protection Agency. 1978. 5 pp.

EPA Method 360.1 Oxygen, Dissolved (Membrane Electrode), (Issued 1971). In: Methods for Chemical Analysis of Water and Wastes. U.S. Environmental Protection Agency. EPA/600/4-79-020. 1983. 2 pp.

EPA Method 365.1 Determination of phosphorus by semi-automated colorimetry, Revision 2. U.S. Environmental Protection Agency. Office of Research and Development. Environmental Monitoring Systems Laboratory. 1993. 18 p.

EPA Method 624.1 Purgeables by GC/MS. U.S Enviromental Protection Agency. Office of Water. EPA 821-R-16-008. Washington, DC. 2016. 42 p.

EPA Method 625.1 Base/Neutrals and Acids by GC/MS. U.S Enviromental Protection Agency. Office of Water. EPA 821-R-16-008. Washington, DC. 2016. 60 p.

K-GCRD-SOP-1097-2. *Determination of iodide in water samples using 0.2 M potassium hydroxide carrier with Lachat flow injection analysis*. 2009. 11 p.

K-GCRD-SOP-1137-0. *Determination of stable hydrogen and oxygen isotope ratios in water samples using a Picarro L2120i cavity ring-down spectrometer (CRDS)*. 2011. 30 p.

K-GCRD-SOP-1151-0. *GWERD SOP for Quality Control Procedures for General Parameters Analyses Using Lachat Flow Injection Analyzers (FIA)*. 2014. 12 p.

K-GCRD-SOP-1165-0. *Standard operating procedure for the determination of various fractions of carbon in aqueous samples using the Shimadzu TOC-VCSH Analyzer*. 2017. 18 p.

K-GCRD-SOP-3329-0. *SOP for the determination of inorganic anions in aqueous samples using the Dionex ICS-2100 Ion Chromatography System*. 2018. 21 p.

Standard Method 4500-NH_3 *Nitrogen (Ammonia)*. Standard Methods for the Examination of Water and Wastewater. 1997. 10 p.

Standard Method 2320B Alkalinity. Standard Methods for the Examination of Water and Wastewater. 1999. 8 p.

Appendix B. Louisville Supporting Information

Table of Contents

Louisville Geochemical Analysis

1.1 Groundwater Monitoring Wells and Piezometers

Table B-1. Locations of wells/piezometers adjacent to stormwater control measures and screened intervals.

Well/Piezometer	Latitude (°)	Longitude (°)	Land Surface Elevation (m-msl)	Top of Screen (m-msl)	Bottom of Screen (m-msl)
Monitoring Wells					
L-190-1-MW-01	38.25965381	-85.77785077	138.07	129.38	126.33
L-190-1-MW-02	38.25942272	-85.77807148	138.15	129.46	126.41
L-190-1-MW-03	38.25931140	-85.77808542	138.17	129.03	125.98
L-190-1-MW-04	38.25908033	-85.77788151	138.37	129.44	126.39
L-190-1-MW-05	38.25911927	-85.77823176	138.52	129.44	126.39
L-190-1-MW-06	38.25886575	-85.77793533	138.01	129.02	125.97
L-190-1-MW-07	38.25882715	-85.77818393	138.33	129.34	126.29
L-190-1-MW-08	38.25869647	-85.77821098	138.35	129.36	126.32
L-190-1-MW-09	38.25857185	-85.77822560	138.03	128.95	125.90
L-190-1-MW-10	38.25835128	-85.77807765	138.07	129.07	126.03
Piezometers					
L-190-1-PW-01	38.25964909	-85.77785196	138.11	126.99	126.38
L-190-1-PW-02	38.25941472	-85.77807254	138.14	126.87	126.26
L-190-1-PW-03	38.25930344	-85.77808658	138.18	126.81	126.20
L-190-1-PW-04	38.25907819	-85.77787357	138.33	127.05	126.44
L-190-1-PW-05	38.25911894	-85.77824188	138.31	126.82	126.21
L-190-1-PW-06	38.25886557	-85.77792553	138.03	126.76	126.15
L-190-1-PW-07	38.25882020	-85.77818565	138.32	126.89	126.28
L-190-1-PW-08	38.25868945	-85.77821371	138.36	126.93	126.32
L-190-1-PW-09	38.25856621	-85.77822528	138.03	126.51	125.90
L-190-1-PW-10	38.25834511	-85.77807841	138.06	126.63	126.02

1.2 Porewater Samplers

Table B-2. Soil porewater sampler locations and probe elevations.

Instrument	Latitude (°)	Longitude (°)	Probe Elevation (m-msl)
L-190-1-LW-1A	38.25938056	-85.77803333	133.85
L-190-1-LW-1C	38.25938056	-85.77803333	131.62
L-190-1-LW-1D	38.25938056	-85.77803333	135.00
L-190-1-LW-1E	38.25938056	-85.77803333	128.83
L-190-1-LW-2A	38.25923056	-85.77805833	133.68
L-190-1-LW-2C	38.25923056	-85.77805833	131.66
L-190-1-LW-2D	38.25923056	-85.77805833	135.46
L-190-1-LW-2E	38.25923056	-85.77805833	128.94
L-190-1-LW-4A	38.25870000	-85.77815000	134.10
L-190-1-LW-4C	38.25870000	-85.77815000	131.98
L-190-1-LW-5A	38.25860556	-85.77816944	134.06
L-190-1-LW-5C	38.25860556	-85.77816944	131.90
L-190-1-LW-6A	38.25854167	-85.77818056	133.72
L-190-1-LW-6C	38.25854167	-85.77818056	132.14
L-190-1-LW-7A	38.25875556	-85.77813889	134.04
L-190-1-LW-7C	38.25875556	-85.77813889	131.26

1.3 Soil Porewater - Major Anions and Cations, pH, Specific Conductivity

1.3.1 Specific Conductivity – Soil Porewater

Specific conductivity ranged from 125 – 3510 µS/cm. There was a significant difference in SPC ($p < 0.001$) depending on whether they were north or south of Main Street (Figure B-1). Generally, the SPC was larger north of Main Street.

Soil porewater clusters 1 and 2 were north of Main Street with cluster 1 being the farthest north and the farthest away from the infiltration gallery at the corner of 17th and Main (Figure 6-6). Specific conductivity in cluster 1 was significantly different ($p < 0.001$) than cluster 2 (Figure B-1). The deepest SPW in cluster 1, LW-1E did not show a trend with time (Figure B-1A). LW-1C, LW-1A, and LW1D showed decreasing SPC trends ($p < 0.001$, $p = 0.118$, and $p = 0.020$, respectively) with LW-1C and LW-1D being significant trends (Figure 6-9A). In cluster, 2 all depths showed decreasing SPC trends (Figure B-1B), LW-2E ($p = 0.009$), LW-2A ($p < 0.001$), and LW-2D ($p = 0.054$) are statistically significant. Overall, SPC was decreasing with time North of Main Street.

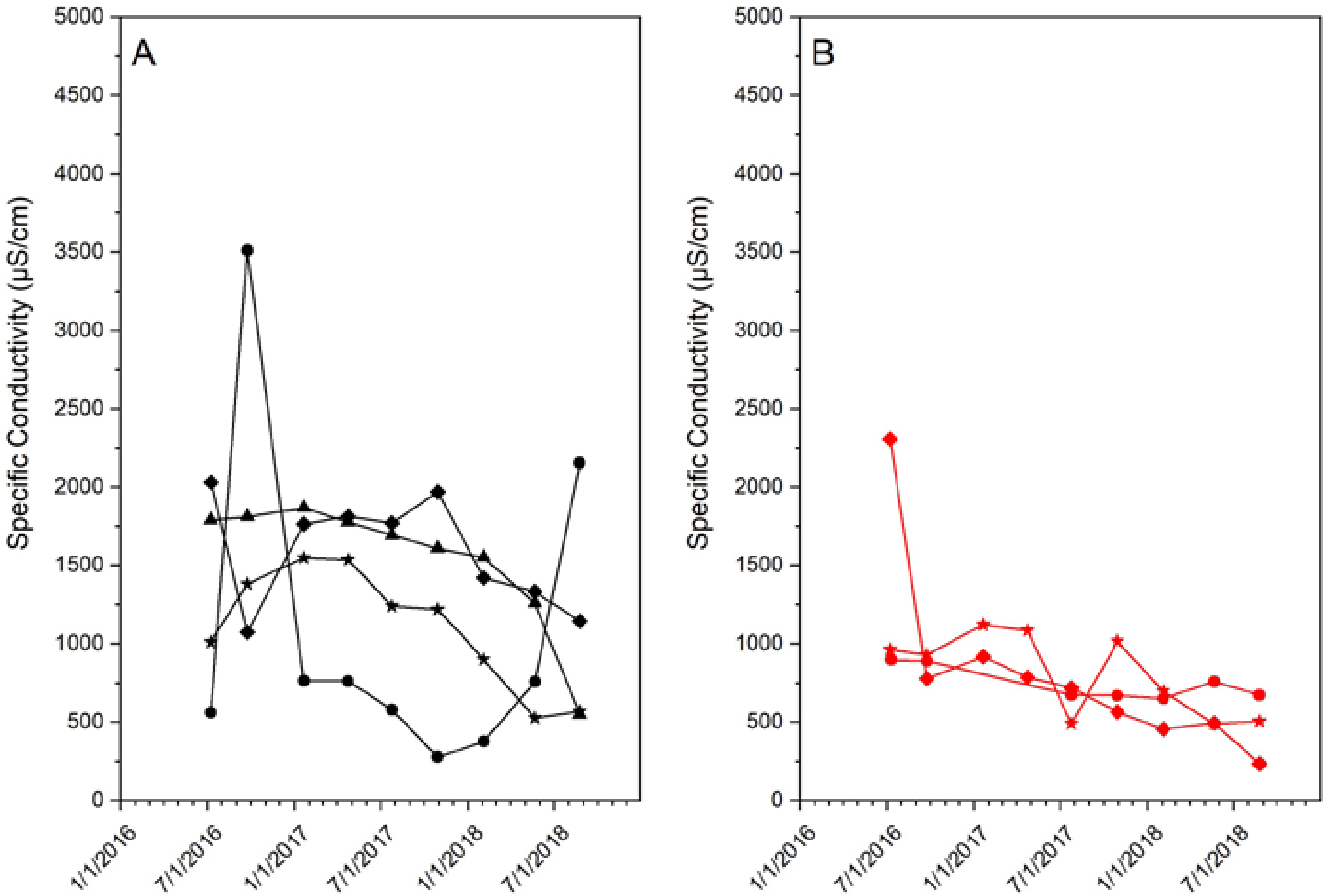

Figure B-1. Changes in Specific Conductivity in relationship to time for the SPWs north of Main Street. A. SPW cluster 1, black circles and lines are LW-1E, black triangles and lines are LW-1C, black diamonds and lines are LW-1A, and black stars and lines are LW-1D. B. SPW cluster 2, red circles and lines are LW-2E, red diamonds and lines are LW-2A, and red stars and lines are LW-2D.

South of Main Street there were four SPW clusters (Figure 6-6) with cluster 7 being the closest to Main Street followed by cluster 4, cluster 5, and cluster 6 moving south of Main Street, respectively. There were no significant differences among these clusters. Figure B-2 shows the relationship between SPC and time in the clusters south of Main Street. In cluster 4 (Figure B-2A), LW-4C and LW-4A showed decreasing trends in SPC with the deepest LW-4C having a significant trend ($p = 0.006$) and LW-4A with significant trend ($p = 0.054$). In cluster 6 (Figure B-2C), LW-6C and LW-6A showed decreasing trends which are not significant. Cluster 7 (Figure B-2D), LW-7C showed a decreasing trend ($p = 0.118$) and LW-7A had no trend in SPC. Finally, LW-5C and LW-5A (Figure B-2B), cluster 5 did not show a trend in SPC data. In more than half of the cases the SPWs south of Main Street showed a decreasing trend in SPC.

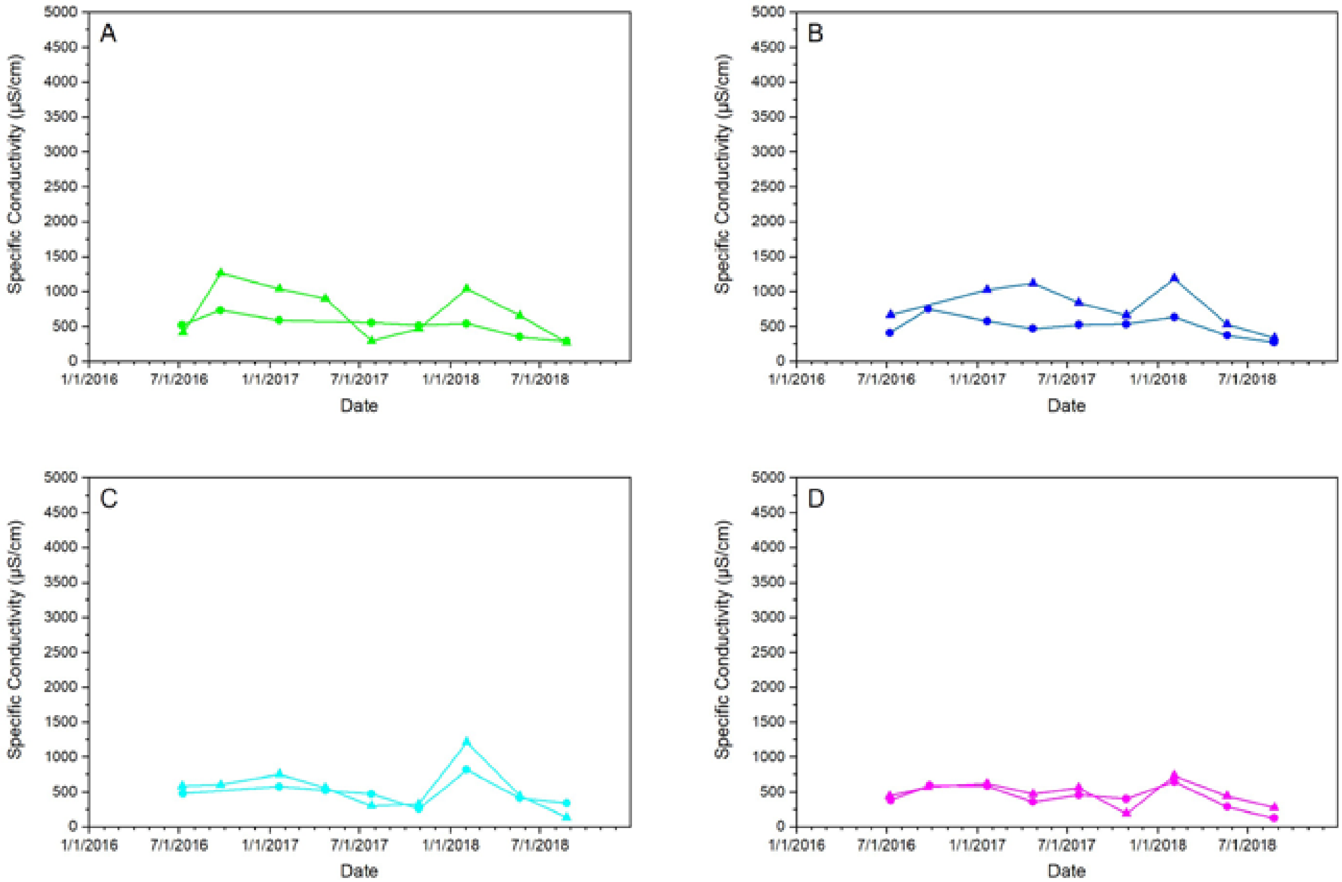

Figure B-2. Changes in Specific Conductivity in relationship to time for the SPWs south of Main Street. A. SPW cluster 4, green circles and lines are LW-4C, green triangles and lines are LW-4A. B. SPW cluster 5, blue circles and lines are LW-5C, blue triangles and lines are LW-5A. C. SPW cluster 6, cyan circles and lines are LW-6C, cyan triangles and lines are LW-6A. D. SPW cluster 7, magenta circles and lines are LW-7C, magenta triangles and lines are LW-7A.

1.3.2 Chloride – Soil Porewater

Chloride concentrations for ranged from 1 – 607 mg/L. There was a significant difference in chloride concentrations ($p < 0.001$) depending on whether they are north or south of Main Street (Figures B-3 and B-4). Generally, the chloride concentration was larger north of Main Street.

Chloride concentrations in cluster 1 were significantly different than in cluster 2 ($p < 0.001$) north of Main Street (Figure B-3). In cluster 1, the deepest SPW, LW-1E showed no trend in chloride concentration (Figure B-3A). However, the shallower SPWs in this cluster showed decreasing significant trends in chloride concentrations (Figure B-3A) (LW-1C and LW-1A $p < 0.001$; LW-1D $p = 0.034$). In cluster 2, however, the deepest SPW (Figure B-3B), LW-2E had decreasing chloride concentrations although not significant ($p = 0.118$). The shallower SPWs (Figure B-3B), as was the case in cluster 1, showed significant decreases in chloride concentrations (LW-2A $p < 0.001$ and LW-2D $p = 0.006$). Except for LW-1E, all SPWs north of Main Street had decreasing chloride concentrations during the study, with some chloride concentrations exceeding the secondary MCL for chloride.

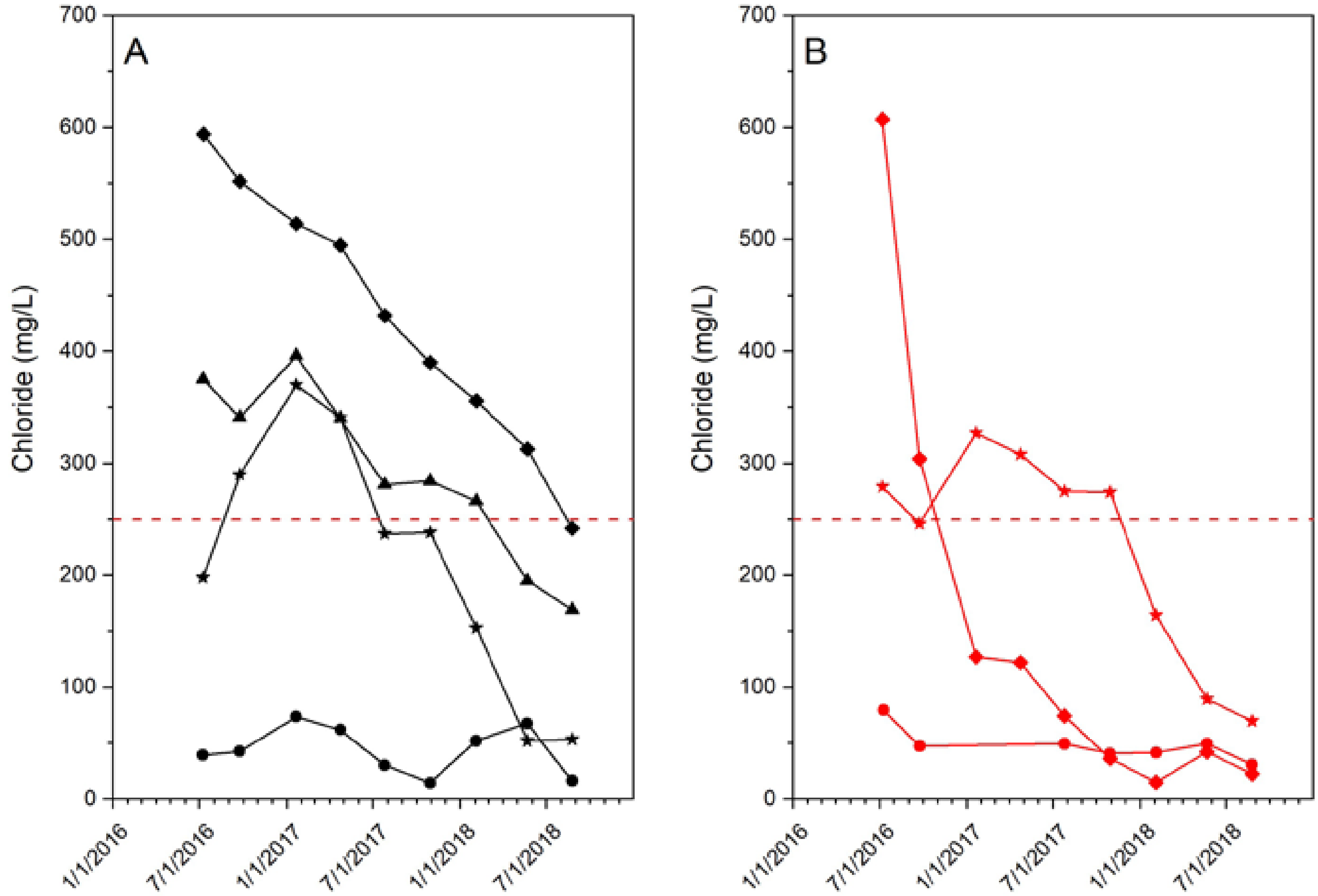

Figure B-3. Changes in chloride concentrations in relationship to time for the SPWs north of Main Street. A. SPW cluster 1, black circles and lines are LW-1E, black triangles and lines are LW-1C, black diamonds and lines are LW-1A, and black stars and lines are LW-1D. B. SPW cluster 2, red circles and lines are LW-2E, red diamonds and lines are LW-2A, and red stars and lines are LW-2D. The red dashed lines represent the chloride secondary MCL (250 mg/L).

South of Main Street there were no significant differences in chloride concentrations between SPW clusters (Figure B-4). The only SPWs that showed a chloride concentration trend were LW-4C and LW-6C and these were decreasing trends (Figure B-4A and A-4C). The trend in LW-4C ($p = 0.011$) and LW-6C ($p = 0.082$) were significant. All other SPW showed no trend in chloride concentrations (Figure B-4). Except for LW-4C, all other SPWs had a spike in chloride concentrations in February 2018 and potentially another spike in January 2017 in SPWs LW-4A, LW-6A, LW-7A and LW-7C (Figure B-4). In general, chloride concentrations were remaining relatively constant south of Main Street during the study, but there were spikes in chloride concentrations in several SPWs in the winter months likely caused by the application of de-icing materials on the road surface. Concentrations in only two SPWs (LW-6A and LW-7C) exceeded the chloride secondary MCL, both occurring in February 2018 (Figure B-4C and B-4D).

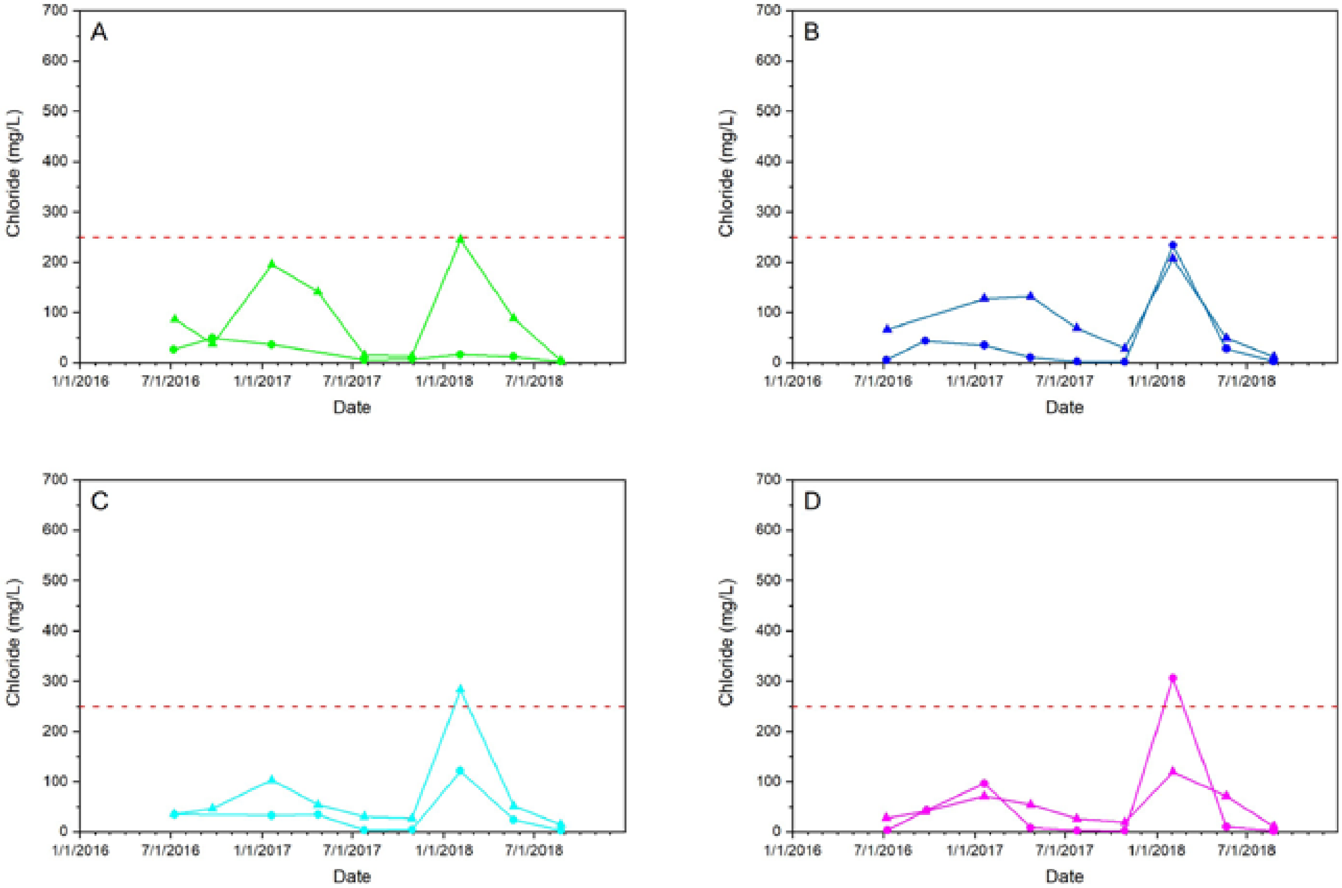

Figure B-4. Changes in chloride concentrations in relationship to time for the SPWs south of Main Street. A. SPW cluster 4, green circles and lines are LW-4C, green triangles and lines are LW-4A. B. SPW cluster 5, blue circles and lines are LW-5C, blue triangles and lines are LW-5A. C. SPW cluster 6, cyan circles and lines are LW-6C, cyan triangles and lines are LW-6A. D. SPW cluster 7, magenta circles and lines are LW-7C, magenta triangles and lines are LW-7A. The red dashed lines represent the chloride secondary MCL (250 mg/L).

1.3.3 Bicarbonate – Soil Porewater

There were no significant differences in bicarbonate concentration between SPWs north and south of Main Street (Figures B-5 and B-6). Bicarbonate concentrations ranged from 4 – 420 mg HCO_3^-/L.

Figure B-5 shows the changes in bicarbonate concentration with time for SPWs south of Main Street. There was a significant difference in bicarbonate concentration in SPW cluster 4 and cluster 5 compared to cluster 7 (p = 0.030 and p = 0.016, respectively). All other cluster combinations show no significant differences in bicarbonate concentrations (Figure B-5A, B-5B, B-5D). There were no trends in bicarbonate data South of Main Street.

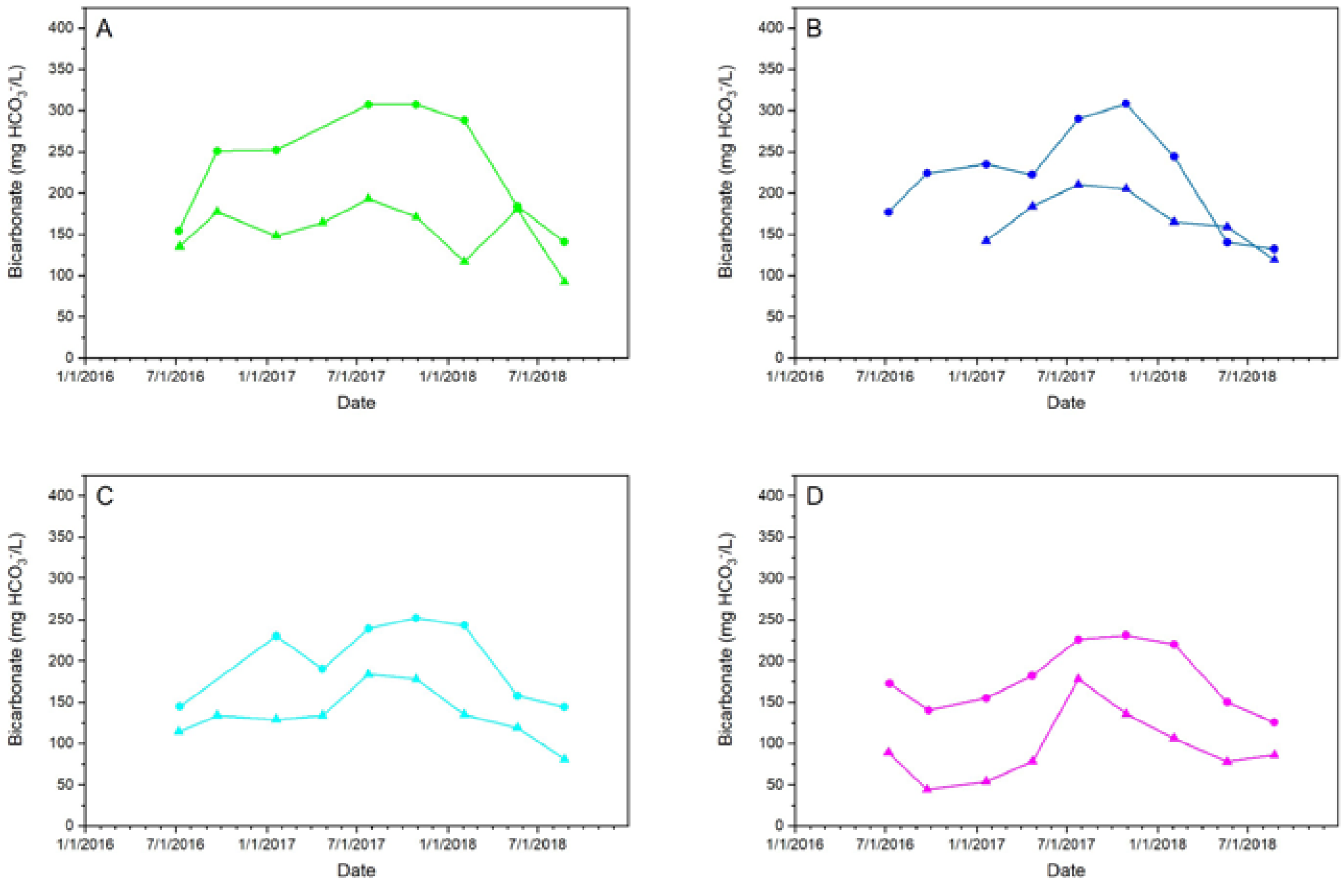

Figure B-5. Changes in Bicarbonate concentrations in relationship to time for the SPWs south of Main Street. A. SPW cluster 4, green circles and lines are LW-4C, green triangles and lines are LW-4A. B. SPW cluster 5, blue circles and lines are LW-5C, blue triangles and lines are LW-5A. C. SPW cluster 6, cyan circles and lines are LW-6C, cyan triangles and lines are LW-6A. D. SPW cluster 7, magenta circles and lines are LW-7C, magenta triangles and lines are LW-7A.

Bicarbonate concentrations in cluster 1 and cluster 2, north of Main Street were significantly different ($p < 0.001$), with cluster 1 larger than cluster 2 bicarbonate concentrations (Figure B-6). Figure B-6A shows the trends in bicarbonate concentrations during the study. There were no trends in the bicarbonate concentrations in LW-1E, LW-1C, and LW-1D, but in LW-1A the bicarbonate concentrations were significantly increasing ($p = 0.020$) (Figure B-6A). Contrasting cluster 2 to cluster 1, the deepest SPW, LW-2E the bicarbonate concentration was decreasing ($p = 0.054$) and in the shallower SPWs, LW-2A and LW-2D, the bicarbonate concentrations were significantly increasing ($p = 0.028$ and $p = 0.006$, respectively) (Figure B-6B).

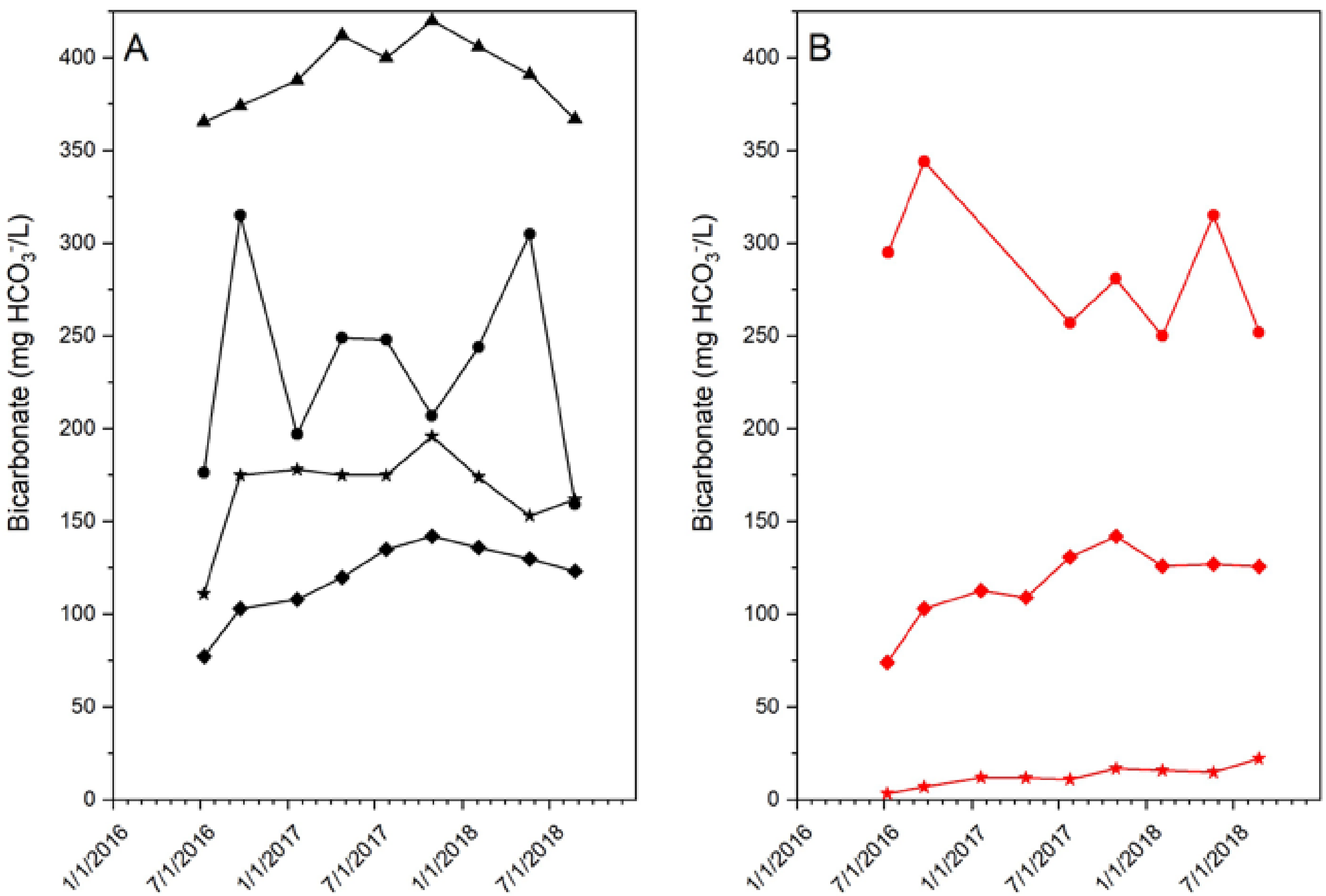

Figure B-6. Changes in bicarbonate concentrations in relationship to time for the SPW's north of Main Street. A. SPW cluster 1, black circles and lines are LW-1E, black triangles and lines are LW-1C, black diamonds and lines are LW-1A, and black stars and lines are LW-1D. B. SPW cluster 2, red circles and lines are LW-2E, red diamonds and lines are LW-2A, and red stars and lines are LW-2D.

1.3.4 Sulfate – Soil Porewater

Sulfate concentrations in this study ranged from 6.36 – 235 mg/L. Much like bicarbonate there were no significant differences in sulfate concentration North or South of Main Street (Figures B-7 and B-8) and there were no exceedances of the secondary MCL (250 mg/L) for sulfate during the study to date.

Data for sulfate north of Main Street is plotted in Figure B-7. The sulfate concentrations in cluster 2 were significantly larger than cluster 1 ($p = 0.002$). In cluster 1, the sulfate concentrations in LW-1E and LW-1D, the deepest and shallowest SPWs (Figure B-7A) were decreasing ($p = 0.118$ and $p = 0.082$, respectively). In LW-1C and LW-1A the sulfate concentrations are significantly increasing ($p < 0.001$; Figure B-7A). Figure B-7B, are plots of the sulfate concentrations with time for cluster 2. In the deepest SPW in this cluster, LW-2E, there was no trend sulfate concentrations (Figure B-7B). Sulfate concentrations in LW-2A, intermediate depth in cluster 2 (Figure B-7B), had a decreasing trend ($p = 0.020$) and in the shallowest depth, LW-2D, the sulfate concentrations were increasing significantly ($p = 0.054$).

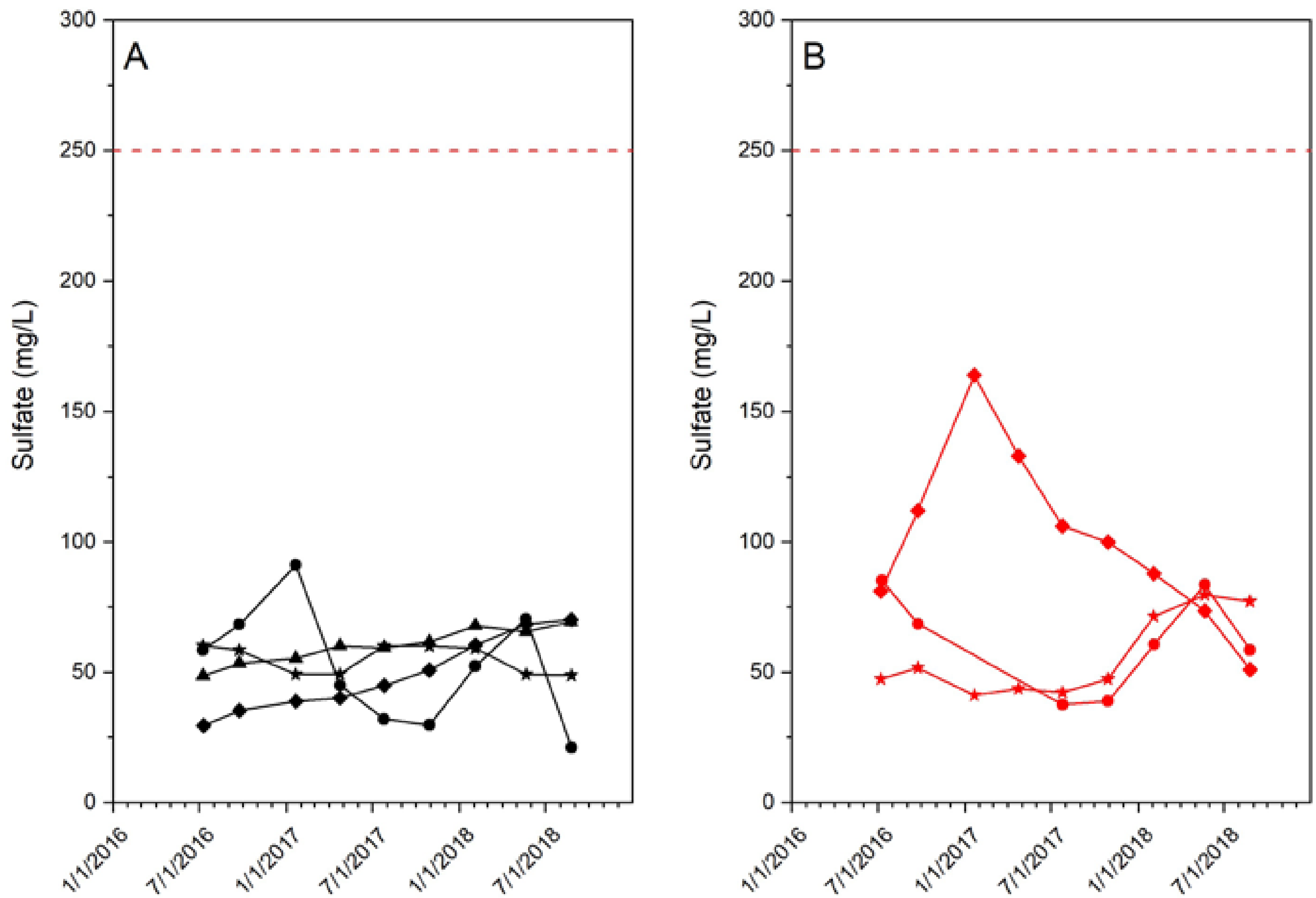

Figure B-7. Changes in sulfate concentrations with respect to time for the SPW's north of Main Street. A. SPW cluster 1, black circles and lines are LW-1E, black triangles and lines are LW-1C, black diamonds and lines are LW-1A, and black stars and lines are LW-1D. B. SPW cluster 2, red circles and lines are LW-2E, red diamonds and lines are LW-2A, and red stars and lines are LW-2D. The red dashed lines indicate the secondary MCL for sulfate (250 mg/L).

Data for sulfate concentrations versus time are plotted in Figure B-8 for SPW clusters south of Main Street. There were no significant differences in sulfate concentrations among cluster 4, cluster 5, cluster 6, and cluster 7. The sulfate concentration trends were all decreasing with time (Figure B-8). Sulfate concentration was significantly decreasing in LW-4C and LW-4A ($p = 0.011$ and $p = 0.006$, respectively); LW-6C and LW-6A ($p = 0.003$ and $p = 0.034$, respectively); and LW-7C ($p = 0.034$). Sulfate concentrations were also significantly decreasing in LW-5C ($p = 0.054$), LW-5A ($p = 0.082$), and LW-7A ($p = 0.082$).

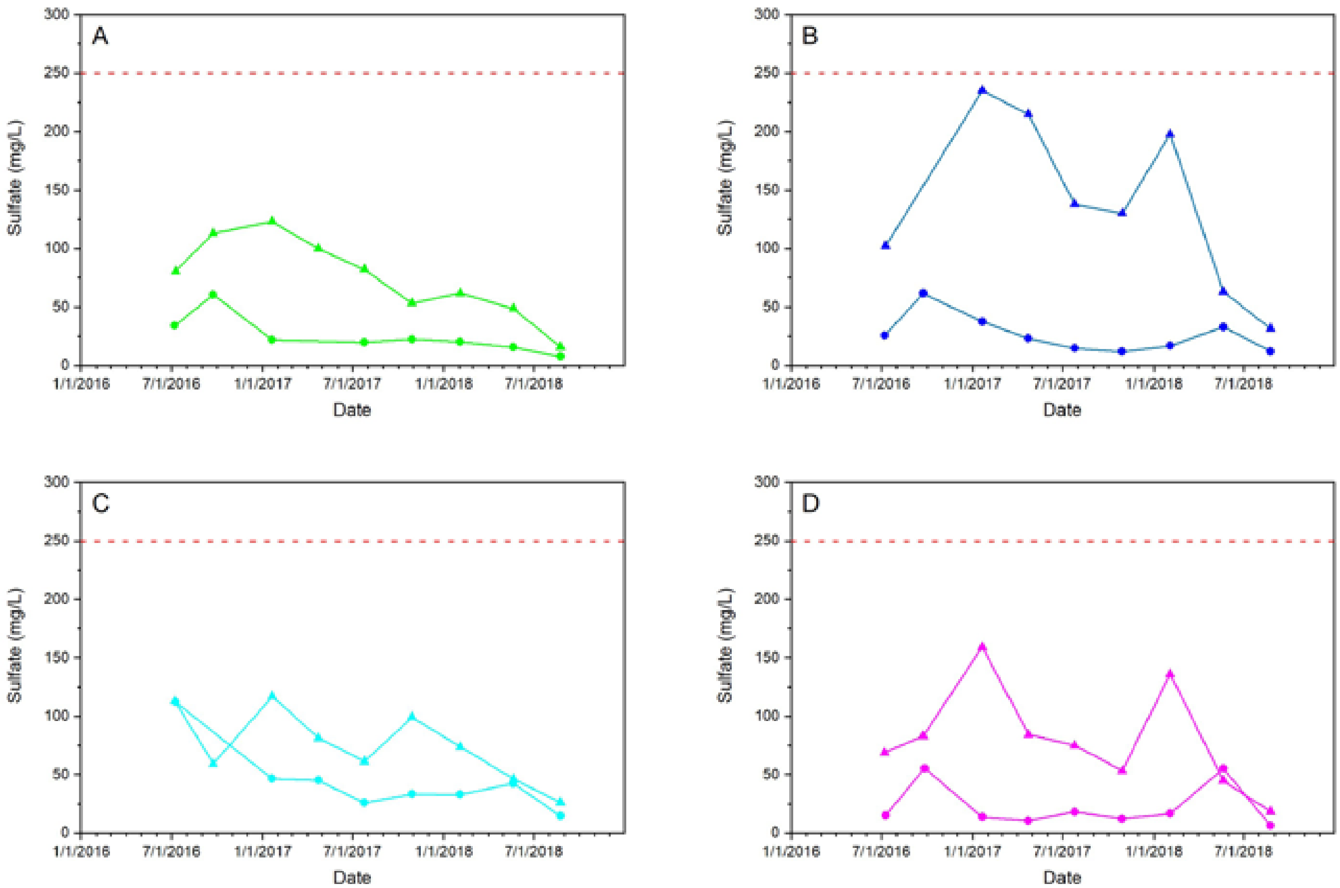

Figure B-8. Changes in sulfate concentrations in relationship to time for the SPWs south of Main Street. A. SPW cluster 4, green circles and lines are LW-4C, green triangles and lines are LW-4A. B. SPW cluster 5, blue circles and lines are LW-5C, blue triangles and lines are LW-5A. C. SPW cluster 6, cyan circles and lines are LW-6C, cyan triangles and lines are LW-6A. D. SPW cluster 7, magenta circles and lines are LW-7C, magenta triangles and lines are LW-7A. Red dashed lines indicate the secondary MCL for sulfate (250 mg/L).

1.3.5 Calcium – Soil Porewater

There were no significant differences in calcium concentration comparing the north side or south side of Main Street in this study in the SPW. Calcium concentrations ranged from 6.35 – 198 mg/L. Figures B-9 and B-10 show the calcium concentrations in the SPW during the study.

North of Main Street, SPW clusters 1 and 2 had statistically different calcium concentrations ($p < 0.001$) and calcium concentrations for each SPW is shown in Figure B-9. The calcium concentrations in cluster 1 (furthest from infiltration point) were greater than those of cluster 2. In SPW cluster 1, there was no trend in calcium data in LW-1E (Figure B-9A), but there were decreasing calcium concentrations in the shallower SPWs LW-1C, LW-1A, and LW-1D. These decreasing trends were statistically significant LW-1C ($p = 0.002$), LW-1A ($p < 0.001$), and LW-1D ($p = 0.009$). In cluster 2 (Figure B-9B), decreasing concentrations in calcium were found over the duration of the study in all the SPWs. The decrease in calcium was significant in LW-2E ($p = 0.082$), LW-2A and LW-2D ($p < 0.001$). Overall, in both clusters north of Main Street there were significant decreases in calcium concentration with time.

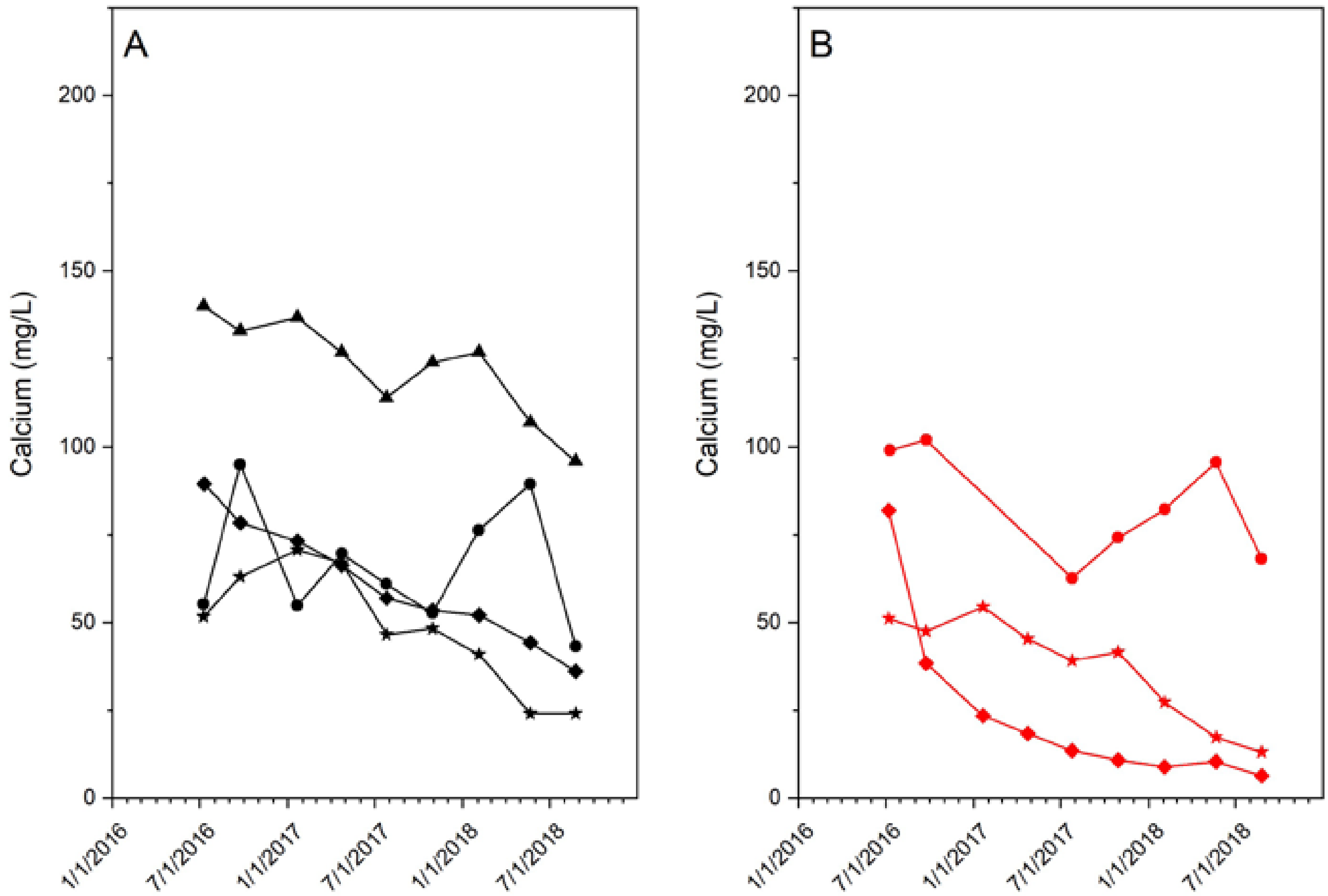

Figure B-9. Changes in calcium concentrations with respect to time for the SPW's north of Main Street. A. SPW cluster 1, black circles and lines are LW-1E, black triangles and lines are LW-1C, black diamonds and lines are LW-1A, and black stars and lines are LW-1D. B. SPW cluster 2, red circles and lines are LW-2E, red diamonds and lines are LW-2A, and red stars and lines are LW-2D.

Data for the changes in calcium concentrations in SPWs south of Main Street are plotted in Figure B-10. There were no statistical differences in calcium concentrations in the four SPW clusters. Except for LW-4A there were no trends in calcium concentration with time for SPWs south of Main Street. LW-4A (Figure B-10A) had decreasing calcium concentrations that were significant ($p = 0.054$). In February 2018 there was a discernable spike in the calcium concentration in most of the SPW samplers in February 2018.

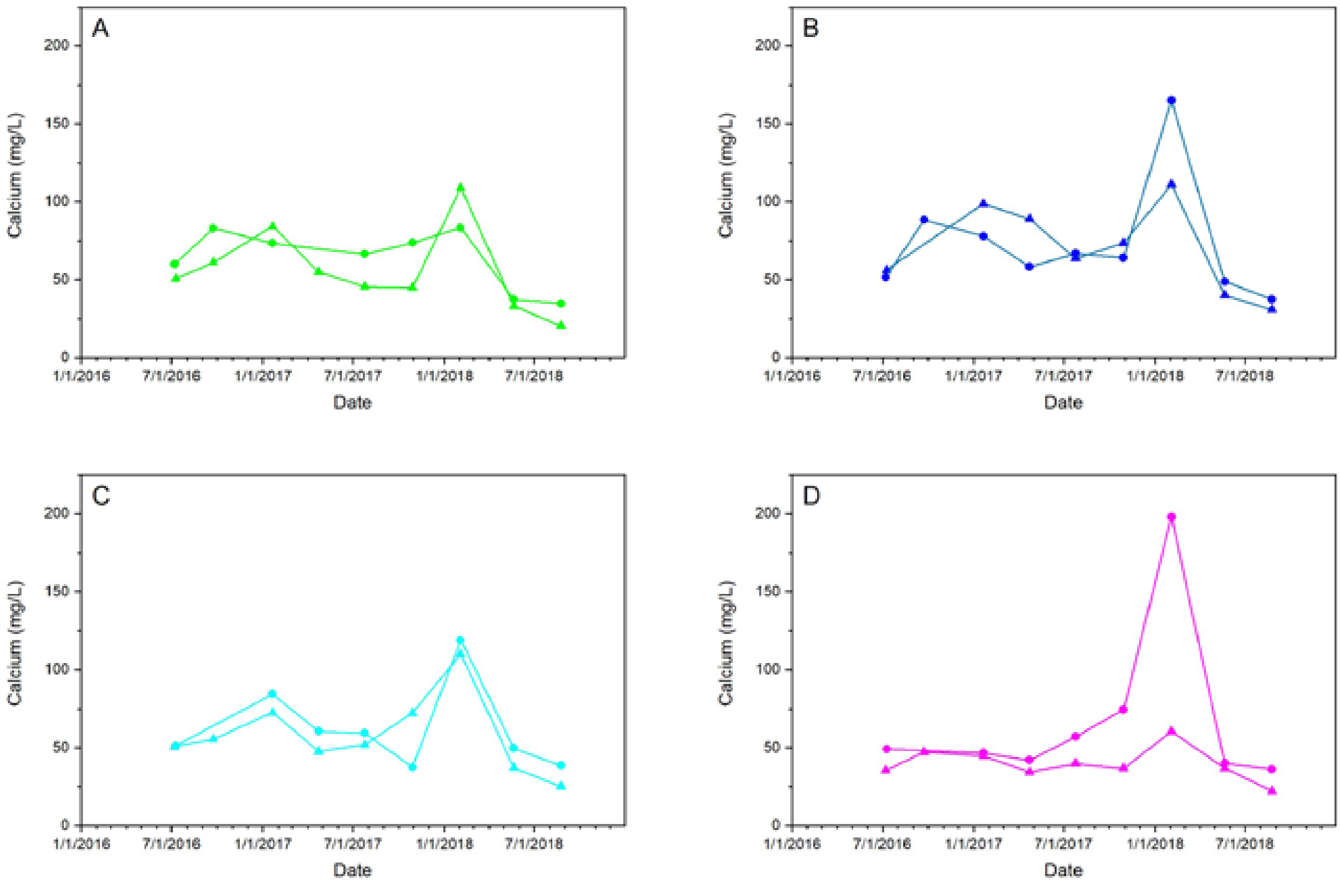

Figure B-10. Changes in calcium concentrations in relationship to time for the SPWs south of Main Street. A. SPW cluster 4, green circles and lines are LW-4C, green triangles and lines are LW-4A. B. SPW cluster 5, blue circles and lines are LW-5C, blue triangles and lines are LW-5A. C. SPW cluster 6, cyan circles and lines are LW-6C, cyan triangles and lines are LW-6A. D. SPW cluster 7, magenta circles and lines are LW-7C, magenta triangles and lines are LW-7A.

1.3.6 Potassium – Soil Porewater

Soil porewater potassium concentrations ranged from 1.80 – 14.3 mg/L. The plots of potassium concentration versus time are shown in Figures B-11 and B-12. Potassium concentrations were significantly different ($p < 0.001$) north and south of Main Street. The potassium concentrations are larger north of Main Street.

The two SPW clusters north of Main Street, cluster 1 and cluster 2, had significantly different potassium concentrations ($p < 0.001$). Cluster 1, the more northern cluster from the infiltration gallery, had larger potassium concentrations than cluster 2 nearer the infiltration gallery. As shown in Figure B-11A, the deepest SPW samplers (LW-1E and LW-1C) do not show any trends in potassium concentration. But, the shallower SPWs in this cluster, have decreasing trends in potassium concentration during the study (Figure B-11A). The decreasing trends in LW-1A ($p = 0.003$) and in LW-1D ($p = 0.054$) were significant ($p = 0.054$). In SPW cluster 2 (Figure B-11B), there were decreasing potassium concentrations with time at all depths. These decreasing trends were significant LW-2E ($p = 0.003$), LW-2A ($p < 0.001$) and LW-2D ($p = 0.034$).

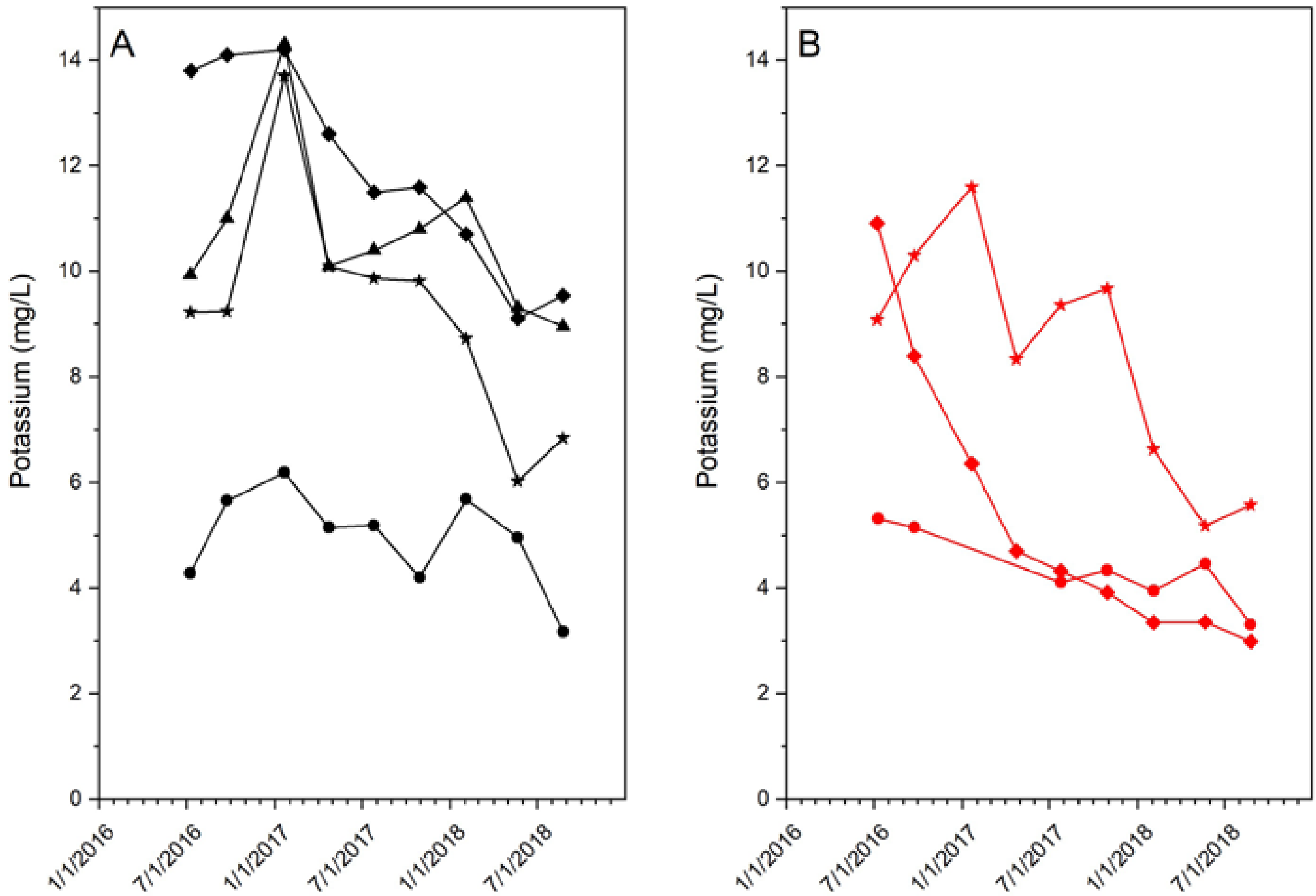

Figure B-11. Changes in potassium concentrations with respect to time for the SPWs north of Main Street. A. SPW cluster 1, black circles and lines are LW-1E, black triangles and lines are LW-1C, black diamonds and lines are LW-1A, and black stars and lines are LW-1D. B. SPW cluster 2, red circles and lines are LW-2E, red diamonds and lines are LW-2A, and red stars and lines are LW-2D.

The potassium concentrations in SPW clusters south of Main Street, with one exception, were not different. In cluster 5, the potassium concentrations were significantly larger than the potassium concentrations in cluster 7 ($p = 0.031$). Figure B-12 shows the changes in potassium concentrations with time for the four clusters. In the four clusters the potassium concentrations in the deepest SPW samplers all had decreasing trends (Figure B-12). The deep SPWs LW-4C (Figure B-12A), LW-5C (Figure B-12B), LW-6C (Figure B-12C) the decreasing trends were significant ($p = 0.006$, $p = 0.011$, and $p = 0.020$, respectively). In LW-7C (Figure B-12D) there was a decreasing trend and was significant ($p = 0.082$). In cluster 7 (Figure B-12D), the shallowest SPW also showed decreasing potassium concentrations over time and this trend was significant ($p = 0.001$). In the other clusters, the shallowest SPWs showed no trends in potassium concentrations.

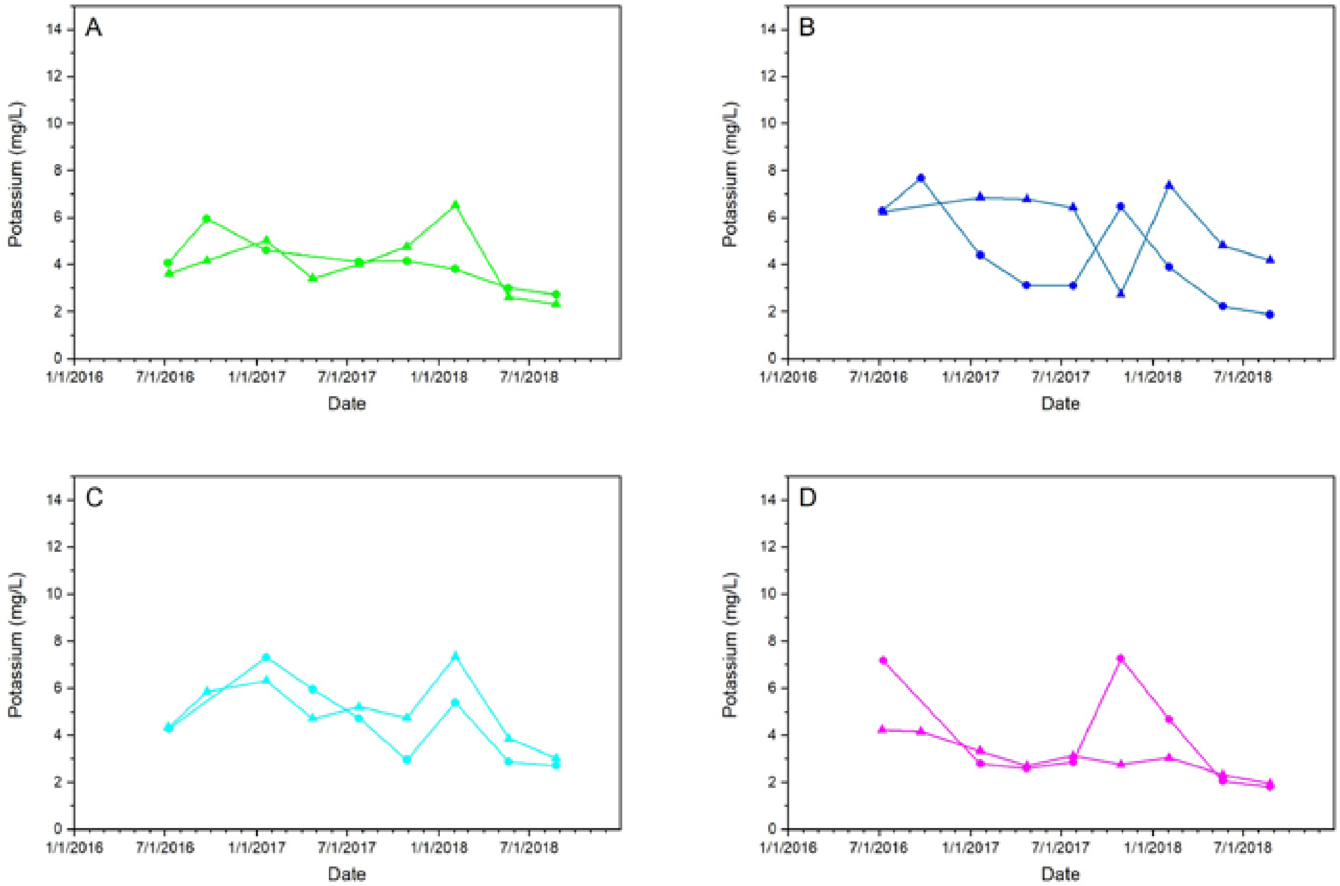

Figure B-12. Changes in potassium concentrations in relationship to time for the SPWs south of Main Street. A. SPW cluster 4, green circles and lines are LW-4C, green triangles and lines are LW-4A. B. SPW cluster 5, blue circles and lines are LW-5C, blue triangles and lines are LW-5A. C. SPW cluster 6, cyan circles and lines are LW-6C, cyan triangles and lines are LW-6A. D. SPW cluster 7, magenta circles and lines are LW-7C, magenta triangles and lines are LW-7A.

1.3.7 Magnesium – Soil Porewater

The magnesium concentrations ranged from 2.81 – 50.4 mg/L. The magnesium concentrations north and south of Main Street in the SPWs were not significantly different. The concentrations of magnesium with respect to time are shown in Figures B-13 and B-14.

Magnesium concentration in the SPW clusters north of Main Street did not show a significant difference. As would be expected the trends in magnesium concentrations for the most part mimic the trends in calcium in clusters 1 and 2. In cluster 1 (Figure B-13A), the deepest SPW samplers, LW-1E and LW-1C showed no trend in magnesium concentrations with time. In the shallower SPW samplers, LW-1A and LW-1D, magnesium concentration decreased with time and these trends were significant ($p < 0.001$ and $p = 0.011$, respectively). However, in cluster 2 (Figure B-13B), all SPW depths had decreasing trends in magnesium concentration during the study. The decreasing trends were significant in all SPW samplers in cluster 2 (LW-1E, $p = 0.034$; LW-1A, $p < 0.001$; and LW-1D, $p = 0.006$).

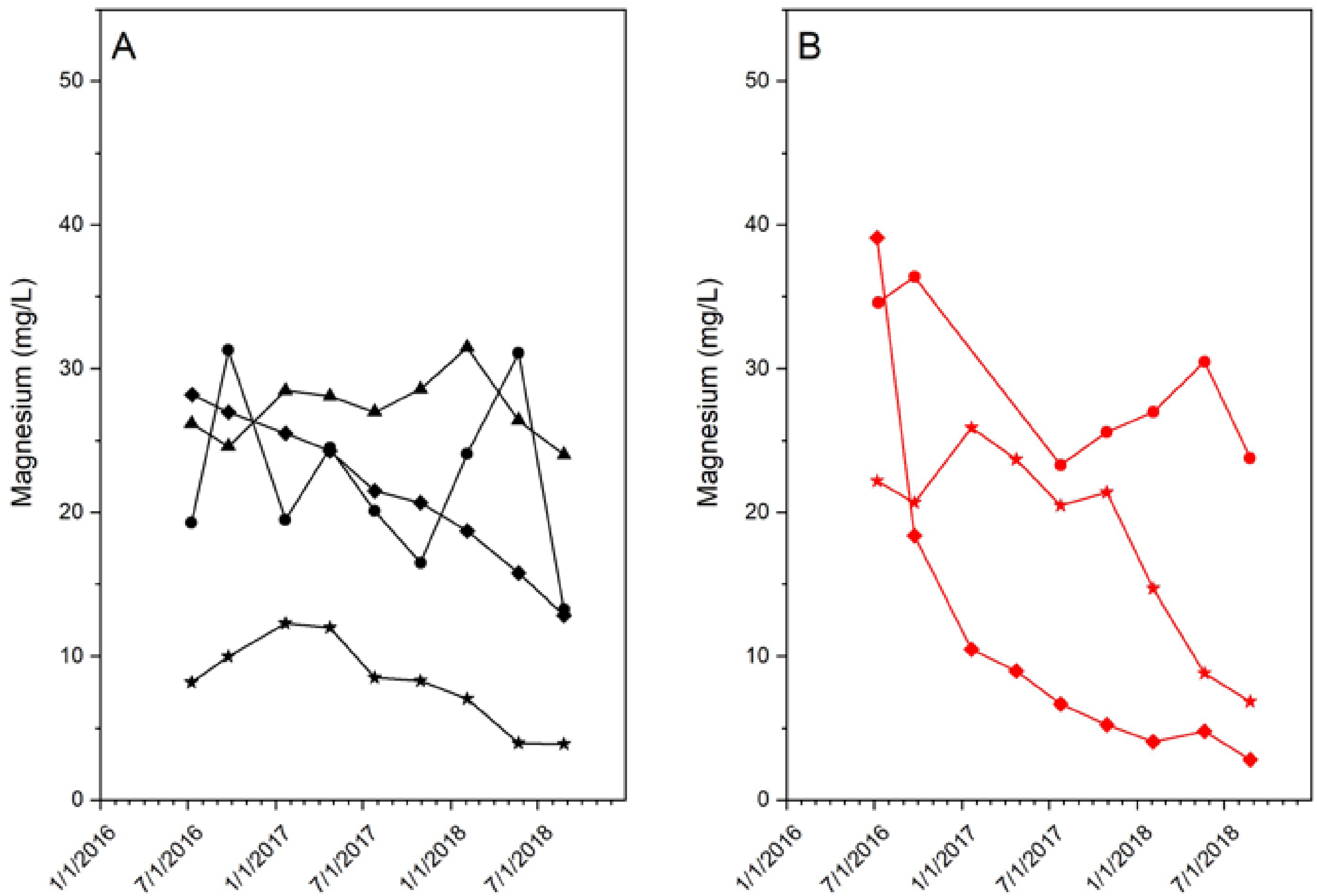

Figure B-13. Changes in magnesium concentrations with respect to time for the SPWs north of Main Street. A. SPW cluster 1, black circles and lines are LW-1E, black triangles and lines are LW-1C, black diamonds and lines are LW-1A, and black stars and lines are LW-1D. B. SPW cluster 2, red circles and lines are LW-2E, red diamonds and lines are LW-2A, and red stars and lines are LW-2D.

Magnesium concentrations were similar in all the SPW clusters south of Main Street. Only cluster 4 (Figure B-14A) and cluster 6 (Figure B-14C) had SPW samplers with decreasing magnesium trends during the study. In cluster 4, LW-4A had a decreasing trend and this trend was significant ($p = 0.054$). In cluster 6, both LW-6C and LW-6A had decreasing magnesium concentrations. The decreasing trend in LW-6C ($p = 0.006$) and LW-6A were ($p = 0.054$) significant. There were not trends in magnesium concentration in other clusters or SPW samples. There was an apparent spike in magnesium concentrations in February 2018.

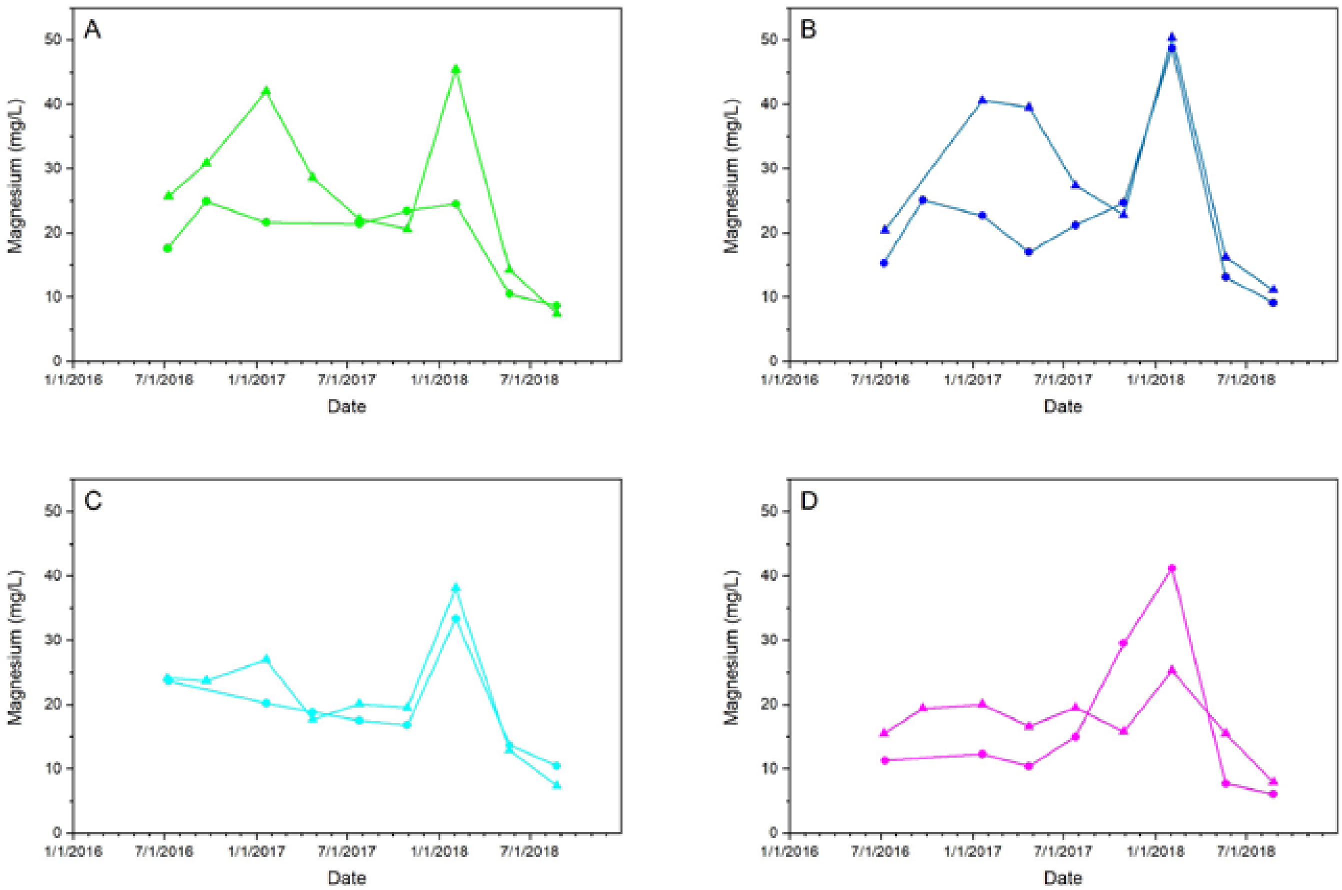

Figure B-14. Changes in magnesium concentrations in relationship to time for the SPWs south of Main Street. A. SPW cluster 4, green circles and lines are LW-4C, green triangles and lines are LW-4A. B. SPW cluster 5, blue circles and lines are LW-5C, blue triangles and lines are LW-5A. C. SPW cluster 6, cyan circles and lines are LW-6C, cyan triangles and lines are LW-6A. D. SPW cluster 7, magenta circles and lines are LW-7C, magenta triangles and lines are LW-7A.

1.3.8 Sodium – Soil Porewater

Sodium concentrations varied considerably in this study. Sodium ranged from 1.57 – 334 mg/L during the study. Plots of sodium concentration versus time are shown in Figures B-15 and B-16. There was a significant difference in sodium concentrations north of Main Street compared to south of Main Street ($p < 0.001$).

North of Main Street, clusters 1 and 2 had significantly different sodium concentrations ($p < 0.001$). Sodium concentrations farther way from the infiltration gallery (cluster 1) had larger sodium concentrations than cluster 2 nearer the gallery. In cluster 1, the deepest SPW sampler (LW-1E) showed no trend in sodium concentrations during the study (Figure B-15A). The shallower SPW samplers in cluster 1 (LW-1C, LW-1A, and LW-1D) had decreasing trends in sodium concentration with time (Figure B-15A). In LW-1C, LW-1D and LW-1A the trends were significant, $p = 0.002$, $p < 0.001$, $p = 0.054$, respectively. In SPW cluster 2 (Figure B-15B), the only SPW sampler with a trend in sodium concentrations was LW-2A and this trend was significant ($p < 0.001$).

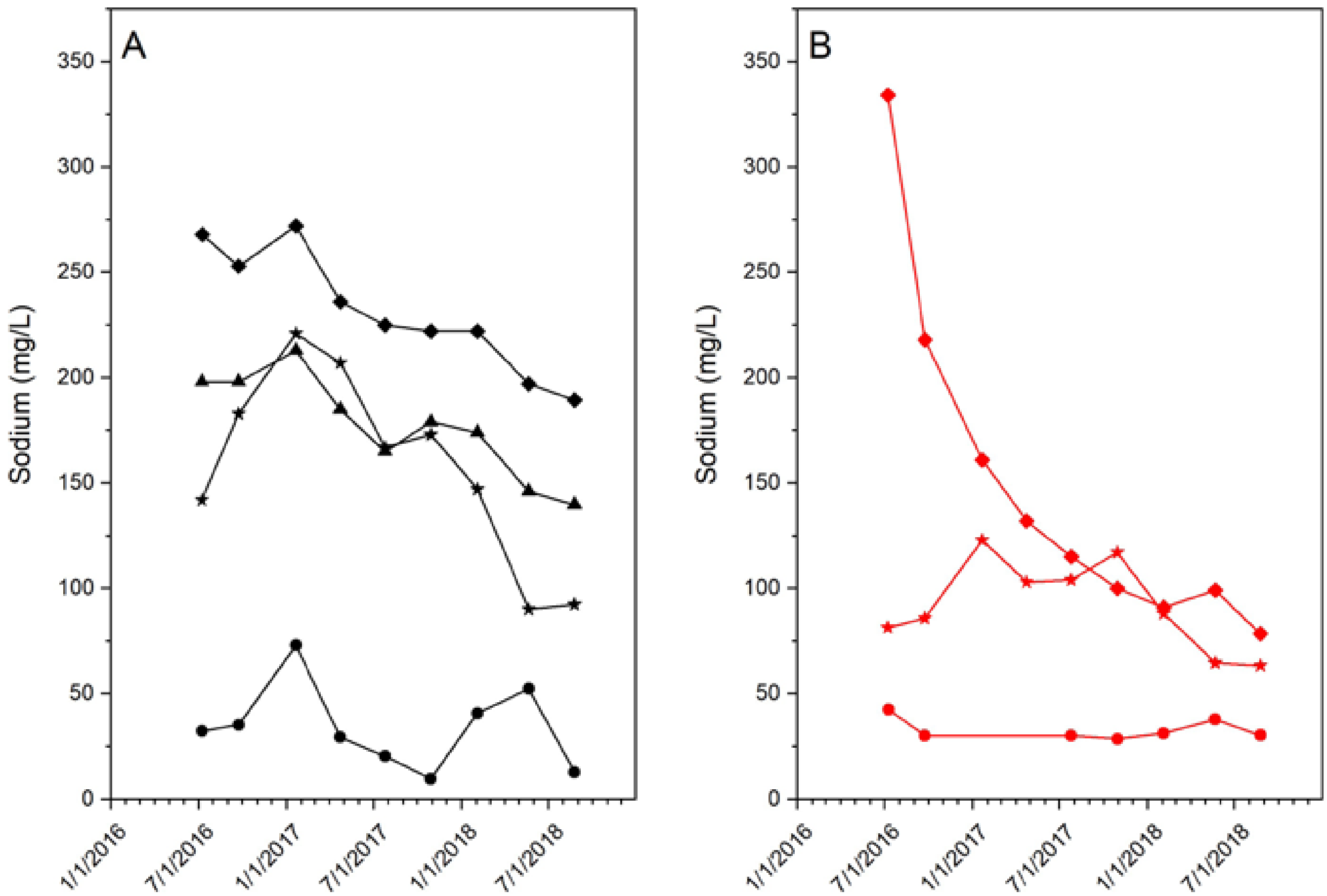

Figure B-15. Changes in sodium concentrations with respect to time for the SPW's north of Main Street. A. SPW cluster 1, black circles and lines are LW-1E, black triangles and lines are LW-1C, black diamonds and lines are LW-1A, and black stars and lines are LW-1D. B. SPW cluster 2, red circles and lines are LW-2E, red diamonds and lines are LW-2A, and red stars and lines are LW-2D.

In the SPW clusters south of Main Street there was no significant difference in sodium concentrations between clusters. In cluster 7, nearest to the infiltration gallery (Figure B-16D), both LW-7C and LW-7A had decreasing sodium concentrations during the study, although these were not significant trends. Moving away from the infiltration gallery, in cluster 4 (Figure B-16A), only LW-4C showed a decreasing sodium concentration trend and was significant ($p = 0.082$). There was no trend in sodium concentrations in cluster 5 (Figure B-16B). In cluster 6 (Figure 6-24C), the farthest from the infiltration gallery south of Main Street, only LW-6C had a decreasing trend in sodium concentration during the study and this trend was not significant.

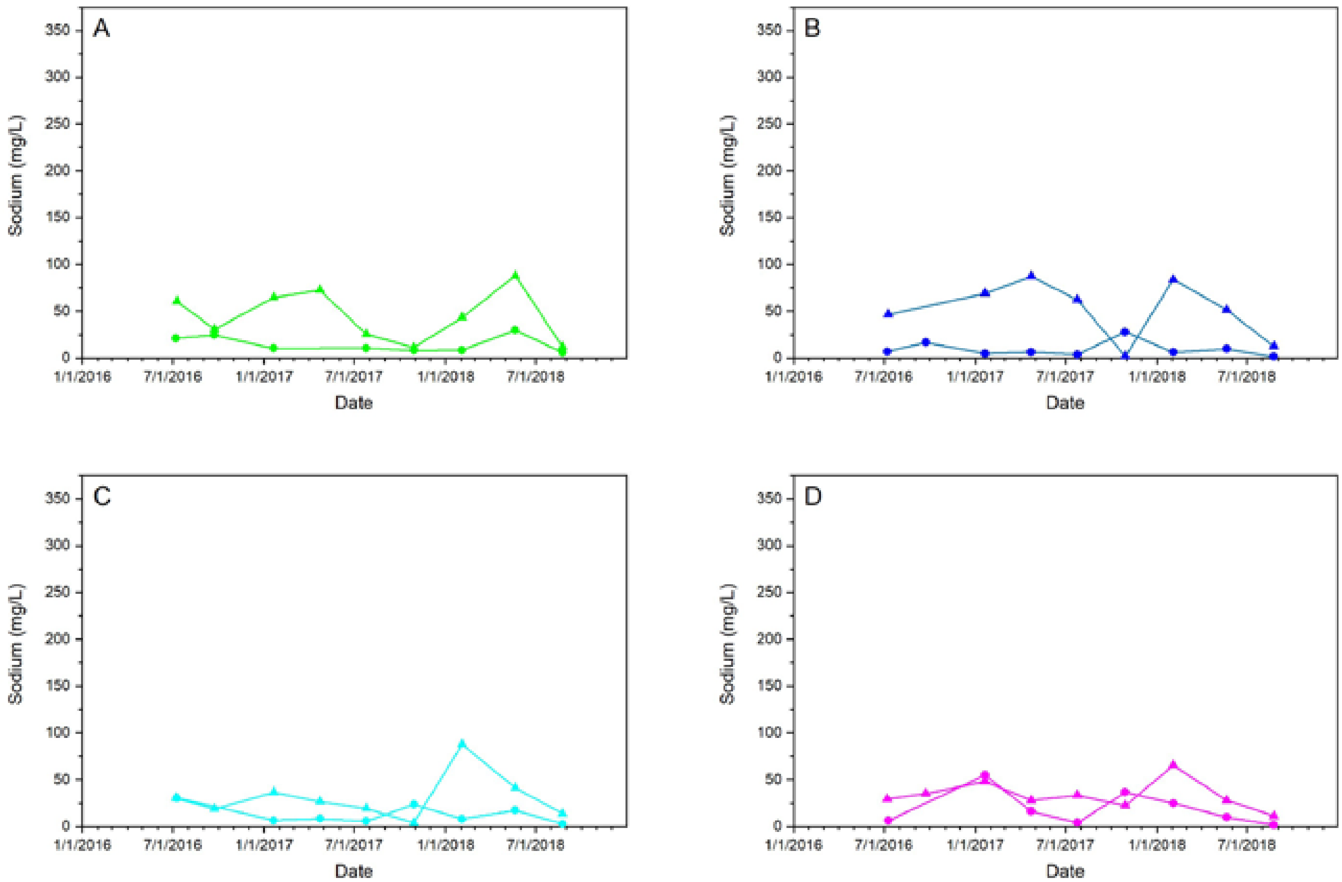

Figure B-16. Changes in sodium concentrations in relationship to time for the SPWs south of Main Street. A. SPW cluster 4, green circles and lines are LW-4C, green triangles and lines are LW-4A. B. SPW cluster 5, blue circles and lines are LW-5C, blue triangles and lines are LW-5A. C. SPW cluster 6, cyan circles and lines are LW-6C, cyan triangles and lines are LW-6A. D. SPW cluster 7, magenta circles and lines are LW-7C, magenta triangles and lines are LW-7A.

1.3.9 pH – Soil Porewater

The pH ranged from 5.03 – 9.03 in the SPWs. As suggested by this range there were samples that exceeded the secondary MCL for pH in the study. There were no significant differences in pH between SPW samplers north and south of Main Street. Plots of pH versus time for pH north and south of Main Street are shown in Figures B-17 and B-18.

Most of the secondary MCL (sMCL) exceedances for pH were in the SPW clusters north of Main Street. In cluster 1, pH exceeded the secondary MCL four times (Figure B-17A). The secondary MCL was exceeded in LW-1A in July 2016 (pH= 6.28), in January 2017 (pH= 9.03), and in October 2017 (pH= 8.66). The pH in LW-1D exceeded the secondary MCL in July 2016 (pH = 6.31). The secondary MCL was exceeded in cluster 2 on four occasions (Figure B-17B). The secondary MCL was exceeded in LW-2D in July 2016 (pH = 5.03), in September 2016 (pH = 5.90), and in May 2018 (pH = 6.46). LW-2A had one exceedance in July 2016 (pH = 6.16). The pH was significantly higher ($p = 0.029$) in SPW cluster 1 (farther from the gallery) than SPW cluster 2 (nearer the gallery). In cluster 1, pH was increasing in LW-1C and LW-1D (Figure B-17A). The increasing pH in LW-1C ($p = 0.016$) and LW-1D ($p = 0.054$) were significant. There were no pH trends in LW-1E and LW-1A. Cluster 2 on the other hand, had increasing pH with time in LW-2E and LW-2A. Both pH trends were significant ($p = 0.071$ and $p = 0.082$, respectively).

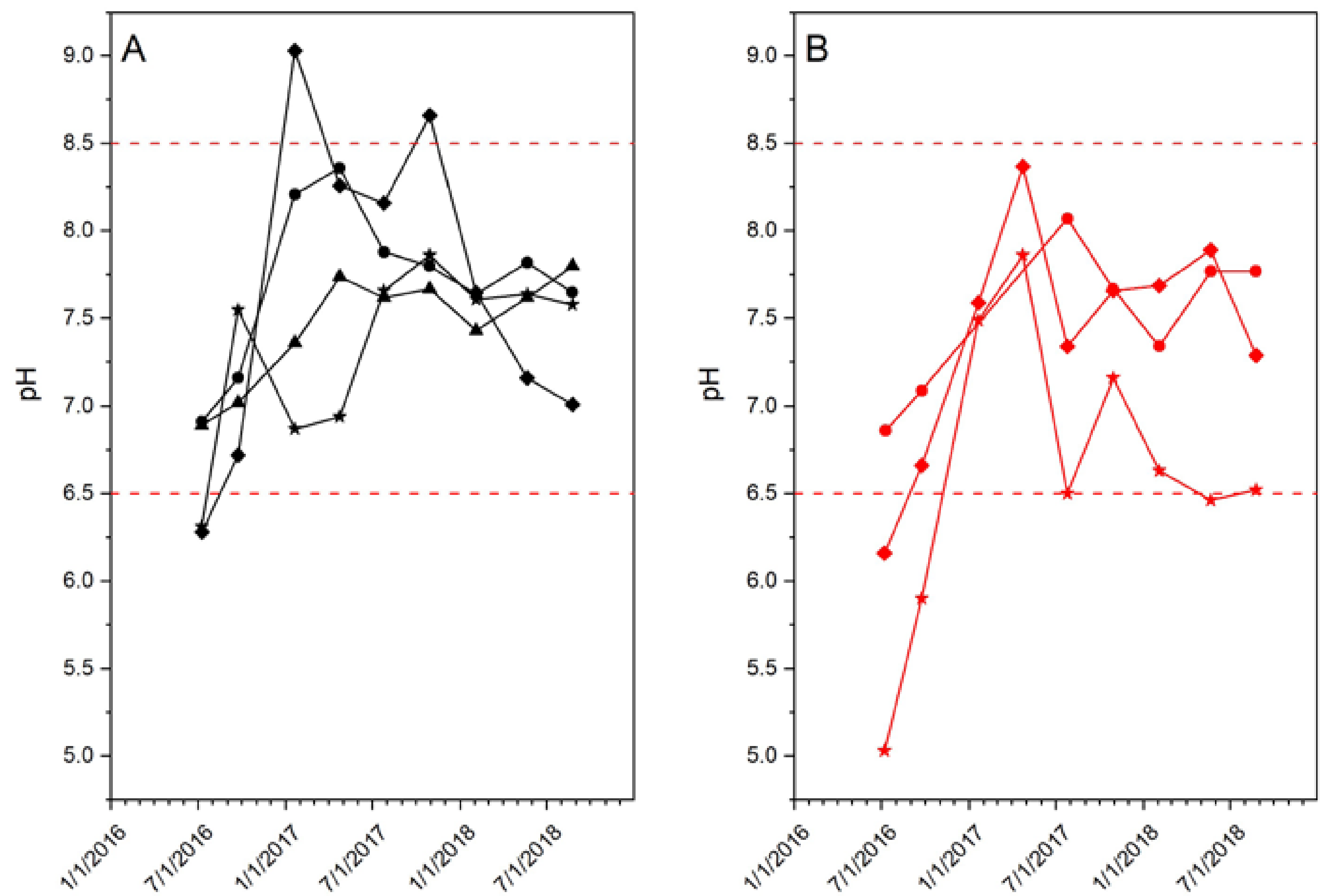

Figure B-17. Changes in pH with respect to time for the SPWs north of Main Street. A. SPW cluster 1, black circles and lines are LW-1E, black triangles and lines are LW-1C, black diamonds and lines are LW-1A, and black stars and lines are LW-1D. B. SPW cluster 2, red circles and lines are LW-2E, red diamonds and lines are LW-2A, and red stars and lines are LW-2D. The red dashed lines are the secondary MCLs for pH (pH<6.5 and pH>8.5).

South of Main Street there was only one secondary MCL exceedance for pH (Figure B-18D). In July 2016 the pH secondary MCL was exceeded in LW-7A (pH= 6.46). There were statistically no differences in pH for any of the four clusters south of Main Street. In SPW cluster 4 and 5 (Figures B-18A and B-18B) there were no trends in pH. In cluster 6 (Figure B-18C), LW-6A showed an increasing pH trend and it was significant ($p = 0.054$). Similarly, in cluster 7 (Figure B-18D), only LW-7A had an increasing pH trend and it was a significant trend ($p = 0.034$).

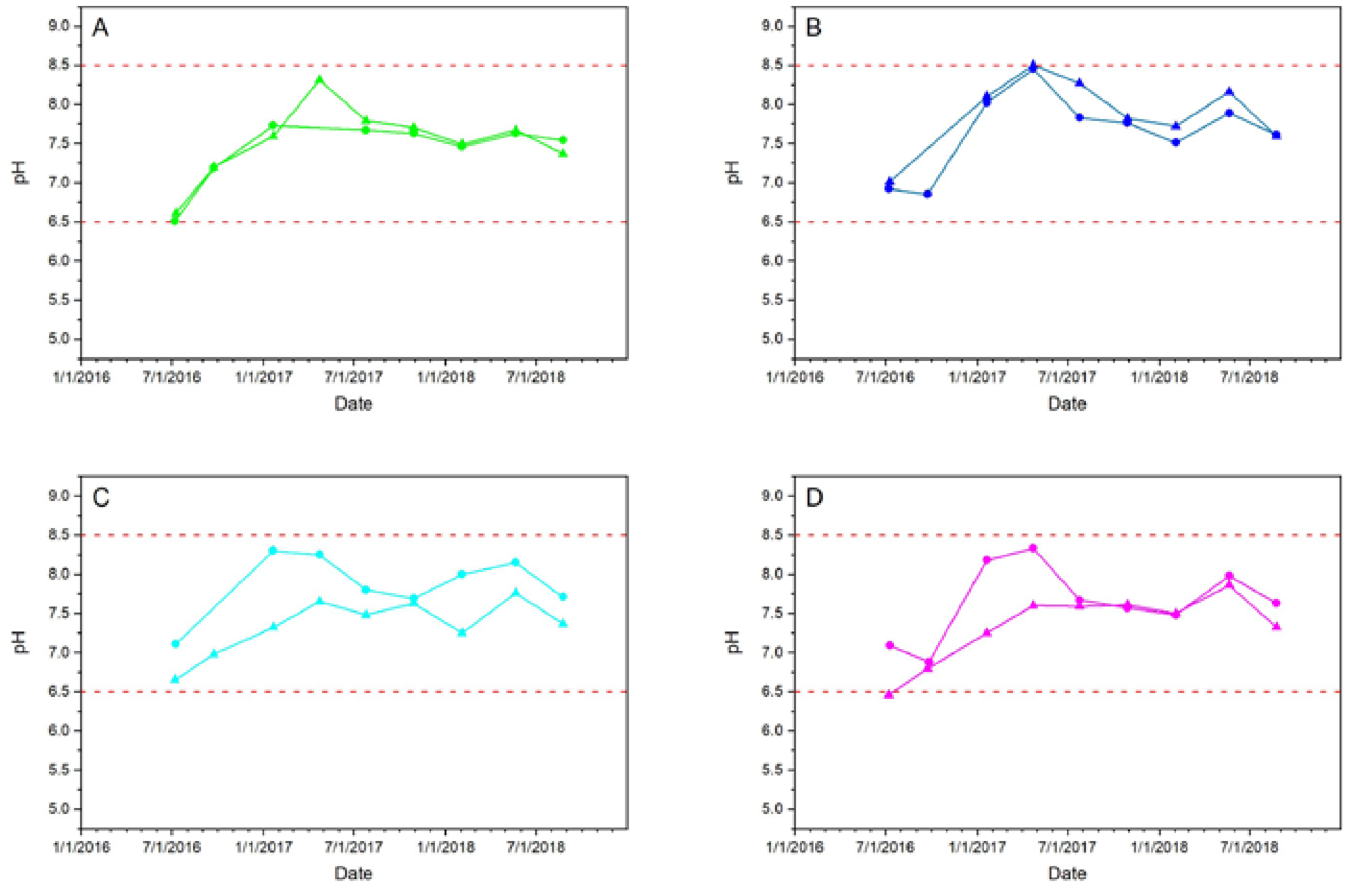

Figure B-18. Changes in pH in relationship to time for the SPWs south of Main Street. A. SPW cluster 4, green circles and lines are LW-4C, green triangles and lines are LW-4A. B. SPW cluster 5, blue circles and lines are LW-5C, blue triangles and lines are LW-5A. C. SPW cluster 6, cyan circles and lines are LW-6C, cyan triangles and lines are LW-6A. D. SPW cluster 7, magenta circles and lines are LW-7C, magenta triangles and lines are LW-7A. The red dashed lines are the secondary MCLs for pH (pH<6.5 and pH>8.5).

1.4 Other Soil Porewater Constituents

1.4.1 Fluoride

Fluoride concentrations varied from 0.02 – 0.95 mg/L in the SPW samples. There was a significant difference in fluoride concentrations in the samples north and south of Main Street ($p < 0.001$). The fluoride concentrations south of Main Street were greater than the concentrations north of Main Street. The concentrations of fluoride during the study for each SPW sampler are shown in Figure B-19 (north of Main Street) and Figure B-20 (south of Main Street).

The concentrations of fluoride during the study north of Main Street are shown in Figure B-19. There were no statistical differences in concentration between clusters 1 and 2 ($p = 0.805$). In cluster 1, only the shallow SPW sampler (LW-1E) had a decreasing trend which was significant ($p = 0.071$; Figure B-19A). All other depths showed no trend in fluoride concentrations. In cluster 2 (Figure B-19B), two samplers (LW-2E and LW-2A) had an increasing trend in fluoride concentrations ($p = 0.016$ and $p = 0.003$, respectively). The shallowest SPW sampler (LW-2D) did not show trend.

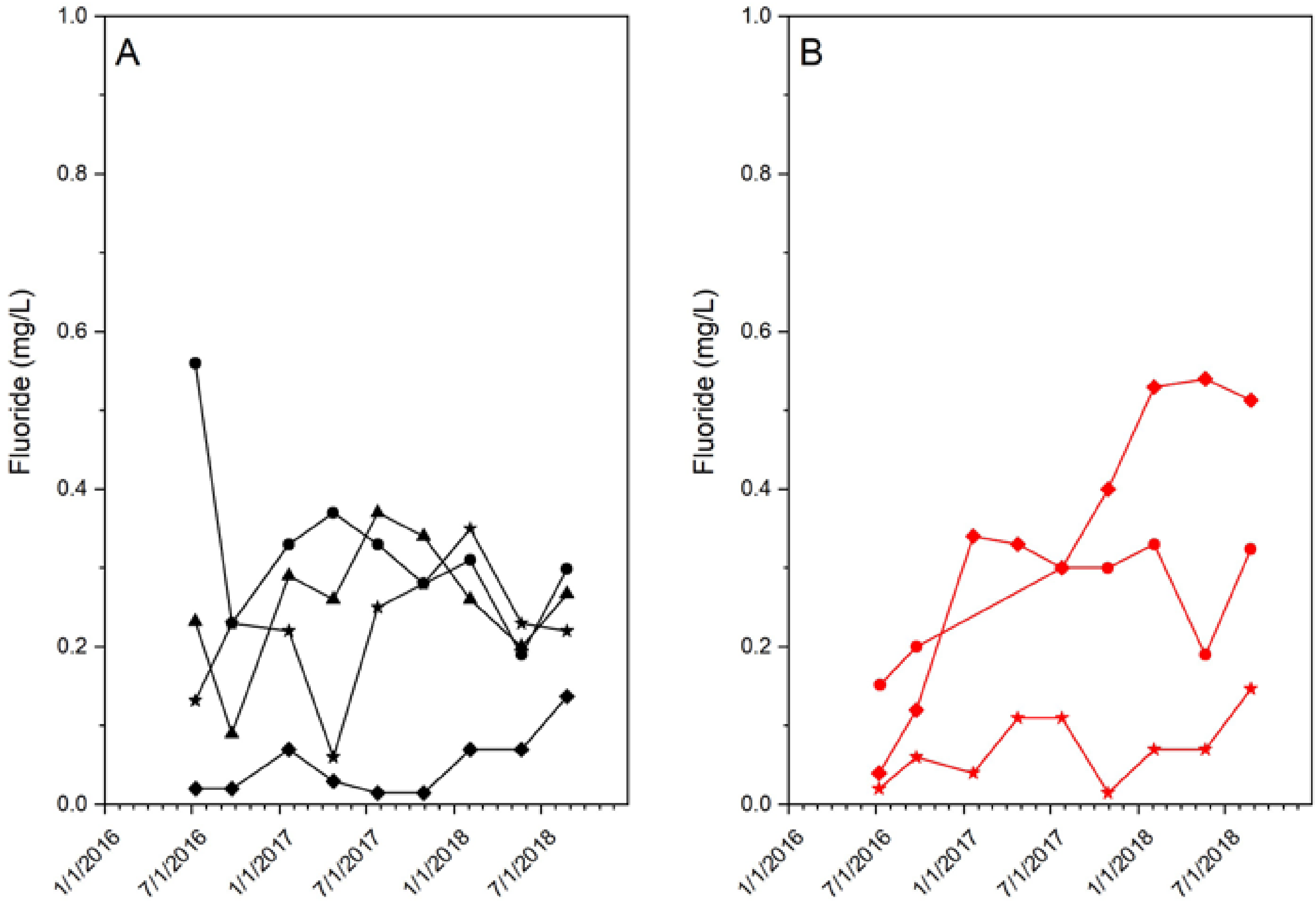

Figure B-19. Changes in fluoride concentration with respect to time for the SPWs north of Main Street. A. SPW cluster 1 and B. SPW cluster 2. Black circles and lines are LW-1E, black triangles and lines are LW-1C, black diamonds and lines are LW-1A, and black stars and lines are LW-1D. B. SPW cluster 2, red circles and lines are LW-2E, red diamonds and lines are LW-2A, and red stars and lines are LW-2D.

Figure B-20 shows the concentrations of fluoride south of Main Street. There were no significant differences between SPW clusters except for when cluster 4 is compared with cluster 7. In this case there was a statistically significant difference in fluoride concentrations ($p = 0.036$). In cluster 4 (Figure B-20A), LW-4A had a decreasing trend and was significant ($p = 0.071$) and LW-4C had no trend. LW-4C showed a spike in the fluoride concentration in February 2018. Cluster 5 and 6 (Figures B-20B and C) had significantly decreasing trends in fluoride concentration in LW-5C ($p = 0.003$), LW-5A ($p = 0.001$), LW-6C ($p = 0.046$), and LW-6A ($p = 0.028$). LW-6A showed a slight spike in fluoride concentration in February 2018 (Figure B-20C). Finally, in cluster 7 (Figure B-20D), LW-7C fluoride concentrations significantly decreased ($p = 0.006$), and there was no trend in the fluoride data for LW-7A. LW-7A showed a spike in the fluoride data in February 2018.

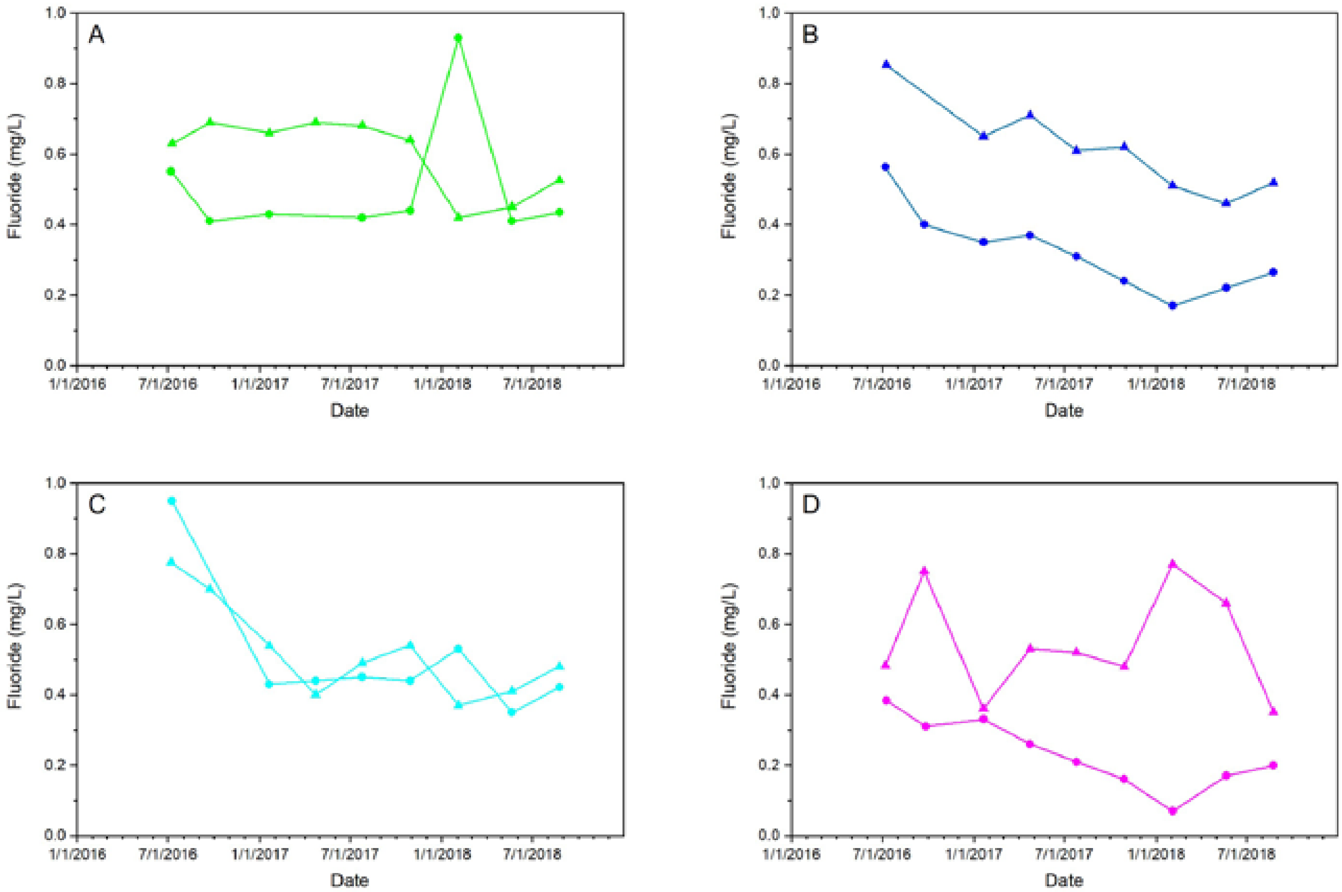

Figure B-20. Changes in fluoride concentration in relationship to time for the SPWs south of Main Street. A. SPW cluster 4, B. SPW cluster 5, C. SPW cluster 6, and D. SPW cluster 7. Green circles and lines are LW-4C, green triangles and lines are LW-4A. B. SPW cluster 5, blue circles and lines are LW-5C, blue triangles and lines are LW-5A. C. SPW cluster 6, cyan circles and lines are LW-6C, cyan triangles and lines are LW-6A. D. SPW cluster 7, magenta circles and lines are LW-7C, magenta triangles and lines are LW-7A.

1.4.2 Nitrate + Nitrite

Nitrate + Nitrite concentrations ranged from 0.01 – 10.4 mg N/L in the SPW. In the case of nitrate + nitrite there was no significant difference in concentrations north and south of Main Street. There were no significant differences in nitrate + nitrite concentrations between clusters 1 and 2 north of Main Street. There is no significant difference in the nitrate + nitrite concentrations in SPW clusters south of Main Street. The SPW samples did have one exceedance of the nitrate + nitrite MCL in LW 5A.

1.4.3 Phosphate

Soil porewater phosphate concentration ranged from 0.013 – 0.341 mg P/L in this study. There was not a significant difference in phosphate concentrations between SPW samples collected north and south of Main Street. There was no statistical difference in phosphate data between SPW clusters 1 and 2 north of Main Street. As was the case with the phosphate data north of Main Street, south of Main Street there was no significant differences in phosphate concentrations between clusters.

1.4.4 Dissolved Organic Carbon

The range of DOC in the SPW samples at this study site was 0.66 – 4.85 mg/L. The concentrations of DOC north and south of Main Street were not significantly different. North of Main Street there were no significant differences in DOC concentrations between SPW clusters 1 and 2.

1.4.5 Barium

The concentration of barium ranged from 0.25 – 210 µg/L in the SPW samples. There was a significant difference in barium concentrations north and south of Main Street ($p < 0.001$). There were no differences in concentrations between the two clusters north of Main Street ($p = 0.065$). There were no differences in barium concentrations in the four SPW clusters overall south of Main Street.

1.5 Background Groundwater Quality

Table B-3. Statistical comparisons between NWIS groundwater data and Louisville Study data from the monitoring wells and piezometers.

Parameter	Monitoring Wells		Piezometers	
	Significant Difference	p-value	Significant Difference	p-value
Alkalinity	Yes	0.020	Yes	0.009
pH	Yes	<0.001	Yes	<0.001
Specific Conductivity	Yes	<0.001	Yes	<0.001
Total Dissolved Solids	Yes	<0.001	Yes	<0.001
Bicarbonate	Yes	<0.001	Yes	<0.001
Chloride	Yes	<0.001	Yes	<0.001
Sulfate	Yes	<0.001	Yes	<0.001
Calcium	Yes	<0.001	Yes	<0.001
Magnesium	Yes	<0.001	Yes	<0.001
Sodium	Yes	<0.001	Yes	<0.001
Potassium	Yes	<0.001	Yes	<0.001
Dissolved Organic Carbon	Yes	0.015	Yes	0.007
Nitrate + Nitrite	Yes	<0.001	Yes	<0.001
Phosphate	Yes	<0.001	Yes	<0.001
Fluoride	Yes	<0.001	Yes	<0.001
Iron	Yes	<0.001	Yes	<0.001
Manganese	Yes	<0.001	Yes	<0.001

Table B-4. Study specific background ranges determined for the Louisville GI Study.

Parameter	Units	Total Number of Analyses	Number of Analyses Used	Mean	Std Dev	Median	Min	Max	Lower Critical Value	Upper Critical Value	Percent of Samples Included
Temperature	°C	220	209	18.58	0.96	18.50	16.50	20.83	16.66	20.50	95.0
Specific Conductance	µS/cm	220	200	1024	139	1040	746	1302	746	1302	90.9
Total Dissolved Solids	mg/L	220	200	666	98	676	456	854	BDL[1]	1450	90.9
Dissolved Oxygen	mg/L	220	204	2.13	1.53	1.98	0.11	5.71	BDL	5.19	92.7
pH		220	202	7.01	0.12	7.03	6.76	7.26	6.77	7.25	91.8
Eh	mV	120	111	322.5	66.9	312.9	186.2	455.2	188.8	456.3	92.5
Turbidity	mg/L	219	209	31.8	45.9	12.4	0.41	249.0	BDL	123.6	95.4
Alkalinity	mg $CaCO_3$/L	219	210	318	40	320	224	417	237	399	95.9
Dissolved Organic Carbon	mg/L	220	200	0.54	0.12	0.53	0.36	0.86	0.3	0.78	90.9
Dissolved Inorganic Carbon	mg/L	220	199	90	11	93	66	113	68	113	90.5
Dissolved Carbon Dioxide	mg CO_2/L	220	204	75	26	74	19	131	23	127	92.7
Bicarbonate	mg HCO_3/L	220	208	381	45	285	263	496	291	471	94.5
Carbonate	mg CO_3/L	220	215	0.2	0.05	0.21	0.08	0.32	0.1	0.3	97.7
Bromide	mg/L	220	197	0.07	0.04	0.06	0.005	0.18	BDL	0.15	89.5
Chloride	mg/L	220	203	71.6	23.7	73.8	25.6	122	24.2	119	92.3
Sulfate	mg/L	220	206	75.7	16.8	76.9	39.8	112.0	42.0	109	93.6
Fluoride	mg/L	220	198	0.20	0.05	0.20	0.08	0.31	0.10	0.30	90.0
Iodide	µg/L	120	115	5.61	3.50	5.40	0.75	17.5	BDL	12.6	95.8
Nitrate + Nitrite	mg N/L	220	210	4.20	1.50	4.10	1.31	7.23	1.20	7.20	95.5
Total Nitrogen	mg N/L	218	213	4.29	1.57	4.21	1.06	7.50	1.15	7.43	97.7
Phosphate	mg P/L	220	211	0.064	0.037	0.055	0.004	0.167	BDL	0.138	95.9
Total Phosphorous	mg P/L	110	102	0.058	0.016	0.056	0.028	0.093	0.026	0.09	92.7
Aluminum	µg/L	171	164	4.6	8.1	1	0.5	51.32	BDL	20.79	95.9
Arsenic	µg/L	195	170	0.94	0.2	0.9	0.52	1.41	0.54	1.34	87.2
Boron	µg/L	220	220	143.77	68.56	162	80	291	6.65	280.89	100.0
Barium	µg/L	220	206	64.16	14.98	64	25	121.13	34.2	94.12	93.6
Calcium	mg/L	220	198	113.06	14.64	115	79.69	144.3	83.78	142.34	90.0
Cobalt	µg/L	195	183	0.4	0.2	0.3	0.3	1.3	BDL	0.8	93.8
Chromium	µg/L	195	192	1.9	3.4	1	0.3	29.0	1.4	5.4	98.5
Copper	µg/L	170	163	1.5	2.5	1.0	0.3	16	BDL	6.6	95.9

[1]BDL = below detection limit

Table B-4 (continued). Study specific background ranges determined for the Louisville GI Study.

Parameter	Units	Total Number of Analyses	Number of Analyses Used	Mean	Std Dev	Median	Min	Max	Lower Critical Value	Upper Critical Value	Percent of Samples Included
Iron	µg/L	220	212	31	21	25	25	156	BDL	73	96.4
Potassium	mg/L	220	197	5.45	1.00	5.55	3.21	7.84	3.45	7.45	89.5
Lithium	µg/L	220	210	7	3	5	5	15	1	14	95.5
Magnesium	mg/L	220	206	37.2	5.64	37.9	24.9	48.6	25.9	48.5	93.6
Manganese	µg/L	195	183	17	25	6.0	0.3	124	BDL	67	93.8
Molybdenum	µg/L	194	175	0.8	0.3	0.9	0.4	1.7	0.1	1.5	90.2
Sodium	mg/L	220	208	43.9	11.3	43.7	17.0	73.6	21.2	66.6	94.5
Nickel	µg/L	195	194	1.2	1.4	0.6	0.3	6.4	BDL	4.0	99.5
Antimony	µg/L	195	168	0.3	0.1	0.3	0.3	0.6	0.1	0.5	86.2
Selenium	µg/L	195	179	2.5	1.0	2.5	0.5	4.8	0.5	4.5	91.8
Silicon	mg/L	220	202	8.80	0.88	8.92	6.79	10.6	7.04	10.6	91.8
Strontium	µg/L	220	210	218	34	220	135	299	150	286	95.5
$d^{18}O$	‰	220	191	-6.37	0.24	-6.38	-0.69	-5.80	-6.85	-5.89	86.8
$d^{2}H$	‰	220	194	-38.56	1.92	-38.67	-43.28	-33.89	-42.40	-34.72	88.2

[1]BDL = below detection limit

Table B-5. Statistics comparing parameter concentrations in monitoring well and piezometers.

Parameter	Significant Difference	p-value
Alkalinity	No	0.897
Barium	No	0.236
Calcium	No	0.758
Chloride	No	0.904
Chromium	Yes	0.014
Copper	No	0.370
Dissolved Organic Carbon	No	0.694
Fluoride	No	0.805
Bicarbonate	No	0.488
Iodide	Yes	0.020

Parameter	Significant Difference	p-value
Potassium	No	0.380
Magnesium	No	0.816
Sodium	No	0.977
Nitrate + Nitrite	No	0.869
pH	No	0.501
Phosphate	No	0.058
Sulfate	No	0.708
Specific Conductivity	No	0.989
Strontium	No	0.742

1.6 Groundwater Major Anions and Cations, pH, Specific Conductivity

1.6.1 SPC – Groundwater

The site-specific background ranges for SPC was determined to be 746 – 1302 µS/cm (Table B-3) and there is no significant difference in SPC north and south of Main Street. Figure B-21 shows SPC trends during the study. North of Main Street, SPC was found to be decreasing with time in all the wells (Figure B-21A). MW-01 ($p = 0.054$), MW-02 ($p = 0.037$), MW-03 ($p = 0.010$), MW-04 ($p = 0.054$), and MW-05 ($p = 0.025$) had decreasing trends and the trends were significant. South of Main Street (Figure B-21B), only MW-07 and MW-10 had decreasing SPC trends during the study, and the SPC trend in MW-07 ($p = 0.037$) and MW-10 ($p = 0.054$) were significant.

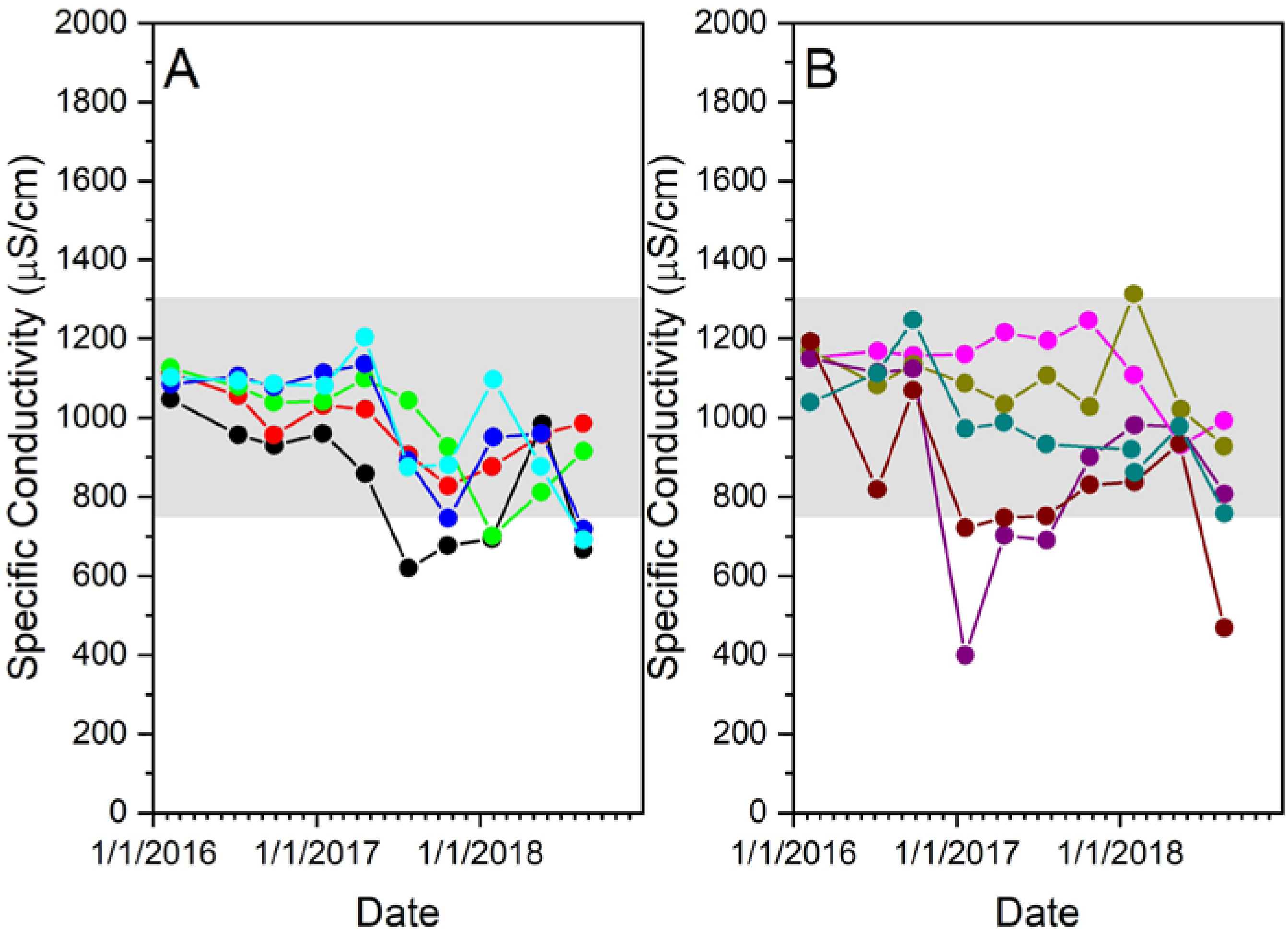

Figure B-21. Plots showing the changes in SPC with time for A. Wells north of Main Street and B. Wells south of Main Street. Black circles and lines show data for MW-01, red circles and lines show data for MW-02, green circles and lines show data for MW-03, blue circles and lines show data for MW-04, cyan circles and lines show data for MW-05, magenta circles and lines show data for MW-06, dark yellow circles and lines show data for MW-07, purple circles and lines show data for MW-08, wine-colored circles and lines show data for MW-09, and dark cyan circles and lines show data for MW-10. Gray shaded areas represent the background site-specific concentration.

1.6.2 pH – Groundwater

The site-specific background range for pH was determined to be 6.77 – 7.26 and there were no significant differences in pH north and south of Main Street. The pH was different between the summer and winter ($p < 0.001$); summer and autumn ($p = 0.011$); and spring and autumn ($p = 0.015$). North of Main Street except for MW-02 (Figure B-22A), there was increasing pH trend with time. These were significant trends in MW-01 ($p = 0.034$), MW-03 ($p = 0.004$), MW-04 ($p = 0.008$), and MW-05 ($p = 0.016$). South of Main Street, Figure B-22B, there were no statistical trends in pH except for MW-09. The pH trend in MW-09 had an increasing trend and was significant ($p = 0.089$). There were no sMCL exceedances in pH during the study.

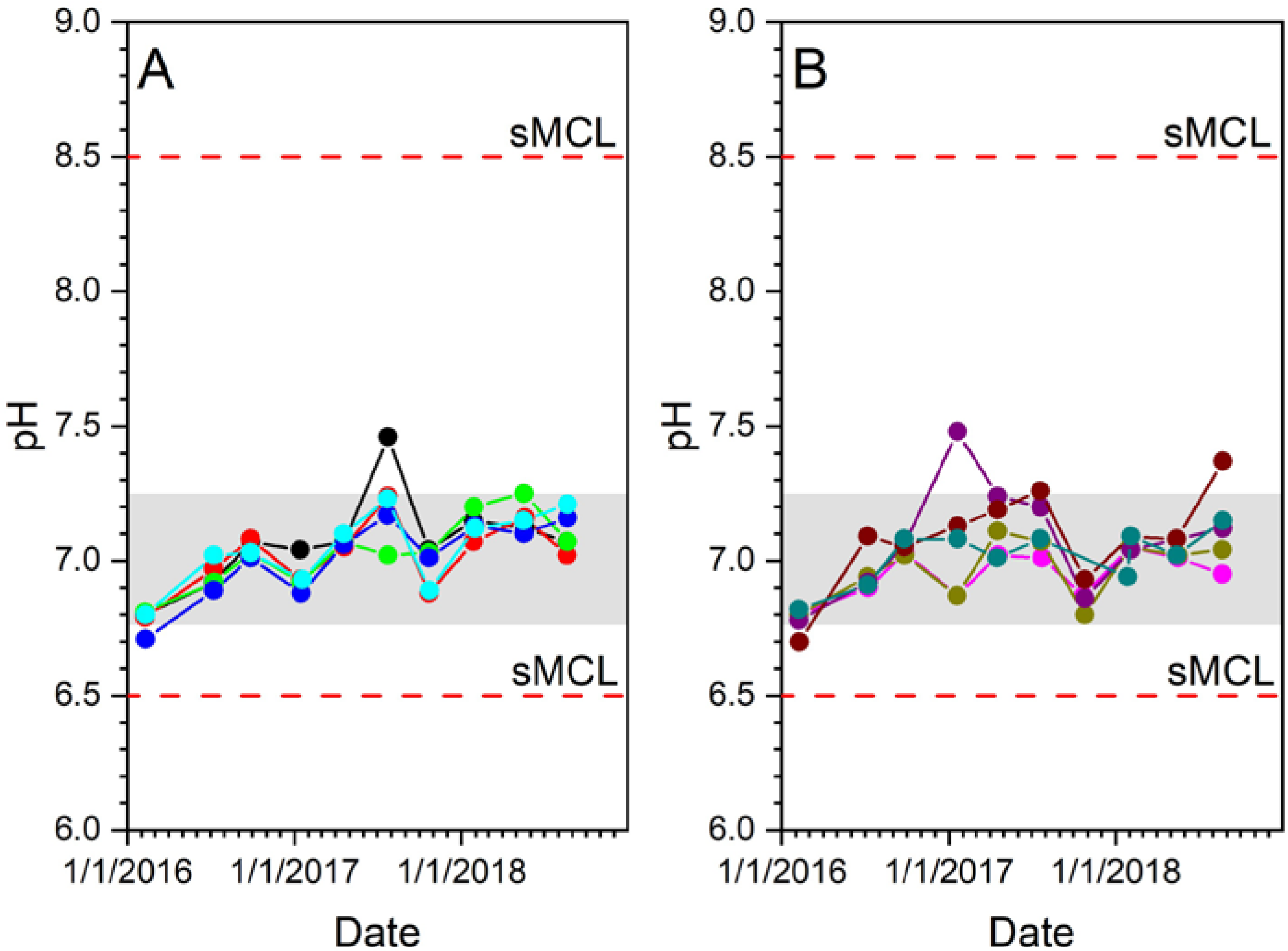

Figure B-22. Plots showing the changes in pH with time for A. Wells north of Main Street and B. Wells south of Main Street. Black circles and lines show data for MW-01, red circles and lines show data for MW-02, green circles and lines show data for MW-03, blue circles and lines show data for MW-04, cyan circles and lines show data for MW-05, magenta circles and lines show data for MW-06, dark yellow circles and lines show data for MW-07, purple circles and lines show data for MW-08, wine-colored circles and lines show data for MW-09, and dark cyan circles and lines show data for MW-10. Gray shaded areas represent the site-specific background. Red dashed lines show the sMCL for pH (6.5 and 8.5).

1.6.3 Chloride – Groundwater

The site-specific chloride background range was determined to be 24.2 – 119 mg/L. Chloride concentrations north and south of Main Street were significantly different (p = 0.030). The chloride concentrations south of Main Street were larger than north of Main Street. Figure B-23 shows the changes in chloride concentrations with time. There was no trend in chloride concentrations north of Main Street in wells MW-02 and MW-05 (Figure B-23A). In wells MW-01, MW-03, and MW-04 there were significant decreasing trends in chloride concentrations (p = 0.010, p = 0.016, and p = 0.010, respectively). South of Main Street, two wells (Figure B-23B) showed decreasing trends in chloride concentration. These trends were significant. These wells were MW-07 (p = 0.054) and MW-10 (p = 0.076). MW-06, MW-08, and MW-09 did not show any trends in chloride concentration during the study. There were no exceedances of this sMCL.

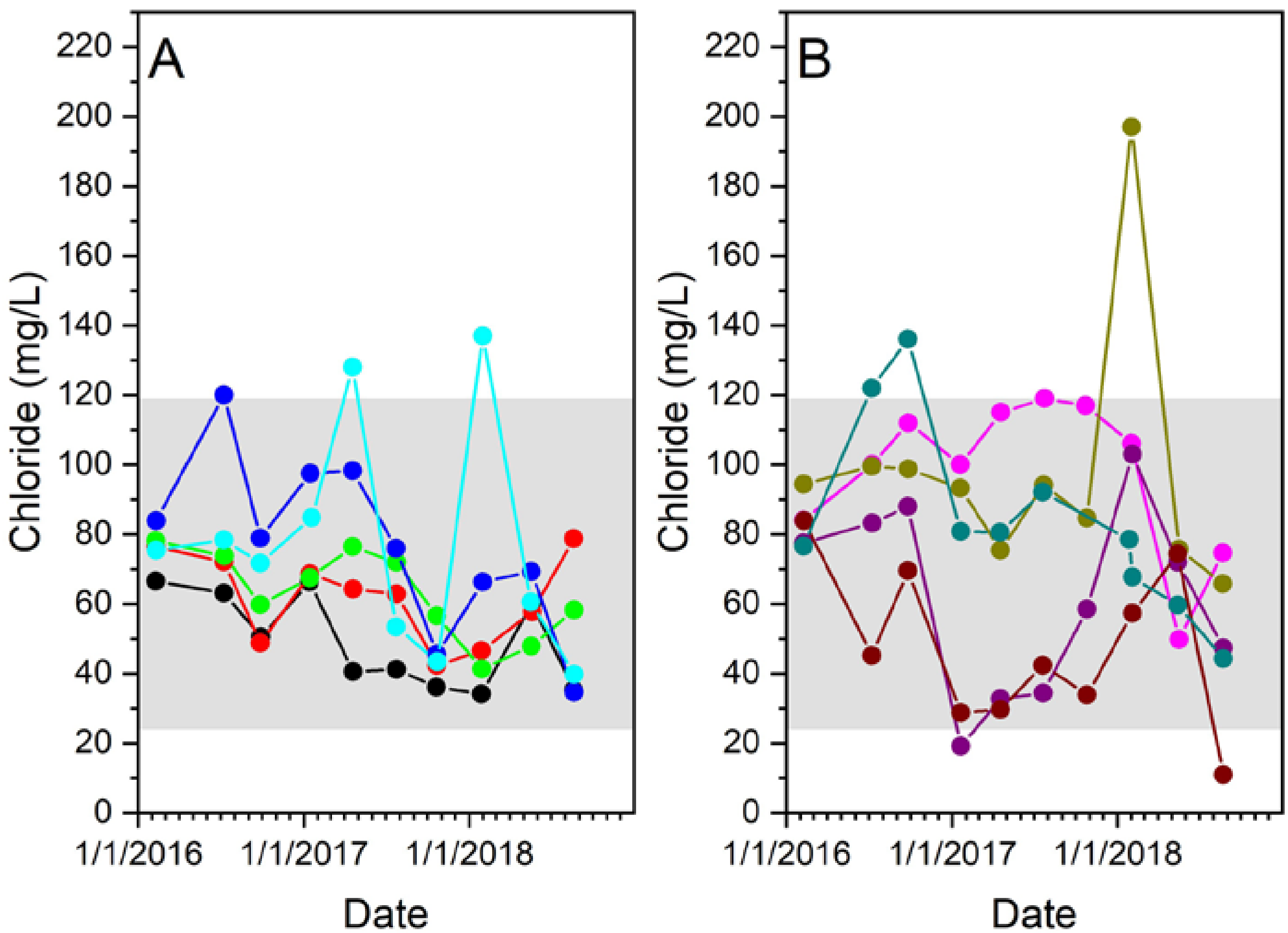

Figure B-23. Plots showing the changes in chloride concentration with time for A. Wells north of Main Street and B. Wells south of Main Street. Black circles and lines show data for MW-01, red circles and lines show data for MW-02, green circles and lines show data for MW-03, blue circles and lines show data for MW-04, cyan circles and lines show data for MW-05, magenta circles and lines show data for MW-06, dark yellow circles and lines show data for MW-07, purple circles and lines show data for MW-08, wine-colored circles and lines show data for MW-09, and dark cyan circles and lines show data for MW-10. Gray shaded areas represent the site-specific background.

1.6.4 Bicarbonate – Groundwater

The site-specific background concentrations for bicarbonate were found to range from 263 – 496 mg HCO_3/L. Figure B-24A shows the changes in bicarbonate concentration with time north of Main Street. North of Main Street, three wells showed significant decreasing trends in bicarbonate concentrations MW-02 ($p = 0.005$), MW-03 ($p = 0.016$), and MW-05 ($p = 0.001$). South of Main Street (Figure B-24B), only two wells showed decreasing trends in bicarbonate concentrations MW06 ($p = 0.006$) and MW-07 ($p = 0.037$). All other wells both north and south of Main Street showed no trend in bicarbonate concentrations.

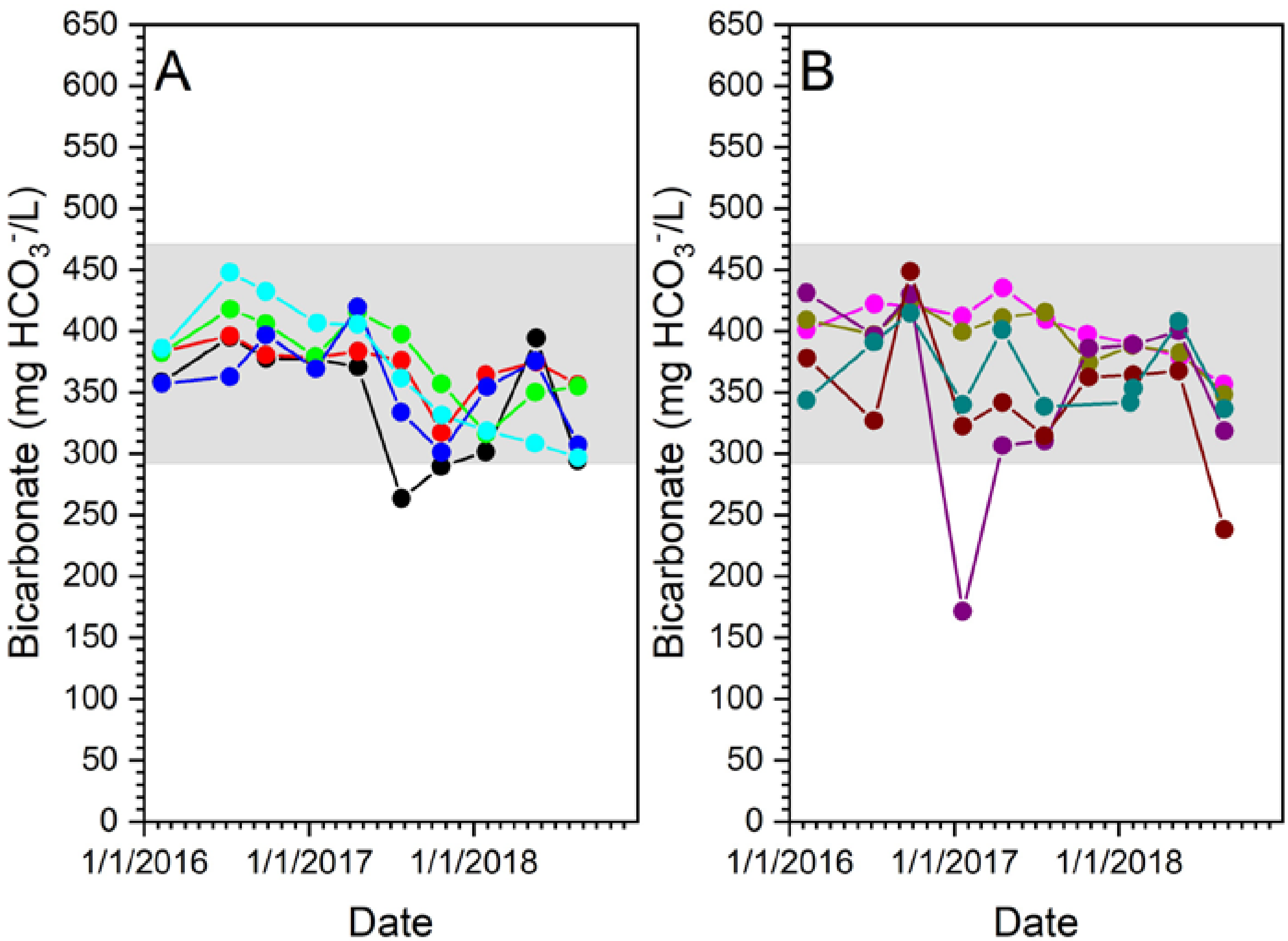

Figure B-24. Plots showing the changes in bicarbonate concentration with time for A. Wells north of Main Street and B. Wells south of Main Street. Black circles and lines show data for MW-01, red circles and lines show data for MW-02, green circles and lines show data for MW-03, blue circles and lines show data for MW-04, cyan circles and lines show data for MW-05, magenta circles and lines show data for MW-06, dark yellow circles and lines show data for MW-07, purple circles and lines show data for MW-08, wine-colored circles and lines show data for MW-09, and dark cyan circles and lines show data for MW-10. Gray shaded areas represent the site-specific background.

1.6.5 Sulfate – Groundwater

The site-specific background was determined to range from 42.0 – 109 mg/L. The sulfate concentrations north and south of Main Street were found to be significantly different ($p = 0.045$) and there was also a significant difference in sulfate concentration between the winter and summer ($p = 0.017$). The changes in sulfate concentrations with time are plotted in Figure B-25. Figure B-25A shows the changes in sulfate concentration north of Main Street. All wells north of Main Street had decreasing sulfate concentrations with time. MW-01, MW-02, MW-03, MW-04, and MW-05 decreasing trends were significant (p-values ranging from 0.004 – 0.076). Four of the five wells south of Main Street showed decreasing sulfate concentrations (Figure B-25B). MW-06 ($p = 0.024$), MW-07 ($p = 0.006$), MW-09 ($p = 0.025$), and MW-10 ($p = 0.037$) all had significantly decreasing trends in sulfate concentration. MW-08 showed no trend in sulfate concentrations over the duration of the study being reported. Sulfate, like chloride, has a sMCL of 250 mg/L. No samples during the study had sulfate concentrations exceeding the sMCL of sulfate.

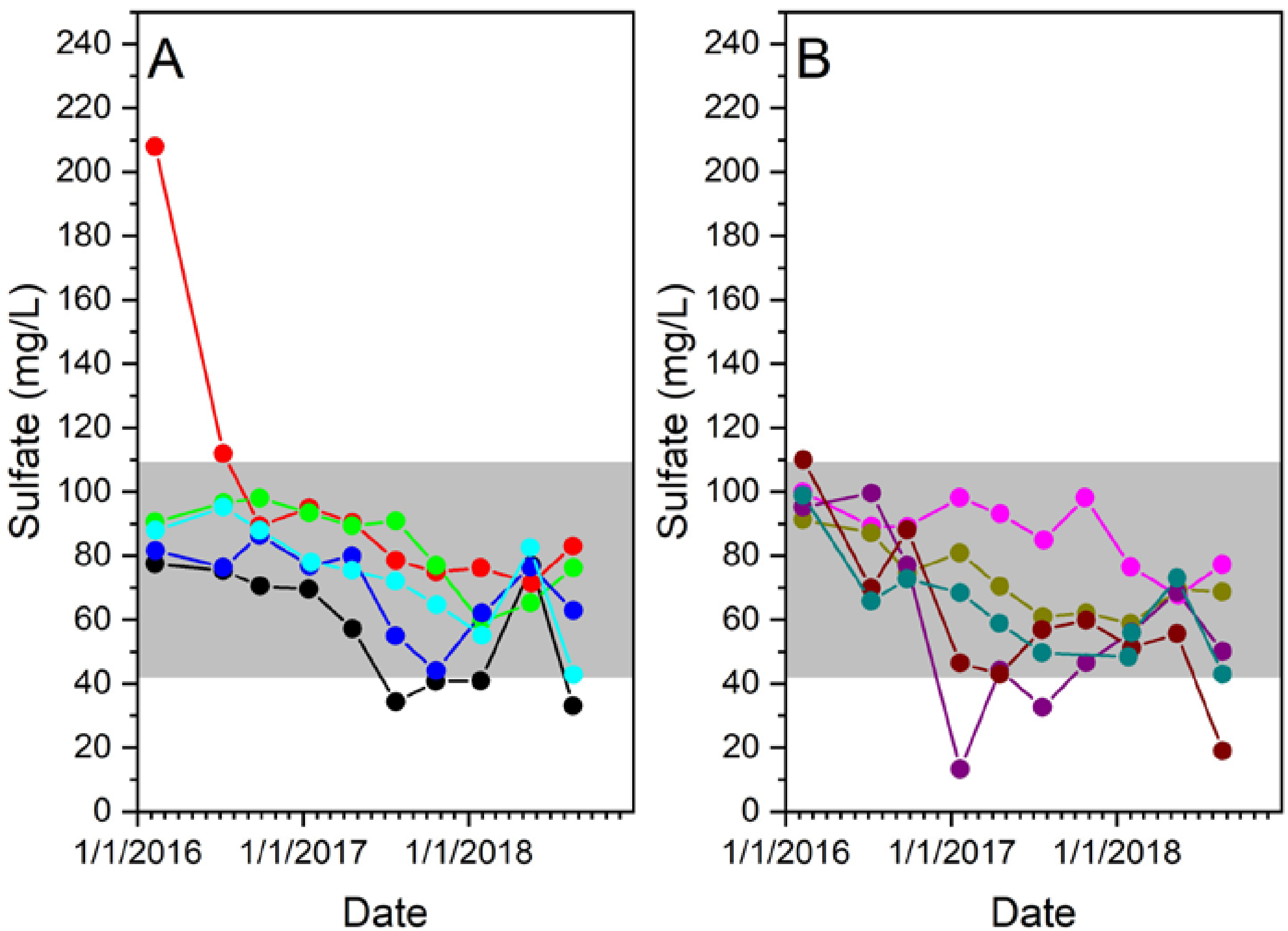

Figure B-25. Plots showing the changes in sulfate concentrations with time for A. Wells north of Main Street and B. Wells south of Main Street. Black circles and lines show data for MW-01, red circles and lines show data for MW-02, green circles and lines show data for MW-03, blue circles and lines show data for MW-04, cyan circles and lines show data for MW-05, magenta circles and lines show data for MW-06, dark yellow circles and lines show data for MW-07, purple circles and lines show data for MW-08, wine-colored circles and lines show data for MW-09, and dark cyan circles and lines show data for MW-10. Gray shaded areas represent the site-specific background.

1.6.6 Calcium – Groundwater

The site-specific calcium background ranged from 83.8 – 142 mg/L. The concentrations of calcium were not different north and south of Main Street. Concentrations of calcium were different between the summer and winter (p = 0.002) and between summer and autumn (p = 0.019). Changes in calcium concentrations in wells north of Main Street are plotted in Figure B-26A. Only one well MW-02 showed no trend in calcium concentrations. In all other wells north of Main Street, there were significantly decreasing calcium concentrations with time (p-values ranged from 0.016 – 0.44). Wells south of Main Street (MW-06 – 10) did not show a trend in calcium concentrations during the study (Figure B-26B).

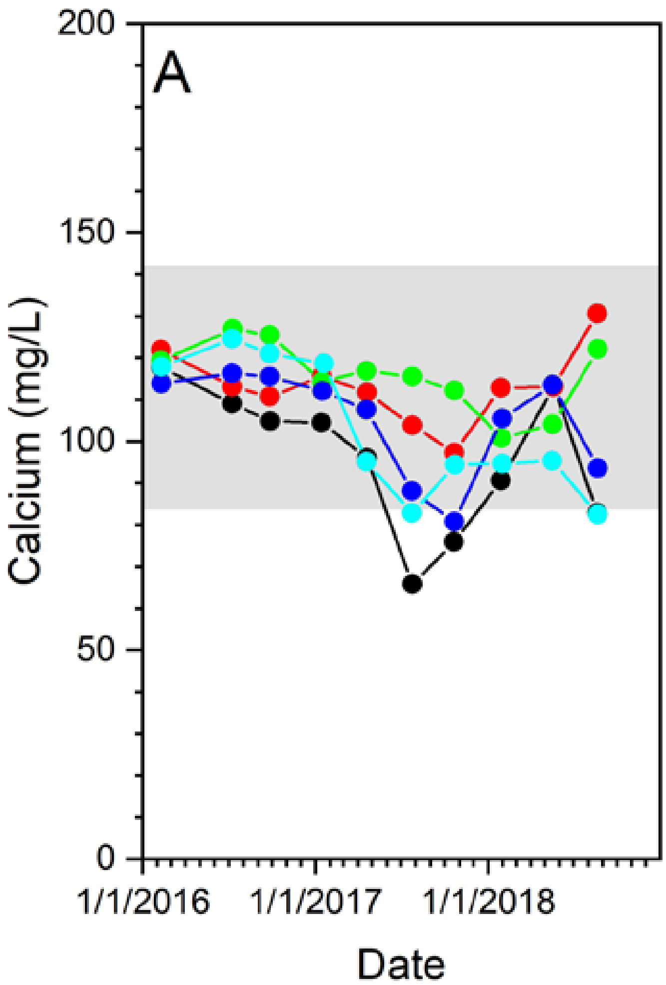

Figure B-26. Plots showing the changes in calcium concentrations with time for A. Wells north of Main Street and B. Wells south of Main Street. Black circles and lines show data for MW-01, red circles and lines show data for MW-02, green circles and lines show data for MW-03, blue circles and lines show data for MW-04, cyan circles and lines show data for MW-05, magenta circles and lines show data for MW-06, dark yellow circles and lines show data for MW-07, purple circles and lines show data for MW-08, wine-colored circles and lines show data for MW-09, and dark cyan circles and lines show data for MW-10. Gray shaded areas represent the site-specific background.

1.6.7 Magnesium – Groundwater

The site-specific magnesium background was established to range from 25.9 – 48.5 mg/L. There was no difference in magnesium concentrations north and south of Main Street. The magnesium concentration changes over time for wells north of Main Street are plotted in Figure B-27A. All the wells north of Main Street show decreasing concentrations of magnesium with time, and the trends are all significant (p = 0.002 – 0.025). South of Main Street, only three wells showed decreasing magnesium concentration (Figure B-27B). The three wells were MW-07, MW-09, and were significant trends (p = 0.037, p = 0.019 and p = 0.078, respectively).

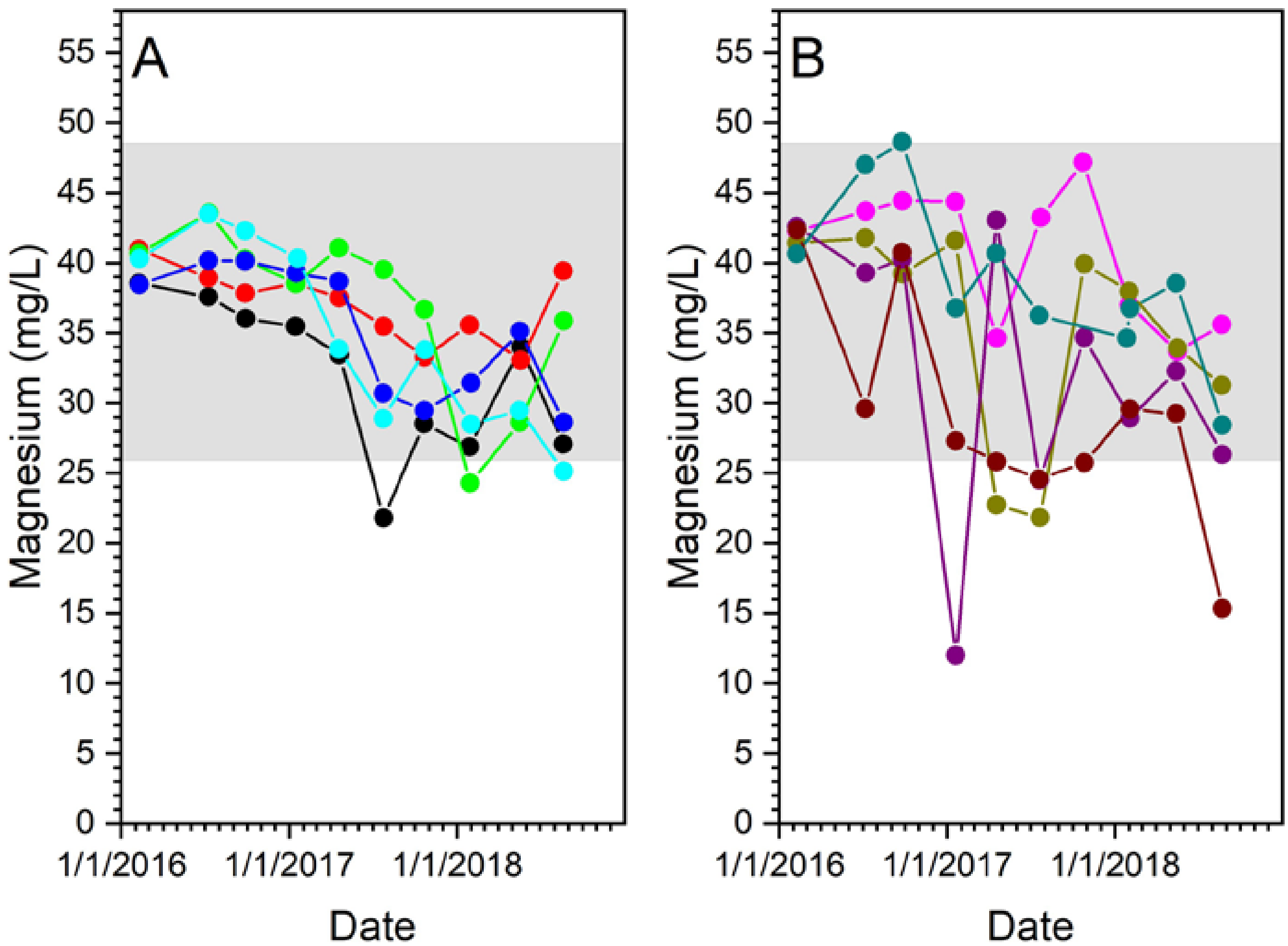

Figure B-27. Plots showing the changes in magnesium concentrations with time for A. Wells north of Main Street and B. Wells south of Main Street. Black circles and lines show data for MW-01, red circles and lines show data for MW-02, green circles and lines show data for MW-03, blue circles and lines show data for MW-04, cyan circles and lines show data for MW-05, magenta circles and lines show data for MW-06, dark yellow circles and lines show data for MW-07, purple circles and lines show data for MW-08, wine-colored circles and lines show data for MW-09, and dark cyan circles and lines show data for MW-10. Gray shaded areas represent the site-specific background.

1.6.8 Sodium – Groundwater

Based on the analysis, the site-specific background ranged from 21.2 – 66.6 mg/L. North and south of Main Street did not show any differences in sodium concentration. The sodium concentrations over time for this study are plotted in Figure B-28. South of Main Street (Figure B-28B), only MW-10 showed a decreasing trend in sodium concentrations and was significant (p = 0.054). Two wells north of Main Street showed sodium concentration trends (Figure B-28A). In MW-02 and MW-04 the decreasing sodium concentrations were significant (p = 0.054). All other wells in the study did not show sodium concentration trends (Figure B-28).

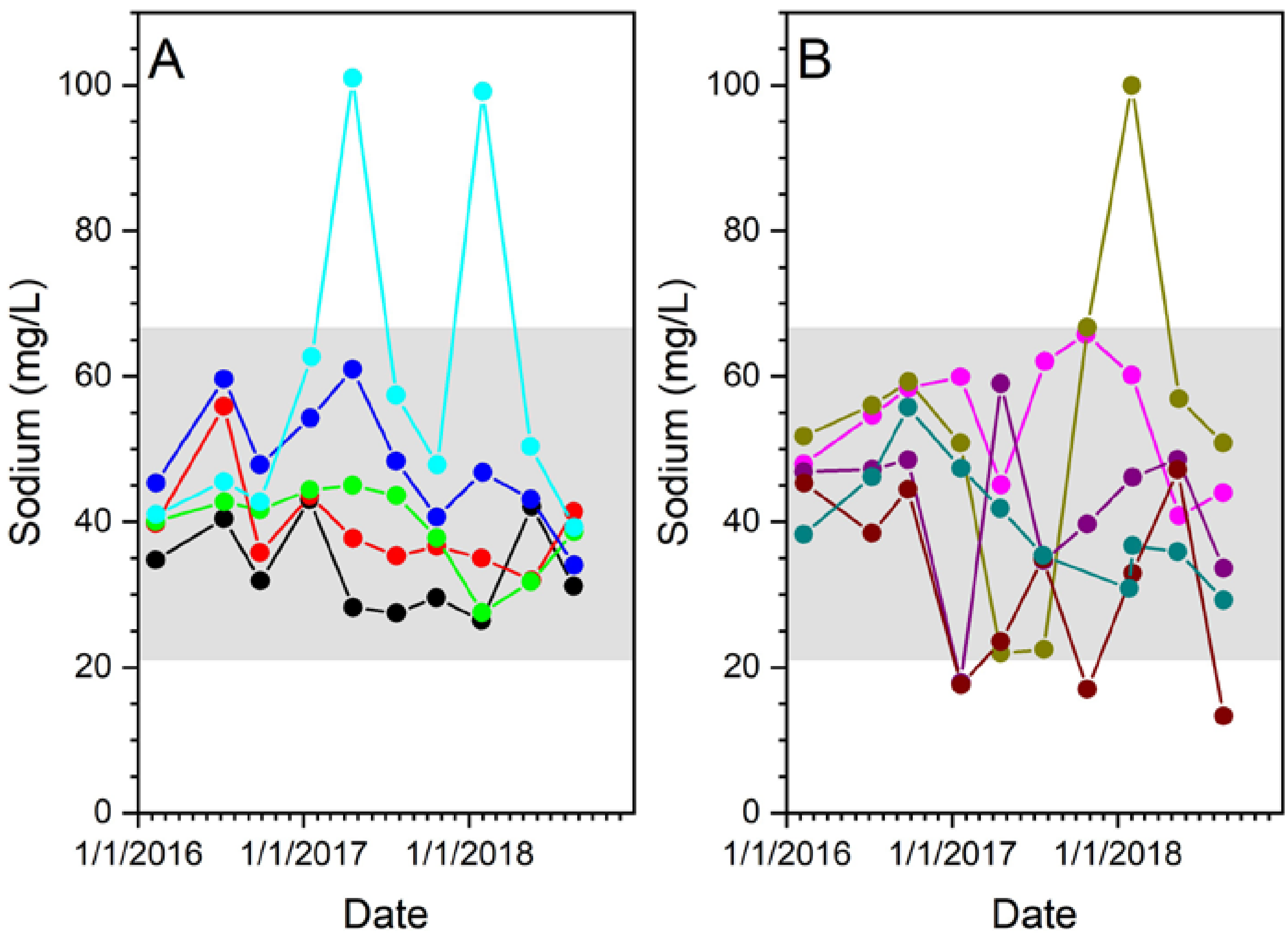

Figure B-28. Plots showing the changes in sodium concentrations with time for A. Wells north of Main Street and B. Wells south of Main Street. Black circles and lines show data for MW-01, red circles and lines show data for MW-02, green circles and lines show data for MW-03, blue circles and lines show data for MW-04, cyan circles and lines show data for MW-05, magenta circles and lines show data for MW-06, dark yellow circles and lines show data for MW-07, purple circles and lines show data for MW-08, wine-colored circles and lines show data for MW-09, and dark cyan circles and lines show data for MW-10. Gray shaded areas represent the site-specific background.

1.6.9 Potassium – Groundwater

The site-specific potassium background was determined to range from 3.45 – 7.45 mg/L. For potassium, there was a significant difference in concentrations between wells north of Main Street and wells south of Main Street ($p = 0.015$). Samples north of Main Street generally had larger concentrations of potassium than south of Main Street. The changes in potassium concentrations for wells north of Main Street are shown in Figure B-29A. In wells MW-01 and MW-05, the potassium concentrations are decreasing with time, and the decreases were significant ($p = 0.006$ and $p = 0.010$, respectively). In well MW-03, the potassium concentrations were significantly increasing with time ($p = 0.037$). All other wells north of Main Street did not show a trend in potassium concentrations with time. South of Main Street (Figure B-29B), MW-08 and MW-09 had decreasing potassium concentrations with time. In MW-08 and MW-09 the trend was significant ($p = 0.089$ and $p = 0.025$, respectively). The other three wells, MW-06, MW-07, and MW-10 did not have a potassium concentration trend.

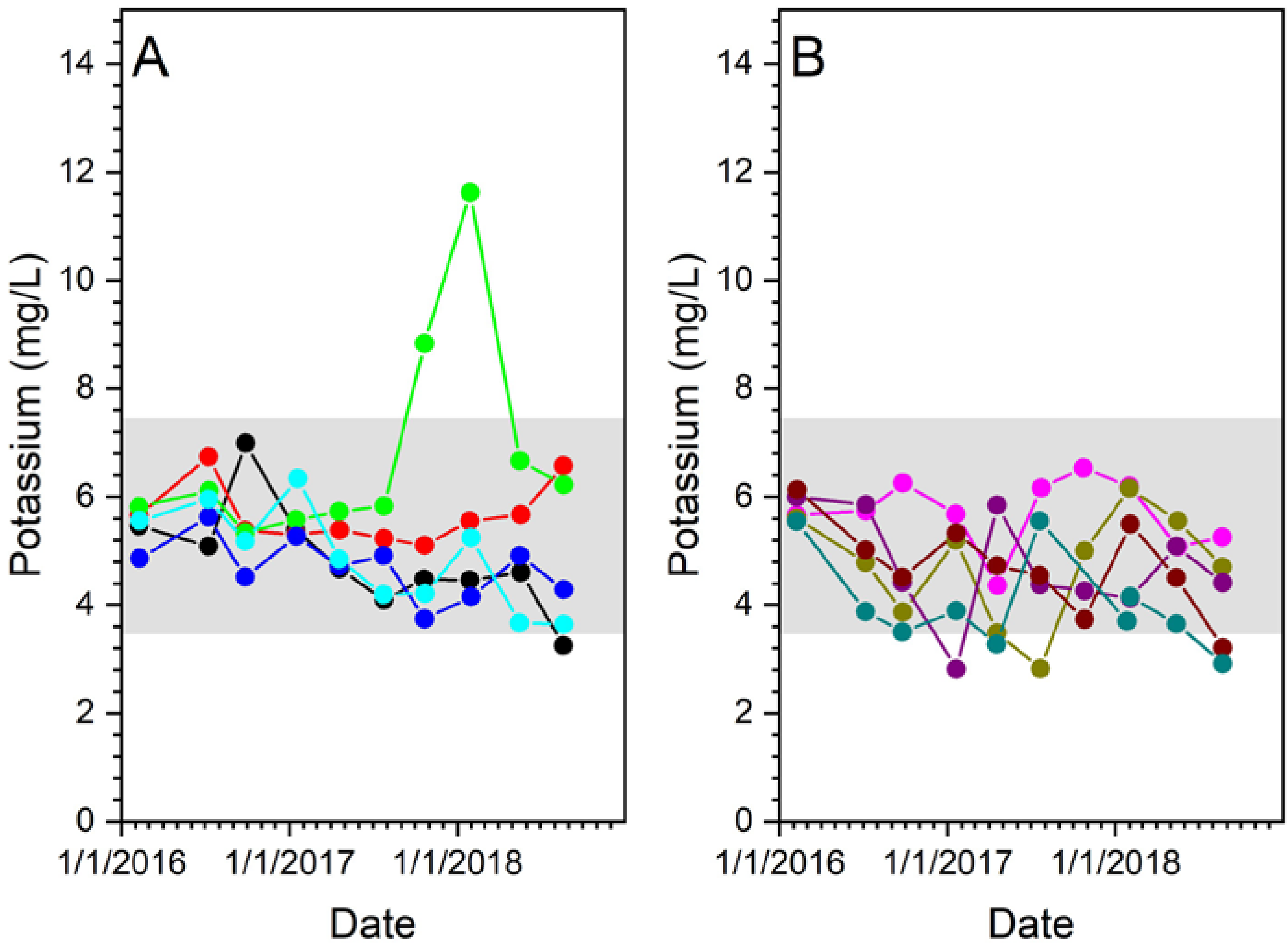

Figure B-29. Plots showing the changes in potassium concentrations with time for A. Wells north of Main Street and B. Wells south of Main Street. Black circles and lines show data for MW-01, red circles and lines show data for MW-02, green circles and lines show data for MW-03, blue circles and lines show data for MW-04, cyan circles and lines show data for MW-05, magenta circles and lines show data for MW-06, dark yellow circles and lines show data for MW-07, purple circles and lines show data for MW-08, wine-colored circles and lines show data for MW-09, and dark cyan circles and lines show data for MW-10. Gray shaded areas represent the site-specific background.

1.7 Other Chemical Constituents

1.7.1 Dissolved Organic Carbon

There was no significant difference in DOC concentrations north and south of Main Street. The site-specific background concentrations range for DOC was estimated to be 0.30 – 0.78 mg/L. In July 2016, MW-04 had DOC concentration outside the background concentrations; in January 2018 MW-03 had DOC concentrations outside background concentrations; and in August 2018, MW-01 had concentrations outside background concentrations.

1.7.2 Fluoride

There were significant differences in fluoride concentrations north and south of Main Street ($p < 0.001$). The fluoride concentrations south of Main Street were greater than those north of Main Street. The range for site-specific background fluoride concentrations was from 0.10 – 0.30 mg/L. During two samplings, October 2017 and January 2018, the concentrations of fluoride in MW-03 were less than the site-specific background. MW-08 fluoride concentrations were outside (larger than) the site-specific background in January and April 2017 for MW-08; April 2017 and July 2017 for MW-09; and October 2017 for MW-10.

1.7.3 Iodide

There were no significant differences in iodide concentrations depending on whether the samples were north or south of Main Street. The site-specific background iodide concentrations ranged for <MDL – 12.6 µg/L. Wells MW-03, MW-04, and MW-05 did have iodide concentrations that were larger than the site-specific background range. These occurred in July 2016 (MW-04), January 2017 (MW-03), July 2017 (MW-05), and had a large spike in February 2018 (MW-03). The large spike in iodide concentration in February 2018 did not have a corresponding spike in chloride concentration. Only two times south of Main Street did the iodide concentration fall outside the site-specific background range during the study. These were in January 2007 (MW-09) and July 2017 (MW-07).

1.7.4 Nitrate + Nitrite

There were significant differences in nitrate + nitrite concentrations ($p = 0.004$). North of Main Street had a larger concentration than south of Main Street. These differences were between summer and winter ($p < 0.001$) and between summer and autumn ($p = 0.007$). Site-specific background nitrate + nitrite was determined to range from 1.20 – 7.20 mg N/L. Only one sample was slightly outside (larger than) the site-specific background north of Main Street. This was MW-05 in February 2016. No samples north of Main Street exceeded the MCL for Nitrate (10 mg N/L). Five samples south of Main Street were outside the site-specific background concentration range for nitrate + nitrite. Two samples (MW-09 and MW-10) were greater than range in February 2016. Three samples were lower than the range: MW-08 (January 2017), MW-08 (July 2017), and MW-09 (August 2018). As was the case with sample north of Main Street, there were no nitrate MCL exceedances south of Main Street.

1.7.5 Phosphate

During this study, the site-specific phosphate concentrations ranged from 0.004 – 0.167 mg P/L. There was a significant difference ($p = 0.002$) between groundwater phosphate concentrations north and south of Main Street, with phosphate concentrations being larger north of Main Street. Several of the samples north of Main Street were outside (greater) than site-specific background concentrations in wells MW-01 and MW-03. In January 2017, January 2018, May 2018, and August 2018 the concentrations were outside the background in MW-01. For MW-03, January 2018, May 2018, and August 2018 were larger than the site-specific background range. Only two samples in the wells south of Main Street had phosphate concentrations greater than the site-specific background. These samples were MW-09 in May 2018 and MW-06 in August 2018.

1.7.6 Barium

The site-specific background concentrations of barium range from 34 – 94 µg/L. There were no significant differences in barium concentration north and south of Main Street. North of Main Street, MW-03 did have four sampling points that were outside the site-specific background range. These occurred in October 2017, February 2018, May 2018, and August 2018. For three of these dates (October 2017, May 2018, and August 2018), the concentration of barium was larger than the site-specific background range for barium. In February 2018, the barium concentration was lower. South of Main Street, MW-07 had two dates when the barium concentrations were outside the site-specific background barium concentrations January 2017 (lower) and February 2018 (higher). Likewise, MW-08 (July 2017) and MW-09 (August 2018) had barium concentrations outside the site-specific background for barium and in both cases the barium concentrations were lower.

1.7.7 Chromium

There was no difference in concentration between north and south of Main Street. Based on the data collected, the site-specific background concentrations for chromium were determined to range from 1.4 – 5.4 µg/L. North of Main Street, there were two samples that were outside the site-specific background range for chromium. These both happened in May 2018 in wells MW-04 and MW-05. The MCL for chromium was exceeded in the May 2018 MW-04 sample. The wells MW-04 and MW-05 are the closest wells to the infiltration gallery. During the study, the site-specific background range for chromium was exceeded four times, two times in May 2018 and August 2018. In May 2018, the site-specific background was exceeded in wells MW-06 and MW-08. In August 2018 the exceedances happened in wells MW-06 and MW-07. South of Main Street, the chromium concentration did not exceed the chromium MCL.

1.7.8 Nickel

The site-specific background nickel concentration range was determined to be <MDL – 4.0 µg/L. There were no differences in nickel concentrations north and south of Main Street. There were no nickel concentrations in any of the wells that were outside the site-specific background concentrations for nickel.

1.8 An example of a process that could potentially mitigate the current rates in phosphate trends

Figure B-30 shows the results of geochemical modeling of the Ca-F-HPO_4^{2-} system. The concentrations of Ca, F, and PO_4 were initially set at the mean concentrations of these parameters in the August 2018 sampling event. The PO_4 concentrations were allowed to increase at the rate reported in Table 6-8. During the model run, calcium and fluoride concentrations were fixed at the mean August 2018 concentrations. It should be noted that phosphate sorption is a potential mechanism of importance, but the parameters need to model this phenomenon are not available, so this model only reflects the precipitation dissolution controls on phosphate. However, this model will be adequate to show potentially how geochemical processes can alter the rates of change previously determined.

In Figure B-30A, in initial solution concentrations (i.e., when cumulative HPO42- is zero) are the mean concentrations for calcium, fluoride, and phosphate in the August 2018 sampling. The model indicates that as phosphate is added to the system, the solution concentrations of calcium and fluoride should decrease. The decrease in fluoride concentrations is more rapid that that of calcium. Initially, the model predicts that the amount of fluorapatite increases rapidly, and then the precipitation of levels off. As the fluorapatite amount levels off, there is a change in the rate of phosphate increase in solution, and the decrease in fluoride concentrations level off. Also, at the point where the increase in fluorapatite levels off, the appearance of hydroxyapatite is indicated. The formation of hydroxyapatite is responsible for the increase in phosphate concentration and the leveling off of the rate of decrease in fluoride concentrations. As the formation of hydroxyapatite happens again, there is a change in rate of increase in phosphate concentrations. Figure B-30B is a plot of calcium, fluoride and phosphate concentrations in the solid phase. In the solid phase, the fluoride concentrations increase with increasing fluorapatite formation. When fluorapatite concentrations level off, so do the fluoride concentrations in the solid. This suggests that equilibrium between the solution and solid phase occurred. The concentrations of calcium and phosphate increase in the solid phase throughout the model run. There is a change in the rate of increase in the concentrations of calcium and phosphate that corresponds to the shift from the formation of fluorapatite to the formation of hydroxyapatite. This discussion demonstrates that the rates of change in potential constituents of concern can change in time. Extrapolations of data are important tools for inference, but caution should be exercised when predicting long term trends in chemical behavior in complex systems.

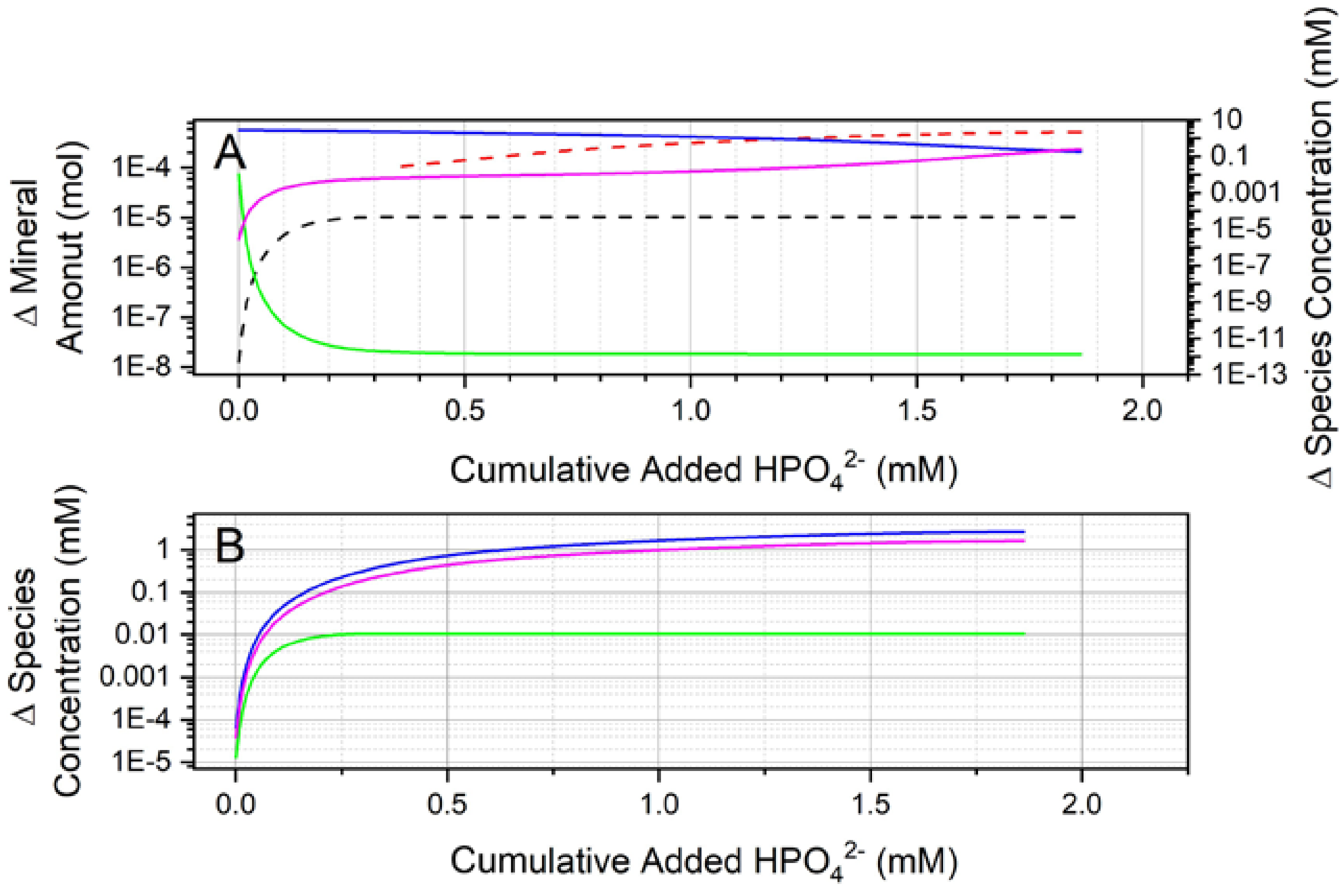

Figure B-30. Geochemical modeling showing potentially how the groundwater could respond to increasing phosphate concentrations. A. Bulk solution species changes and solid phase formation. B. Solid phase species concentrations. Black dashed lines represent fluorapatite, red dashed lines represent hydroxyapatite, green solid lines represent fluoride concentrations, blue solid lines represent calcium concentrations, and magenta solid lines represent phosphate concentrations.

Appendix C. Yakima Supporting Information

Table of Contents

Subsurface Monitoring Network

Table C-1. Monitoring well coordinates, surface elevation total depth (as elevation), and top of screen elevations at the Yakima study site.

Well ID	Longitude	Latitude	Surface Elevation	Total Depth (as Elevation)	Top of Screen Elevation
	°	°	m-msl	m-msl	m-msl
MW 2	-120.465910	46.581311	303.89	298.40	299.31
MW 3	-120.465209	46.580125	338.63	332.46	333.38
MW 4	-120.471444	46.575989	304.80	297.64	298.56
MW 5	-120.469670	46.574860	302.06	295.88	296.79
MW 6	-120.466264	46.573732	301.14	294.84	295.75
BCF 836	-120.468339	46.576253	302.36	295.32	296.23
BCF 837	-120.468709	46.573624	300.84	293.78	294.69
BCF 838	-120.468579	46.572208	299.92	292.94	293.85
BCF 839	-120.467753	46.570903	299.92	292.88	293.80

Table C-2. Outfall sampling locations.

Sampling Location	Longitude	Latitude
	°	°
Outfall 01	-120.468115	46.576302
Outfall 02	-120.467315	46.575258
Outfall 03	-120.466091	46.573800
Outfall 04	-120.466242	46.572246
Outfall 05	-120.466417	46.570999

Background Groundwater Quality

The results of statistical analysis comparing NWIS groundwater quality data to study groundwater data is given in Table C-3.

Table C-3. Statistical comparisons between NWIS groundwater data and Yakima Study data from the groundwater monitoring wells.

Analyte	Significant Difference	Probability
pH	Yes	< 0.001
Specific Conductivity	No	1.000
Total Dissolved solids	No	0.951
Dissolved Carbon Dioxide	Yes	< 0.001
Bicarbonate	Yes	< 0.001
Nitrate + Nitrite	No	0.115
Chloride	Yes	< 0.001
Fluoride	Yes	< 0.001
Sulfate	No	0.654
Barium	No	0.660
Calcium	Yes	0.041
Copper	Yes	0.007
Iron	No	0.151
Potassium	No	0.978
Magnesium	Yes	0.011
Manganese	Yes	< 0.001
Sodium	No	0.355
Silicon	Yes	0.026

Table C-4. Study specific background ranges determined using the 2-sigma method for the Yakima Study.

Parameter	Units	N	n	Mean	Std Dev	Median	Min	Max	Lower Critical Value	Upper Critical Value	Percent Used
Temperature	°C	251	239	15.09	3.47	15.12	8.00	23.26	8.15	22.03	95.2
Specific Conductance	µS/cm	252	244	333	122	345	76	628	88	577	96.8
Total Dissolved Solids	mg/L	252	244	216	80	224	50	408	57	375	96.8
Dissolved Oxygen	mg/L	241	210	1.18	1.39	0.61	0.00	4.96	BDL[1]	3.96	87.1
pH	-----	252	224	6.47	0.28	6.48	5.83	7.09	5.91	7.03	88.9
Alkalinity	mg $CaCO_3$/L	253	226	91	21	95	44	143	48	134	89.3
Dissolved Organic Carbon	mg/L	252	234	1.02	0.61	0.86	0.33	3.18	BDL	2.24	92.9
Dissolved Inorganic Carbon	mg/L	251	227	26.54	8.88	28.6	7.44	47.6	8.78	44.3	90.4
Dissolved Carbon Dioxide	mg CO_2/L	221	200	57.9	23.9	60.7	7.86	114	10.1	106	90.5
Bicarbonate	mg HCO_3^-/L	250	228	85.9	31.1	88.5	23.6	148	23.6	148	91.2
Carbonate	mg CO_3^{2-}/L	221	214	0.019	0.020	0.012	0.000	0.106	BDL	0.059	96.8
Nitrate + Nitrite	mg N/L	247	226	2.09	2.16	2.09	0.005	7.78	BDL	6.41	91.5
Ammonia	mg N/L	254	248	0.053	0.129	0.006	0.001	0.76	BDL	0.311	97.6
Bromide	mg/L	254	238	0.07	0.05	0.05	0.02	0.29	BDL	0.17	93.7
Chloride	mg/L	254	236	25.6	13.8	27.0	1.61	55.7	BDL	53.2	92.9
Sulfate	mg/L	254	232	16.2	7.62	16.4	2.23	36.9	0.98	31.5	91.3
Fluoride	mg/L	224	206	0.09	0.05	0.09	0.01	0.22	BDL	0.19	92.0
Iodide	µg/L	245	224	4.98	2.92	4.83	0.75	13.1	BDL	10.82	91.4
Phosphate	mg P/L	28	25	0.589	0.690	0.250	0.113	2.490	BDL	1.969	89.3
Aluminum	µg/L	63	62	2.0	3.2	0.5	0.5	18.3	BDL	8.4	98.4
Arsenic	µg/L	63	60	1.0	1.0	0.8	0.3	6.0	BDL	3.0	95.2
Boron	µg/L	224	207	83	17	80	80	191	49	118	92.4
Barium	µg/L	254	239	17	6.9	17	5.0	33	3.2	31	94.1
Calcium	mg/L	254	238	29.2	9.49	31.0	9.16	51.1	10.3	48.2	93.7
Cobalt	µg/L	63	58	0.9	0.8	0.7	0.3	3.2	BDL	2.2	92.1
Chromium	µg/L	63	59	0.3	0.1	0.3	0.3	0.6	0.1	0.5	93.7
Copper	µg/L	63	60	1.1	0.7	0.9	0.3	3.1	BDL	2.4	95.2
Iron	µg/L	254	216	98	232	25	1	1370	BDL	563	85.0

[1]BDL = below detection limit

Table C-4 (continued). Study specific background ranges determined using the 2-sigma method for the Yakima Study.

Parameter	Units	N	n	Mean	Std Dev	Median	Min	Max	Lower Critical Value	Upper Critical Value	Percent Used
Potassium	mg/L	254	242	3.81	1.55	4.13	0.73	8.74	0.71	6.91	95.3
Magnesium	µg/L	254	238	10.9	3.79	11.3	3.29	19.5	3.36	18.5	93.7
Manganese	µg/L	63	59	352	368	325	0.3	1237	BDL	1089	93.7
Molybdenum	µg/L	63	57	0.6	0.3	0.4	0.4	1.5	BDL	1.3	90.5
Sodium	mg/L	254	228	14.7	5.38	14.8	3.97	28.8	3.94	25.5	89.8
Nickel	µg/L	63	57	2.0	1.6	1.5	0.3	5.7	BDL	5.2	90.5
Silicon	mg/L	254	242	17.2	3.20	18.1	10.5	22.5	10.8	23.6	95.3
Strontium	µg/L	254	236	135	39	137	49	224	56	213	92.9
Vanadium	µg/L	63	60	1.8	1.0	1.9	0.3	4.2	BDL	3.8	95.2
$d^{18}O$	‰	252	231	-14.01	0.39	-14.09	-14.92	-12.96	-14.79	-13.23	91.7
$d^{2}H$	‰	252	233	-104.13	2.89	-105.13	-109.91	-98.36	-109.91	-98.35	92.5

[1]BDL = below detection limit

Major Anions and Cations, pH, Specific Conductivity

3.1 Specific Conductivity

Site-specific background for specific conductivity ranged from 76 – 628 µS/cm in the groundwater and 69 – 835 µS/cm in the outfall samples during the study (Figure C-1). There was a significant difference between the upgradient wells and the outfall samples ($p < 0.001$) and a nearly significant difference between the wells near the outfall and the upgradient wells ($p = 0.051$). The outfall samples (Figure C-1A) had larger SPC than the upgradient wells (Figure C-1C), and SPC was larger in the wells near the outfall (Figure C-1B) and the upgradient wells. There was no significant difference in SPC between the wells near the outfall and the outfall. This suggests that the wells near the outfall have SPC that is between the upgradient wells and outfall samples.

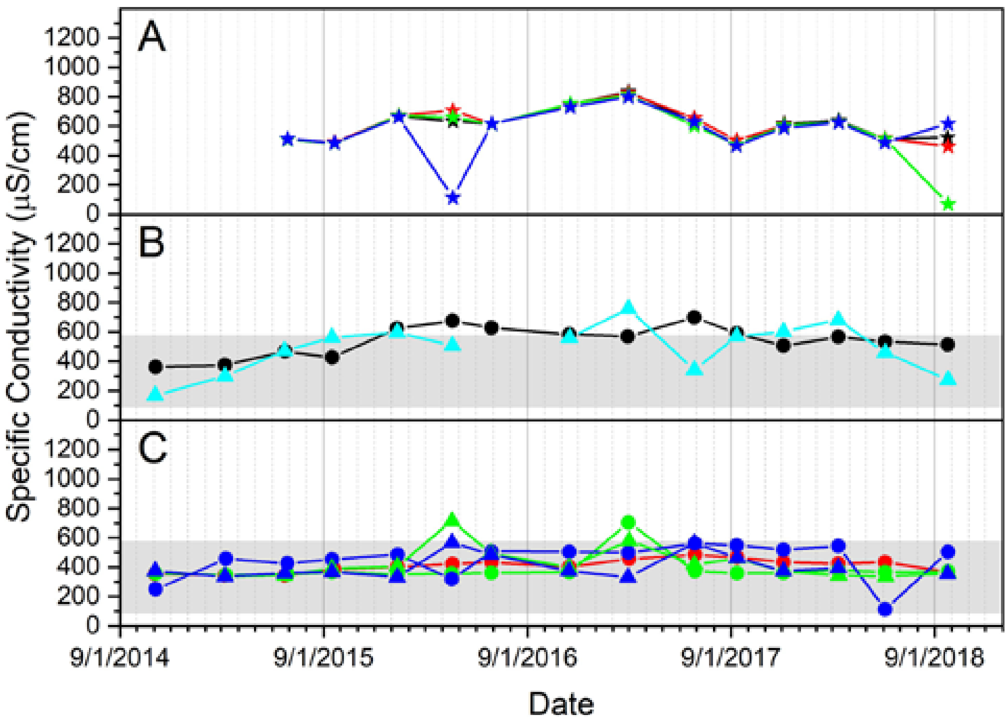

Figure C-1. Time series plots for specific conductivity in A. Outfalls samples, B. Wells near the outfall, and C. Upgradient wells. Gray shaded areas indicate the range of the site-specific background for SPC in groundwater (Table C-4). Black circles and lines are BCF836 data, red circles and lines are BCF837 data, green circles and lines are BCF838 data, blue circles and lines are BCF839 data, green triangles and lines are MW-04 data, blue triangles and lines are MW-05 data, cyan triangles and lines are MW-06 data, black stars and lines are Outfall 1 data, red stars and lines are Outfall 2 data, green stars and lines are Outfall 3 data, and blue stars and lines are Outfall 4 data. Gray shaded areas represent the site-specific background ranges in the Yakima Study.

The SPC showed increasing trends in three of five upgradient wells (Figure C-1C). These trends were significant, and the wells were BCF837 ($p = 0.011$), BCF838 ($p = 0.004$), and BCF839 ($p = 0.030$). The upgradient wells MW-04 and MW-05 did not have a trend in SPC during the study period. In the wells near the outfall, only MW-06 showed an increasing, but not significant, SPC trend ($p = 0.117$). (Figure C-1B). There were no trends in SPC in the outfall samples (Figure C-1A). In the upgradient wells, only three samples were outside the site-specific background for SPC. In the wells near the outfall, ten samples were outside the site-specific background for SPC. The SPC in the wells near the outfalls did not exceed the site-specific background range until after the treated wastewater was released into the outfall channels (Figure C-1). This suggests that the wells near the outfall were influenced by the infiltrating treated wastewater.

3.2 pH

During the study, site-specific background for pH ranged from 5.83 – 7.09 in the groundwater samples and ranged from 6.65 – 7.86 in the outfall samples (Figure C-2). It should be noted that in the November 2014 and March 2015 samplings of groundwater, there were problems with the pH sonde and the low values for pH in these events may be a result of these problems. There were significant differences in pH in wells upgradient and the outfall ($p < 0.001$) and wells near the outfall and the outfall ($p = 0.002$). The pHs were greater in the outfall samples than in the upgradient wells and in the wells near the outfall (Figure C-2). There were no significant differences in pH between the upgradient wells and the wells near the outfall.

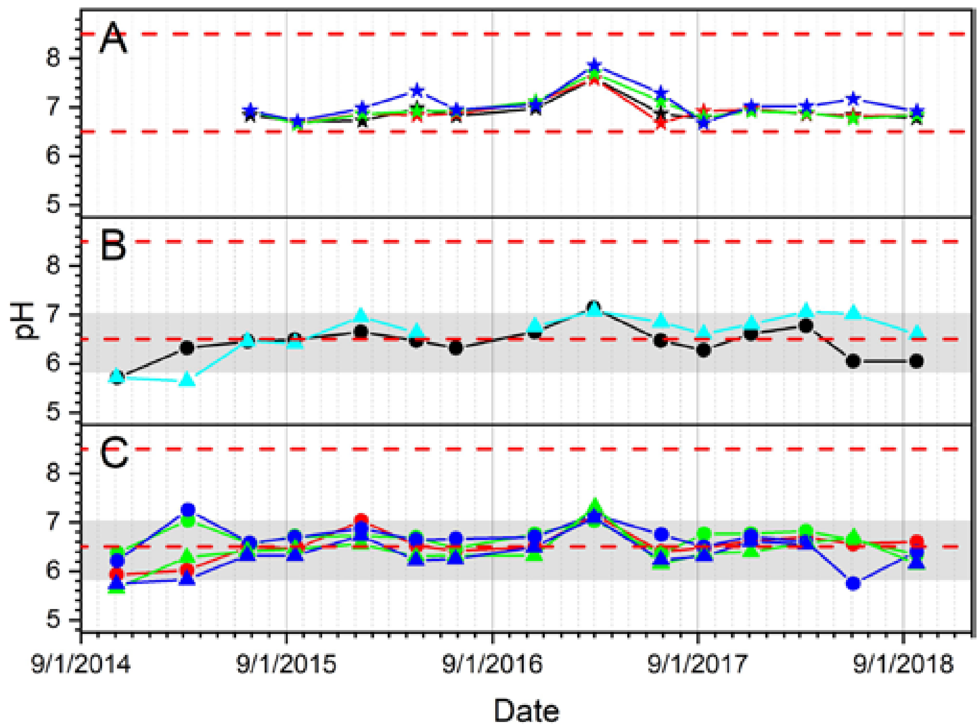

Figure C-2. Time series plots for pH in A. Outfall samples, B. Wells near the outfall, and C. Upgradient wells. Gray shaded areas indicate the range of the site-specific background for pH in groundwater (Table C-4). Red dashed lines show the sMCLs for pH. Black circles and lines are BCF836 data, red circles and lines are BCF837 data, green circles and lines are BCF838 data, blue circles and lines are BCF839 data, green triangles and lines are MW-04 data, blue triangles and lines are MW-05 data, cyan triangles and lines are MW-06 data, black stars and lines are Outfall 1 data, red stars and lines are Outfall 2 data, green stars and lines are Outfall 3 data, and blue stars and lines are Outfall 4 data. Gray shaded areas represent the site-specific background ranges in the Yakima Study.

As was the case with SPC, there were trends in pH in three of the wells upgradient. There was a significant increasing pH trend in BCF837 ($p = 0.027$) and non-significant increasing pH trends in wells MW-04 and MW-05 ($p = 0.127$ in both wells) (Figure C-2C). In the wells near the outfall (Figure C-2B), BCF836 did not have a trend in pH, but there was significant increasing pH in well MW-06 ($p = 0.011$). There were no trends in pH in any of the Outfall samples (Figure C-2A).

There were no sMCL exceedances in any of the outfall samples (Figure C-2A); however, there were sMCL exceedances in several samples upgradient and wells near the outfalls. The upgradient wells (Figure C-2C) in November 2014 all exceeded the sMCL and BCF837, MW-04, and MW-05 in March 2015. Again, these exceedances could be related to the pH sonde problem discussed earlier. Beyond the initial two events, there were 28 other exceedances of the sMCLs for pH in the upgradient wells and these exceedances were all lower pH than the sMCL of 6.50 (Figure C-2C). As was the case with the upgradient wells, the initial two samplings had pH sMCL exceedances in the wells near the outfall, BCF836 and MW-06 (Figure C-2B). These exceedances could also be related to the problems with the pH sonde. The only other sMCL exceedance for pH in MW-06 was in September 2016 (Figure C-2B). BCF836 had an additional seven pH sMCL exceedances (Figure C-2B). Like the upgradient wells, the sMCL exceedances in the wells near the outfall were less than the pH sMCL of 6.50.

3.3 Chloride

Site-specific background chloride concentrations in the groundwater ranged from 1.61 – 55.7 mg/L and chloride concentrations ranged from 5.25 – 66.2 mg/L in the outfall samples (Figure C-3). There were no significant differences in chloride concentrations between groundwater upgradient and near the outfalls as well as there were no significant differences in chloride concentrations between the wells near the outfalls and outfall samples. However, there was a significant difference between the upgradient chloride concentrations and the chloride concentrations in the outfall ($p = 0.002$). The chloride concentrations in the outfall were greater than the chloride concentrations upgradient. The chloride concentrations in wells near the outfall are between those upgradient and those in the outfall samples.

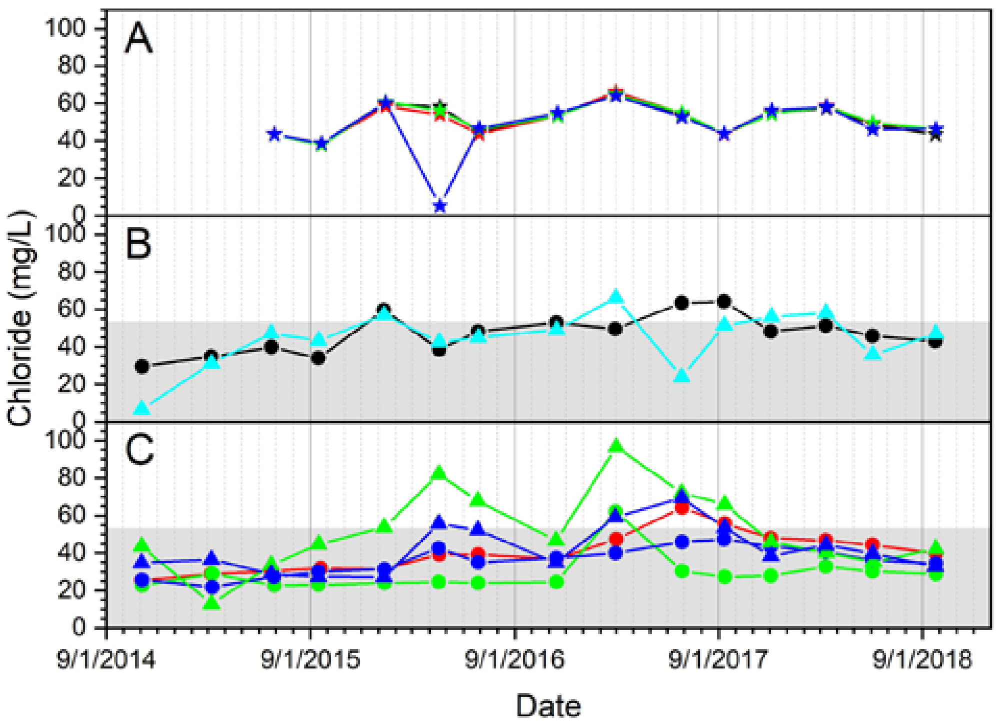

Figure C-3. Time series plots for chloride concentrations in A. Outfall samples, B. Wells near the outfall, and C. Upgradient wells. Gray shaded areas indicate the range of the site-specific background for chloride in groundwater (Table C-4). Black circles and lines are BCF836 data, red circles and lines are BCF837 data, green circles and lines are BCF838 data, blue circles and lines are BCF839 data, green triangles and lines are MW-04 data, blue triangles and lines are MW-05 data, cyan triangles and lines are MW-06 data, black stars and lines are Outfall 1 data, red stars and lines are Outfall 2 data, green stars and lines are Outfall 3 data, and blue stars and lines are Outfall 4 data. Gray shaded areas represent the site-specific background ranges in the Yakima Study.

In the upgradient wells (Figure C-3C), there were significant increasing chloride concentrations in wells BCF837 ($p = 0.001$), BCF838 ($p < 0.001$), and BCF839 ($p = 0.005$). There were no trends in chloride in the other upgradient wells, MW-04 and MW-05. In both wells near the outfall (Figure B-3B) there were increasing trends in chloride concentrations. The increasing chloride trend in BCF836 ($p = 0.041$) and MW-06 ($p = 0.069$) were significant. There were no trends in chloride concentration in the outfall samples (Figure C-3A).

The sMCL for chloride is 250 mg/L. There were no exceedances of the chloride sMCL in the swamples collected.

3.4 Bicarbonate

Bicarbonate concentrations in the outfall samples ranged from 45 – 270 mg HCO_3^-/L and site-specific background in the groundwater ranged from 23.6 – 148 mg HCO_3^-/L (Figure C-4). There were no significant differences in bicarbonate between the upgradient wells and wells near the outfall or upgradient wells and outfall samples or outfall samples and wells near the outfall.

Upgradient, only well BCF837 showed an increasing trend in bicarbonate (Figure C-4C) and this was a significant trend ($p = 0.030$). In the wells near the outfall (Figure 7-8B), only MW-06 showed a significant increasing trend ($p = 0.001$). There were no trends in bicarbonate concentrations in the outfall samples.

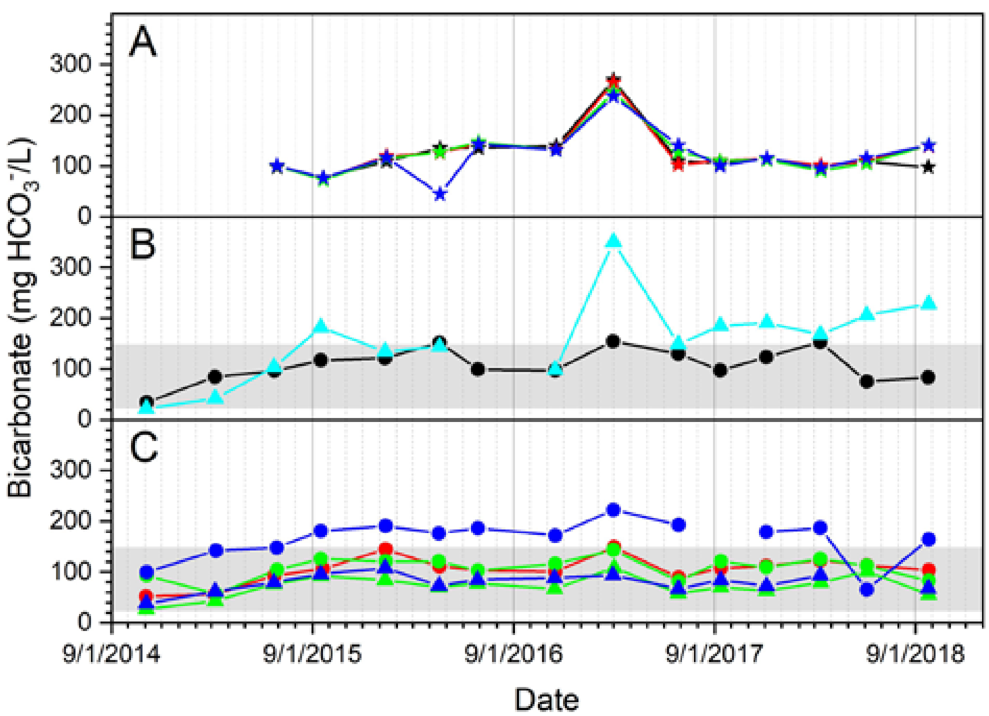

Figure C-4. Time series plots for bicarbonate concentrations in A. Outfall samples, B. Wells near the outfall, and C. Upgradient wells. Gray shaded areas indicate the range of the site-specific background for bicarbonate in groundwater (Table C-4). Black circles and lines are BCF836 data, red circles and lines are BCF837 data, green circles and lines are BCF838 data, blue circles and lines are BCF839 data, green triangles and lines are MW-04 data, blue triangles and lines are MW-05 data, cyan triangles and lines are MW-06 data, black stars and lines are Outfall 1 data, red stars and lines are Outfall 2 data, green stars and lines are Outfall 3 data, and blue stars and lines are Outfall 4 data. Gray shaded areas represent the site-specific background ranges in the Yakima Study.

3.5 Sulfate

The site-specific background concentrations of sulfate in the groundwater ranged from 2.23 – 36.9 mg/L and the sulfate concentrations in the outfall samples ranged from 6.39 – 85.4 mg/L in this study (Figure C-5). The sulfate concentrations in the wells near the outfall and the outfall samples were not significantly different. There was a significant difference in sulfate concentrations between the upgradient wells and the outfall samples ($p < 0.001$) and between the upgradient wells and the wells near the outfall ($p < 0.001$). The sulfate concentrations were larger in the wells near the outfall were larger than the concentration in the outfall samples (Figure C-5). This suggests that the groundwater near the outfall may be being influenced by the infiltrating water from the outfalls.

In the upgradient wells, only BCF837 showed a trend in the sulfate concentrations (Figure C-5C) and this was a significantly increasing trend ($p = 0.037$). There were no trends in sulfate concentrations in wells near the outfall or in the outfall samples.

The sMCL for sulfate is 250 mg/L. There were no exceedances in the sulfate sMCL in the samples collected.

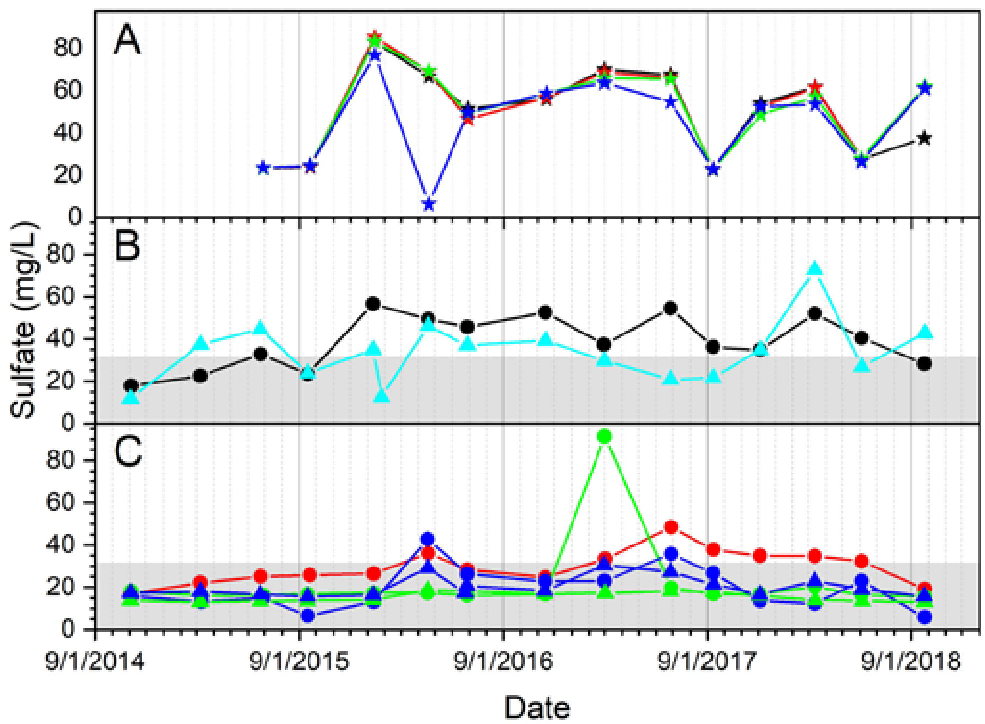

Figure C-5. Time series plots for sulfate concentrations in A. Outfall samples, B. Wells near the outfall, and C. Upgradient wells. Gray shaded areas indicate the range of the site-specific background for sulfate in groundwater (Table C-4). Black circles and lines are BCF836 data, red circles and lines are BCF837 data, green circles and lines are BCF838 data, blue circles and lines are BCF839 data, green triangles and lines are MW-04 data, blue triangles and lines are MW-05 data, cyan triangles and lines are MW-06 data, black stars and lines are Outfall 1 data, red stars and lines are Outfall 2 data, green stars and lines are Outfall 3 data, and blue stars and lines are Outfall 4 data. Gray shaded areas represent the site-specific background ranges in the Yakima Study.

3.6 Calcium

Site-specific background calcium concentrations in the groundwater ranged from 9.16 – 51.1 mg/L and <0.50 – 35.0 mg/L in the outfall samples (Figure C-6). The concentrations of calcium were significantly different from the outfall samples in both the upgradient wells ($p < 0.001$) and wells near the outfall ($p < 0.001$). The upgradient wells and wells near the outfall did not have significantly different calcium concentrations.

Calcium showed significant increasing concentrations in 3 of the 5 upgradient wells (Figure C-6C), BCF837 ($p < 0.001$), BCF838 ($p = 0.001$) and BCF839 ($p < 0.001$). Only BCF836 showed an increasing and significant ($p = 0.024$) calcium trend in the wells near the outfall (Figure C-6B). There were no trends in calcium concentration in the outfall samples (Figure C-6A).

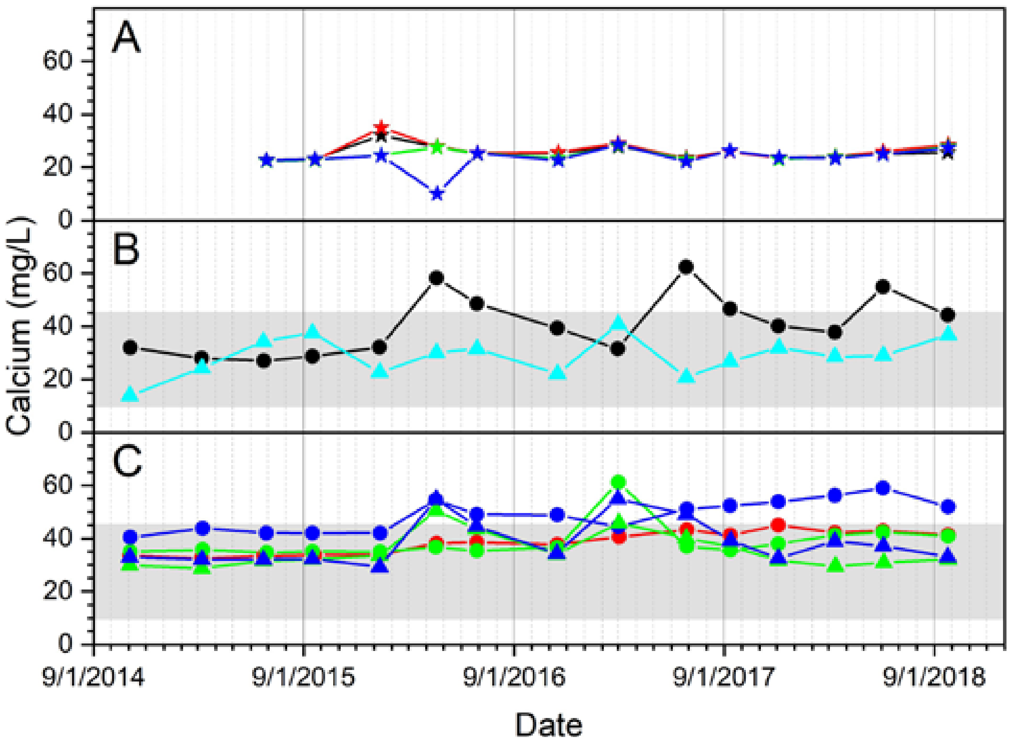

Figure C-6. Time series plots for calcium concentrations in A. Outfall samples, B. Wells near the outfall, and C. Upgradient wells. Gray shaded areas indicate the range of the site-specific background for calcium in groundwater (Table C-4). Black circles and lines are BCF836 data, red circles and lines are BCF837 data, green circles and lines are BCF838 data, blue circles and lines are BCF839 data, green triangles and lines are MW-04 data, blue triangles and lines are MW-05 data, cyan triangles and lines are MW-06 data, black stars and lines are Outfall 1 data, red stars and lines are Outfall 2 data, green stars and lines are Outfall 3 data, and blue stars and lines are Outfall 4 data. Gray shaded areas represent the site-specific background ranges in the Yakima Study.

3.7 Magnesium

Groundwater site-specific background magnesium concentrations ranged from 3.29 – 19.5 mg/L and 0.07 – 20.8 mg/L in the outfall samples (Figure C-7). There were no significant differences in magnesium concentration between the different water sources and there were no seasonal differences in magnesium concentration.

Like calcium, there were only trends in magnesium concentrations in the same three wells upgradient (Figure C-7C). The increasing trends in magnesium concentration were significant in the wells BCF837 ($p = 0.013$), BCF838 ($p = 0.004$), and BCF 839 ($p = 0.009$). Unlike calcium, both the wells near the outfall (Figure C-7B) had increasing magnesium concentrations and these trends were significant, BCF836 ($p = 0.027$) and MW-06 ($p = 0.041$). There were no trends in the magnesium concentrations in the outfall samples (Figure C-7A).

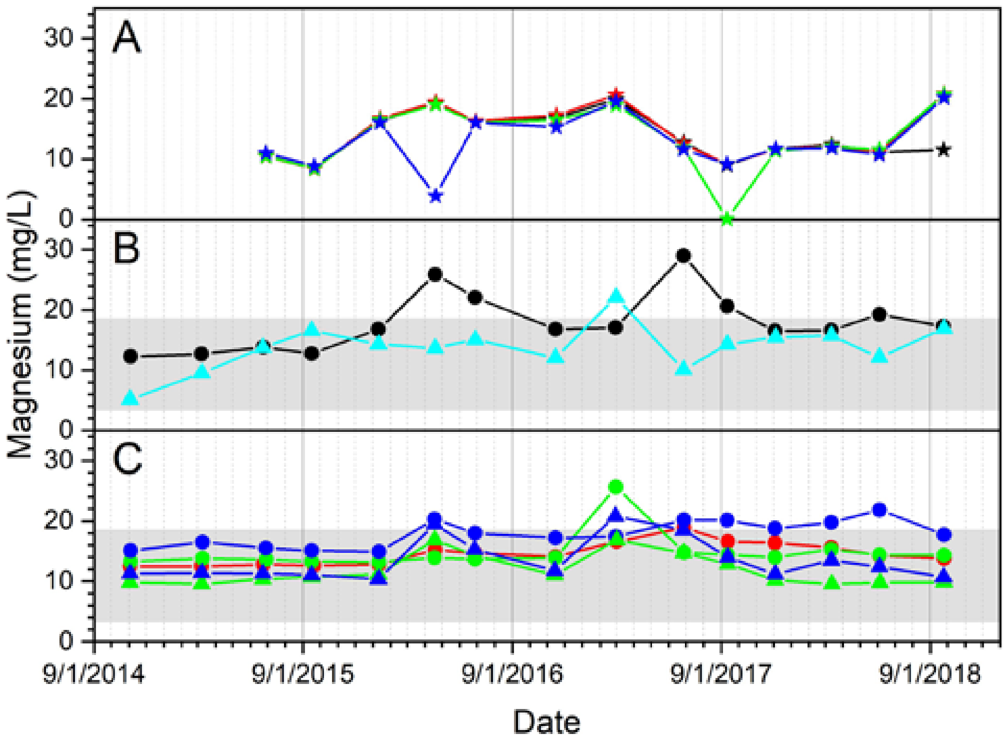

Figure C-7. Time series plots for magnesium concentrations in A. Outfall samples, B. Wells near the outfall, and C. Upgradient wells. Gray shaded areas indicate the range of the site-specific background for magnesium in groundwater (Table C-4). Black circles and lines are BCF836 data, red circles and lines are BCF837 data, green circles and lines are BCF838 data, blue circles and lines are BCF839 data, green triangles and lines are MW-04 data, blue triangles and lines are MW-05 data, cyan triangles and lines are MW-06 data, black stars and lines are Outfall 1 data, red stars and lines are Outfall 2 data, green stars and lines are Outfall 3 data, and blue stars and lines are Outfall 4 data. Gray shaded areas represent the site-specific background ranges in the Yakima Study.

3.8 Potassium

Site-specific background potassium concentrations in the Yakima Study ranged from 0.73 – 8.74 mg/L in the groundwater and 0.50 – 29.2 mg/L in the outfall samples (Figure C-8). The concentrations of potassium were significantly different ($p < 0.001$) between the outfall samples and the upgradient groundwater. The outfall samples had greater potassium concentrations than the upgradient wells. Likewise, the potassium concentrations between the wells near the outfall and the outfall samples were significantly different ($p < 0.001$). The outfall samples potassium concentrations were greater than those of the wells near the outfall. There was also a significant difference in potassium concentrations between the wells near the outfall and upgradient wells ($p < 0.001$). The wells near the outfall had higher potassium concentrations than the upgradient wells. This suggests that the wells near the outfall potentially resulted from the mixing of the upgradient water with the infiltrated outfall water.

In the upgradient wells, there were increasing potassium concentrations with time in all the wells except for MW-04 (Figure C-8C). In wells BCF837, BCF838, and BCF839, these increasing trends were significant ($p = 0.003$, $p = 0.003$, and $p = 0.001$, respectively). In MW-05, the increasing trend in potassium was not significant ($p = 0.138$). Potassium was significantly increasing in MW-06 ($p = 0.004$), but potassium showed no trend in BCF836 (Figure C-8B). There were no trends in potassium in the outfall samples (Figure C-8A).

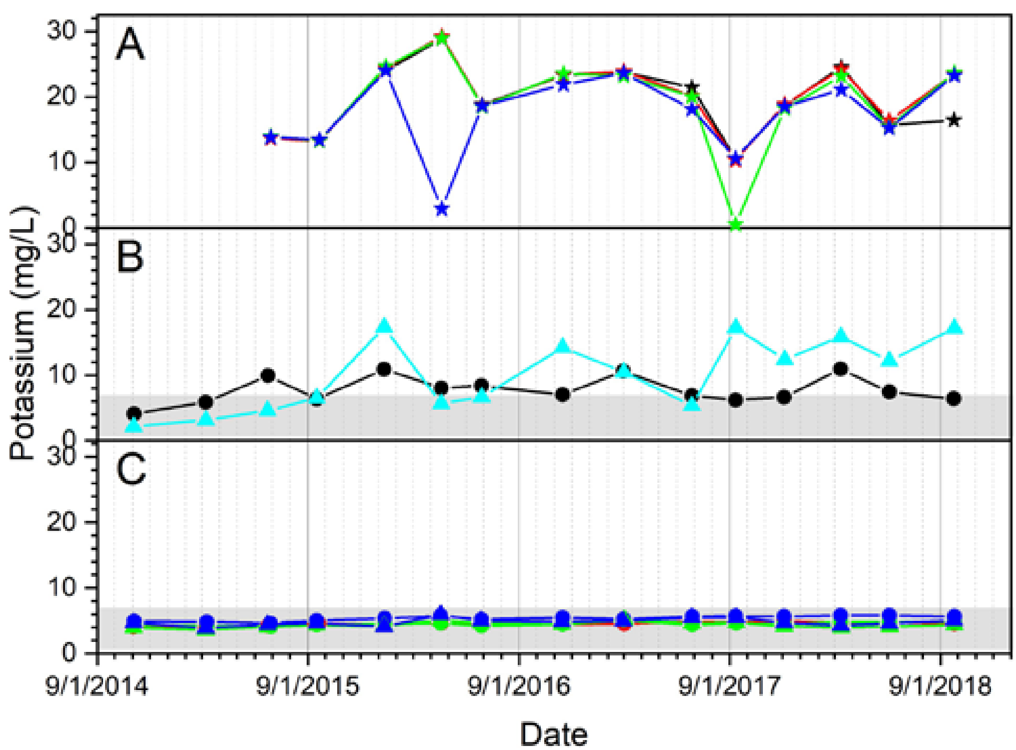

Figure C-8. Time series plots for potassium concentrations in A. Outfall samples, B. Wells near the outfall, and C. Upgradient wells. Gray shaded areas indicate the range of the site-specific background for potassium in groundwater (Table C-4). Black circles and lines are BCF836 data, red circles and lines are BCF837 data, green circles and lines are BCF838 data, blue circles and lines are BCF839 data, green triangles and lines are MW-04 data, blue triangles and lines are MW-05 data, cyan triangles and lines are MW-06 data, black stars and lines are Outfall 1 data, red stars and lines are Outfall 2 data, green stars and lines are Outfall 3 data, and blue stars and lines are Outfall 4 data. Gray shaded areas represent the site-specific background ranges in the Yakima Study.

3.9 Sodium

Site-specific background sodium concentrations in the groundwater ranged from 3.97 – 28.8 mg/L. The sodium concentrations in the outfall samples ranged from <2.00 – 89.0 mg/L in this study (Figure C-9). There were significant differences in sodium concentration between upgradient wells and the wells near the outfall ($p < 0.001$). The wells near the outfall had higher sodium concentrations than the upgradient wells. The upgradient wells were also significantly different than the outfall samples ($p < 0.001$), with the outfall samples having higher sodium concentrations than the upgradient wells. The wells near the outfall and outfall samples were also significantly different ($p = 0.048$). The outfall samples had slightly higher sodium concentrations than the wells near the outfall. The sodium concentration differences also suggest that the wells near the outfall potentially resulted from the mixing of upgradient groundwater with infiltrated outfall water.

Sodium concentrations showed increasing concentrations in all the wells upgradient (Figure C-9C). These increasing trends were significant in BCF837 ($p < 0.001$), BCF838 ($p = 0.061$), BCF839 ($p = 0.005$), MW-04 ($p = 0.083$), and MW-05 ($p = 0.007$). In the wells near the outfall (Figure C-9B), only MW-06 showed and increasing trend in sodium concentration ($p = 0.001$). Sodium did show an increasing concentration trend in the two sampling points nearest to the beginning of the outfall trenches (Figure C-9A). These sodium concentration trends were in Outfall 1 and Outfall 2, but the trends were not significant in Outfall 1 ($p = 0.123$) but were significant in Outfall 2 ($p = 0.064$).

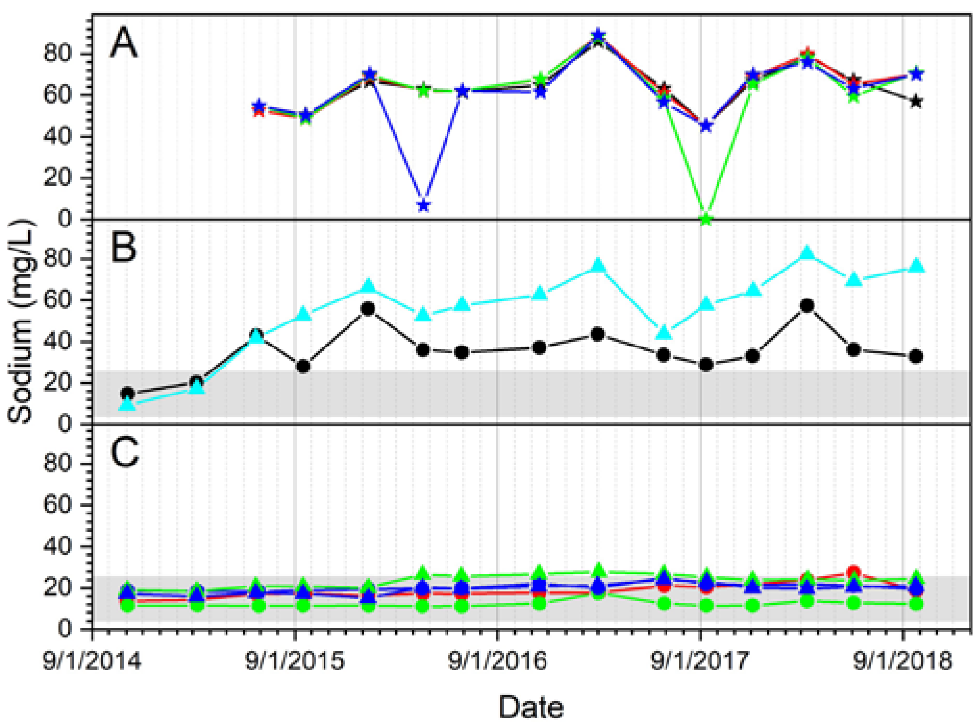

Figure C-9. Time series plots for sodium concentrations in A. Outfall samples, B. Wells near the outfall, and C. Upgradient wells Gray shaded areas indicate the range of the site-specific background for sodium in groundwater (Table C-4). Black circles and lines are BCF836 data, red circles and lines are BCF837 data, green circles and lines are BCF838 data, blue circles and lines are BCF839 data, green triangles and lines are MW-04 data, blue triangles and lines are MW-05 data, cyan triangles and lines are MW-06 data, black stars and lines are Outfall 1 data, red stars and lines are Outfall 2 data, green stars and lines are Outfall 3 data, and blue stars and lines are Outfall 4 data. Gray shaded areas represent the site-specific background ranges in the Yakima Study.

Other Chemical Constituents

4.1 Nitrate + Nitrite

Nitrate + nitrite is an analysis which does not distinguish between these two nitrogen species. Figure C-10 is a plot of Eh versus pH showing the N speciation and the study data. This figure indicates that denitrification processes could potentially happen in most samples. A few samples do not indicate that denitrification would occur, and in these samples, only nitrate would be present. A few samples indicate that nitrite could be present. Many of the samples would indicate that nitrate should be fully denitrified to nitrogen, but there is still measurable nitrate + nitrite in these samples. This would suggest that one of two things is happening. The water in the aquifer is not at equilibrium or there is oxidation of the nitrogen happening in the sample bottle after the sample is taken and before analysis. The analysis conducted cannot distinguish between these possibilities. It is noteworthy that if ammonia was present in the water that in all cases ammonia would be thermodynamically unstable suggesting the more oxidized N species more stable.

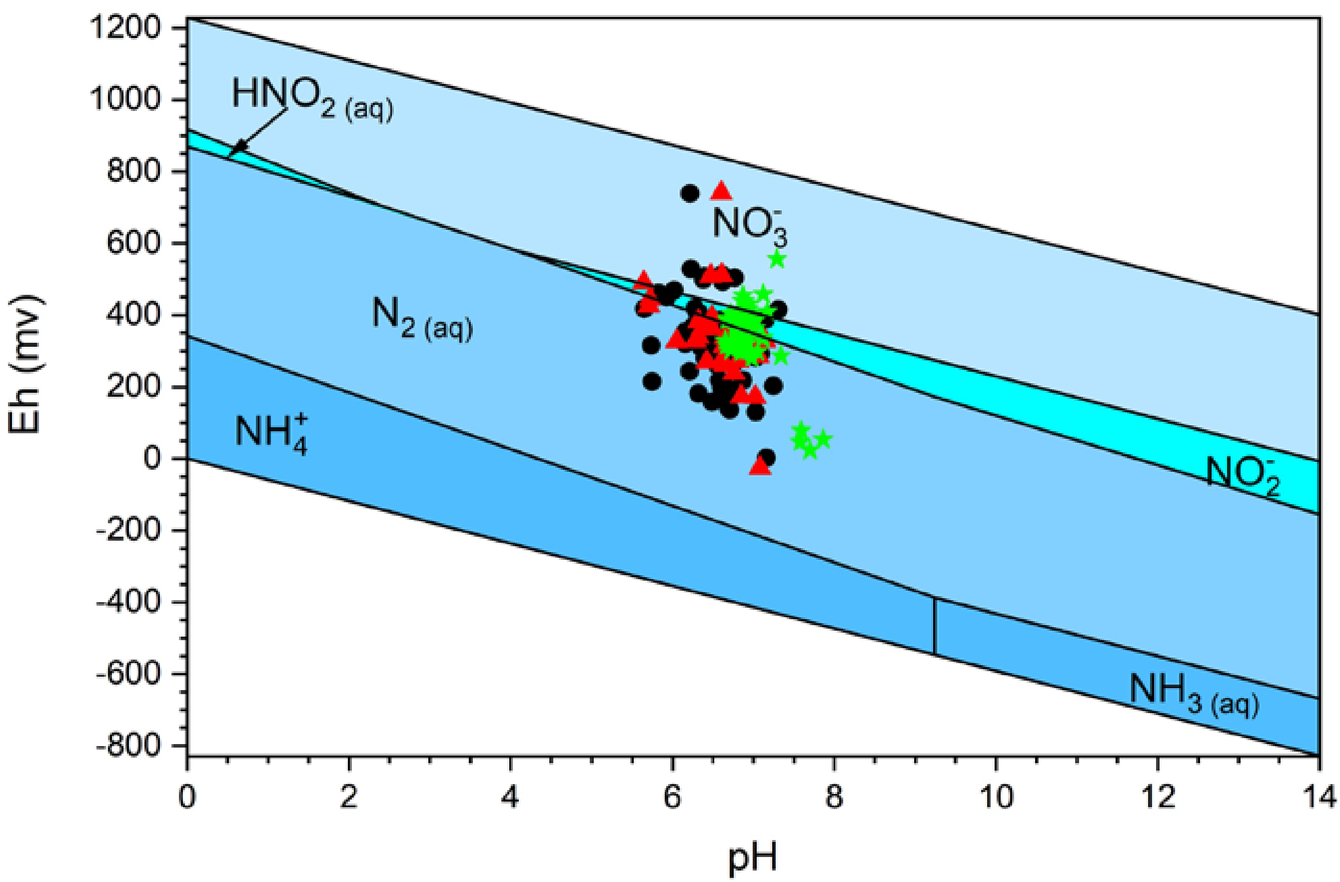

Figure C-10. Eh-pH diagram for N-system. Black circles are upgradient groundwater, red triangles are groundwater in wells near the outfall, and green stars are treated wastewater samples in the outfall.

4.2 Fluoride

Figure 7-24 are log F^- activity versus pH plots of the Ca-F-PO_4 system and the Ca-F system. In the Ca-F-PO_4 system, Figure C-11A, all the data collected in this study are oversaturated with respect to fluorapatite suggesting that fluorapatite would control the F solubility and that fluorapatite should be forming. On the other hand, in the Ca-F system (Figure C-11B), all the data collected indicates undersaturated conditions with respect to F. This would suggest that any fluorite in the aquifer would be dissolving and the F concentrations should be increasing. Only BCF837 and MW-06 had increasing trends in F concentrations; however, it is unknown if fluorite dissolution is the actual reason for this trend.

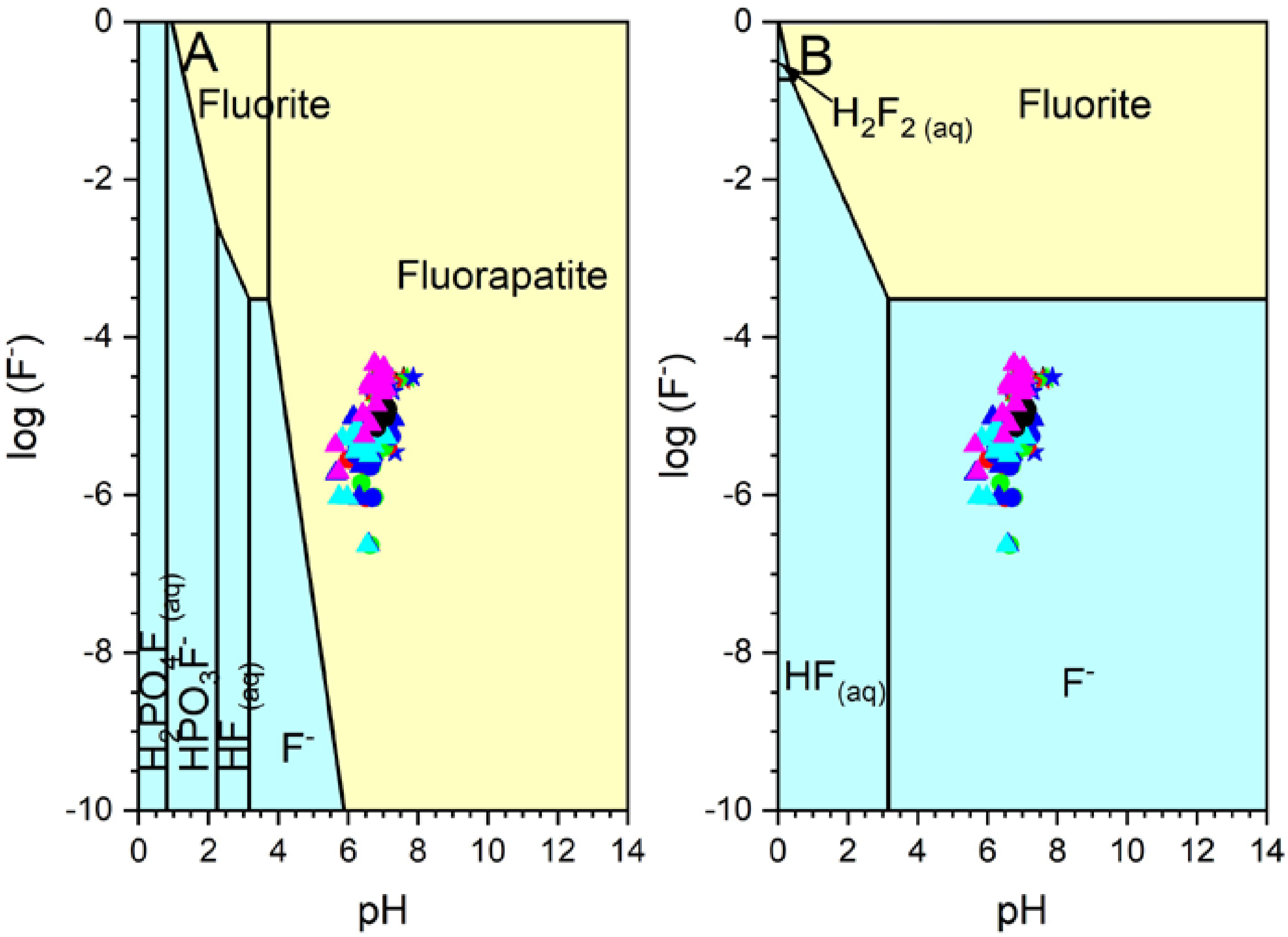

Figure C-11. Log F^- activity vs. pH. A. Ca-F-PO_4 system and B. Ca-F system. Blue shade areas show solution species and yellow shaded areas show solid phases. Black circles and lines are MW-01, red circles are MW-02, green circles are MW-03, blue circles are MW-04, cyan circles are MW-05, magenta circles are MW-06, dark yellow circles are MW-07, purple circles are MW-08, wine-colored circles are MW-09 and dark cyan circles are MW-10.

4.3 Phosphate

Plots of log HPO_4^{2-} versus pH for the Ca-F-HPO_4^{2-} system and Ca-HPO_4^{2-} system for the upgradient wells are shown in Figure C-12. Most of the upgradient samples plot in the fluorapatite field or along the border of the fluorapatite/$H_2PO_4^-$ fields of the Ca-F-HPO_4^{2-} system (Figure C-12A). There were a few samples that plotted in the $H_2PO_4^-$ field. There was no temporal pattern to the upgradient data. This suggests that the upgradient groundwater at the study site is in equilibrium or slightly oversaturated with respect to fluorapatite. Conversely, all the upgradient groundwater samples plot as aqueous species in the Ca-HPO_4^{2-} system (Figure C-12B). This suggests that fluorapatite is controlling phosphate concentrations in the upgradient water during the study.

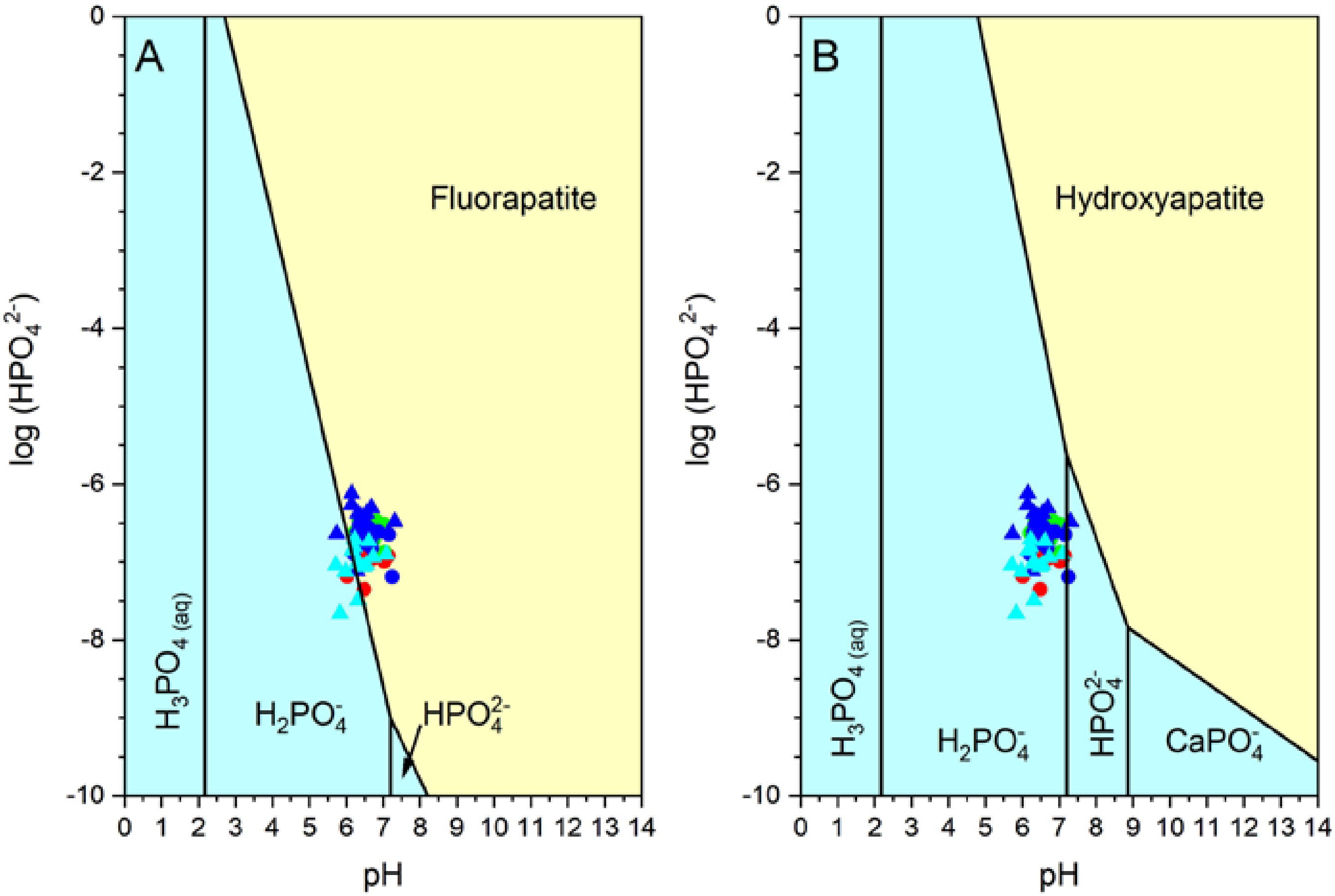

Figure C-12. Upgradient groundwater log HPO_4^{2-} activity vs. pH. A. Ca-F-HPO_4^{2-} system and B. Ca-HPO_4^{2-} system. Blue shaded areas show solution species and yellow shaded areas show solid phases. The red circles are BCF837, green circles are BCF838, blue circles are BCF839, blue triangles are MW-04, and cyan triangles are MW-05.

Plots of log HPO_4^{2-} versus pH for the Ca-F-HPO_4^{2-} system and Ca-HPO_4^{2-} system for the infiltrated treated wastewater in the outfalls are shown in Figure C-13. All the treated wastewater plot in the fluorapatite field of the Ca-F-HPO_4^{2-} system (Figure C-13A). There was no temporal pattern to the upgradient data. This suggests that the treated wastewater in the study site is oversaturated with respect to fluorapatite. It is likely that most of the treated wastewater is in equilibrium with hydroxyapatite or slightly under/oversaturated with hydroxyapatite. This can be seen in the Ca-HPO_4^{2-} system (Figure C-13B) and suggests that hydroxyapatite is controlling phosphate concentrations in the treated wastewater samples during the study and potentially why the phosphate concentrations showed no trends during the study.

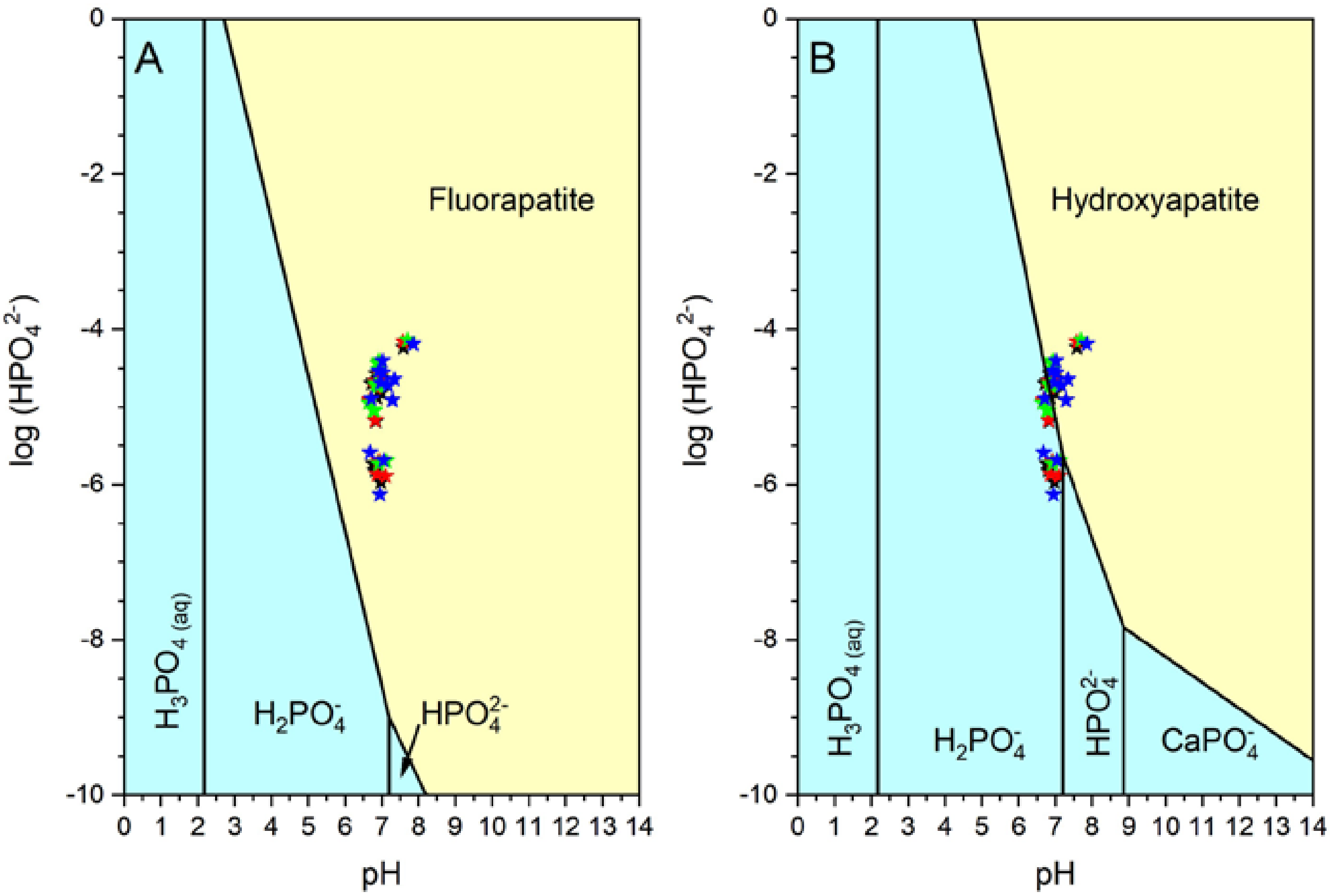

Figure C-13. Treated wastewater in the outfalls log HPO_4^{2-} activity vs. pH. A. Ca-F-HPO_4^{2-} system and B. Ca-HPO_4^{2-} system. Blue shaded areas show solution species and yellow shaded areas show solid phases. The black stars are Outfall 1, red stars are Outfall 2, green stars are Outfall 3, and blue stars are Outfall 4.

Plots of log HPO_4^{2-} versus pH for the Ca-F-HPO_4^{2-} system and Ca-HPO_4^{2-} system for the wells near the outfalls are shown in Figure C-14. Initially both wells BCF836 and MW-06 were undersaturated with respect to fluorapatite field of the Ca-F-HPO_4^{2-} system (Figure C-14A). The infiltration began in the outflows the phosphate concentrations began to increase, and the wells near the outfalls became over saturated with respect to fluorapatite (blue arrow in Figure C-14A shows the relative trajectory). This suggests that the wells near the outfall in the study site became oversaturated with respect to fluorapatite with time. BCF836 was undersaturated with respect to hydroxyapatite throughout the study but was approaching equilibrium in the later events (Figure C-14B). MW-06 did reach equilibrium with respect to hydroxyapatite in the later events of the study. This suggests that as the phosphate concentrations in the wells near the outfall increased, they were approaching equilibrium with hydroxyapatite. This was the case in the treated wastewater in the outfalls. If the phosphate concentrations in the treated wastewater do not increase, it would likely serve as the maximum concentration (end member) for the phosphate concentrations in MW-06 and BCF836.

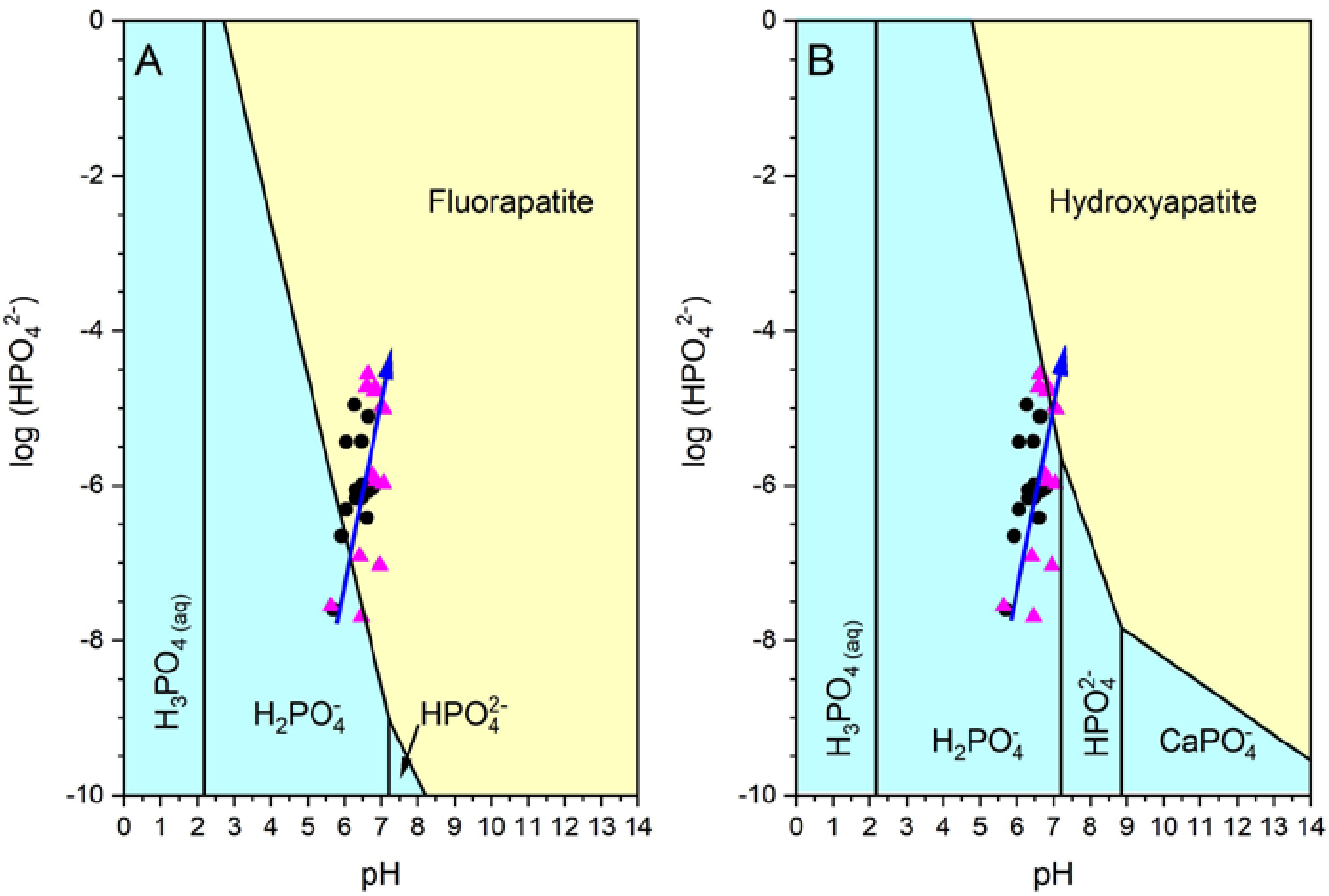

Figure C-14. Wells near the outfalls log HPO_4^{2-} activity vs. pH. A. Ca-F-HPO_4^{2-} system and B. Ca-HPO_4^{2-} system. Blue shaded areas show solution species and yellow shaded areas show solid phases. The black circles are BCF836 and magenta triangles are MW-06. Blue arrows show the relative trajectory of the temporal changes in the wells.

Appendix D. Fort Riley Supporting Information

Table of Contents

Groundwater, Piezometers, Tensiometers, and Porewater Samplers

Table D-1. Sampling locations, Fort Riley, Kansas.

Sample Location	Latitude (degrees)	Longitude (degrees)	Top of Screen Elevation[1] (m msl[3])	Bottom of Screen Elevation[1] (m msl[3])	Probe Elevation[2] (m msl[3])
Monitoring Wells					
FRGW01	39.069348	-96.842821	321.2	318.2	NA[4]
FRGW02	39.068896	-96.842301	321.3	318.3	NA
FRGW03	39.068816	-96.842552	321.8	318.8	NA
FRGW04	39.068857	-96.842927	321.2	318.1	NA
FRGW05	39.068762	-96.842974	321.3	318.2	NA
FRGW06	39.068708	-96.842604	322.2	319.1	NA
FRGW07	39.068644	-96.842239	321.1	318.0	NA
FRGW08	39.068598	-96.843053	320.9	317.8	NA
FRGW09	39.068580	-96.842392	321.1	318.0	NA
FRGW10	39.069030	-96.842428	322.2	319.1	NA
FRGW11	39.069118	-96.843254	321.5	318.5	NA
FRGW12	39.068986	-96.842630	321.1	318.0	NA
FRGW13	39.068801	-96.842386	321.1	318.1	NA
Piezometers					
FRPW01	39.069361	-96.842813	315.9	315.3	NA
FRPW02	39.069335	-96.842827	317.7	317.1	NA
FRPW03	39.068854	-96.842943	315.6	315.0	NA
FRPW04	39.068852	-96.842911	317.5	316.9	NA
FRPW05	39.068708	-96.842624	318.2	317.6	NA
FRPW06	39.068647	-96.842262	317.5	316.9	NA
FRPW07	39.068604	-96.843071	315.8	315.2	NA
FRPW08	39.068592	-96.843038	317.2	316.6	NA
FRPW09	39.068581	-96.842409	317.6	317.0	NA
FRPW10	39.069315	-96.843789	317.3	316.7	NA
FRPW11	39.071151	-96.839792	317.8	317.1	NA
FRPW12	39.068263	-96.841283	317.8	317.2	NA

[1]Monitoring wells and piezometers;
[2]Soil porewater samplers and tensiometers;
[3]msl = Mean sea level;
[4]NA = Not applicable.

Table D-1 (continued). Sampling locations, Fort Riley, Kansas.

Sample Location	Latitude (degrees)	Longitude (degrees)	Top of Screen Elevation[1] (m msl[3])	Bottom of Screen Elevation[1] (m msl[3])	Probe Elevation[2] (m msl[3])
Soil Pore Water Samplers					
FRLW01	39.068946	-96.843008	NA	NA	323.3
FRLW02	39.068940	-96.842988	NA	NA	321.8
FRLW03	39.068900	-96.842917	NA	NA	325.1
FRLW04	39.068900	-96.842917	NA	NA	324.2
FRLW05	39.068900	-96.842917	NA	NA	323.3
FRLW06	39.068874	-96.842907	NA	NA	325.1
FRLW07	39.068874	-96.842907	NA	NA	324.2
FRLW08	39.068874	-96.842907	NA	NA	323.3
FRLW09	39.068888	-96.842810	NA	NA	323.3
FRLW10	39.068882	-96.842790	NA	NA	321.8
FRLW11	39.068810	-96.842939	NA	NA	323.3
FRLW12	39.068810	-96.842939	NA	NA	321.8
Tensiometers					
T1A	39.068943	-96.842998	NA	NA	323.3
T1B	39.068943	-96.842998	NA	NA	321.8
T2A	39.068885	-96.842800	NA	NA	323.3
T2B	39.068885	-96.842800	NA	NA	321.8
T3A	39.068897	-96.842907	NA	NA	325.1
T3B	39.068897	-96.842907	NA	NA	324.2
T3C	39.068897	-96.842907	NA	NA	323.3
T4A	39.068877	-96.842917	NA	NA	325.1
T4B	39.068877	-96.842917	NA	NA	324.2
T4C	39.068877	-96.842917	NA	NA	323.3
T5A	39.068813	-96.842948	NA	NA	323.3
T5B	39.068813	-96.842948	NA	NA	321.8
Infiltration Gallery Wells					
FRIW01-1	39.069007	-96.843163	326.6	325.1	NA
FRIW01-2	39.069000	-96.843139	326.6	325.1	NA
FRIW01-3	39.068993	-96.843117	326.6	325.1	NA
FRIW01-4	39.068986	-96.843094	326.6	325.1	NA

[1]Monitoring wells and piezometers;
[2]Soil porewater samplers and tensiometers;
[3]msl = Mean sea level;
[4]NA = Not applicable.

Table D-1 (continued). Sampling locations, Fort Riley, Kansas.

Sample Location	Latitude (degrees)	Longitude (degrees)	Top of Screen Elevation[1] (m msl[3])	Bottom of Screen Elevation[1] (m msl[3])	Probe Elevation[2] (m msl[3])
Temporary Wells October 2018					
TNS 1-1	39.070126	-96.843517	322.5	319.5	NA
TNS 1-2	39.069995	-96.843574	322.1	319.0	NA
TNS1-3	39.069864	-96.843632	322.3	319.2	NA
TNS1-4	39.069726	-96.843664	322.6	319.6	NA
TNS1-5	39.069596	-96.843724	322.4	319.3	NA
TNS1-6	39.069464	-96.843784	322.1	319.0	NA
TNS1-7	39.069335	-96.843846	322.4	319.4	NA
TNS1-8	39.069205	-96.843907	321.9	318.9	NA
TEW1-1	39.069553	-96.843560	322.9	319.9	NA
TEW1-2	39.069501	-96.843391	323.7	320.6	NA
TEW1-3	39.069337	-96.843132	322.4	319.4	NA
TEW2-1	39.069288	-96.843676	322.1	319.0	NA
TEW2-2	39.069244	-96.843508	323.9	320.8	NA
TEW2-3	39.069152	-96.843218	324.3	321.3	NA
TEW3-1	39.069162	-96.843735	322.3	319.2	NA
TEW3-3	39.069035	-96.843204	322.4	319.3	NA
TEW4	39.068959	-96.843421	320.4	317.4	NA
Alphamach Temperature Profilers					
TP1-1	39.068951	-96.843076	NA	NA	325.2
TP1-2	39.068951	-96.843076	NA	NA	325.5
TP1-3	39.068951	-96.843076	NA	NA	325.8
TP1-4	39.068951	-96.843076	NA	NA	326.1
TP2-1	39.068844	-96.842717	NA	NA	325.2
TP2-2	39.068844	-96.842717	NA	NA	325.5
TP2-3	39.068844	-96.842717	NA	NA	325.8
TP2-4	39.068844	-96.842717	NA	NA	326.1

[1]Monitoring wells and piezometers;
[2]Soil porewater samplers and tensiometers;
[3]msl = Mean sea level;
[4]NA = Not applicable.

Geophysics Figures

2.1 Electrical Resistivity Imaging Survey

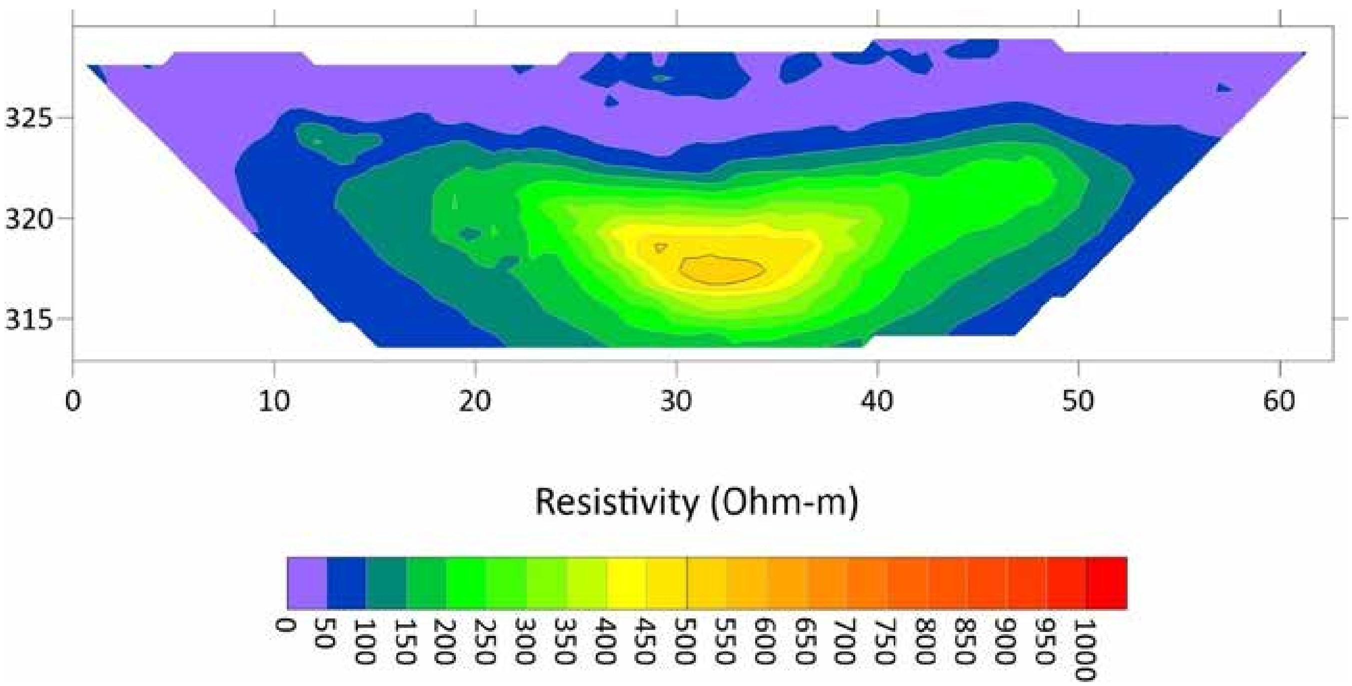

Figure D-1. Electrical resistivity image for transect TIL08-4.

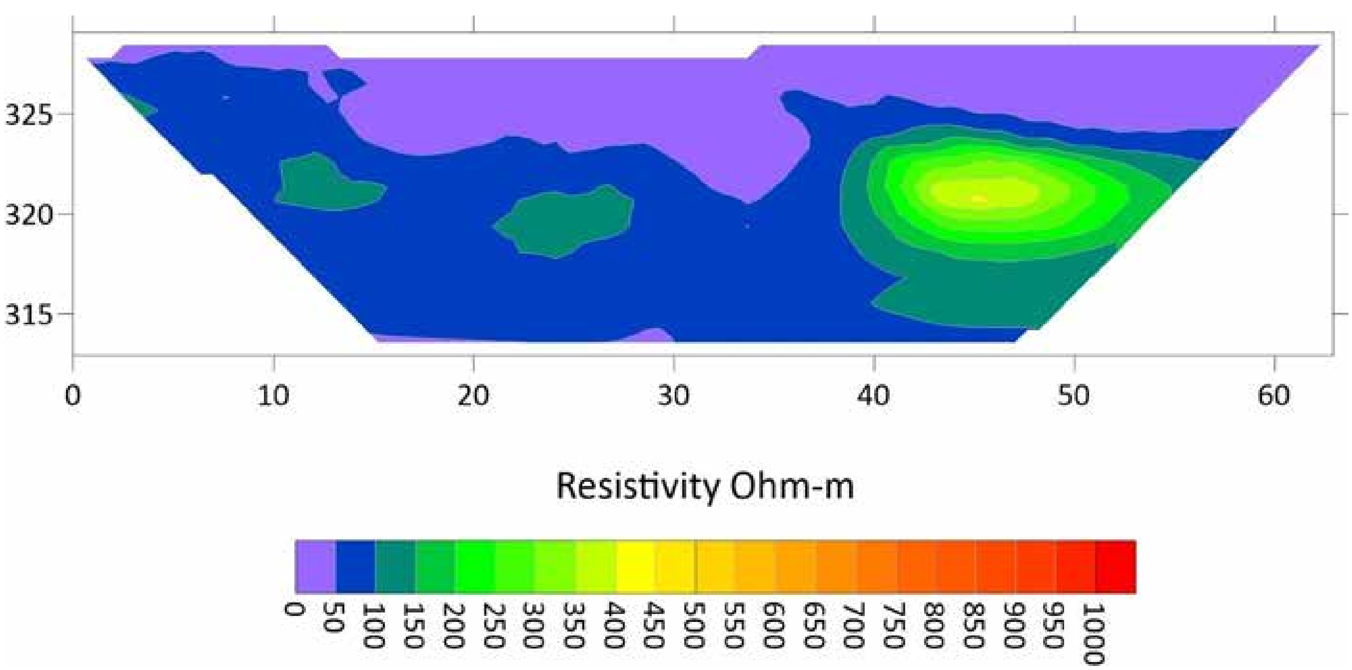

Figure D-2. Electrical resistivity image for transect TIL08-5.

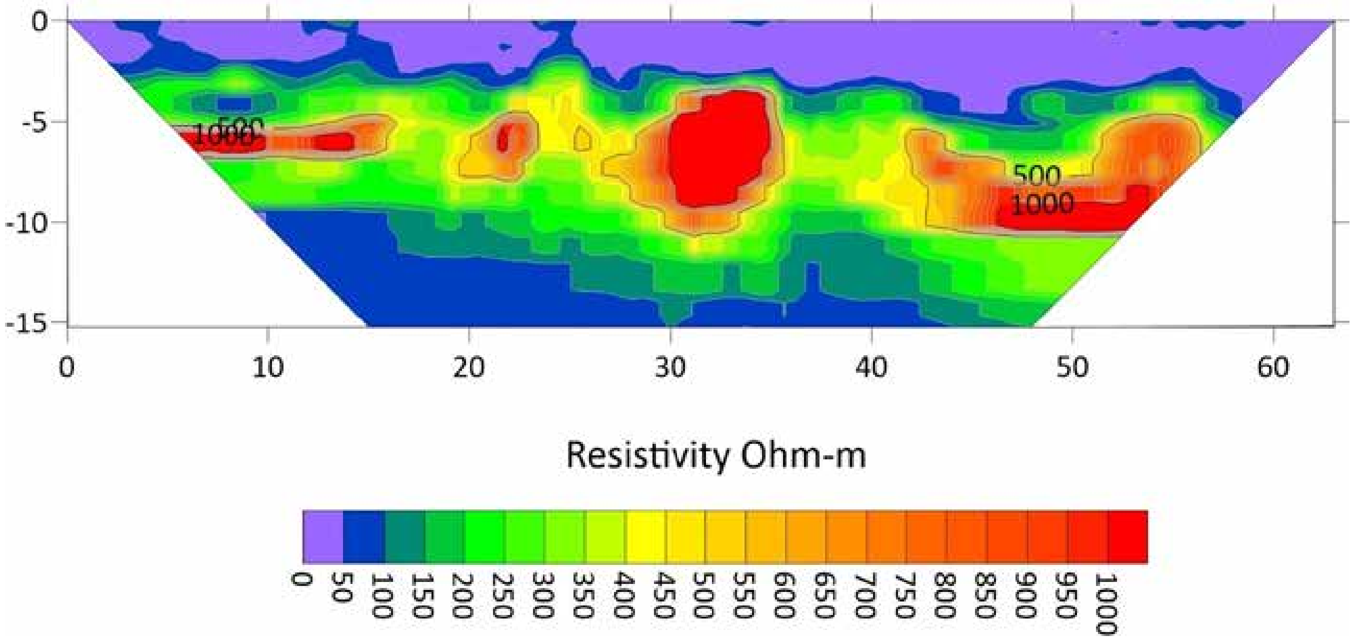

Figure D-3. Electrical resistivity image for transect TIL09-1.

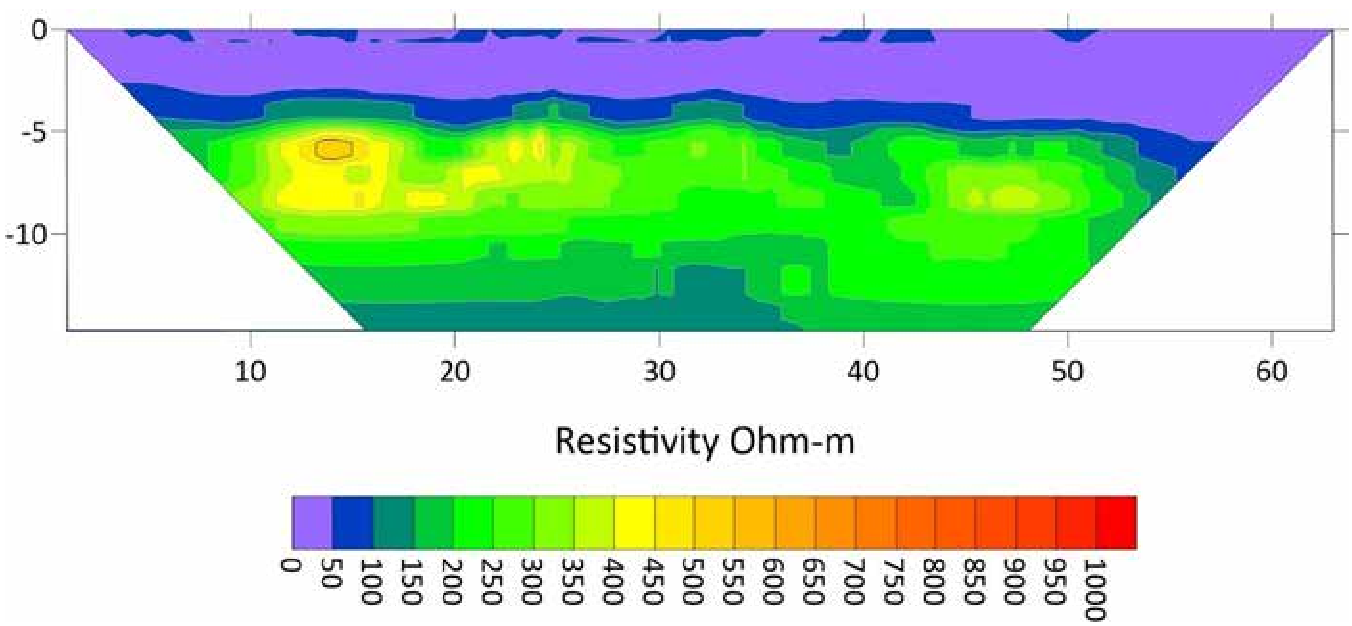

Figure D-4. Electrical resistivity image for transect TIL09-6.

2.2 Borehole Geophysical Methods

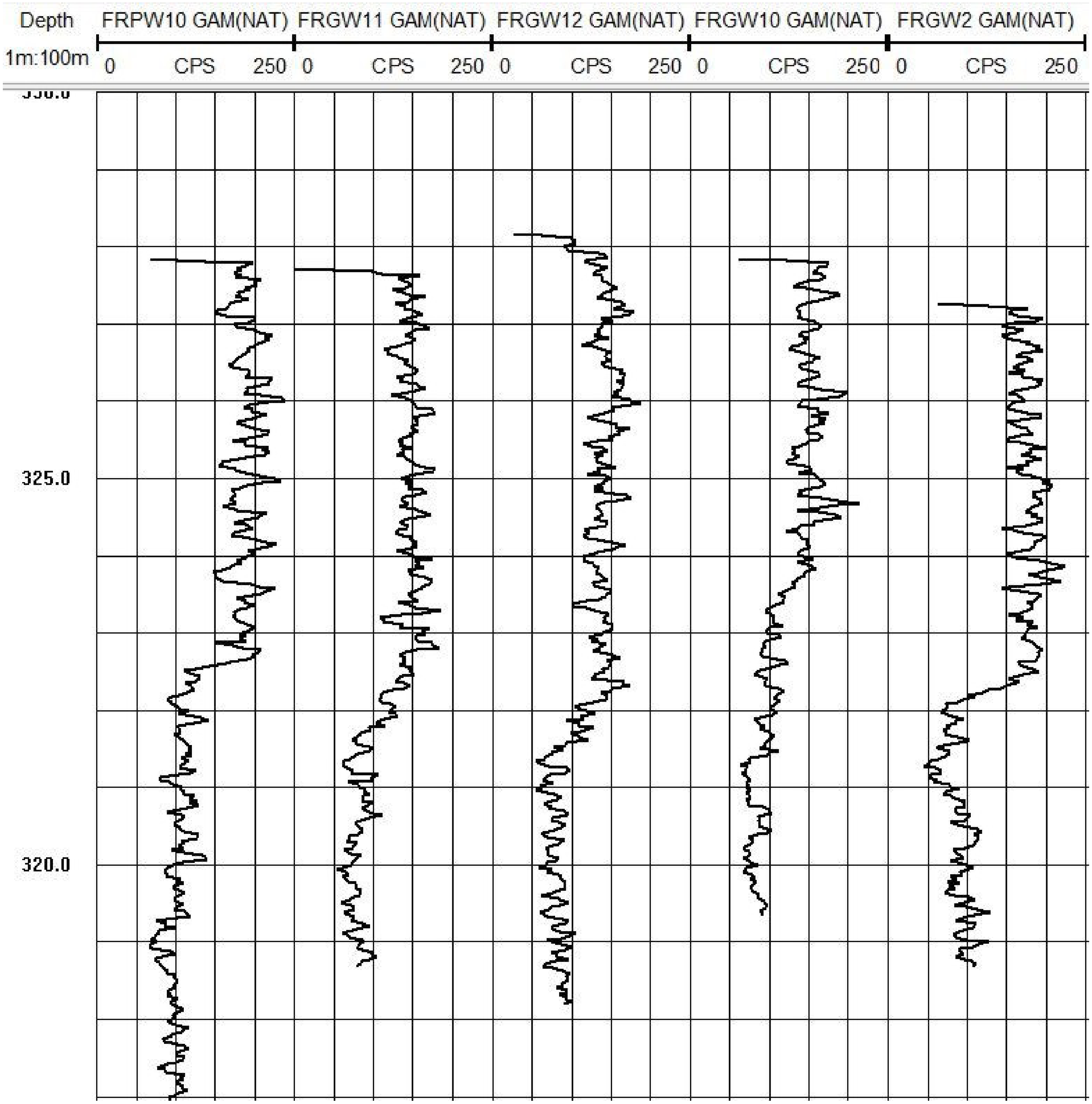

Figure D-5. Natural gamma logs for west (FRPW10) to east (FRGW02) transect.

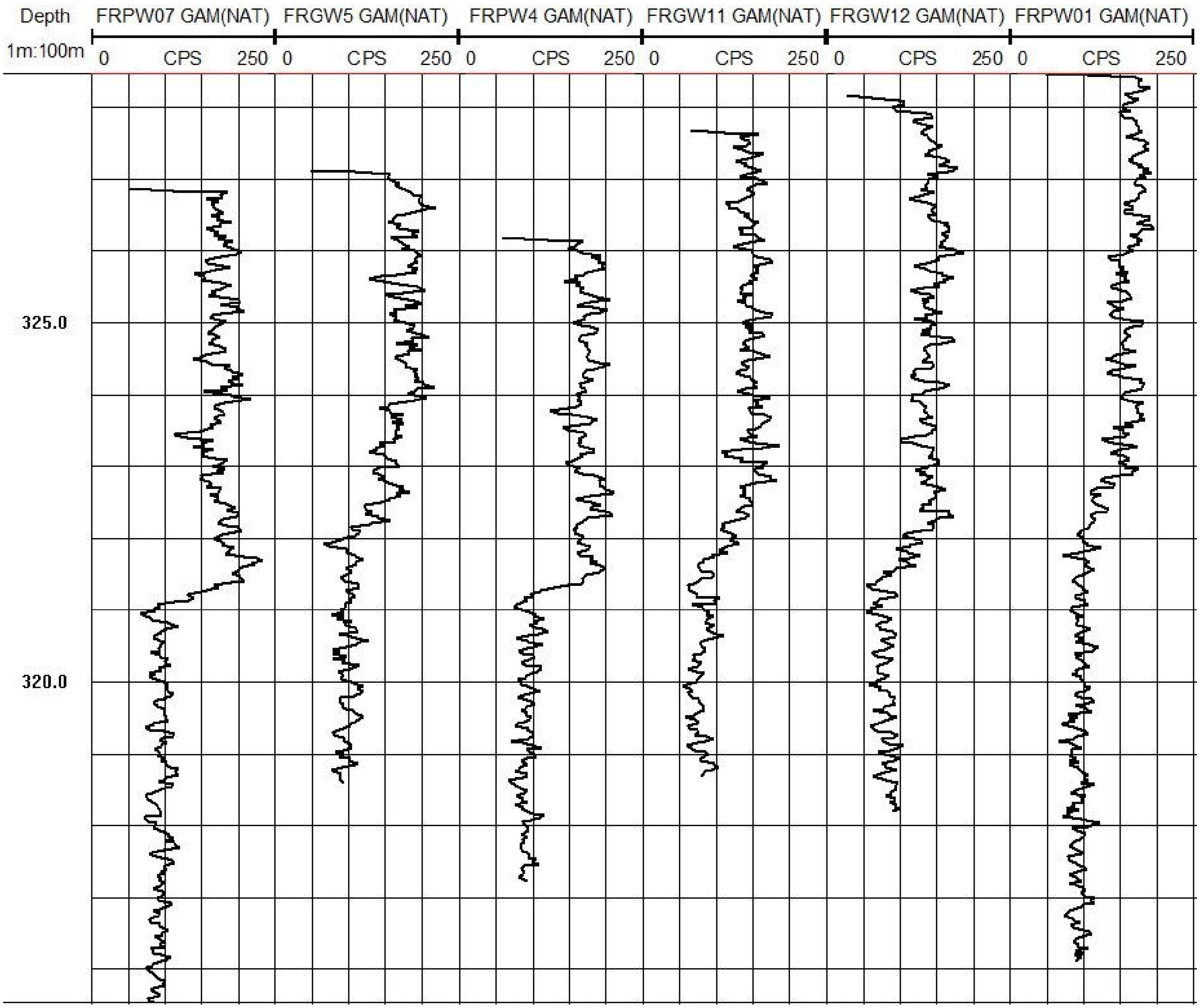

Figure D-6. Natural gamma logs for south (FRPW07) to north (FRPW01) transect.

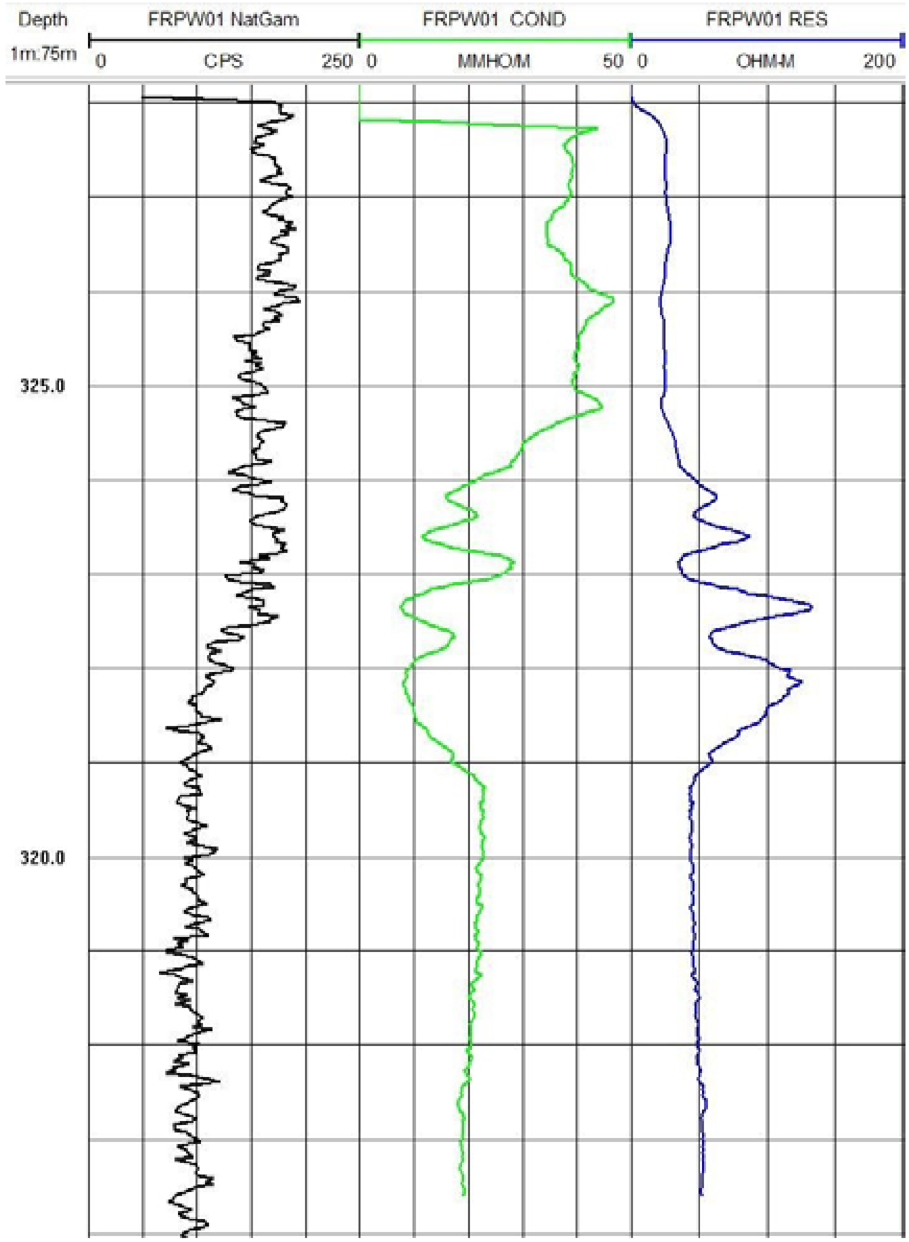

Figure D-7. Borehole geophysical log for FRPW01.

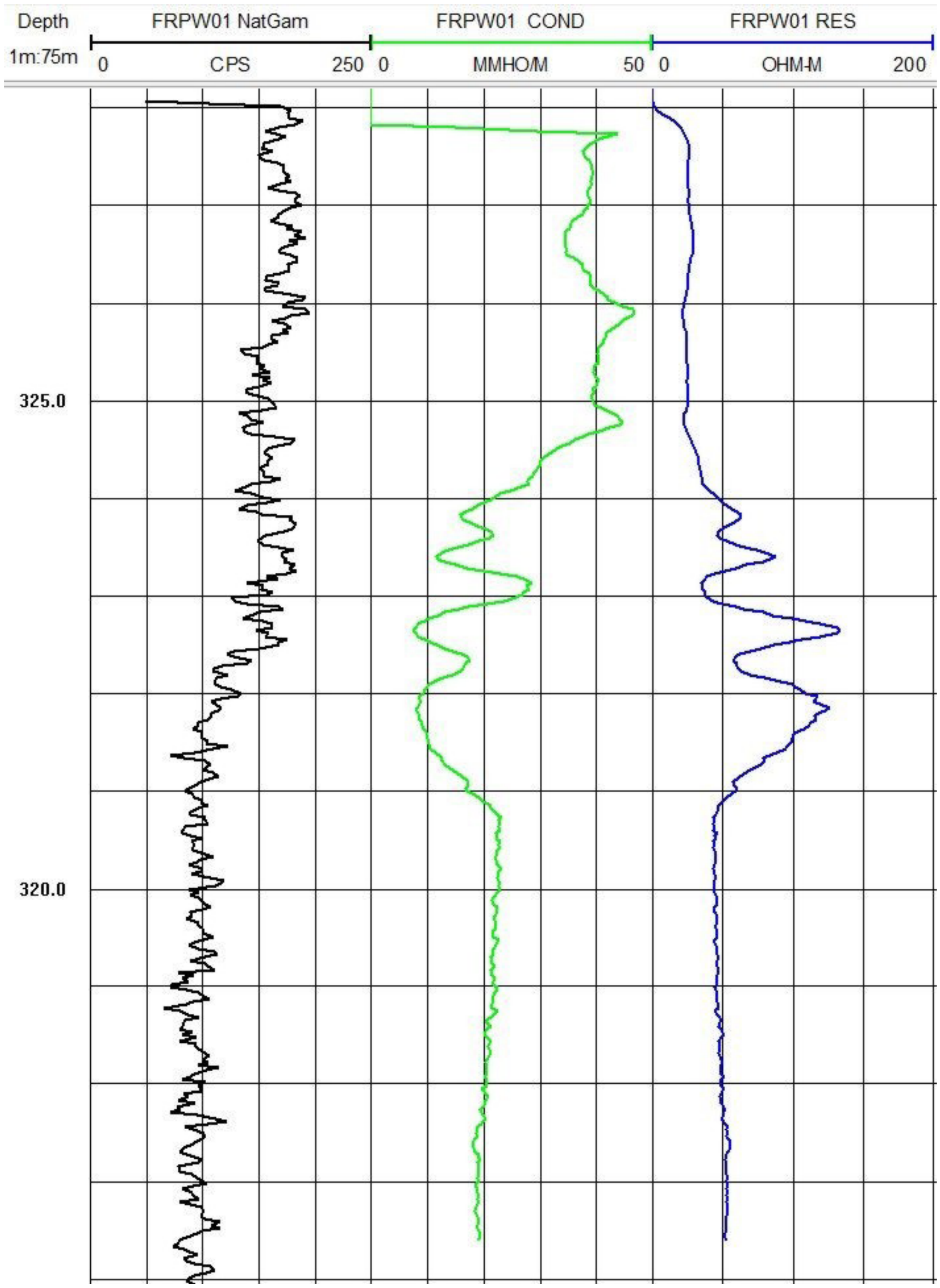

Figure D-8. Borehole geophysical log for FRPW01.

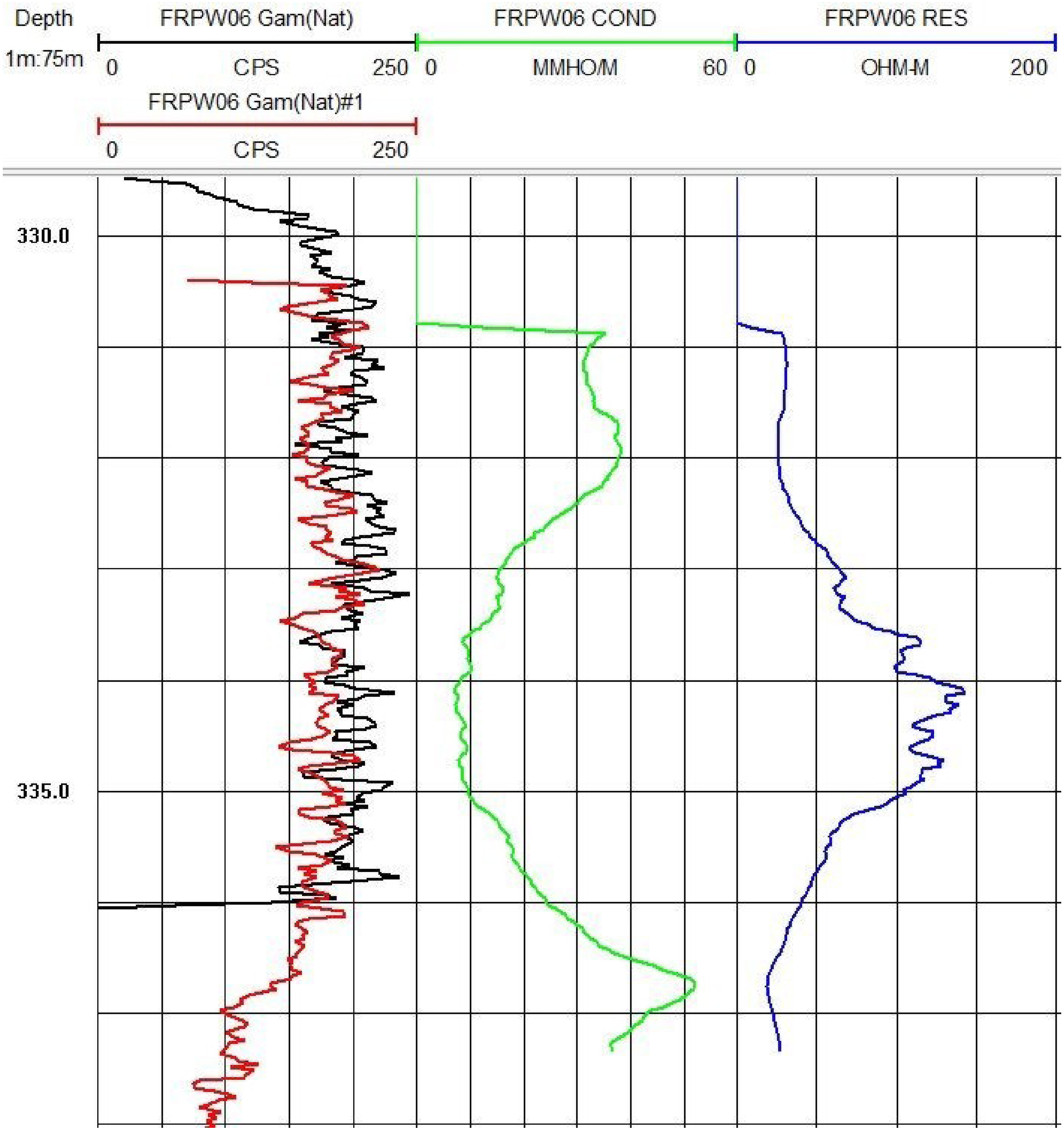

Figure D-9. Borehole geophysical log for FRPW06.

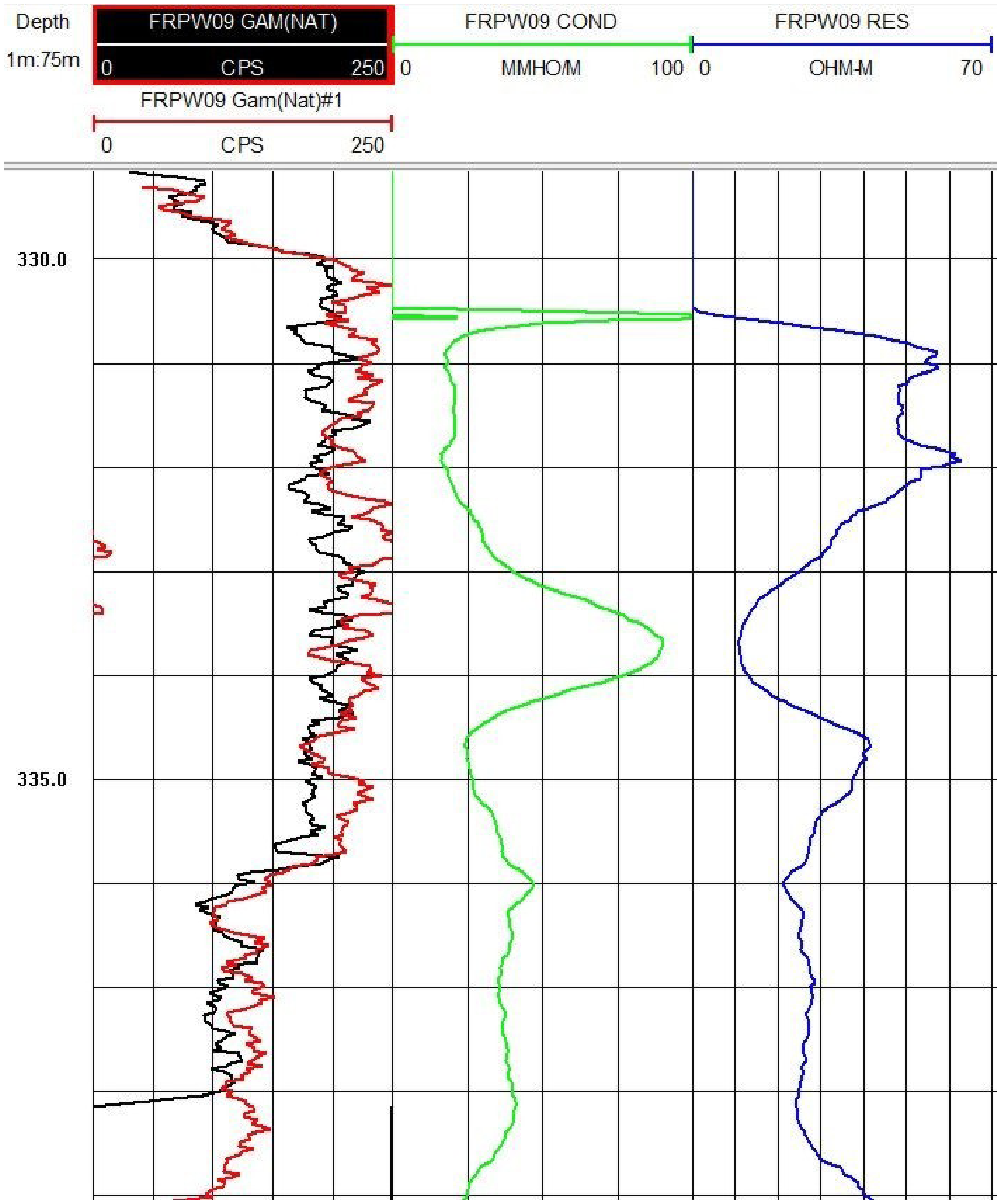

Figure D-10. Borehole geophysical log for FRPW09.

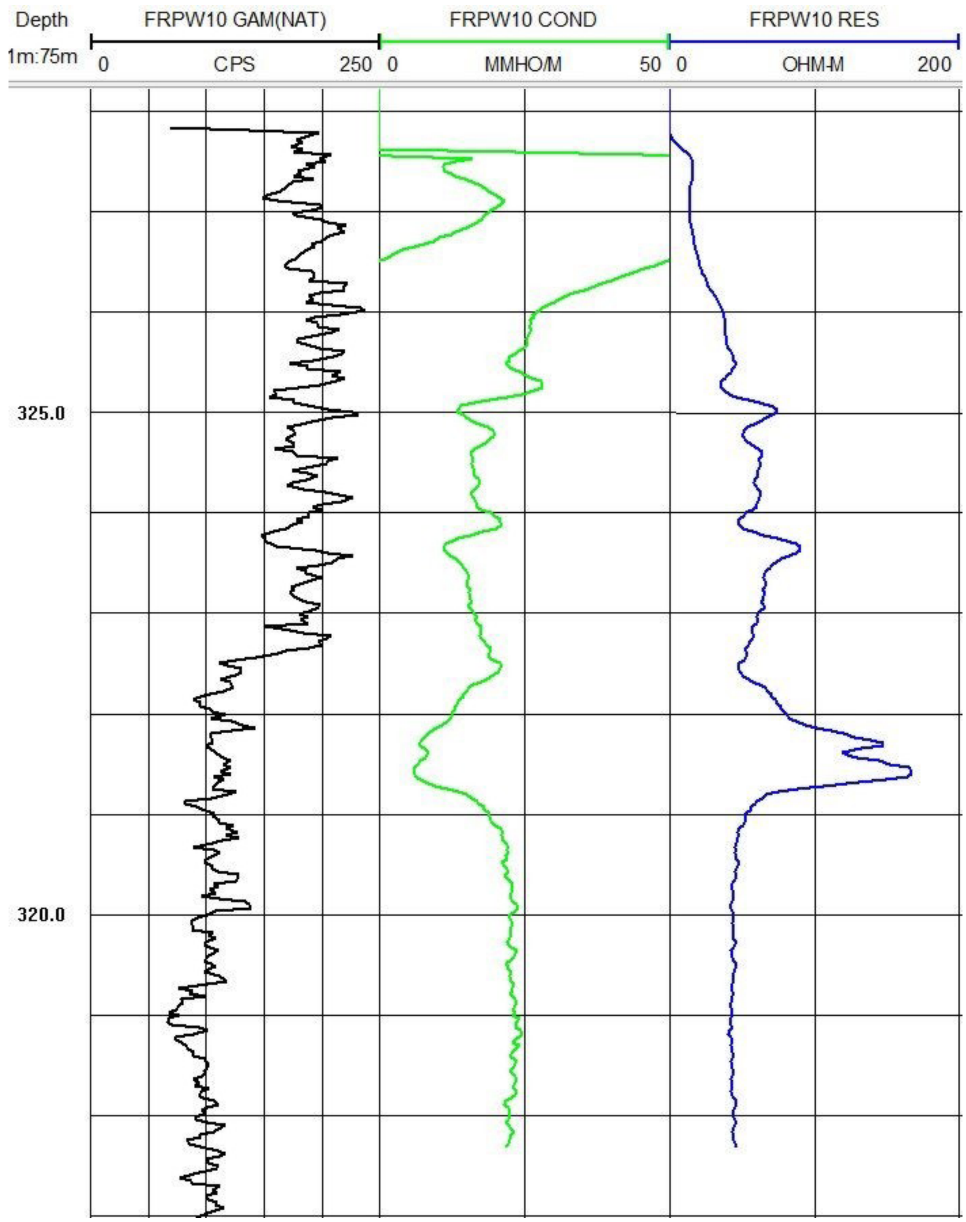

Figure D-11. Borehole geophysical log for FRPW10.

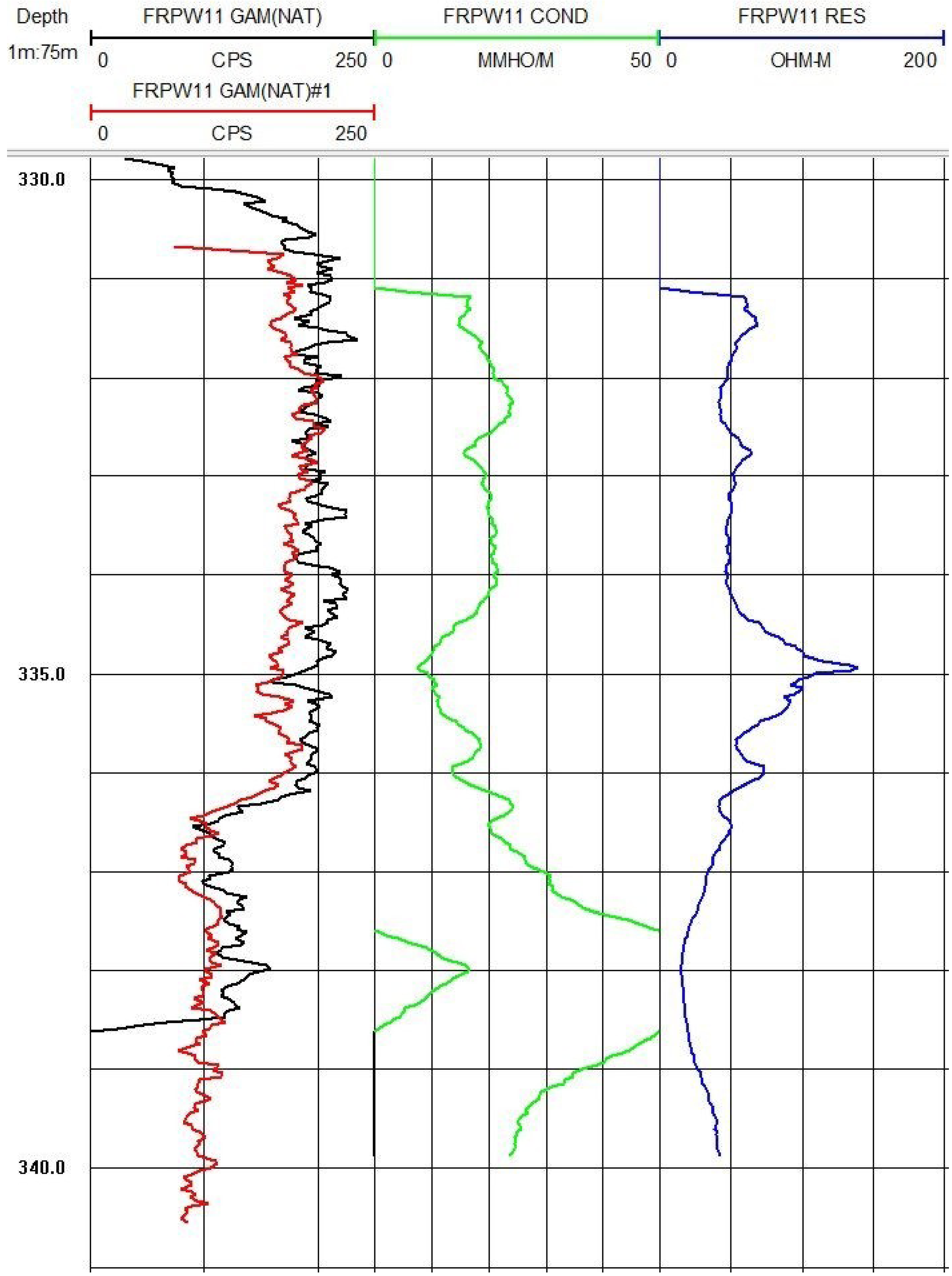

Figure D-12. Borehole geophysical log for FRPW11.

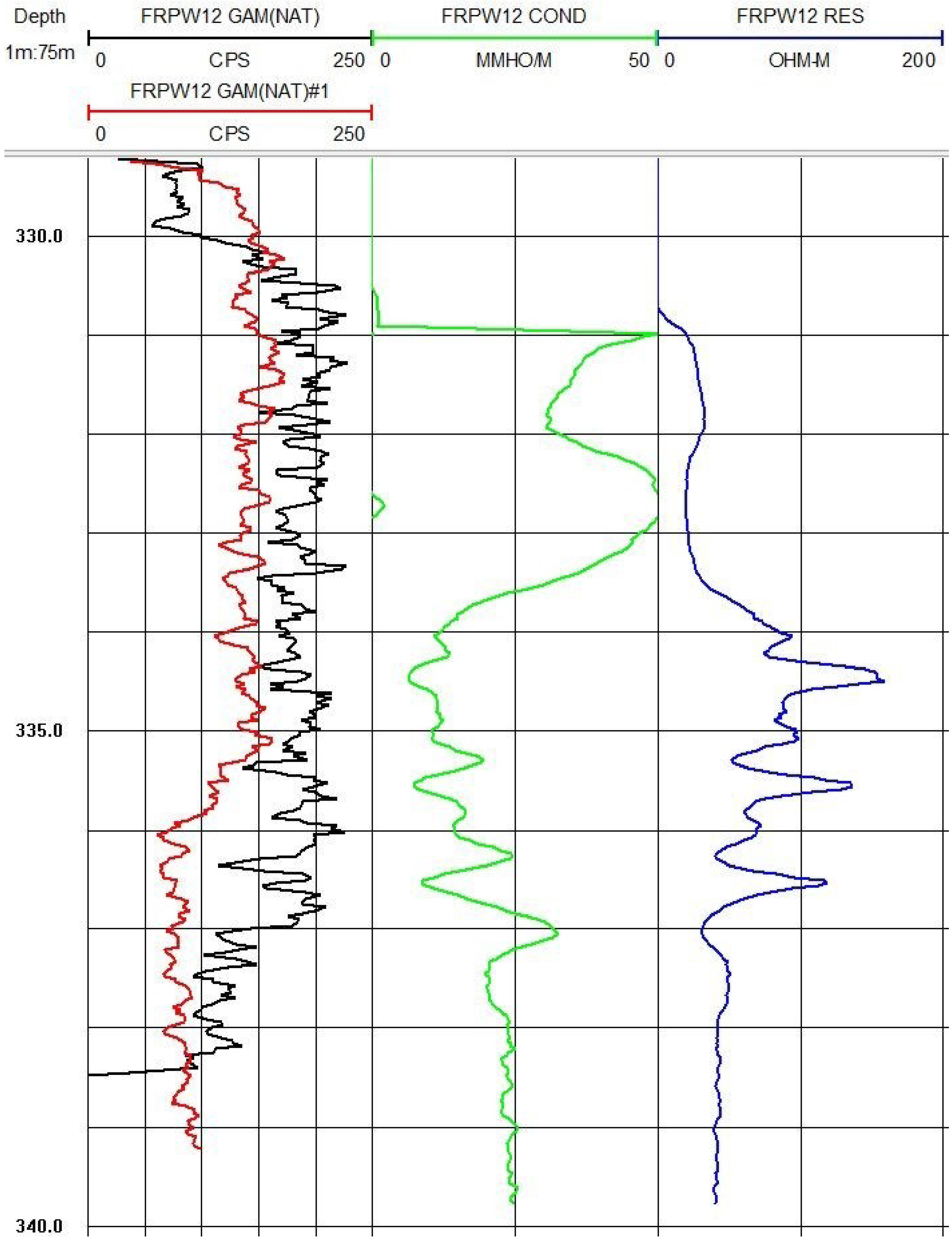

Figure D-13. Borehole geophysical log for FRPW12.

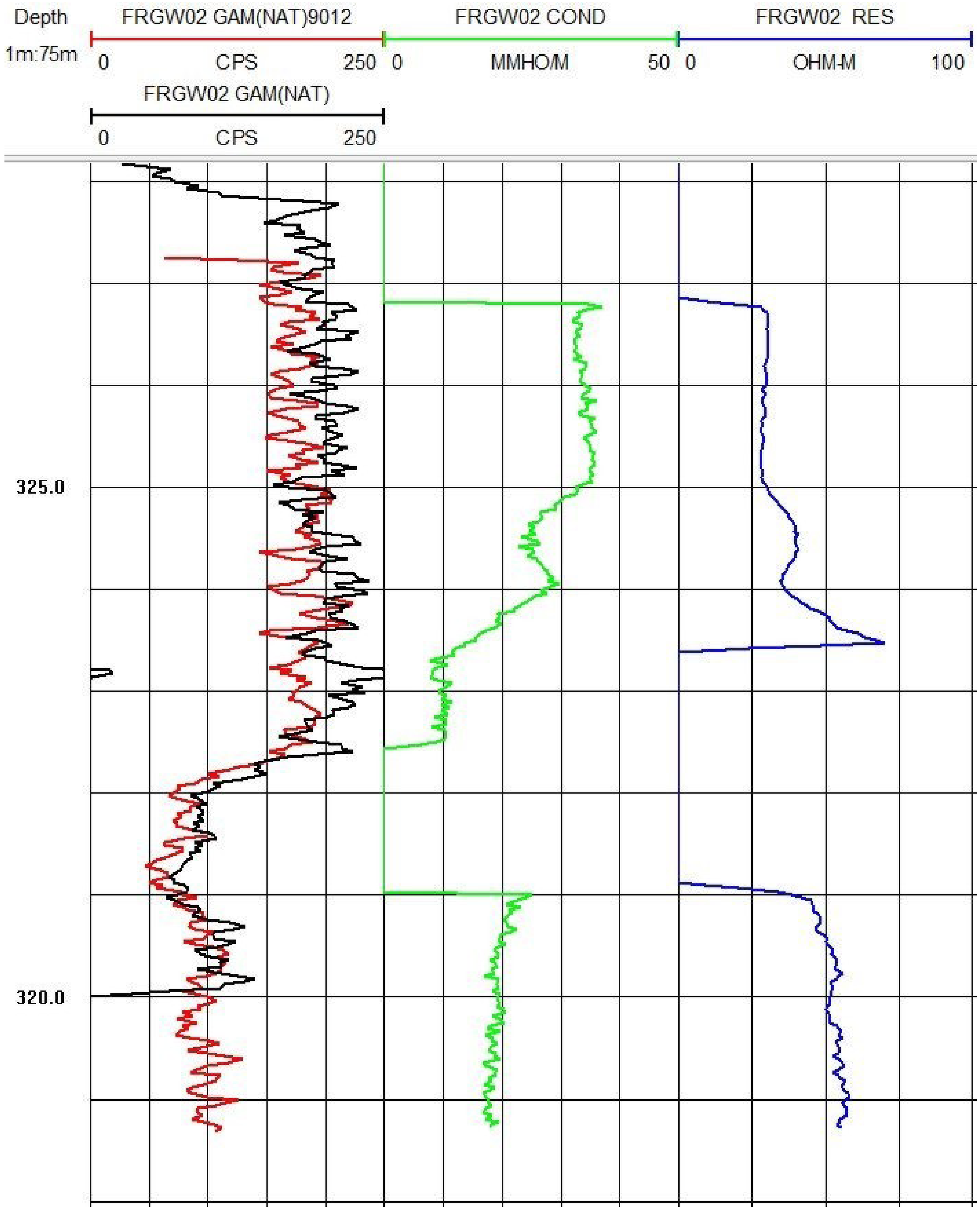

Figure D-14. Borehole geophysical log for FRGW02.

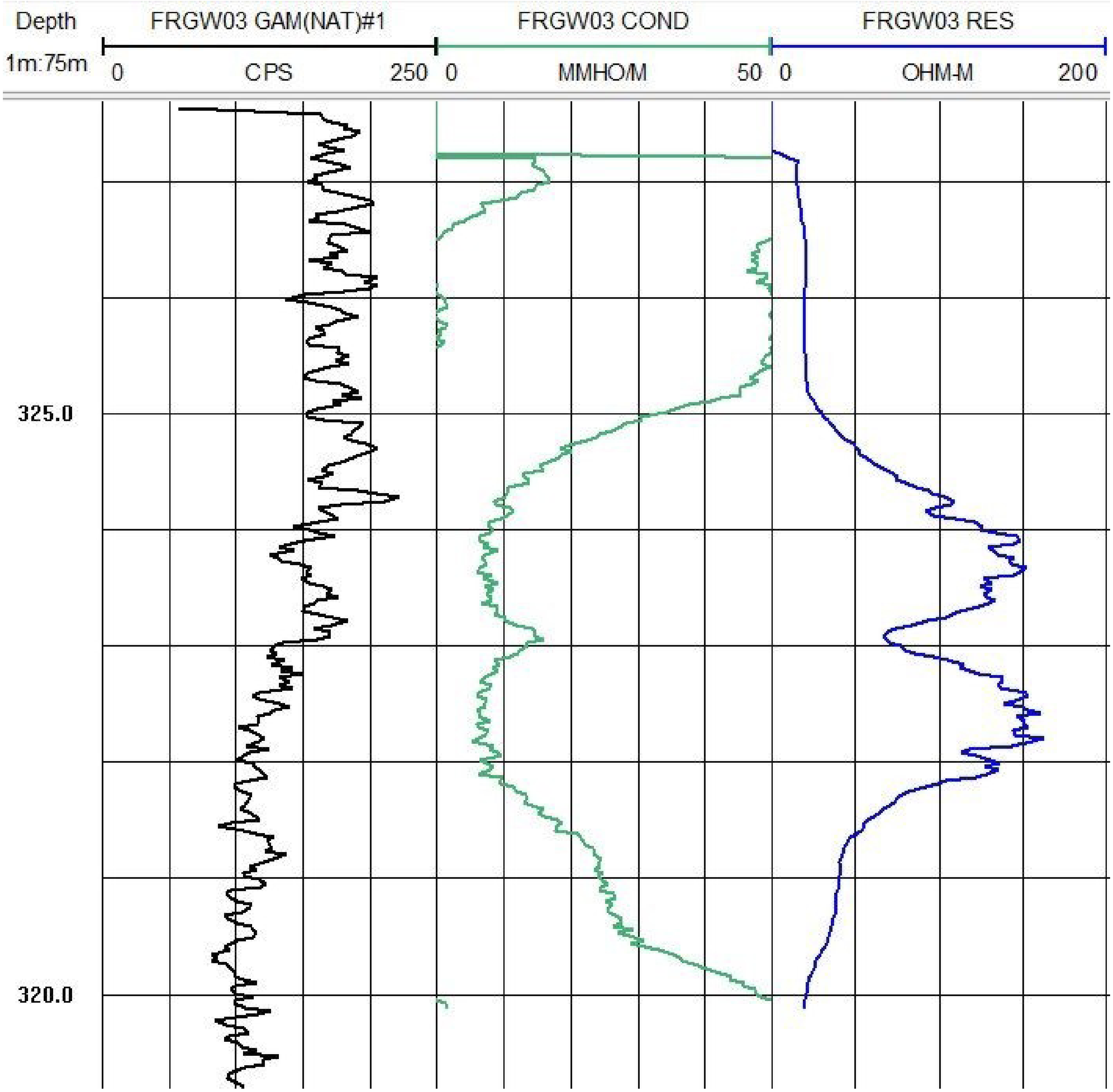

Figure D-15. Borehole geophysical log for FRGW03.

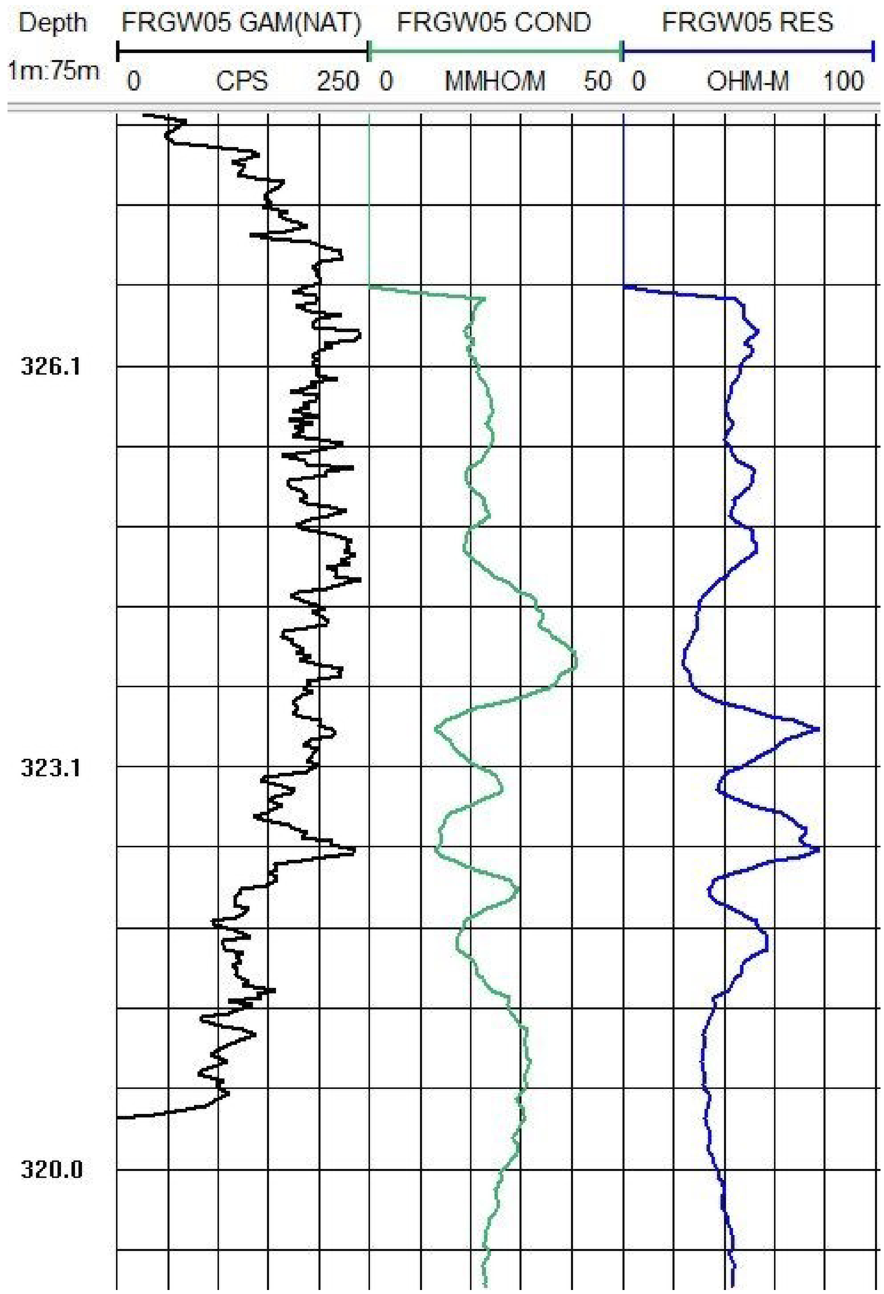

Figure D-16. Borehole geophysical log for FRGW05.

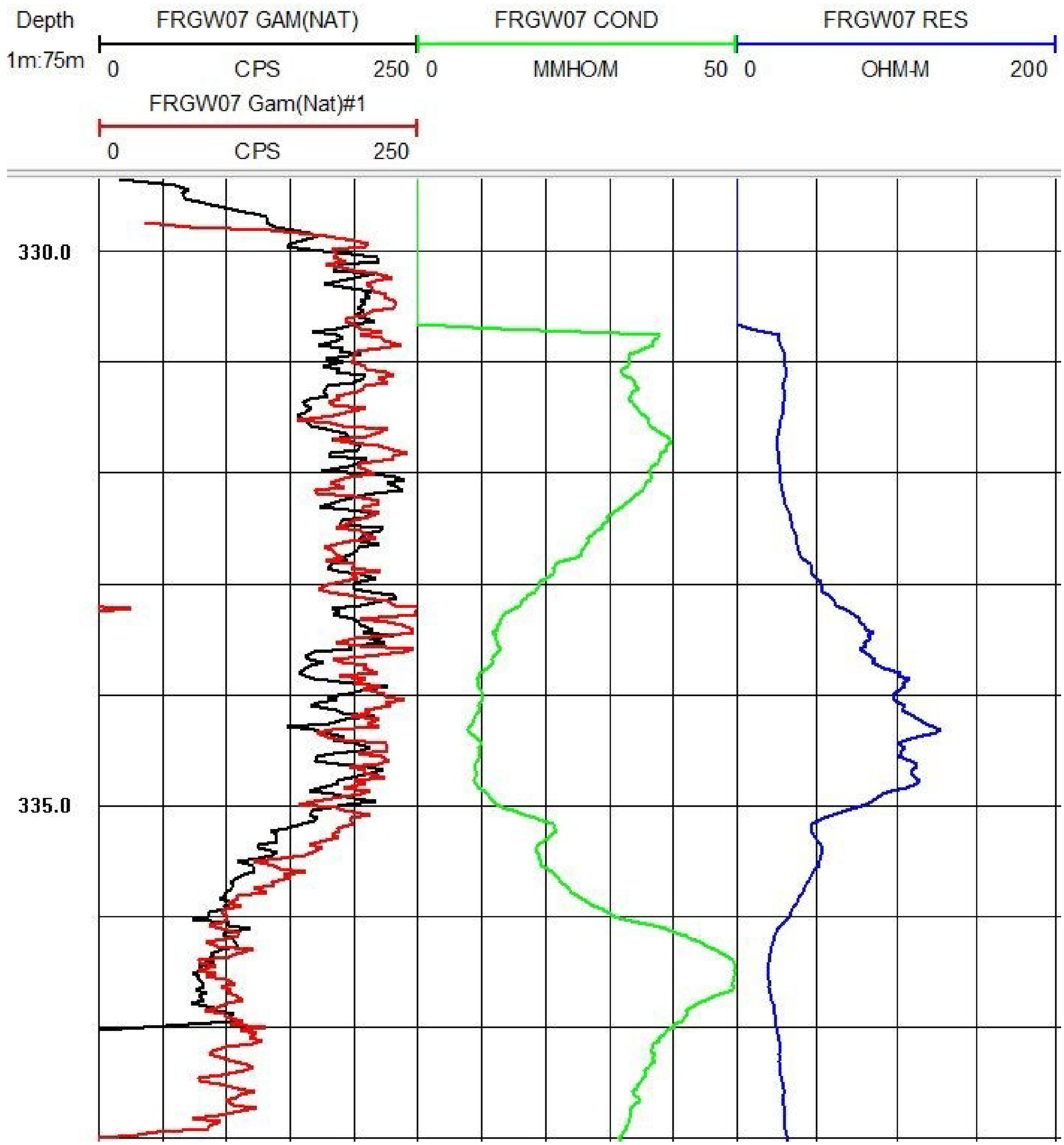

Figure D-17. Borehole geophysical log for FRGW07.

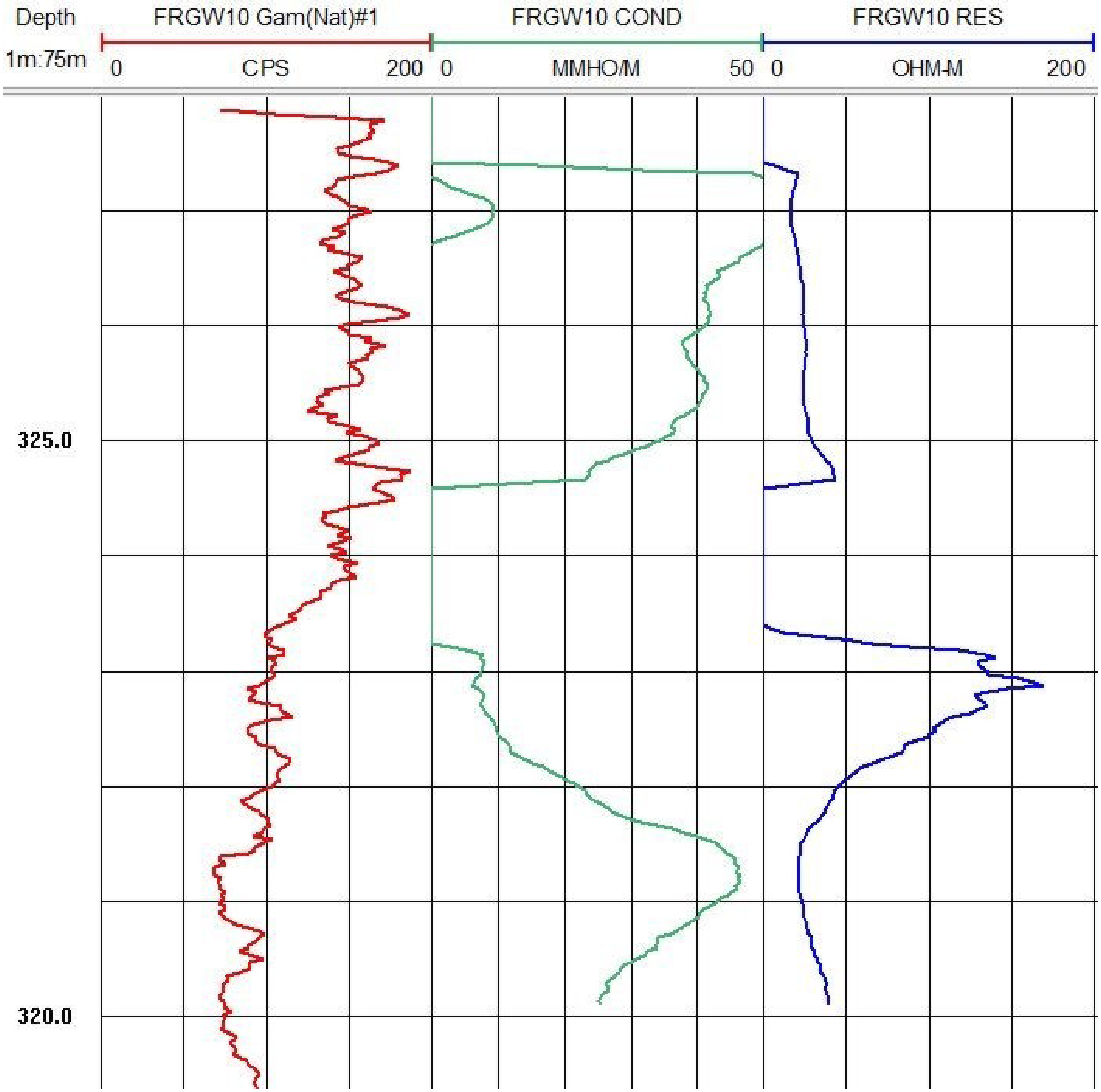

Figure D-18. Borehole geophysical log for FRGW10.

Hydrogeology Figures

3.1 Groundwater Flow Field Characterization

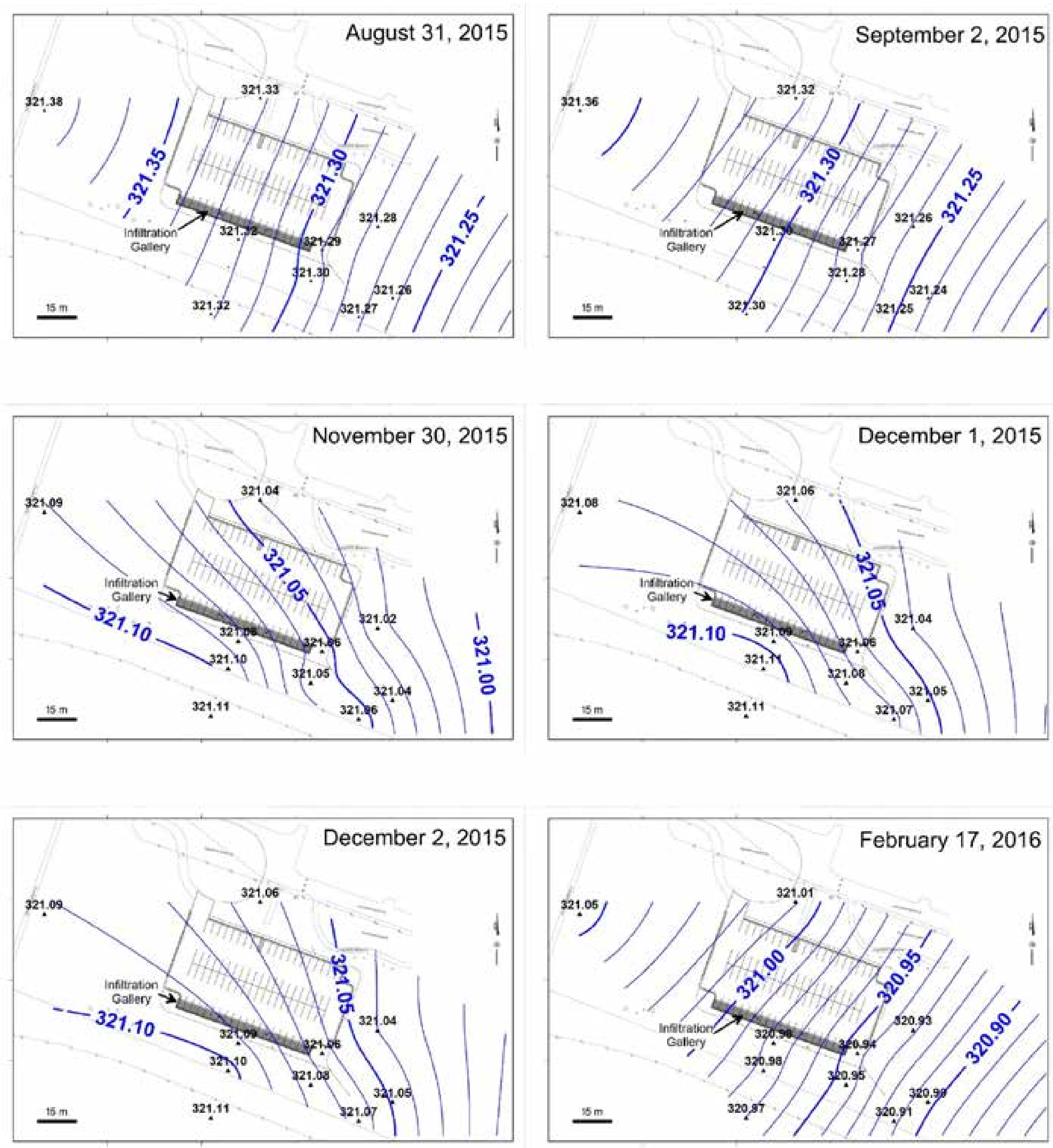

Figure D-19. Potentiometric surface maps representative of water table elevations near the infiltration gallery at the Fort Riley, Kansas, study site. Hydraulic head data were obtained from manual measurements on indicated dates. Water table elevations are posted and contoured (blue contours) using a 0.01 m contour interval.

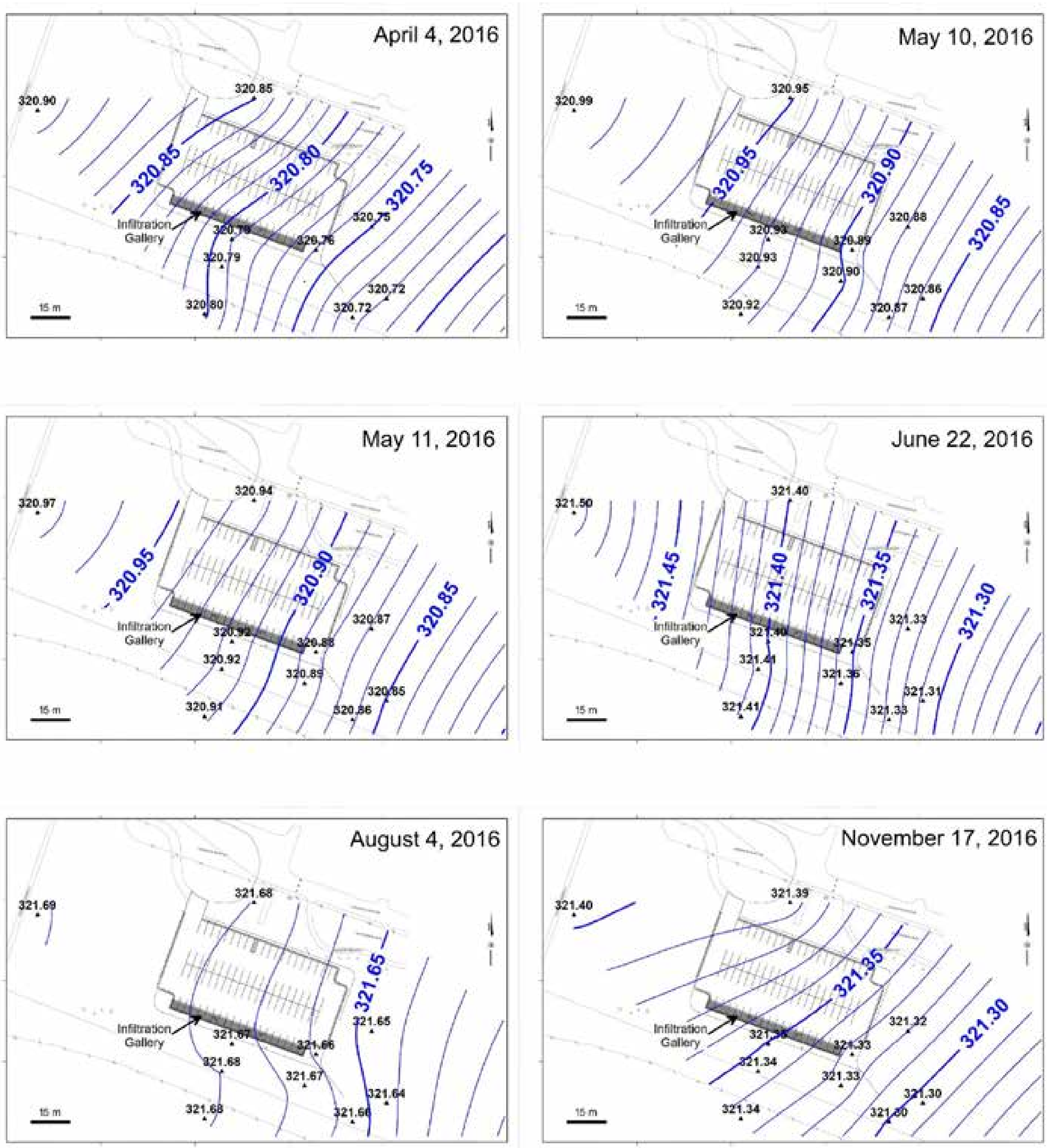

Figure D-19 (continued). Potentiometric surface maps representative of water table elevations near the infiltration gallery at the Fort Riley, Kansas, study site. Hydraulic head data were obtained from manual measurements on indicated dates. Water table elevations are posted and contoured (blue contours) using a 0.01 m contour interval.

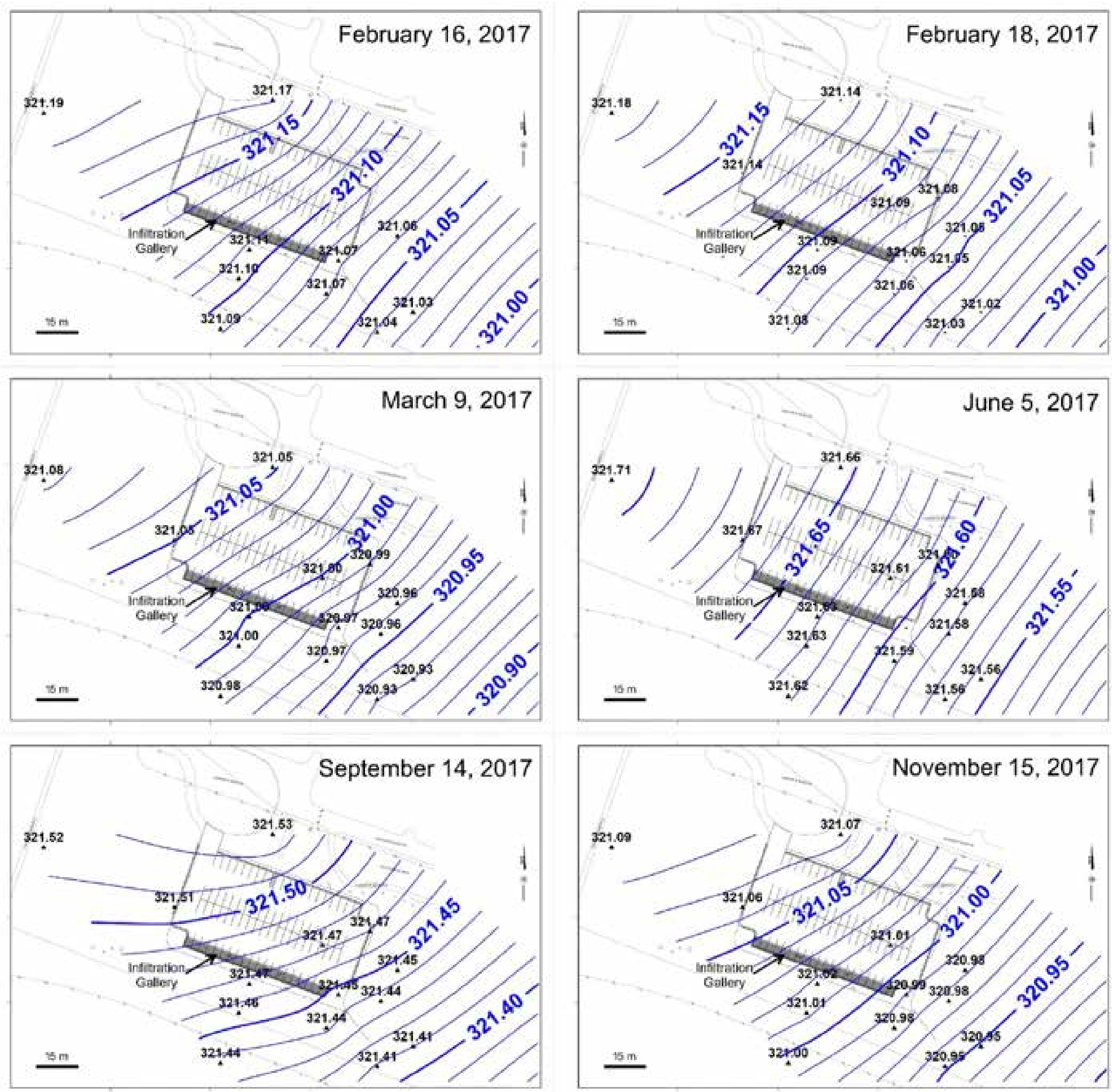

Figure D-19 (continued). Potentiometric surface maps representative of water table elevations near the infiltration gallery at the Fort Riley, Kansas, study site. Hydraulic head data were obtained from manual measurements on indicated dates. Water table elevations are posted and contoured (blue contours) using a 0.01 m contour interval.

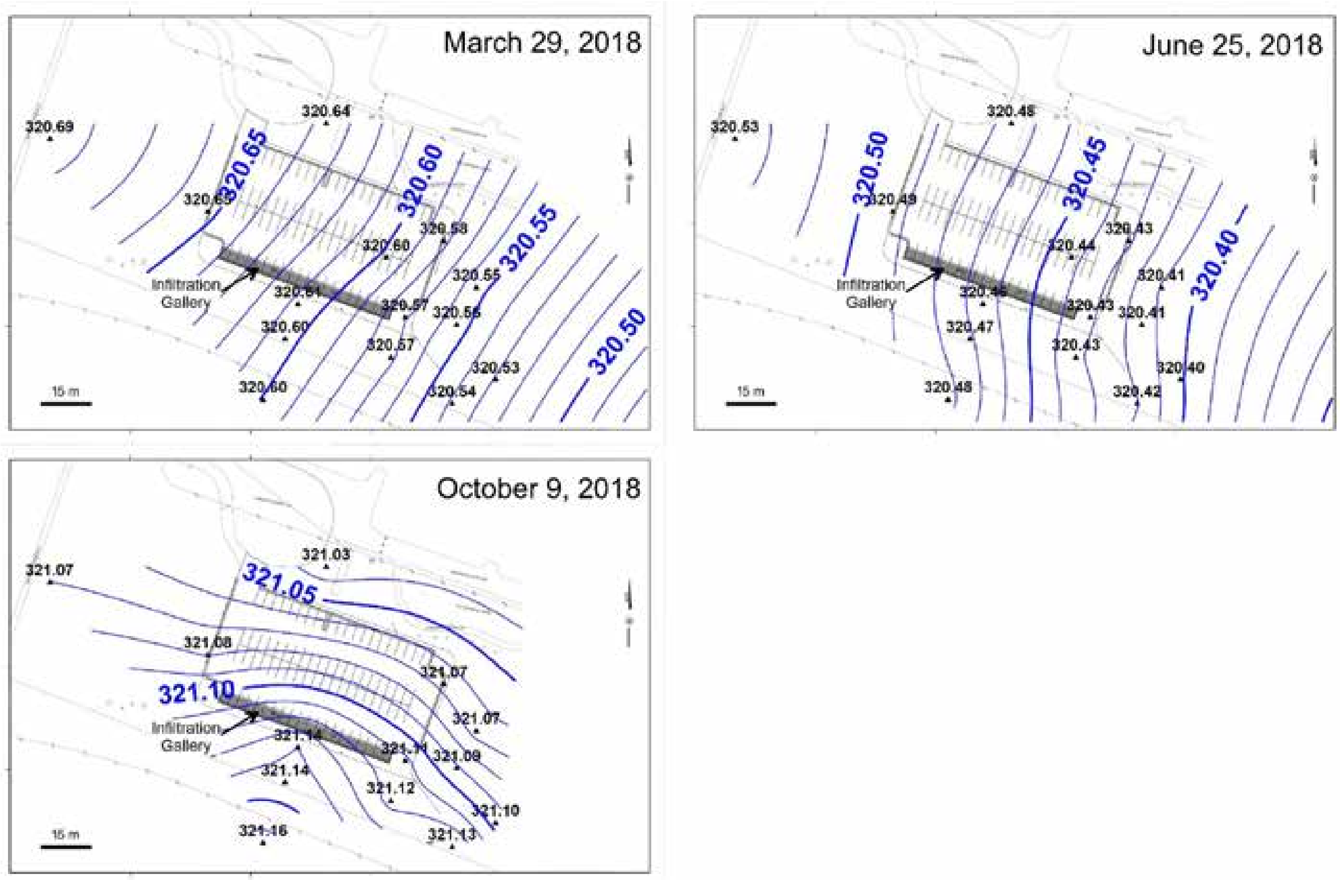

Figure D-19 (continued). Potentiometric surface maps representative of water table elevations near the infiltration gallery at the Fort Riley, Kansas, study site. Hydraulic head data were obtained from manual measurements on indicated dates. Water table elevations are posted and contoured (blue contours) using a 0.01 m contour interval.

Vadose Zone

4.1 Precipitation Patterns during the Study

Table D-2. Monthly precipitation summary for the Fort Riley study, 2015- 2018.

Month	Number of Precipitation Events	Total Precipitation	Mean Precipitation per event	Standard Deviation	Median Precipitation per Event	Maximum Precipitation Event
		mm	mm	mm	mm	mm
2015 (977 mm)						
January	1	4.83	4.83	--	4.83	4.83
February	5	31.0	6.20	11.1	0.76	25.9
March	6	10.9	1.82	1.68	1.52	4.32
April	10	52.3	5.23	7.61	1.52	19.6
May	15	211	14.1	15.7	10.4	64.0
June	10	136	13.6	10.1	12.3	27.9
July	12	132	11.0	19.6	4.45	71.1
August	6	100	16.7	14.2	13.2	41.7
September	6	77.2	12.9	17.5	2.79	43.7
October	2	17.8	8.89	12.6	8.89	17.8
November	8	128	15.9	16.0	13.0	38.9
December	9	76.2	8.47	14.5	1.27	38.6
2016 (957 mm)						
January	4	9.91	2.48	2.65	1.78	6.10
February	2	11.2	5.59	6.47	5.59	10.2
March	10	15.2	1.52	2.04	0.89	6.35
April	6	101	16.9	14.0	17.7	40.9
May	11	179	16.3	17.9	7.37	58.2
June	5	29.2	5.84	10.0	1.52	23.6
July	10	180	18.0	13.3	15.0	40.1
August	10	208	20.8	13.6	19.4	43.9
September	6	82.0	13.7	13.3	12.8	35.1
October	5	123	24.6	28.5	14.7	74.7
November	1	0.76	0.76	--	0.76	0.76
December	1	17.0	17.0	--	17.0	17.0

Table D-2 (continued). Monthly precipitation summary for the Fort Riley study, 2015- 2018.

Month	Number of Precipitation Events	Total Precipitation	Mean Precipitation per event	Standard Deviation	Median Precipitation per Event	Maximum Precipitation Event
		mm	mm	mm	mm	mm
2017 (704 mm)						
January	4	31.0	7.75	13.3	1.40	27.7
February	1	11.9	11.9	--	11.9	11.9
March	8	111	13.9	15.9	5.97	36.1
April	17	118	6.95	7.80	3.30	26.7
May	5	81.3	16.3	16.6	10.7	44.2
June	9	111	12.4	14.6	4.57	41.1
July	5	42.7	8.53	4.72	6.10	16.5
August	7	129	18.4	33.0	7.37	91.9
September	4	19.1	4.76	5.97	1.91	13.7
October	5	49.5	9.91	14.7	2.03	34.5
November	4	3.56	0.89	1.05	0.76	2.03
December	1	2.29	2.29	--	2.29	2.29
2018 (866 mm)						
January	2	7.62	3.81	3.23	3.81	6.10
February	3	10.4	3.47	2.22	4.06	5.33
March	3	14.5	4.83	3.58	4.32	8.64
April	9	30.5	3.39	3.41	1.78	8.89
May	7	87.9	12.6	13.2	5.84	34.3
June	9	50.3	5.59	5.00	3.05	15.2
July	9	112.8	12.5	15.4	6.86	46.2
August	11	129.8	11.8	19.1	3.30	62.0
September	8	175.5	21.9	40.9	9.78	122
October	9	154.9	17.2	12.8	15.5	38.9
November	4	21.1	5.27	2.98	4.57	9.40
December	4	65.3	16.3	8.52	16.1	25.4

4.2 Alkalinity, Major Anions and Cations, pH, Specific Conductivity

4.2.1 Specific Conductivity – Soil Porewater

Specific conductivity for SPWs at the Fort Riley site ranged from 438 – 17,770 µS/cm (Figure D-20). The SPW clusters (1 and 2; Figure D-20A and B, respectively) showed several spikes in SPC when compared with the control FRLW12. In cluster 1, FRLW01 showed SPC spikes in March of 2017 and 2018 but there were no spikes in SPC for FRLW02 (Figure D-20A). Similarly, in cluster 2, there was no spike in SPC for FRLW10, but there were spikes in SPC for FRLW09 in April 2016, March 2017 and 2018 (Figure D-20B). Both FRLW01 and FRLW09 are the shallowest SPWs beneath the infiltration gallery, whereas FRLW02 and FRLW10 are the deepest SPW beneath the infiltration gallery. Specific conductivity in FRLW12 shows a significant decrease in SPC ($p = 0.043$) with time and with the SPC spikes removed FRLW01 also showed a significant decreasing trend in SPC ($p = 0.068$). FRLW02, FRLW09, and FRLW10 showed no trends in SPC. Figure C-20C shows the SPC data with respect to time for SPW cluster 3, FRLW03 and FRLW05 which are 0.6 m form the infiltration gallery wall. Both SPWs showed a spike in SPC in March 2018 and FLRW05 the spike was still present in June 2018 when compared with FRLW12. FRLW03 is the shallowest SPW in this cluster and is at a similar depth to the bottom of the infiltration gallery. FRLW05 is the deepest SPW in this cluster and its depth is the same as FRLW01 and FRLW09. When the spikes are removed, neither of these SPWs show a trend in SPC and the SPC is like that of FRLW12 in magnitude. In SPW cluster 4, FRLW06, FRLW07, and FRLW08, there were spikes in the SPW data in June 2018 (Figure C-20D). This SPW cluster is 3.1 m from the infiltration gallery wall and the depths are the same as in SPWs cluster 3. When the spikes in the data are removed the SPC magnitude was nearly the same as FRLW12 with a significant decreasing trend in SPC in FRLW07 ($p = 0.023$) and no trend in FRLW09. FRLW06 did not show a trend.

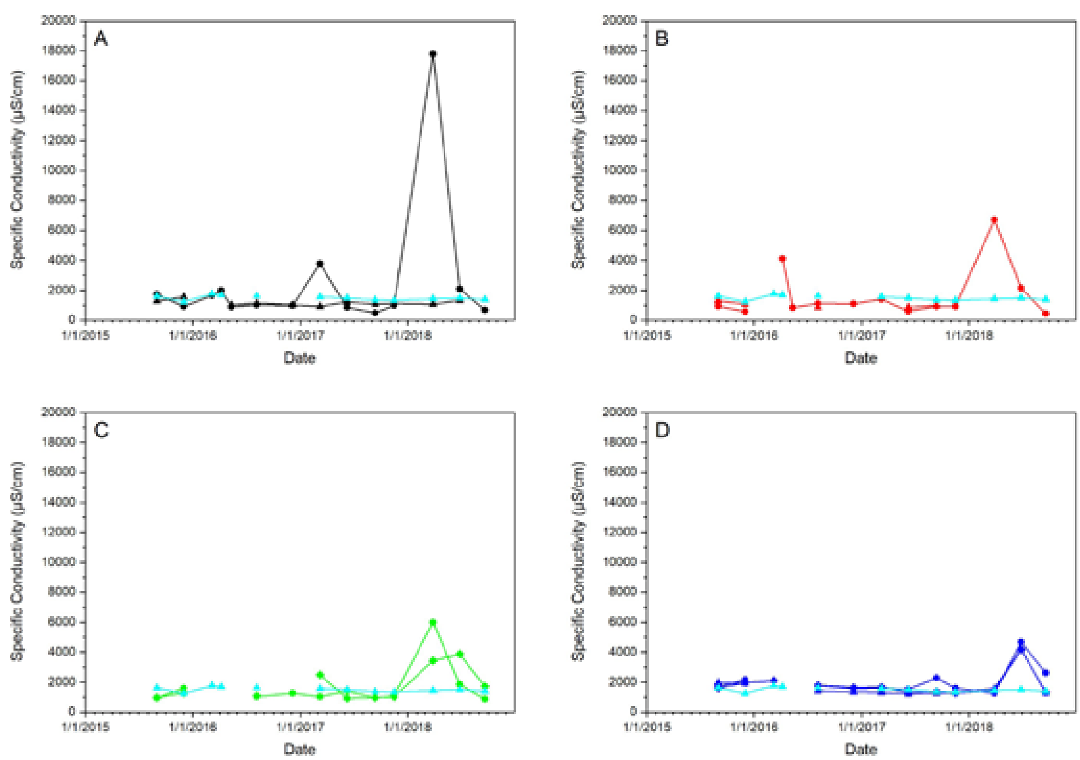

Figure D-20. Changes in Specific Conductivity in relationship to time for the Fort Riley SPWs. In all graphs the cyan triangles and lines represent FRLW12 the unimpacted control. A. SPW cluster 1, black circles and lines are FRLW01, black triangles and lines are FRLW02. B. SPW cluster 2, red circles and lines are FRLW09, red triangles and lines are FRLW10. C. SPC cluster 3, green circles and lines are FRLW03, green diamonds and lines are FRLW05. D. SPW cluster 4, blue circles and lines are FRLW06, blue triangles and lines are FRLW07, blue diamonds and lines are FRLW08.

4.2.2 Chloride – Soil Porewater

Figure D-21 shows the relationship between chloride concentrations and time for the SPW samplers. Chloride concentrations ranged from 0.72 – 6,160 mg/L in SPW samples. As was the case with SPC, chloride showed spikes in concentrations in all the SPW clusters except for the control SPW sampler (FRLW12). In SPW cluster 1 (Figure D-21A), three spikes were observed in FRLW01 in April 2016, March 2017 and 2018. Similarly, in SPW cluster 2 two chloride spikes were observed in FRLW09 (April 2016 and March 2018) and no chloride spike in FRLW10 (Figure D-21B). In the control SPW, FRLW12 there was no trend in the chloride concentrations, which was what was observed for FRLW02 and FRLW10 the deeper SPW beneath the infiltration galleries. However, the shallower SPW beneath the infiltration gallery, FRLW01 and FRLW09 both had decreasing trends in chloride concentration with FRLW01 having a significant trend (p = 0.43). Spikes in the chloride concentrations were also observed in SPW cluster 3 (Figure D-21C). FRLW03 had chloride spikes in May 2016, March 2018 – June 2018 and FRLW05 showed spikes in the chloride concentrations in March 2018 – June 2018. Chloride trends in FRLW03 showed significant decreasing chloride concentrations (p = 0.035), but there was no trend in chloride concentrations in FRLW05. SPW cluster 4 had a spike in chloride concentration in June 2018 in FRLW06, FRLW07, and FRLW08 (Figure D-21D). There were no trends in chloride concentrations in FRLW06 and FRLW08, but there was an increasing trend in chloride concentrations (p = 0.043) in FRLW07.

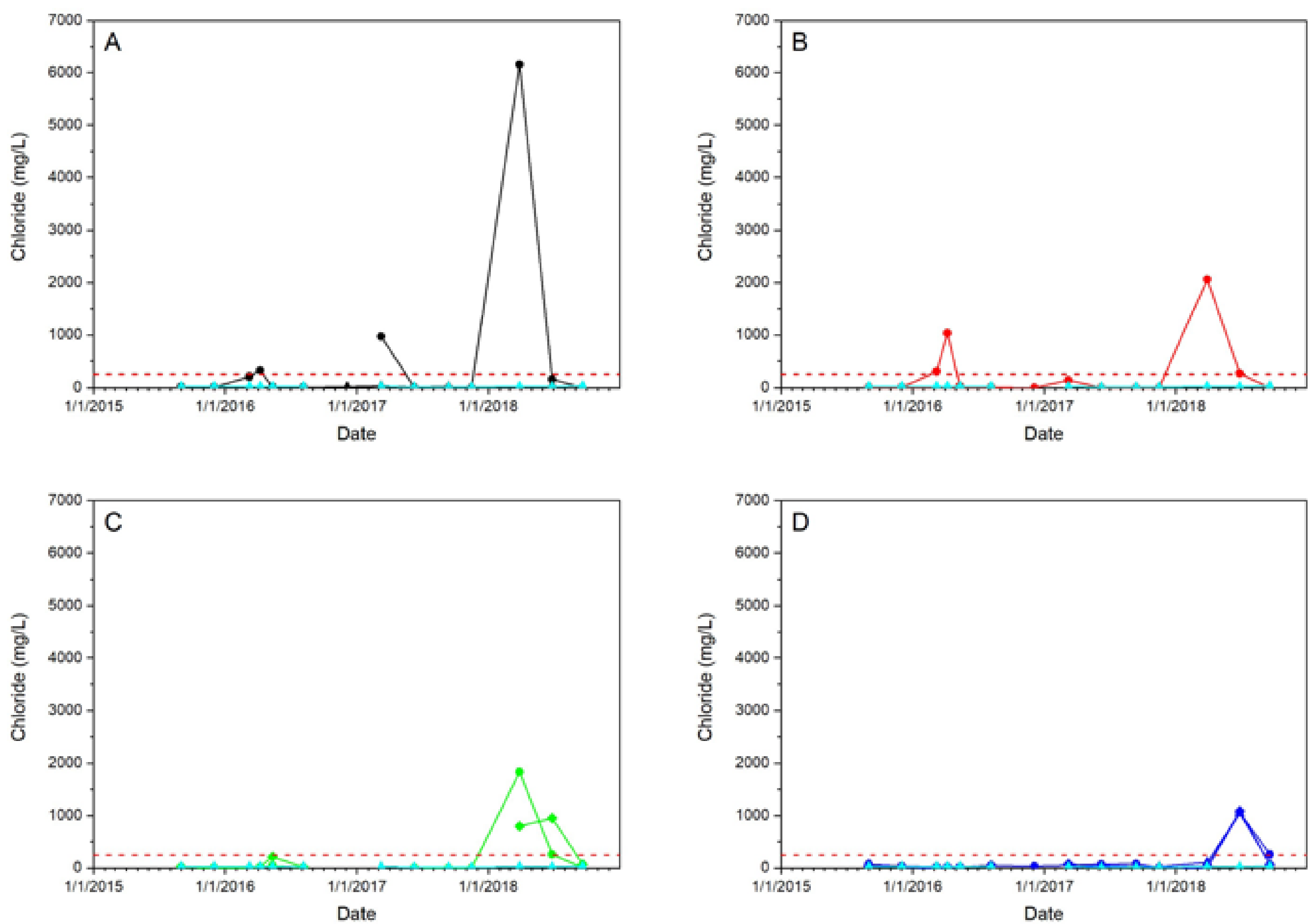

Figure D-21. Changes in chloride in relationship to time for the Fort Riley SPWs. In all graphs the cyan triangles and lines represent FRLW12 the unimpacted control. A. SPW cluster 1, black circles and lines are FRLW01, black triangles and lines are FRLW02. B. SPW cluster 2, red circles and lines are FRLW09, red triangles and lines are FRLW10. C. SPC cluster 3, green circles and lines are FRLW03, green diamonds and lines are FRLW05. D. SPW cluster 4, blue circles and lines are FRLW06, blue triangles and lines are FRLW07, blue diamonds and lines are FRLW08.

4.2.3 Sodium – Soil Porewater

Sodium concentrations ranged from 4.55 – 1,469 mg/L in SPWs. Figure D-22 shows the relationship between sodium concentrations with time for the SPWs. In SPW cluster 1, FRLW01 showed spikes in the sodium concentration in March 2017 and a major spike in sodium concentration in March 2018 (Figure D-22A). The spike in sodium concentration in FRLW01 still had not reached background concentrations by September 2018. Because of the lack of sample volume collected in FRLW02, it was unknown if spikes occurred in March of 2017 or 2018 (Figure D-22A). FRLW12 did not show a trend in sodium concentrations as was the case FRLW02. FRLW01, on the other hand, did show an increasing significant trend in sodium concentrations ($p = 0.098$). SPW cluster 2 sodium concentration spikes were similar to Cluster 1 but the magnitude of the sodium spike in FRLW09 was considerably less than what was observed in FRLW01 (Figure D-22B). The lack of sample volume in FRLW10 when the sodium spikes occurred in FRLW01 and FRLW09 did not allow for the determination if sodium spikes occurred in FRLW10 (Figure D-22B). The trend in FRLW09 showed decreasing sodium concentration ($p = 0.098$), and FRLW10 showed no trend in sodium concentration. Because of the sample volumes collected, no analysis of SPW cluster 3 could be undertaken (Figure D-22C). No sodium spikes were observed in SPW cluster 4 during the study (Figure D-22D). In cluster 4, only FRLW07 showed a trend in sodium concentration and this was a significant decreasing trend ($p = 0.010$).

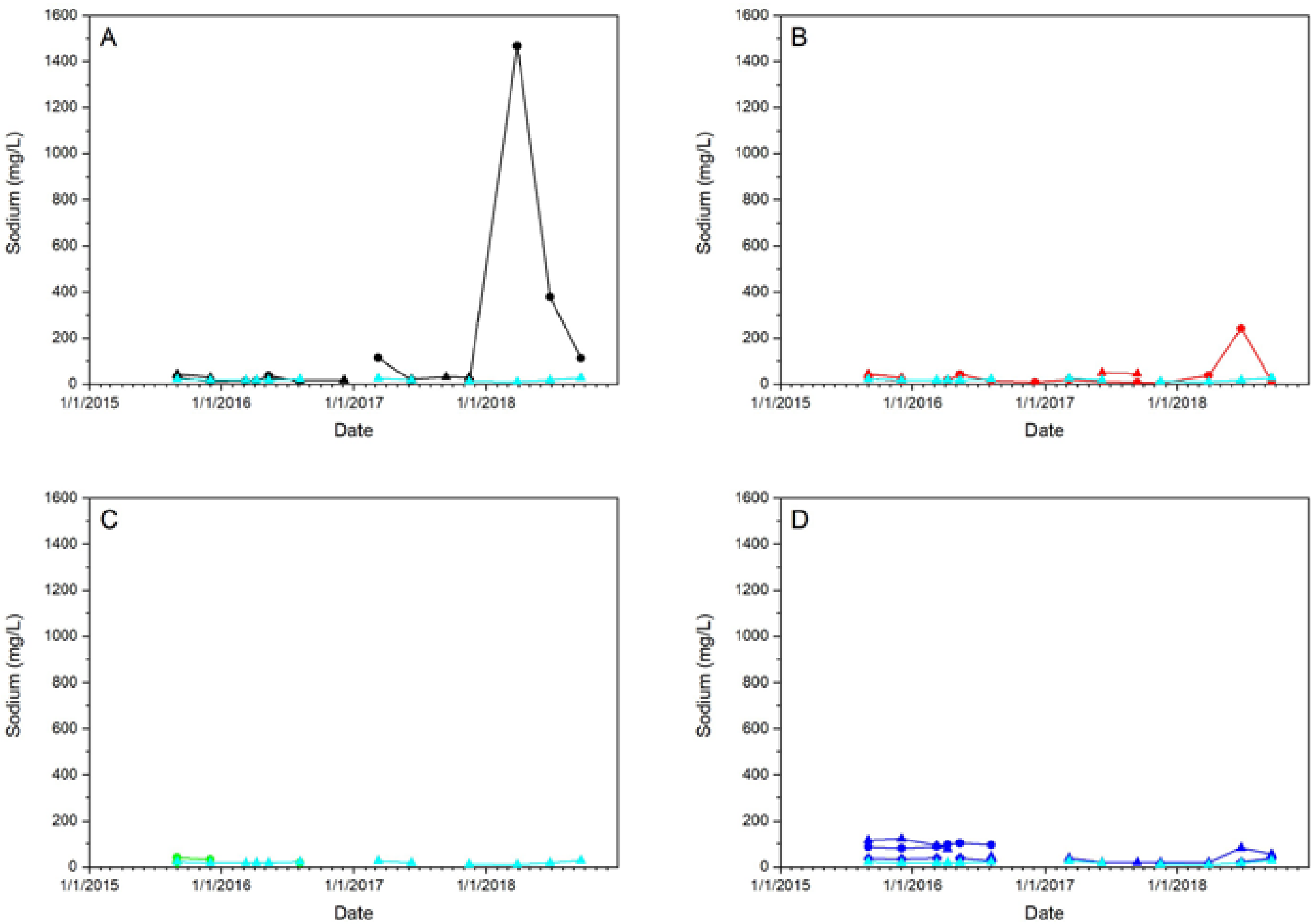

Figure D-22. Changes in sodium in relationship to time for the Fort Riley SPWs. In all graphs the cyan triangles and lines represent FRLW12 the unimpacted control. A. SPW cluster 1, black circles and lines are FRLW01, black triangles and lines are FRLW02. B. SPW cluster 2, red circles and lines are FRLW09, red triangles and lines are FRLW10. C. SPC cluster 3, green circles and lines are FRLW03, green diamonds and lines are FRLW05. D. SPW cluster 4, blue circles and lines are FRLW06, blue triangles and lines are FRLW07, blue diamonds and lines are FRLW08.

4.2.4 Calcium and Magnesium – Soil Porewater

Calcium and magnesium concentrations ranged from 39.3 – 1,289 mg/L and 10.4 – 452 mg/L, respectively. Calcium concentration trends with time are shown in Figure D-23, and magnesium concentration trends with time are shown in Figure D-24. Spikes in calcium and magnesium concentrations in SPW clusters 1, 2, and 3 follow what was previously discussed for sodium; however, the trend in calcium concentration for FRLW12 was decreasing significantly ($p < 0.001$) as were the calcium concentration trend in FRLW01 ($p = 0.020$) and FRLW02 ($p = 0.031$). There were no trends in calcium concentrations in FRLW09 and FRLW10 or any of the SPWs in cluster 4. Magnesium concentration trends followed those of calcium except there was no trend in FRLW12.

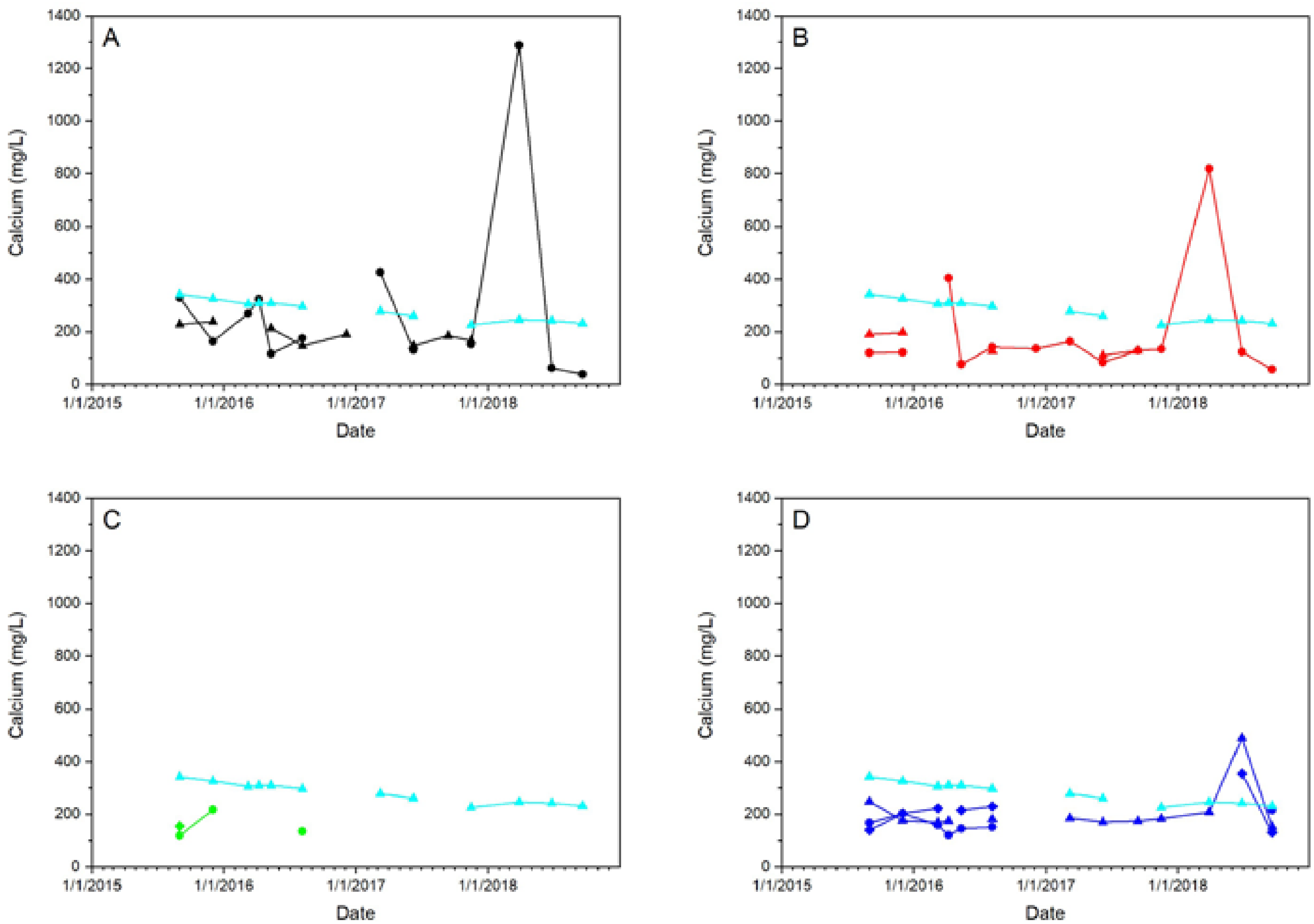

Figure D-23. Changes in calcium in relationship to time for the Fort Riley SPWs. In all graphs the cyan triangles and lines represent FRLW12 the unimpacted control. A. SPW cluster 1, black circles and lines are FRLW01, black triangles and lines are FRLW02. B. SPW cluster 2, red circles and lines are FRLW09, red triangles and lines are FRLW10. C. SPC cluster 3, green circles and lines are FRLW03, green diamonds and lines are FRLW05. D. SPW cluster 4, blue circles and lines are FRLW06, blue triangles and lines are FRLW07, blue diamonds and lines are FRLW08.

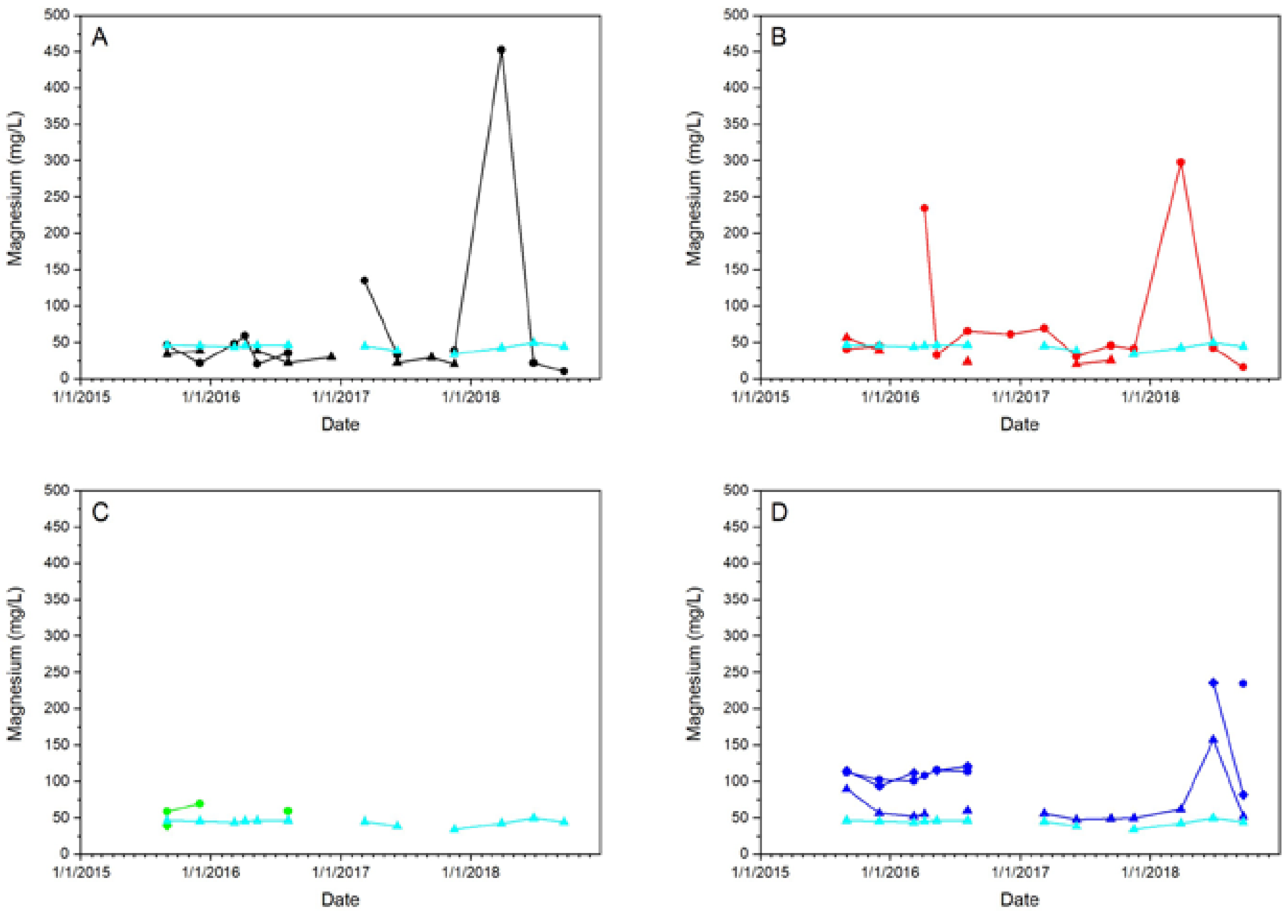

Figure D-24. Changes in magnesium in relationship to time for the Fort Riley SPWs. In all graphs the cyan triangles and lines represent FRLW12 the unimpacted control. A. SPW cluster 1, black circles and lines are FRLW01, black triangles and lines are FRLW02. B. SPW cluster 2, red circles and lines are FRLW09, red triangles and lines are FRLW10. C. SPC cluster 3, green circles and lines are FRLW03, green diamonds and lines are FRLW05. D. SPW cluster 4, blue circles and lines are FRLW06, blue triangles and lines are FRLW07, blue diamonds and lines are FRLW08.

4.2.5 Bicarbonate – Soil Porewater

Changes in bicarbonate concentrations are shown in Figure D-25 and bicarbonate concentrations range from 186 – 1,081 mg HCO_3^-/L in the SPW samples. Because of the difficulty in obtaining sufficient sample volumes during the study, there were many missing data points for bicarbonate in all the SPW sampler locations. Therefore, spikes in bicarbonate concentrations were difficult to identify in most SPW sampler locations. Only FRLW01 in June 2018 was there enough data to identify a spike in bicarbonate concentrations, and this could not be compared to control SPW (Figure D-25A). Trend analysis of bicarbonate concentration accessed for several SPWs given the bicarbonate data collected. There were no trends in bicarbonate concentrations for FRLW01, FRLW08, FRLW09, and FRLW12. Both FRLW02 and FRLW07 had significant decreasing bicarbonate concentrations ($p = 0.028$ and $p = 0.008$, respectively).

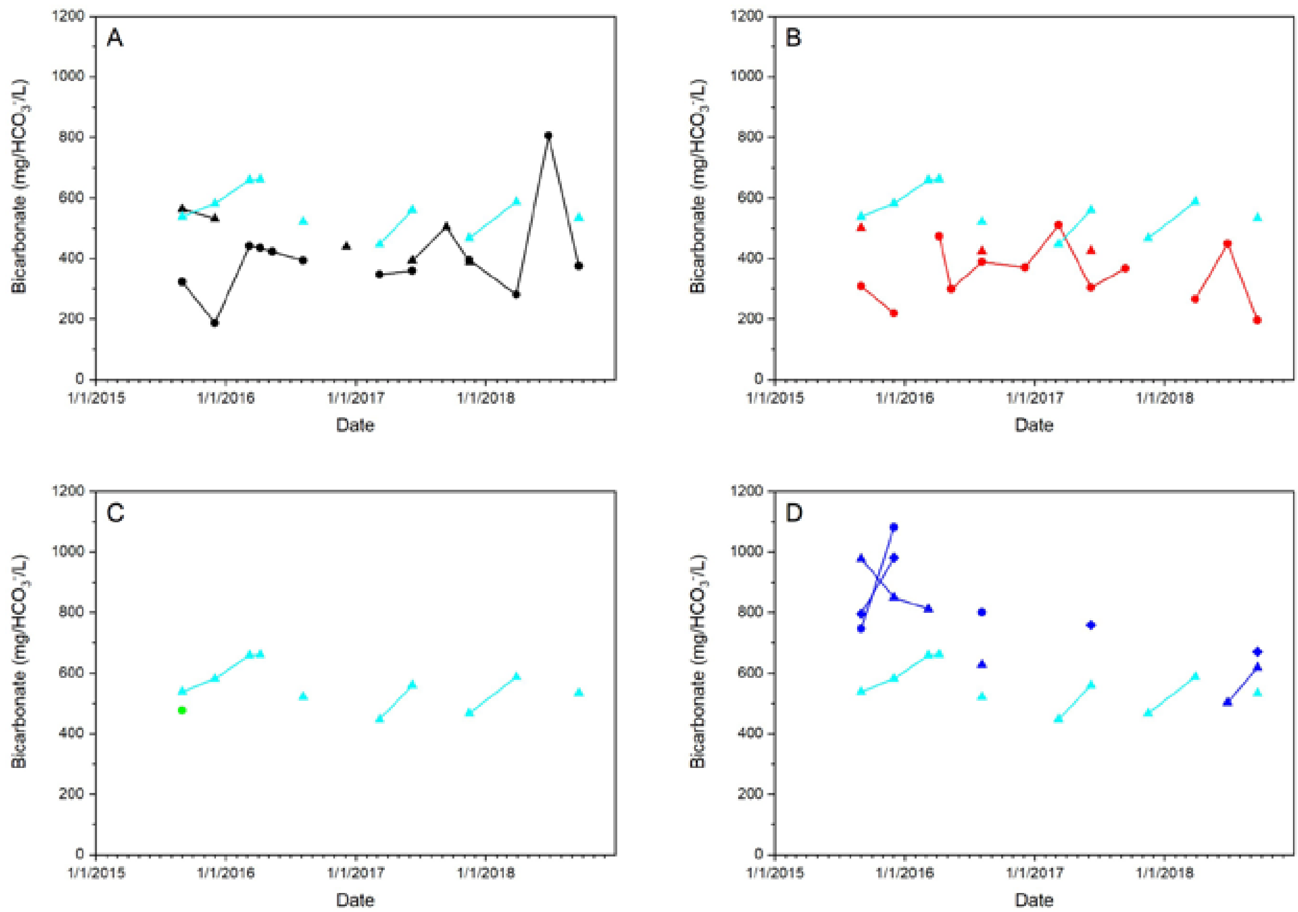

Figure D-25. Changes in bicarbonate in relationship to time for the Fort Riley SPWs. In all graphs the cyan triangles and lines represent FRLW12 the unimpacted control. A. SPW cluster 1, black circles and lines are FRLW01, black triangles and lines are FRLW02. B. SPW cluster 2, red circles and lines are FRLW09, red triangles and lines are FRLW10. C. SPC cluster 3, green circles and lines are FRLW03, green diamonds and lines are FRLW05. D. SPW cluster 4, blue circles and lines are FRLW06, blue triangles and lines are FRLW07, blue diamonds and lines are FRLW08.

4.2.6 Potassium – Soil Porewater

Potassium concentrations in the SPWs ranged from 2.55 – 86.6 mg/L during the study. Figure D-26 shows the changes in potassium concentration as a function of time. In SPW cluster 3, because of the limited sample volume collected, there was one sample collected for FRLW05 and only three dates for FRLW03 (Figure D-26C). For cluster 3, no trend data or spikes in potassium concentrations could be obtained. In SPW cluster 1, there were no clear spikes in the K concentrations, and the potassium concentrations in both FRLW01 and FRLW02 decreased more than in FRLW12. FRLW12 had a decreasing trend in potassium concentration and it was significant ($p = 0.076$). FRLW01 and FRLW02 both had significant decreases in potassium concentration ($p = 0.002$ and $p = 0.007$, respectively). As was the case in SPW cluster 1, SPW cluster 2 had no clear spikes in potassium concentration (Figure D-26B). FRLW09 had a significant decrease in potassium concentration with time ($p < 0.001$), but there was no trend in FRLW10. Finally, in SPW cluster 4, in all depths the potassium concentrations were initially larger than the control, but the concentration decreased with time (Figure D-26D). There were no trends in FRLW06 and in FRLW07 and the potassium concentrations significantly were decreasing ($p = 0.003$). There were significant decreasing potassium concentrations in FRLW08 ($p = 0.068$).

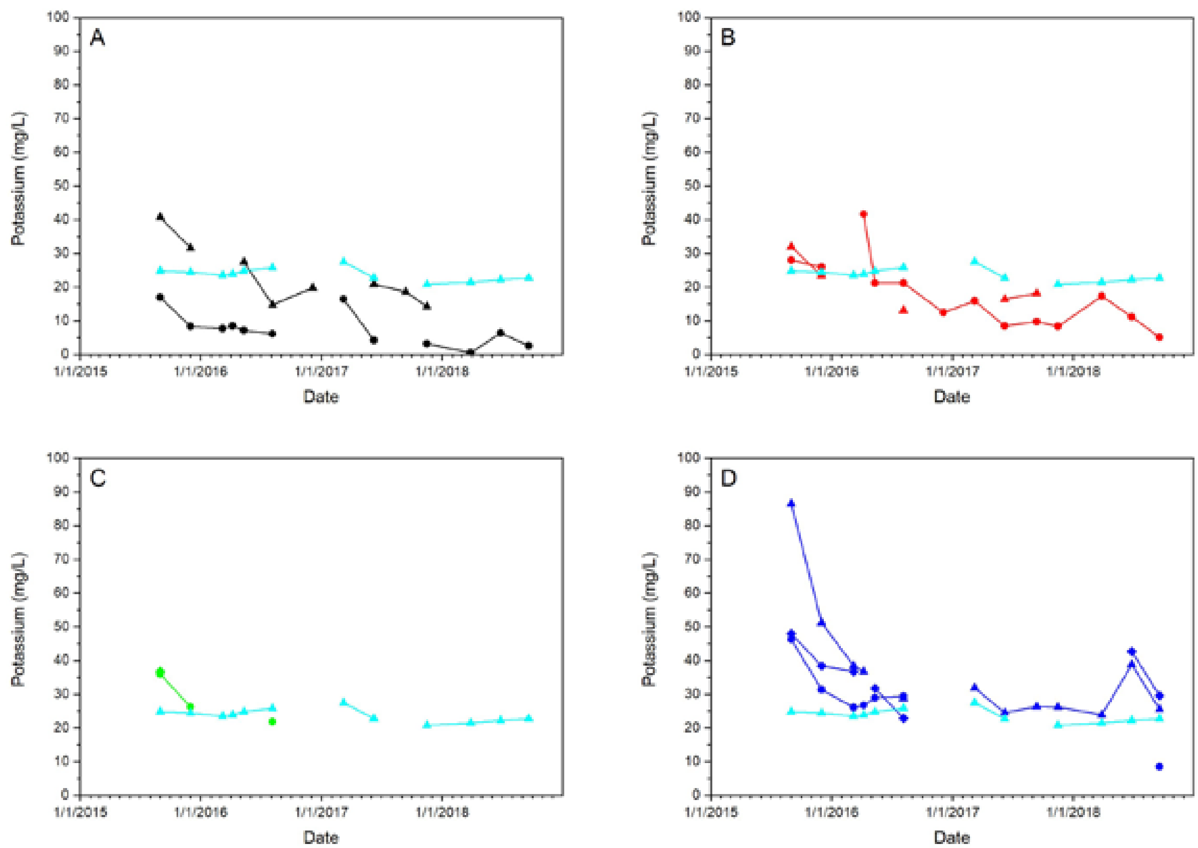

Figure D-26. Changes in potassium in relationship to time for the Fort Riley SPWs. In all graphs the cyan triangles and lines represent FRLW12 the unimpacted control. A. SPW cluster 1, black circles and lines are FRLW01, black triangles and lines are FRLW02. B. SPW cluster 2, red circles and lines are FRLW09, red triangles and lines are FRLW10. C. SPC cluster 3, green circles and lines are FRLW03, green diamonds and lines are FRLW05. D. SPW cluster 4, blue circles and lines are FRLW06, blue triangles and lines are FRLW07, blue diamonds and lines are FRLW08.

4.2.7 pH – Soil Porewater

Figure D-27 shows the time trends for pH in the SPWs. The pH data were quite variable and the pHs ranged from 6.39 – 8.25. Given the variability of pHs in any SPW, it was difficult to assess if spikes in the pH occurred, and there are no trends in pH in any of the SPWs.

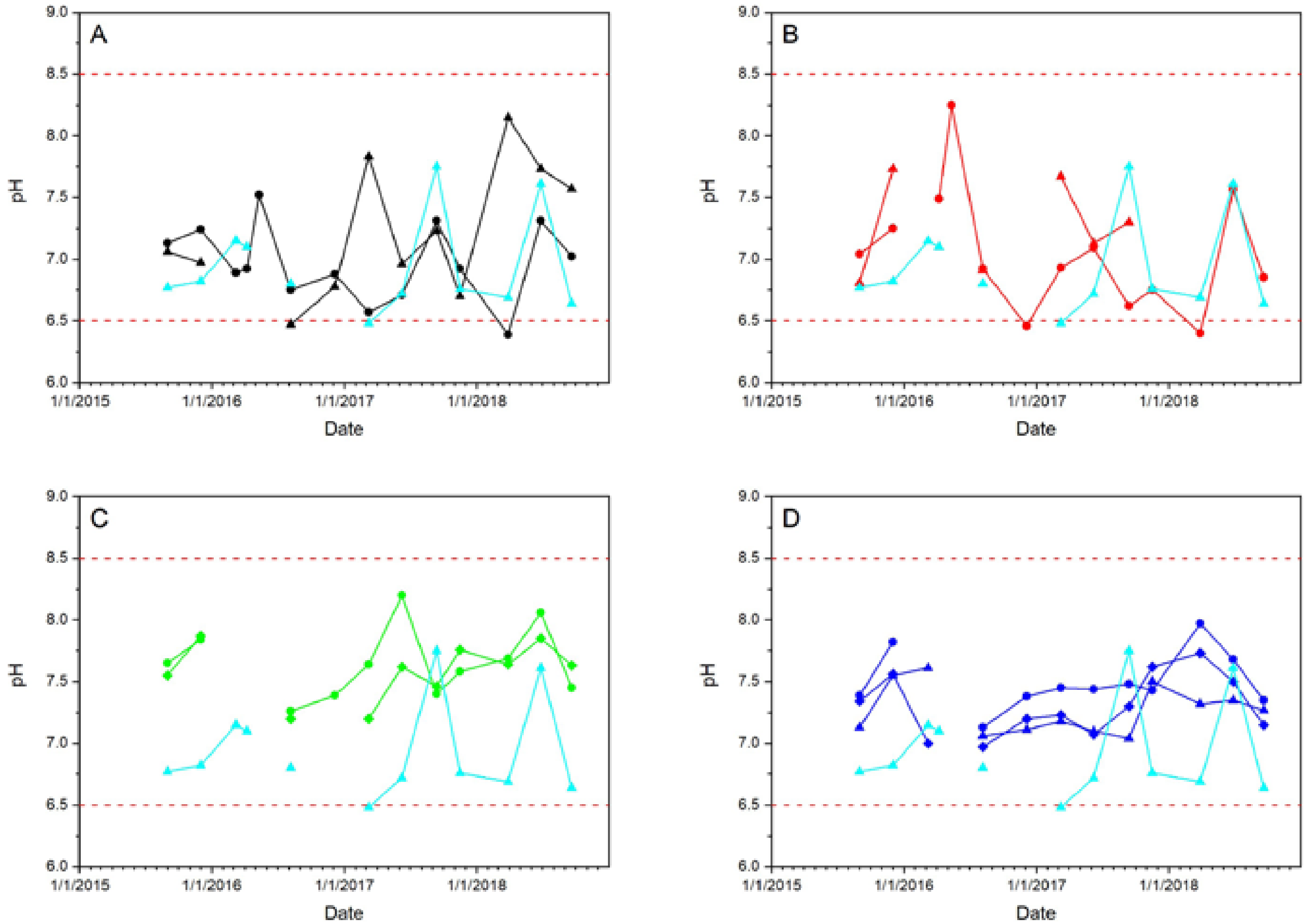

Figure D-27. Changes in pH in relationship to time for the Fort Riley SPWs. In all graphs the cyan triangles and lines represent FRLW12 the unimpacted control. A. SPW cluster 1, black circles and lines are FRLW01, black triangles and lines are FRLW02. B. SPW cluster 2, red circles and lines are FRLW09, red triangles and lines are FRLW10. C. SPC cluster 3, green circles and lines are FRLW03, green diamonds and lines are FRLW05. D.SPW cluster 4, blue circles and lines are FRLW06, blue triangles and lines are FRLW07, blue diamonds and lines are FRLW08.

4.2.8 Sulfate – Soil Porewater

Sulfate concentrations in the SPWs ranged from 29.7 – 766 mg/L (Figure D-28). As was the case with pH, spikes in sulfate concentrations were difficult to assess. However, in the case of sulfate, it was not because of the variability in sulfate concentrations. Rather, it was because of an overall significant decrease in sulfate concentrations throughout the study: FRLW01 ($p = 0.016$), FRLW02 ($p = 0.002$), FRLW03 ($p = 0.008$), FRLW05 ($p = 0.060$), FRLW07 ($p = 0.002$), FRLW08 ($p = 0.038$), FRLW09 ($p = 0.010$), FRLW10 ($p = 0.002$), and FRLW12 ($p < 0.001$).

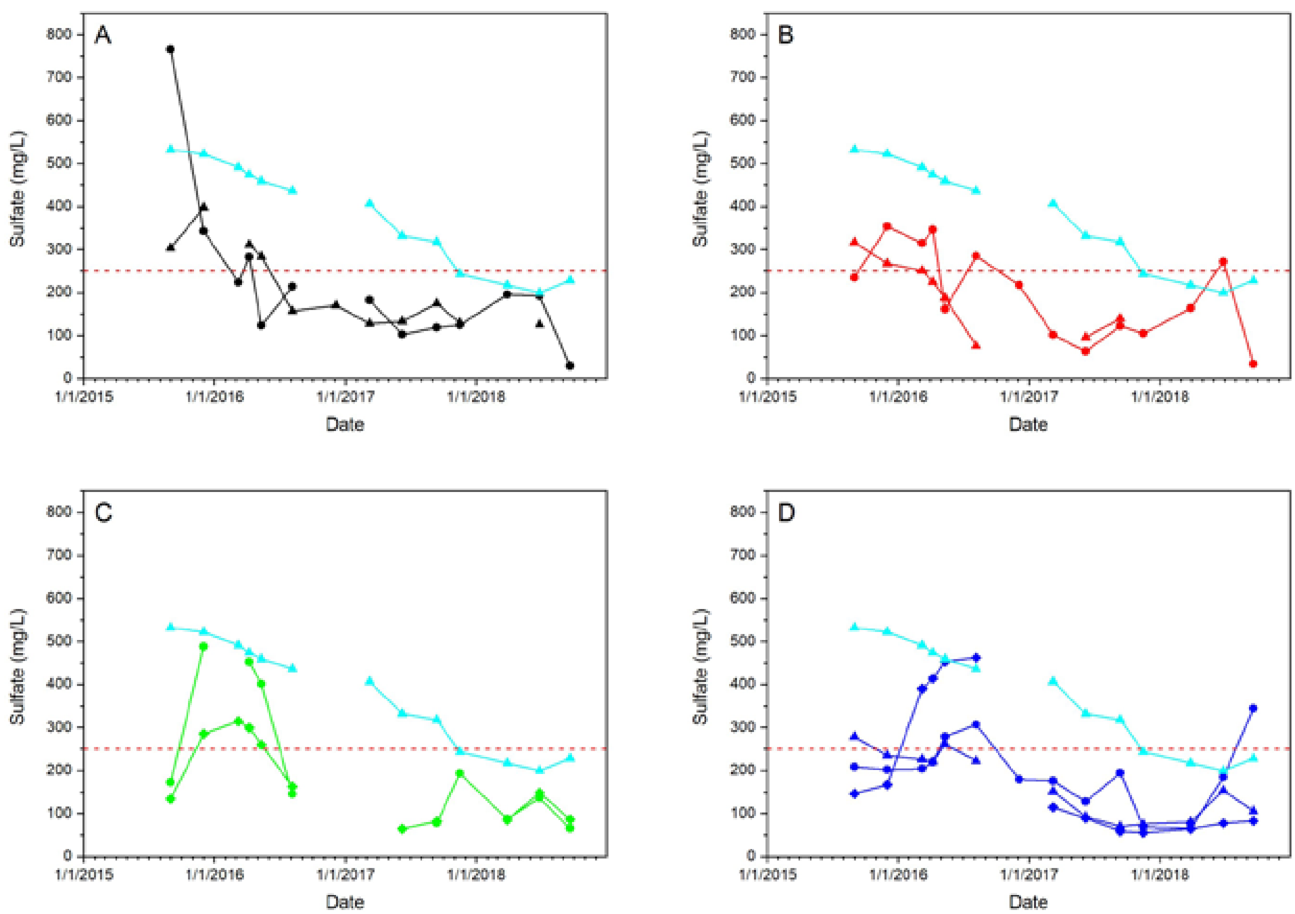

Figure D-28. Changes in sulfate in relationship to time for the Fort Riley SPWs. In all graphs the cyan triangles and lines represent FRLW12 the unimpacted control. A. SPW cluster 1, black circles and lines are FRLW01, black triangles and lines are FRLW02. B. SPW cluster 2, red circles and lines are FRLW09, red triangles and lines are FRLW10. C. SPC cluster 3, green circles and lines are FRLW03, green diamonds and lines are FRLW05. D. SPW cluster 4, blue circles and lines are FRLW06, blue triangles and lines are FRLW07, blue diamonds and lines are FRLW08.

4.3 Other Soil Porewater Constituents

4.3.1 Barium – Soil Porewater

Barium behaved similarly to calcium in the vadose zone, where the same geochemical processes that were controlling calcium concentrations also controlled barium. Barium phases in the soil, barite and witherite are similar to gypsum and calcite that were shown to be at least partially control calcium concentrations (Kabata-Pendias and Mukherjee, 2007a; Madejón, 2013). Barium can potentially be strongly sorbed to argillaceous sediments (clays), manganese minerals titanium oxides, and other oxides and hydroxides. Barium can also be weakly sorbed and participate in ion exchange reactions (Kabata-Pendias and Mukherjee, 2007a; Madejón, 2013). Transport of barium depends on CEC, calcium carbonate and gypsum content, the precipitation of barite and witherite in the sediments and soil of the vadose zone (Madejón, 2013). Based on this information, it is somewhat surprising that barium was mobile when spikes in calcium occurred.

Since calcite and gypsum were the predicted stable calcium solid phases, there should be a correlation of barium with calcium if the transport of barium depends on these phases being present. There was a weak to moderate correlation of barium with calcium (r^2= 0.42). Figure D-29 is a plot of the log Ba^{2+} activity vs pH for the soil porewater samples collected. This figure clearly indicates that from the thermodynamic prospective that the stable barium phases would either be barite or witherite in the soils and vadose zone. The barite SI indicates that barium is in equilibrium or oversaturated with respect to barite. The witherite SI indicates that the Ba in the porewater is in equilibrium or saturated with respect to witherite. This analysis supports that barium phases in the soil or vadose zone were in part controlling barium, but the correlation does not explain 58% of the variability in the correlation with calcium.

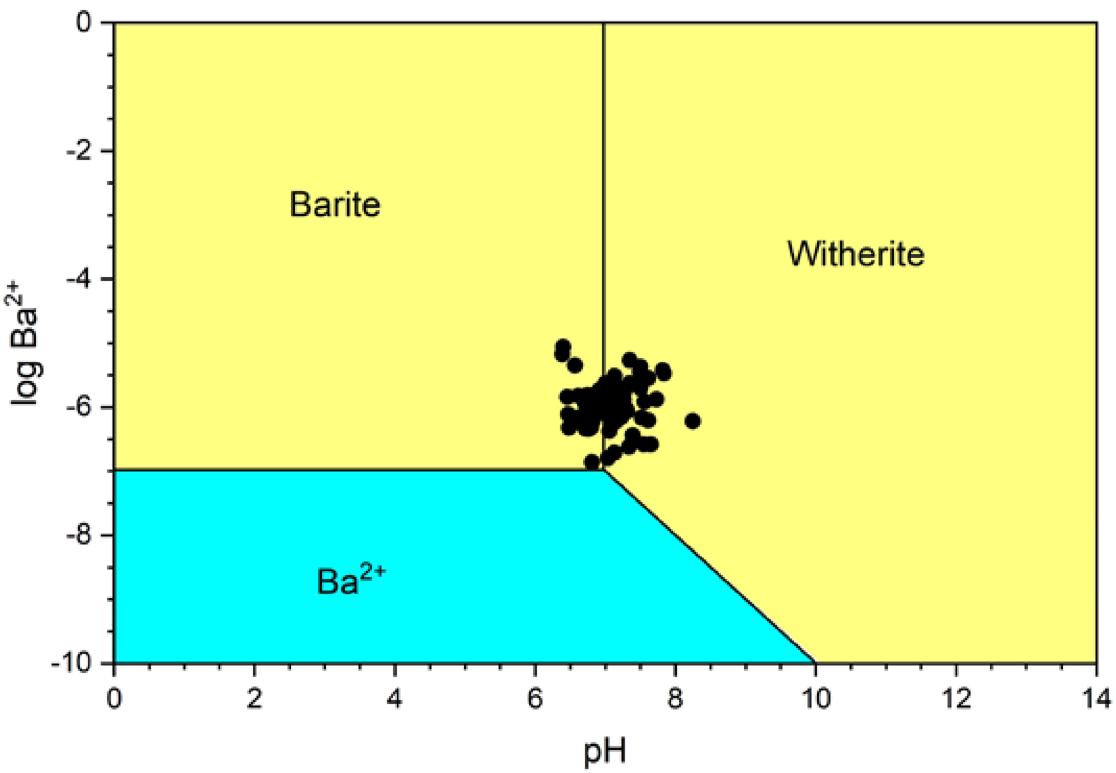

Figure D-29. Log Ba^{2+} activity vs. pH. The yellow shaded areas indicate that solid phases are the stable species and the cyan shaded area indicate that soluble ions or complexes are the stable species. Black dots represent the barium activity of the porewater samples in this study.

4.3.2 Fluoride – Soil Porewater

Changes in fluoride concentrations with time for SPW clusters are shown in Figure D-30. FRLW12 in cluster 5 shows little change in fluoride concentration. In SPW cluster 1, FRLW02 had little change in fluoride concentration, whereas there were observable spikes in fluoride concentration for FRLW01 in December 2015, May 2016, September 2017, and September 2018 (Figure D-30A). In cluster 2, FRLW10 potentially spiked in August 2016, but there was missing data and it is unknown what happened between August 2016 and June 2017 (Figure D-30A). However, in June 2017 the fluoride concentrations were elevated compared to the initial fluoride concentrations. In FRLW09, initially, there were higher fluoride concentrations in September 2015 and December 2015. The fluoride concentrations decreased until April 2016, and then fluoride concentrations appeared to spike in June 2017. After June 2017, the fluoride concentrations leveled off and decreased until March 2018, and then increased until the end of the study period (Figure D-30B). FRLW03, in cluster 3, fluoride data is shown in Figure D-30. Although the data is somewhat sporadic, it appears there is a dip in fluoride concentrations in March 2018. FLRW05's pattern is similar to that of FRLW03, but the fluoride concentration appeared to potentially peak in September 2018 (Figure D-30C). In SPW cluster 4, FRLW06 appeared to have a fluoride concentration spike in December 2015 which later decreased until April 2016. There was a gradual increase in fluoride concentration until June 2018, and then fluoride potentially spiked in September 2018 (Figure D-30C). FRLW07 showed little change in fluoride concentration throughout the study (Figure D-30D). On the other hand, FRLW08 followed the pattern of FRLW06 except there was a dip in fluoride concentration in June 2018 (Figure D-30D).

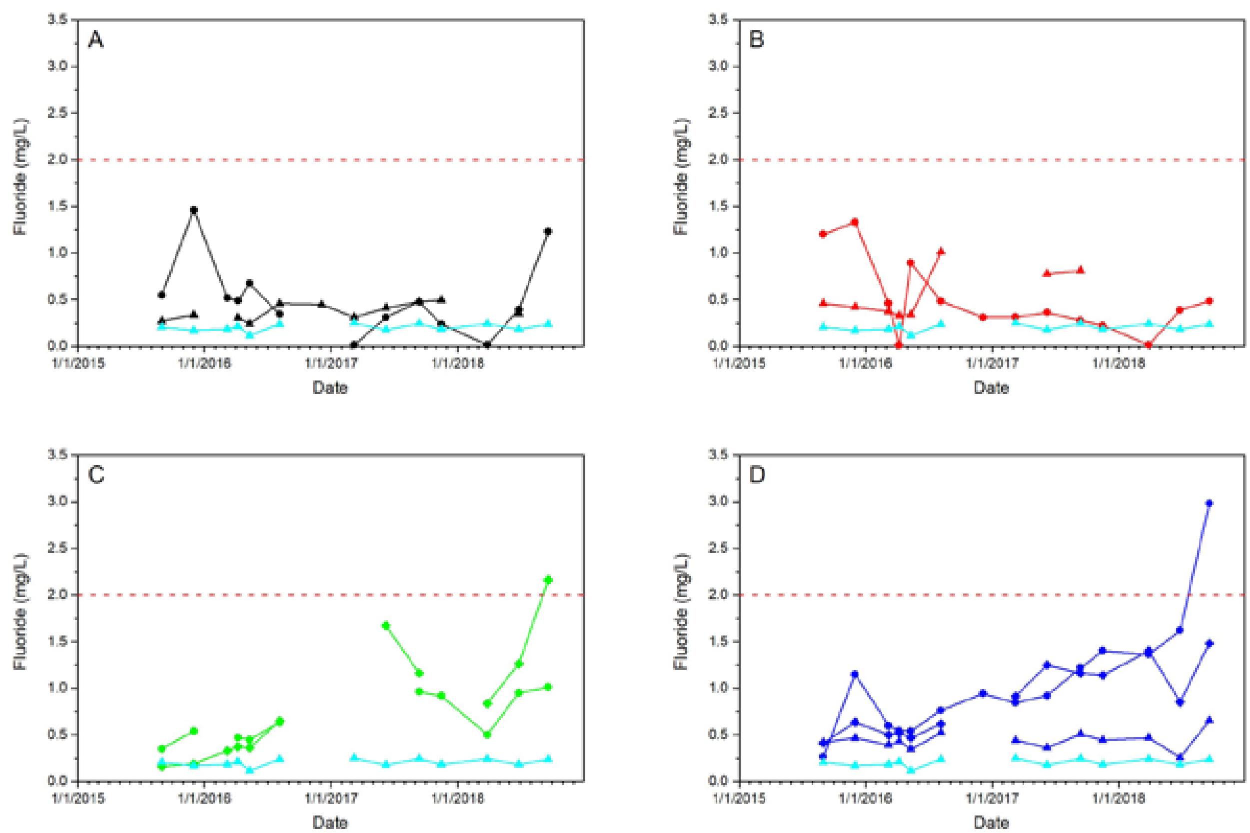

Figure D-30. Changes in fluoride concentration in relationship to time for the Fort Riley SPWs. In all graphs the cyan triangles and lines represent FRLW12 the unimpacted control. A. SPW cluster 1, black circles and lines are FRLW01, black triangles and lines are FRLW02. B. SPW cluster 2, red circles and lines are FRLW09, red triangles and lines are FRLW10. C. SPC cluster 3, green circles and lines are FRLW03, green diamonds and lines are FRLW05. D. SPW cluster 4, blue circles and lines are FRLW06, blue triangles and lines are FRLW07, blue diamonds and lines are FRLW08.

4.4 Stormwater Contaminants

Table D-3. Summary of halogenated aliphatics and aromatics (monocyclic) for Fort Riley soil porewater samples.

	1,2,4-Trichlorobenzene	1,2-Dichlorobenzene	1,3-Dichlorobenzene	1,4-Dichlorobenzene	2,4,5-Trichlorophenol	2,4,6-Trichlorophenol	2,4-Dinitrotoluene	2,6-Dinitrotoluene	Hexachlorobenzene
Units	**µg/L**	**µg/L**	**µg/L**	**µg/L**	**µg/L**	**µg/L**	**µg/L**	**µg/L**	**µg/L**
Total Number of Analyses	20	20	20	20	15	15	5	5	20
Number of Detects	0	2	0	0	0	0	0	0	0
Percent Detects	0	10	0	0	0	0	0	0	0
Mean	-----	0.03	-----	-----	-----	-----	-----	-----	-----
Standard Deviation	-----	-----	-----	-----	-----	-----	-----	-----	-----
Minimum	-----	0.03	-----	-----	-----	-----	-----	-----	-----
25th Percentile	-----	0.03	-----	-----	-----	-----	-----	-----	-----
Median	-----	0.03	-----	-----	-----	-----	-----	-----	-----
75th Percentile	-----	-----	-----	-----	-----	-----	-----	-----	-----
Maximum	-----	0.03	-----	-----	-----	-----	-----	-----	-----

Table D-4. Summary of polycyclic aromatic hydrocarbons for the Fort Riley soil porewater samples.

	Acenaphthene	Acenaphthylene	Anthracene	Benzo(a)anthracene	Benzo(a)pyrene	Benzo(b)fluoranthene	Benzo(g,h,i)perylene	Benzo(k)fluoranthene	Chrysene	Dibenz(a,h)anthracene	Fluoranthene	Fluorene	Indeno(1,2,3-cd)pyrene	Isophorone	Naphthalene	Phenanthrene	Pyrene
Units	**µg/L**	**µg/L**	**µg/L**	**µg/L**	**µg/L**	**µg/L**	**µg/L**	**µg/L**	**µg/L**	**µg/L**	**µg/L**	**µg/L**	**µg/L**	**µg/L**	**µg/L**	**µg/L**	**µg/L**
Total Number of Analyses	20	20	20	20	20	20	20	20	20	20	20	20	20	20	20	16	20
Number of Detects	0	0	0	0	0	0	0	0	0	0	0	0	0	0	0	0	0
Percent Detects	0	0	0	0	0	0	0	0	0	0	0	0	0	0	0	0	0
Mean	-----	-----	-----	-----	-----	-----	-----	-----	-----	-----	-----	-----	-----	-----	-----	-----	-----
Standard Deviation	-----	-----	-----	-----	-----	-----	-----	-----	-----	-----	-----	-----	-----	-----	-----	-----	-----
Minimum	-----	-----	-----	-----	-----	-----	-----	-----	-----	-----	-----	-----	-----	-----	-----	-----	-----
25th Percentile	-----	-----	-----	-----	-----	-----	-----	-----	-----	-----	-----	-----	-----	-----	-----	-----	-----
Median	-----	-----	-----	-----	-----	-----	-----	-----	-----	-----	-----	-----	-----	-----	-----	-----	-----
75th Percentile	-----	-----	-----	-----	-----	-----	-----	-----	-----	-----	-----	-----	-----	-----	-----	-----	-----
Maximum	-----	-----	-----	-----	-----	-----	-----	-----	-----	-----	-----	-----	-----	-----	-----	-----	-----

Table D-5. Summary of pesticides for the Fort Riley soil porewater samples.

	α-BHC	ß-BHC	Chlordane	Dieldrin	Endosulfan I	Endosulfan II	Endosulfan Sulfate	Endrin	γ-BHC	Heptachlor	Heptachlor Epoxide	Isophorone	p,p'-DDD	p,p'-DDE	p,p'-DDT
Units	**µg/L**	**µg/L**	**µg/L**	**µg/L**	**µg/L**	**µg/L**	**µg/L**	**µg/L**	**µg/L**	**µg/L**	**µg/L**	**µg/L**	**µg/L**	**µg/L**	**µg/L**
Total Number of Analyses	20	20	20	20	20	20	20	20	20	20	20	20	20	20	20
Number of Detects	0	0	0	0	0	0	0	0	0	0	0	0	0	0	0
Percent Detects	0	0	0	0	0	0	0	0	0	0	0	0	0	0	0
Mean	-----	-----	-----	-----	-----	-----	-----	-----	-----	-----	-----	-----	-----	-----	-----
Standard Deviation	-----	-----	-----	-----	-----	-----	-----	-----	-----	-----	-----	-----	-----	-----	-----
Minimum	-----	-----	-----	-----	-----	-----	-----	-----	-----	-----	-----	-----	-----	-----	-----
25th Percentile	-----	-----	-----	-----	-----	-----	-----	-----	-----	-----	-----	-----	-----	-----	-----
Median	-----	-----	-----	-----	-----	-----	-----	-----	-----	-----	-----	-----	-----	-----	-----
75th Percentile	-----	-----	-----	-----	-----	-----	-----	-----	-----	-----	-----	-----	-----	-----	-----
Maximum	-----	-----	-----	-----	-----	-----	-----	-----	-----	-----	-----	-----	-----	-----	-----

Table D-6. Summary of phenols, ethers, and phthalates for the Fort Riley soil porewater samples.

	2,4,5-Trichlorophenol	2,4,6-Trichlorophenol	2,4-Dichlorophenol	Pentachlorophenol	4-Bromophenyl-phenylether	4-Chlorophenyl-phenylether	Bis-(2-Ethylhexyl)phthalate	Butylbenzylphthalate	Diethylphthalate	Dimethylphthalate	Di-n-butylphthalate	Di-n-octylphthalate
Units	**µg/L**	**µg/L**	**µg/L**	**µg/L**	**µg/L**	**µg/L**	**µg/L**	**µg/L**	**µg/L**	**µg/L**	**µg/L**	**µg/L**
Total Number of Analyses	15	15	15	15	20	20	16	20	16	20	20	20
Number of Detects	0	0	1	0	0	0	0	3	2	0	1	0
Percent Detects	0	0	7	0	0	0	0	15	13	0	5	0
Mean	-----	-----	0.27	-----	-----	-----	-----	0.03	0.76	-----	0.29	-----
Standard Deviation	-----	-----	-----	-----	-----	-----	-----	0.00	0.77	-----	-----	-----
Minimum	-----	-----	-----	-----	-----	-----	-----	0.03	0.21	-----	-----	-----
25th Percentile	-----	-----	-----	-----	-----	-----	-----	0.03	0.48	-----	-----	-----
Median	-----	-----	0.27	-----	-----	-----	-----	0.03	0.76	-----	0.29	-----
75th Percentile	-----	-----	-----	-----	-----	-----	-----	0.03	1.03	-----	-----	-----
Maximum	-----	-----	-----	-----	-----	-----	-----	0.03	1.30	-----	-----	-----

Groundwater Quality

5.1 Background Groundwater Quality

Table D-7. Statistical comparisons between NWIS and NURE groundwater quality data with the Fort Riley Study data from the monitoring wells and piezometers.

Parameter	Monitoring Wells (GW)		Piezometer Wells (PW)	
	Significant Difference	p-value	Significant Difference	p-value
Alkalinity	Yes	< 0.001	Yes	< 0.001
Dissolved Oxygen	Yes	< 0.001	Yes	< 0.001
pH	Yes	< 0.001	Yes	< 0.001
Specific Conductivity	Yes	< 0.001	Yes	< 0.001
Total Dissolved Solids	Yes	< 0.001	Yes	< 0.001
Bicarbonate	Yes	< 0.001	Yes	< 0.001
Dissolved Carbon Dioxide	Yes	< 0.001	Yes	< 0.001
Dissolved Organic Carbon (DOC)	Yes	< 0.001	No	0.897
Chloride	Yes	< 0.001	Yes	< 0.001
Fluoride	No	0.175	No	0.388
Sulfate	Yes	< 0.001	Yes	< 0.001
Nitrate + Nitrite	Yes	< 0.001	Yes	< 0.001
Phosphate	Yes	< 0.001	Yes	< 0.001
Aluminum	Yes	0.048	Yes	0.017
Arsenic	Yes	< 0.001	Yes	< 0.001
Barium	No	0.978	Yes	0.001
Calcium	Yes	< 0.001	Yes	< 0.001
Copper	Yes	< 0.001	Yes	< 0.001
Iron	Yes	< 0.001	No	0.529
Potassium	Yes	< 0.001	No	0.245
Lithium	Yes	< 0.001	No	0.328
Magnesium	Yes	< 0.001	Yes	< 0.001
Manganese	No	0.802	Yes	< 0.001
Molybdenum	Yes	< 0.001	No	0.899
Sodium	No	0.989	Yes	0.049
Nickel	No	0.868	No	0.052
Selenium	Yes	0.024	No	0.312
Silicon	Yes	0.003	Yes	0.002
Strontium	Yes	0.005	No	0.161
Uranium	Yes	< 0.001	Yes	< 0.001
Vanadium	No	0.638	No	0.065

Table D-8. Study specific background ranges determined for the Fort Riley GI Study.

Parameter	Units	N	n	Mean	Std Dev	Median	Min	Max	Lower Critical Value	Upper Critical Value	Percent of samples Included
Temperature	°C	162	157	17.33	1.70	16.96	14.15	21.2	13.93	20.73	96.9
Specific Conductance	µS/cm	162	154	1402	221	1408	960	1934	960	1844	95.1
Total Dissolved Solids	mg/L	162	154	908	146	913	633	1257	617.13	1199.17	95.1
Dissolved Oxygen	mg/L	162	141	0.44	0.31	0.38	0.07	1.62	BDL[1]	1.06	87.0
pH	-----	162	159	6.73	0.18	6.72	6.12	7.24	6.37	7.09	98.1
Eh	mV	162	146	236.3	39.48	240.3	155.9	322.9	157.34	315.26	90.1
Turbidity	NTU	157	147	38.5	57.1	18.3	0.83	321.0	BDL	152.66	93.6
Alkalinity	mg $CaCO_3$/L	159	141	491	47	495	393	596	397.81	584.45	88.7
Dissolved Organic Carbon	mg/L	162	148	1.88	0.60	1.96	0.86	3.23	0.68	3.08	91.4
Dissolved Inorganic Carbon	mg/L	162	147	152	16.6	151	117	189	118.28	184.76	90.7
Carbon dioxide$_{(aq)}$	mg CO_2/L	162	148	107	29	109	46	170	49	165	91.4
Bicarbonate	mg HCO_3^-/L	162	139	563	59	573	416	695	445.62	681.26	85.8
Carbonate	mg CO_3^{2-}/L	162	160	0.37	2.57	0.15	0.02	32.66	BDL	5.51	98.8
Nitrate + Nitrite	mg N/L	160	143	0.24	0.34	0.13	0.01	1.58	BDL	0.92	89.4
Total Nitrogen	mg N/L	161	153	0.59	0.87	0.31	0.04	4.72	BDL	2.33	95.0
Bromide	mg/L	162	155	0.1	0.08	0.09	0.01	0.29	BDL	0.26	95.7
Chloride	mg/L	162	144	31.34	12.42	29.6	6.98	83.4	6.5	56.18	88.9
Sulfate	mg/L	162	156	231	101	216	48.0	440	28.45	433.33	96.3
Fluoride	mg/L	162	158	0.28	0.07	0.28	0.10	0.48	0.14	0.42	97.5
Iodide	µg/L	162	155	5.65	3.12	6.14	0.75	12.4	BDL	11.89	95.7
Phosphate	mg P/L	162	152	0.053	0.034	0.055	0.001	0.168	BDL	0.121	93.8

[1]BDL = below detection limit

Table D-8 (continued). Study specific background ranges determined for the Fort Riley GI Study.

Parameter	Units	N	n	Mean	Std Dev	Median	Min	Max	Lower Critical Value	Upper Critical Value	Percent of samples Included
Total Phosphorous	mg P/L	153	148	0.074	0.028	0.074	0.008	0.131	0.018	0.13	96.7
Aluminum	µg/L	162	158	7	12	1	0.3	74	BDL	31.2	97.5
Arsenic	µg/L	162	144	4.2	1.7	4.4	0.3	9	0.8	7.6	88.9
Barium	µg/L	162	141	98	21	100	60	164	56	140	87.0
Calcium	mg/L	162	156	216	40.5	218	139	309	135.3	297.3	96.3
Copper	µg/L	161	155	1	0.5	1	0	5	BDL	1.7	96.3
Iron	µg/L	162	147	332	398	206	25	1717	BDL	1128	90.7
Potassium	mg/L	162	158	15.8	5.48	15.2	4.77	27.0	4.85	26.77	97.5
Lithium	µg/L	144	138	38	11	36	16	67	16	60	95.8
Magnesium	mg/L	162	155	42.5	6.68	42.8	26.3	63.2	29.14	55.86	95.7
Manganese	µg/L	162	153	105	75	103	1.1	268	BDL	255.8	94.4
Molybdenum	µg/L	162	155	8.3	3.5	7.7	0.8	16	1.3	15.3	95.7
Sodium	mg/L	162	153	30.4	8.7	29.4	16.7	53.6	13	47.8	94.4
Nickel	µg/L	162	148	2.7	1.5	2.7	0.3	6.3	BDL	5.7	91.4
Selenium	µg/L	162	152	3	3	2	0.5	13	BDL	8.4	93.8
Silicon	mg/L	162	146	15.67	1.41	15.85	12.6	18.8	12.85	18.49	90.1
Strontium	µg/L	162	146	1611	192	1597	1225	2038	1227	1995	90.1
Uranium	µg/L	162	156	43	26	36	0.3	145	BDL	94.9	96.3
Vanadium	µg/L	162	154	2.5	2.7	1.8	0.3	12.6	BDL	7.9	95.1
$d^{18}O$	‰	162	141	-6.31	0.21	-6.31	-6.77	-5.74	-6.73	-5.89	87.0
$d^{2}H$	‰	162	146	-39.33	1.48	-39.18	-43.73	-35.19	-42.29	-36.37	90.1

Table D-9. Statistical comparisons of monitoring wells and piezometer wells in the Fort Riley GI study.

Parameter	Significantly Different	p-value
Alkalinity	Yes	< 0.001
Aluminum	No	0.924
Antimony	No	0.993
Arsenic	No	0.941
Barium	Yes	< 0.001
Bicarbonate	Yes	0.018
Bromide	No	0.974
Calcium	Yes	< 0.001
Carbonate	No	0.881
Chloride	No	0.485
Copper	No	0.170
Dissolved Carbon Dioxide	No	0.897
Dissolved Inorganic Carbon	Yes	< 0.001
Dissolved Organic Carbon	Yes	< 0.001
Dissolved Oxygen	Yes	< 0.001
Eh	No	1.000
Fluoride	No	0.999
Iodide	No	1.000
Iron	Yes	< 0.001
Lithium	Yes	< 0.001
Magnesium	No	0.321

Parameter	Significantly Different	p-value
Manganese	Yes	< 0.001
Molybdenum	Yes	< 0.001
Nickel	Yes	< 0.001
Nitrate + Nitrite	No	0.996
pH	No	1.000
Phosphate	Yes	< 0.001
Potassium	Yes	< 0.001
Selenium	Yes	0.046
Silicon	No	1.000
Sodium	Yes	< 0.001
Specific Conductance	Yes	< 0.001
Strontium	No	0.340
Sulfate	Yes	< 0.001
Temperature	No	0.501
Total Dissolved Solids	Yes	< 0.001
Total Nitrogen	Yes	< 0.001
Total Phosphorous	Yes	< 0.001
Turbidity	Yes	< 0.001
Uranium	Yes	< 0.001
Vanadium	Yes	< 0.001

5.2 Major Anions and Cations, pH, Specific Conductivity

5.2.1 pH – Groundwater

The site-specific background pH in this study ranged from 6.12 – 7.24. Figure D-31 shows the groundwater time series plots for pH. There were no significant differences in pH between the upgradient groundwater, background groundwater, and the downgradient groundwater. There were no trends in pH in the upgradient wells (Figure D-31A) or in the background wells (Figure D-31C). In the downgradient wells (Figure D-31B), the pH was significantly increasing in FRGW04, and FRGW06 ($p = 0.015$ and $p = 0.014$, respectively). In FRGW07, the pH was decreasing and was a significant trend ($p = 0.099$).

There were several sMCL exceedances in pH. FRGW01, FRGW04, and FRGW06 in September 2015; FRGW06 in December 2015 and March 2016; FRGW11 in March of 2017; FRGW01 and FRGW08 in March 2018; and FRGW07 and FRGW09 in September 2018 all had pH < 6.50. Only one pH exceeded the pH > 8.50 and that was FRGW13 in September 2017.

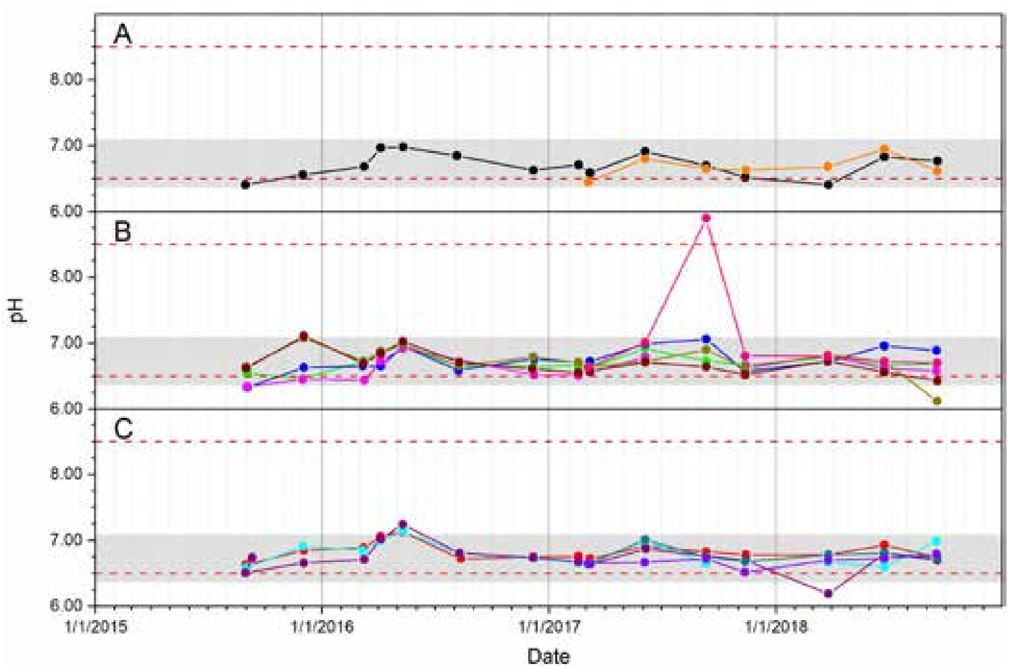

Figure D-31. Time series plots for pH in A. Upgradient wells, B. Downgradient wells, and C. Background wells. The gray shaded regions represent the site-specific background range. Black circles and lines are FRGW01, red circles and lines are FRGW02, green circles and lines are FRGW03, blue circles and lines are FRGW04, cyan circles and lines are FRGW05, magenta circles and lines are FRGW06, dark yellow circles and lines are FRGW07, purple circles and lines are FRGW08, wine-colored circles and lines are FRGW09, dark cyan circles and lines are FRGW10, orange circles and lines are FRGW11, violet circles and lines are FRGW12, and pink circles and lines are FRGW13. The red dashed lines show the pH sMCL of pH= 6.50 and pH= 8.50.

5.2.2 Specific Conductivity – Groundwater

Specific Conductivity (site-specific background) ranged from 960 – 1934 µS/cm in this study (Figure D-32). The SPC in the background wells was significantly different than the upgradient wells ($p < 0.001$) and the downgradient wells ($p < 0.001$). There was no significant difference in SPC between the upgradient wells and downgradient wells. The upgradient wells had the highest SPC values followed by the downgradient wells and then the background wells. The SPC time series data for the upgradient wells is shown in Figure D-32A. In the upgradient wells, only FRGW01 showed a trend in SPC was significantly increasing ($p = 0.024$). In the downgradient wells (Figure D-32B), the SPC was decreasing in FRGW03, FRGW04, and FRGW06. The decreasing SPC was a significant trend in FRGW03 ($p = 0.005$), FRGW04 ($p = 0.069$), and FRGW06 ($p = 0.063$). In the background wells (Figure D-32C) there was increasing SPC trend in well FRGW05. This was a significant trend ($p < 0.001$).

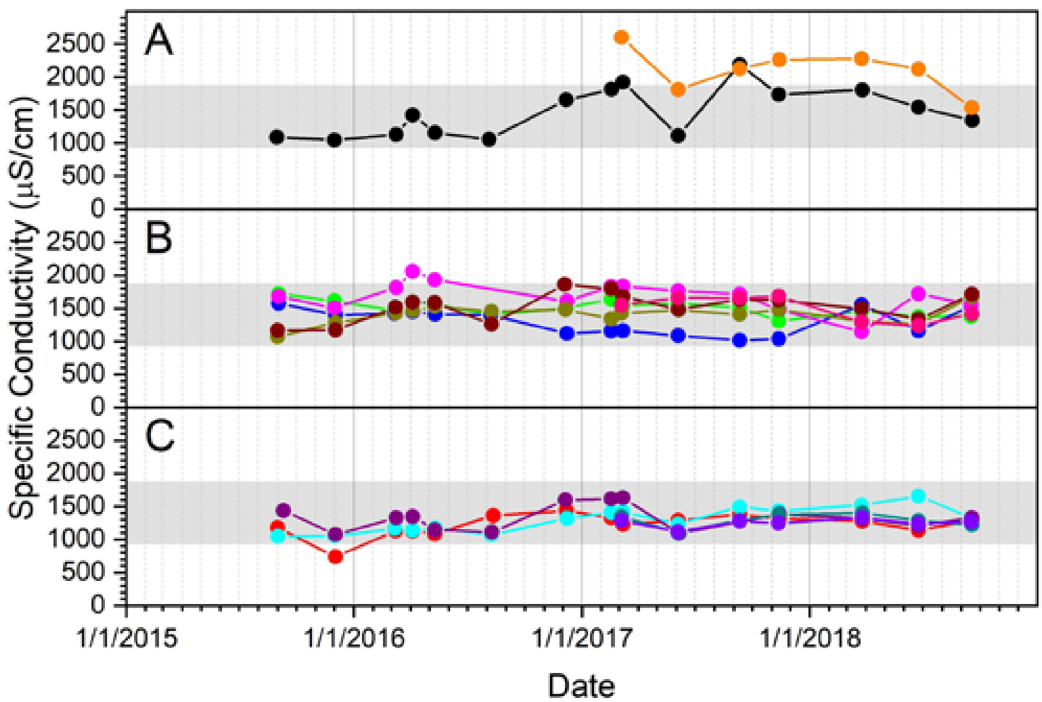

Figure D-32. Time series plots for specific conductivity in A. Upgradient wells, B. Downgradient wells, and C. Background wells. The gray shaded regions represent the site-specific background range. Black circles and lines are FRGW01, red circles and lines are FRGW02, green circles and lines are FRGW03, blue circles and lines are FRGW04, cyan circles and lines are FRGW05, magenta circles and lines are FRGW06, dark yellow circles and lines are FRGW07, purple circles and lines are FRGW08, wine-colored circles and lines are FRGW09, dark cyan circles and lines are FRGW10, orange circles and lines are FRGW11, violet circles and lines are FRGW12, and pink circles and lines are FRGW13.

5.2.3 Calcium – Groundwater

Site-specific background concentrations for calcium ranged from 139 – 309 mg/L during this study (Figure D-33). There were significant differences in calcium concentrations in the upgradient wells and the background wells ($p = 0.007$). However, there were not significant differences in calcium concentrations between the upgradient and downgradient wells. There was also a significant difference in calcium concentrations between the downgradient wells and the background wells ($p < 0.001$). The calcium concentrations were slightly larger in the downgradient wells than the upgradient wells. Both the downgradient and upgradient wells had larger calcium concentrations than the background wells. In the upgradient wells (Figure D-33A), there was an increasing trend in calcium concentrations, and this trend was significant ($p = 0.046$). There were also trends in the downgradient wells' calcium concentrations (Figure D-33B). The downgradient wells that showed significant decreasing trends in calcium concentrations with time were FRGW03 ($p = 0.008$), FRGW04 ($p = 0.003$) and FRGW06 ($p = 0.031$). The only other downgradient well that showed a trend in calcium concentrations was FRGW09. FRGW09 had significantly increasing calcium concentrations ($p = 0.037$) with time. The time series data for the background wells is shown in Figure D-33C. Only one background well (FRGW05) showed a trend in calcium concentrations and this was a significantly increasing trend ($p = 0.003$).

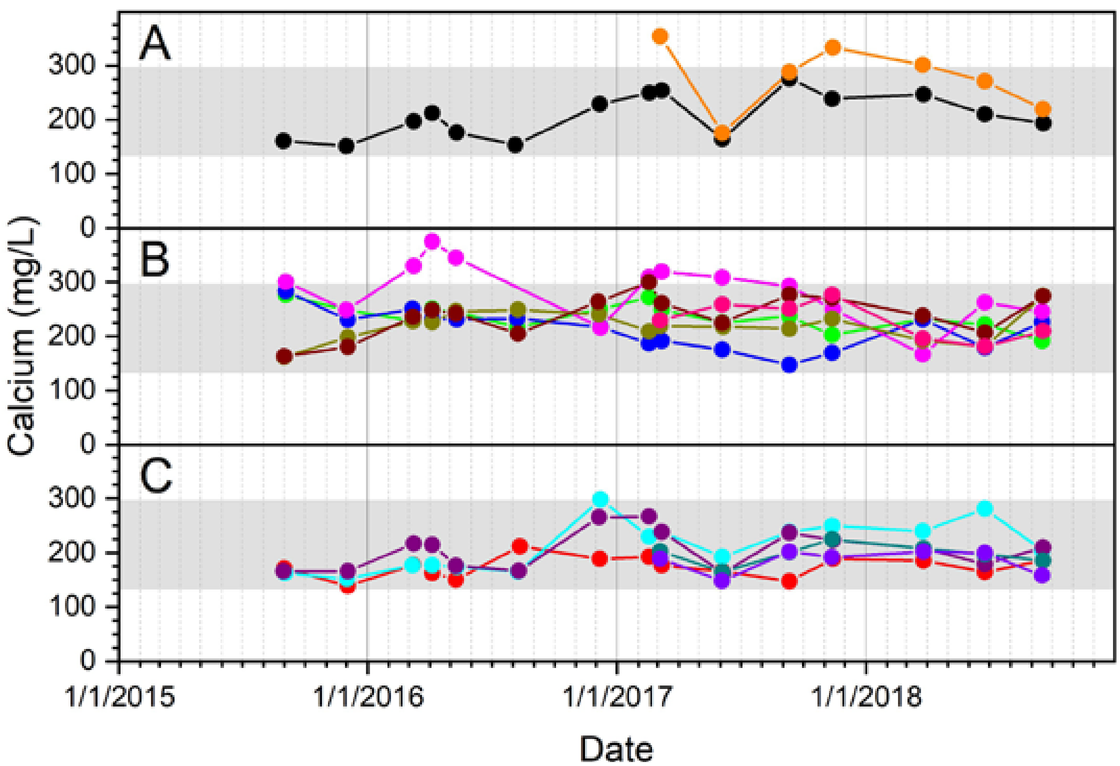

Figure D-33. Time series plots for calcium concentrations in A. Upgradient wells, B. Downgradient wells, and C. Background wells. The gray shaded regions represent the site-specific background range. Black circles and lines are FRGW01, red circles and lines are FRGW02, green circles and lines are FRGW03, blue circles and lines are FRGW04, cyan circles and lines are FRGW05, magenta circles and lines are FRGW06, dark yellow circles and lines are FRGW07, purple circles and lines are FRGW08, wine-colored circles and lines are FRGW09, dark cyan circles and lines are FRGW10, orange circles and lines are FRGW11, violet circles and lines are FRGW12, and pink circles and lines are FRGW13.

5.2.4 Magnesium – Groundwater

The site-specific background concentrations of magnesium in the groundwater in this study ranged from 26.3 – 63.2 mg/L (Figure D-34). There were significant differences in magnesium concentrations between the upgradient wells and the background wells ($p = 0.001$). The upgradient wells had larger magnesium concentrations than the background wells. However, unlike calcium, there were differences in magnesium concentration between the upgradient and downgradient wells ($p = 0.001$), and again, the upgradient wells had larger concentrations than the downgradient wells. There were no differences in magnesium concentration between the background wells and the downgradient wells. The time series magnesium concentration data for the upgradient wells is presented in Figure D-34A. As has been the case with previous parameters, only FRGW01 shows increasing magnesium concentrations with time and this was a significant trend ($p = 0.021$). Several downgradient wells showed decreasing magnesium concentrations (Figure D-34B). These decreasing trends in magnesium concentrations were significant in FRGW03 ($p < 0.001$), FRGW13 ($p = 0.031$), and FRGW04 ($p = 0.083$). The background wells (Figure D-34C), FRGW05, FRGW08, and FRGW12 all had trends in magnesium concentrations. FRGW05 and FRGW08 both had increasing magnesium concentrations with time. The trend in FRGW05 ($p = 0.046$) and FRGW08 ($p = 0.083$). FRGW12 showed decreasing magnesium concentration during the study, and this trend was significant ($p = 0.060$).

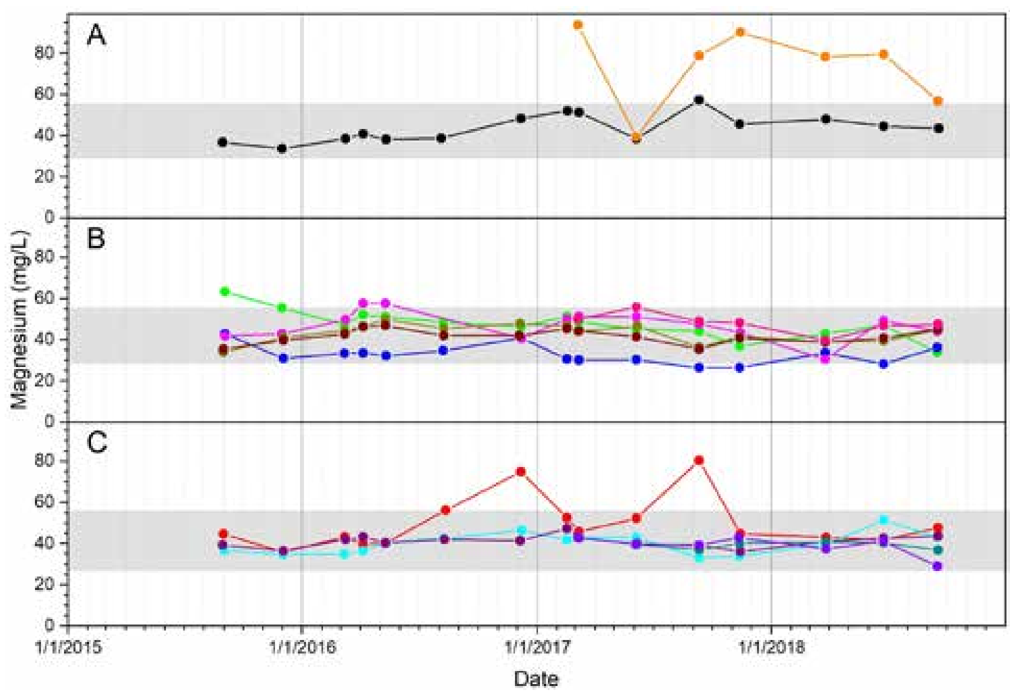

Figure D-34. Time series plots for magnesium concentrations in A. Upgradient wells, B. Downgradient wells, and C. Background wells. The gray shaded regions represent the site-specific background range. Black circles and lines are FRGW01, red circles and lines are FRGW02, green circles and lines are FRGW03, blue circles and lines are FRGW04, cyan circles and lines are FRGW05, magenta circles and lines are FRGW06, dark yellow circles and lines are FRGW07, purple circles and lines are FRGW08, wine-colored circles and lines are FRGW09, dark cyan circles and lines are FRGW10, orange circles and lines are FRGW11, violet circles and lines are FRGW12, and pink circles and lines are FRGW13.

5.2.5 Sodium – Groundwater

Sodium concentrations in the groundwater ranged from 16.7 – 87.4 mg/L (Figure D-35). There were significant differences in sodium concentrations between the background wells and the upgradient wells ($p = 0.043$), and the upgradient wells had larger sodium concentrations than the background wells. There were also significant differences in sodium concentrations between the background wells and the downgradient wells ($p < 0.001$). The downgradient wells had larger sodium concentrations than the background wells. There were not any significant differences in sodium concentrations between the upgradient wells and the downgradient wells. The time series sodium concentrations for the upgradient wells are plotted in Figure D-35A. There were trends in the sodium concentrations in both upgradient wells. There were significant increasing trends in sodium concentrations in FRGW01 ($p = 0.027$) and in FRGW11 ($p = 0.060$). Figure D-35B shows the time series plot of sodium concentrations in the downgradient wells. In two of the downgradient wells, FRGW06 and FRGW07, there were increasing sodium concentrations with time. The increasing trend in FRGW06 ($p = 0.063$) and FRGW07 ($p = 0.006$) were significant. In the downgradient wells (Figure D-35C), only FRGW02 and FRGW05 showed trends in the sodium concentrations and these were increasing trends. In FRGW05 and FRGW02, the sodium concentrations were significantly increasing with time ($p = 0.051$ and $p = 0.009$, respectively).

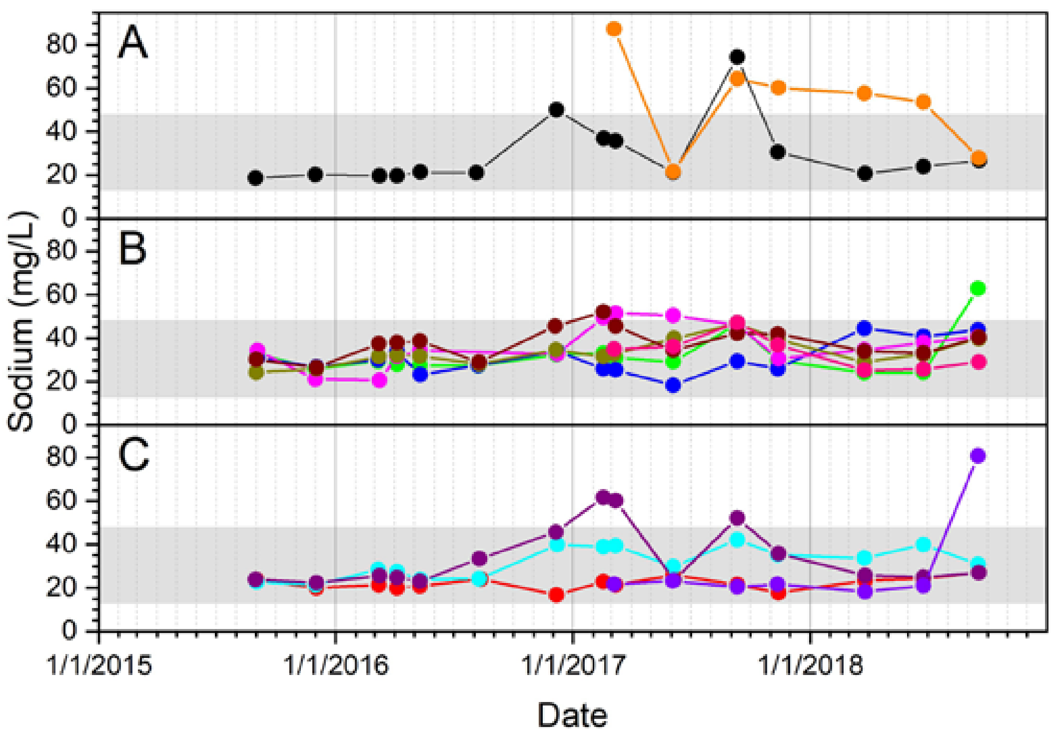

Figure D-35. Time series plots for sodium concentrations in A. Upgradient wells, B. Downgradient wells, and C. Background wells. The gray shaded regions represent the site-specific background range. Black circles and lines are FRGW01, red circles and lines are FRGW02, green circles and lines are FRGW03, blue circles and lines are FRGW04, cyan circles and lines are FRGW05, magenta circles and lines are FRGW06, dark yellow circles and lines are FRGW07, purple circles and lines are FRGW08, wine-colored circles and lines are FRGW09, dark cyan circles and lines are FRGW10, orange circles and lines are FRGW11, violet circles and lines are FRGW12, and pink circles and lines are FRGW13.

5.2.6 Potassium – Groundwater

Potassium ranged from 4.77 – 34.1 mg/L in this study (Figure D-36). Potassium concentrations in the background wells were significantly different than both the upgradient wells ($p < 0.001$) and downgradient wells ($p < 0.001$). There were no significant differences in the potassium concentrations in the upgradient wells and the downgradient wells. The upgradient and downgradient wells both had larger potassium concentrations than in the background wells. There were no trends in potassium concentrations in the upgradient wells (Figure D-36A). There were trends in potassium concentrations in the downgradient wells FRGW03, FRGW04, FRGW07, and FRGW09 (Figure D-36B). In these wells, only FRGW04 showed a decreasing trend in potassium concentrations with time, and this was a significant trend ($p = 0.090$). For FRGW03, FRGW07, and FRGW09 the potassium concentrations were increasing during the study. In FRGW03, FRGW07 and FRGW09, these increasing potassium trends were significant ($p = 0.057$, $p = 0.015$ and $p = 0.011$, respectively). The time series potassium concentration data for the background wells is shown in Figure D-36C. The background wells FRGW02 and FRGW05 both had increasing potassium concentrations with time. In wells FRGW02 and FRGW05, this increasing trend was significant ($p = 0.099$ and $p = 0.046$, respectively).

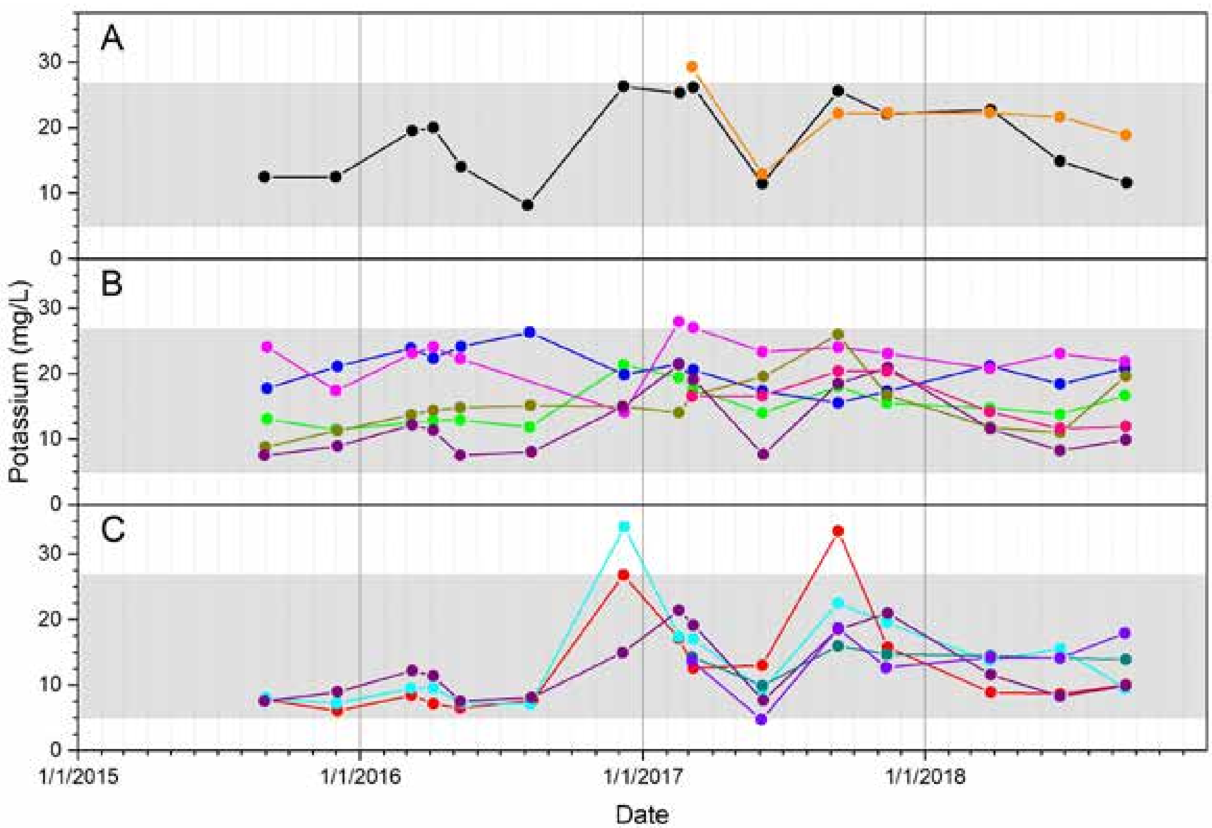

Figure D-36. Time series plots for potassium concentrations in A. Upgradient wells, B. Downgradient wells, and C. Background wells. The gray shaded regions represent the site-specific background range. Black circles and lines are FRGW01, red circles and lines are FRGW02, green circles and lines are FRGW03, blue circles and lines are FRGW04, cyan circles and lines are FRGW05, magenta circles and lines are FRGW06, dark yellow circles and lines are FRGW07, purple circles and lines are FRGW08, wine-colored circles and lines are FRGW09, dark cyan circles and lines are FRGW10, orange circles and lines are FRGW11, violet circles and lines are FRGW12, and pink circles and lines are FRGW13.

5.2.7 Bicarbonate – Groundwater

Bicarbonate concentrations ranged from 296 – 872 mg HCO_3^-/L during the study (Figure D-37). There were no significant differences in bicarbonate concentrations between the upgradient wells, downgradient wells, and the background wells. There were no trends in bicarbonate concentrations in the upgradient wells (Figure D-37A). Figure D-37B shows the time series bicarbonate concentrations in the downgradient wells. Only one of the downgradient wells, FRGW04, showed a trend in the bicarbonate concentrations and had significantly increasing bicarbonate concentrations ($p = 0.024$). The downgradient wells, FRGW02 and FRGW05, showed bicarbonate concentrations trends (Figure D-37C). In FRGW02 and FRGW05, there were significantly increasing bicarbonate concentrations ($p = 0.037$ and $p = 0.003$, respectively).

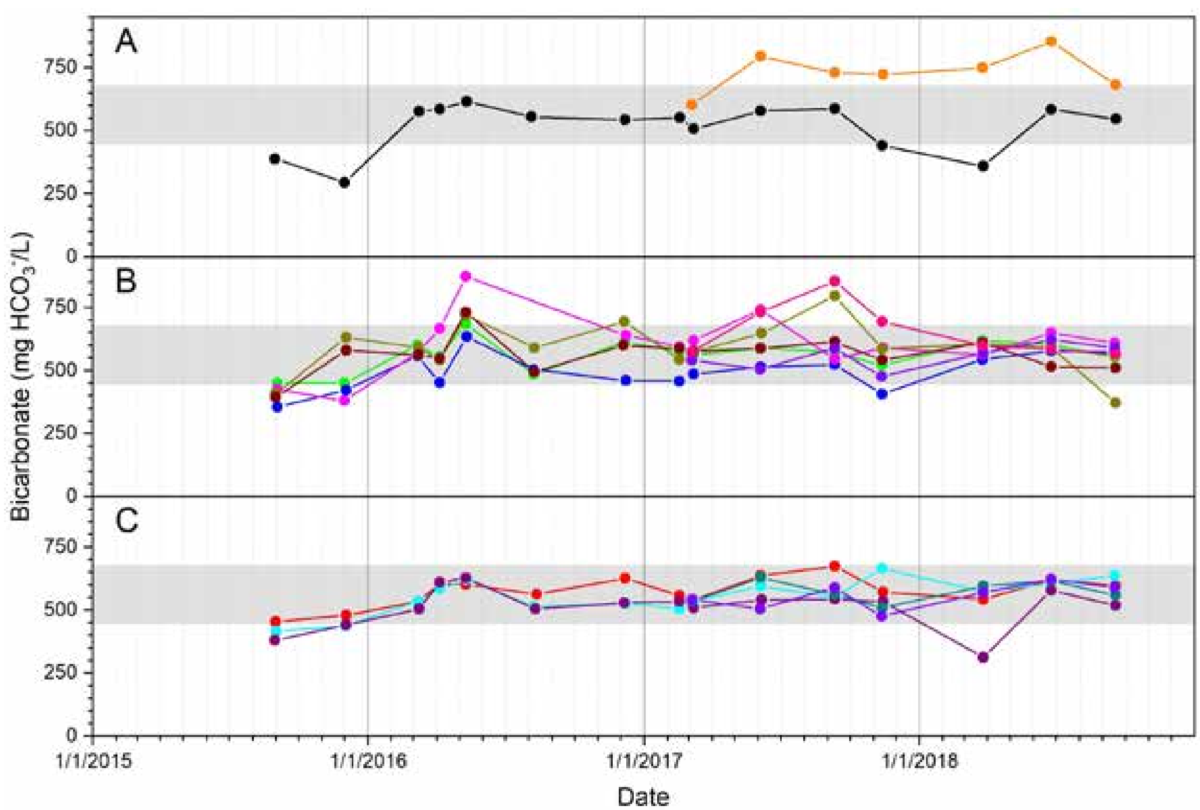

Figure D-37. Time series plots for bicarbonate concentrations in A. Upgradient wells, B. Downgradient wells, and C. Background wells. The gray shaded regions represent the site-specific background range. Black circles and lines are FRGW01, red circles and lines are FRGW02, green circles and lines are FRGW03, blue circles and lines are FRGW04, cyan circles and lines are FRGW05, magenta circles and lines are FRGW06, dark yellow circles and lines are FRGW07, purple circles and lines are FRGW08, wine-colored circles and lines are FRGW09, dark cyan circles and lines are FRGW10, orange circles and lines are FRGW11, violet circles and lines are FRGW12, and pink circles and lines are FRGW13.

5.2.8 Sulfate – Groundwater

Sulfate concentration in this study ranged from 48.0 – 581 mg/L (Figure D-38). There were significant differences in sulfate concentrations between the background wells and the upgradient wells ($p < 0.001$) and between the background wells and the downgradient wells ($p < 0.001$). There was also a significant difference between the upgradient wells and the downgradient wells ($p < 0.001$). The highest concentrations of sulfate were in the downgradient wells followed by the upgradient wells which had higher SO_4 concentrations than the background wells. The upgradient sulfate concentrations with time are given in Figure D-38A. Only FRGW01 in the upgradient wells showed a significantly decreasing trend in sulfate concentrations with time ($p = 0.005$). The time series data for the downgradient wells is shown in Figure D-38B. Most of the downgradient wells showed decreasing sulfate concentrations with time. These decreasing sulfate trends were significant in FRGW03 ($p < 0.001$), FRGW04 ($p < 0.001$) and FRGW13 ($p = 0.077$). Two of the background wells (Figure C-38C), FRGW05 and FRGW10 showed trends in the sulfate concentrations with time. FRGW05 had increasing sulfate concentrations which was significant ($p = 0.006$); however, the trend in FRGW10 was decreasing sulfate concentrations with time and this trend was significant ($p = 0.060$).

The sMCL for sulfate of 250 mg/L was exceeded in all the downgradient wells in multiple samplings. In the upgradient wells, only FRGW11 exceeded the sMCL for sulfate on three samplings. The background wells, FRGW08 (8 samplings) and FRGW05 (6 samplings), exceeded the sMCL for sulfate.

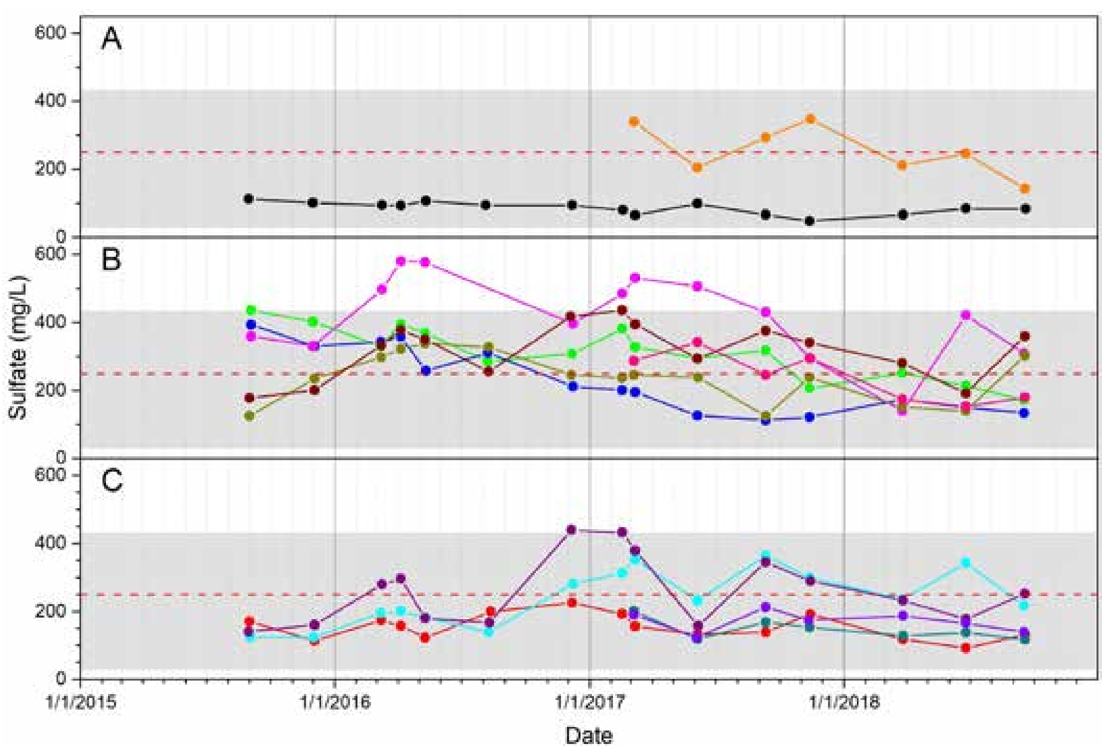

Figure D-38. Time series plots for sulfate concentrations in A. Upgradient wells, B. Downgradient wells, and C. Background wells. The gray shaded regions represent the site-specific background range. Black circles and lines are FRGW01, red circles and lines are FRGW02, green circles and lines are FRGW03, blue circles and lines are FRGW04, cyan circles and lines are FRGW05, magenta circles and lines are FRGW06, dark yellow circles and lines are FRGW07, purple circles and lines are FRGW08, wine-colored circles and lines are FRGW09, dark cyan circles and lines are FRGW10, orange circles and lines are FRGW11, violet circles and lines are FRGW12, and pink circles and lines are FRGW13. The red dashed line represents the sulfate sMCL of 250 mg/L.

5.2.9 Chloride – Groundwater

The concentrations of chloride ranged from 6.98 – 351 mg/L in the groundwater (Figure D-39). There were no significant differences in chloride concentrations between the background wells and the downgradient wells. There were significant differences in chloride concentration between the upgradient wells and the background wells ($p < 0.001$) and between the upgradient wells and the downgradient wells ($p < 0.001$). The chloride concentrations were larger in the upgradient wells than in the downgradient wells or background wells. There was an increasing chloride concentration trend in the upgradient well FRGW01 (Figure D-39A) and was significant ($p = 0.004$). The downgradient wells (Figure D-39B), FRGW03, FRGW04, and FRGW09, also showed increasing trends in chloride concentrations. These were significant trends ($p = 0.007$, $p = 0.003$ and $p = 0.007$, respectively). In the background wells, there were also trends in the chloride concentrations (Figure D-39C). In FRGW02 and FRGW05, there were significant increasing chloride concentrations with time ($p < 0.001$ and $p = 0.009$, respectively). FRGW08 had decreasing chloride concentrations during the study period and this was a significantly decreasing trend ($p = 0.030$).

Chloride has a sMCL of 250 mg/L. The chloride sMCL was not exceeded in any of the background wells or the downgradient wells. In the upgradient wells, the chloride sMCL was exceeded 3 times in FRGW01 (March 2017, September 2017, and March 2018), and the chloride sMCL was exceeded 1 time in FRGW11 on March 2018.

The chloride concentrations in FRGW01 (upgradient) spiked in concentration April 2016, in March of 2017, September 2017, and March 2018. The upgradient concentrations in FRGW11 were on average larger than the other wells, but potentially peaked in March 2018 and rapidly declined afterwards. In the downgradient wells, chloride concentrations only potentially showed peaks in chloride concentrations in FRGW04 in March and September 2018. In the background wells, there were potentially muted chloride spikes in FRGW02 (March 2018) and FRGW10 in November 2017. It is unclear what caused the upgradient spikes in chloride concentrations. For both FRGW01 and FRGW11, it is possible that the spikes in chloride concentrations are from a source upgradient of these two wells moving through the aquifer to these wells. This is possible since it was shown earlier that upgradient concentrations were higher in some parameter than the site wells. Another possibility exists for FRGW01. The spikes in chloride concentrations may reflect de-icing agents applied to the sidewalks around the school or the upgradient residential community. The background wells FRGW02 and FRGW10 are both downgradient of FRGW01, and the potential spikes observed could be from the migration of groundwater from around FRGW01 with higher chloride concentrations moving through these wells. This would explain why this potential peak arrives first in FRGW10 since it is closer to FRGW01 than FRGW02. The spike in FRGW04 is likely from the transport of groundwater with higher initial concentrations of chloride. It would be expected that de-icing agents would cause a larger chloride spike. Therefore, de-icing agents cannot be ruled out as a cause for this apparent chloride spike in FRGW04.

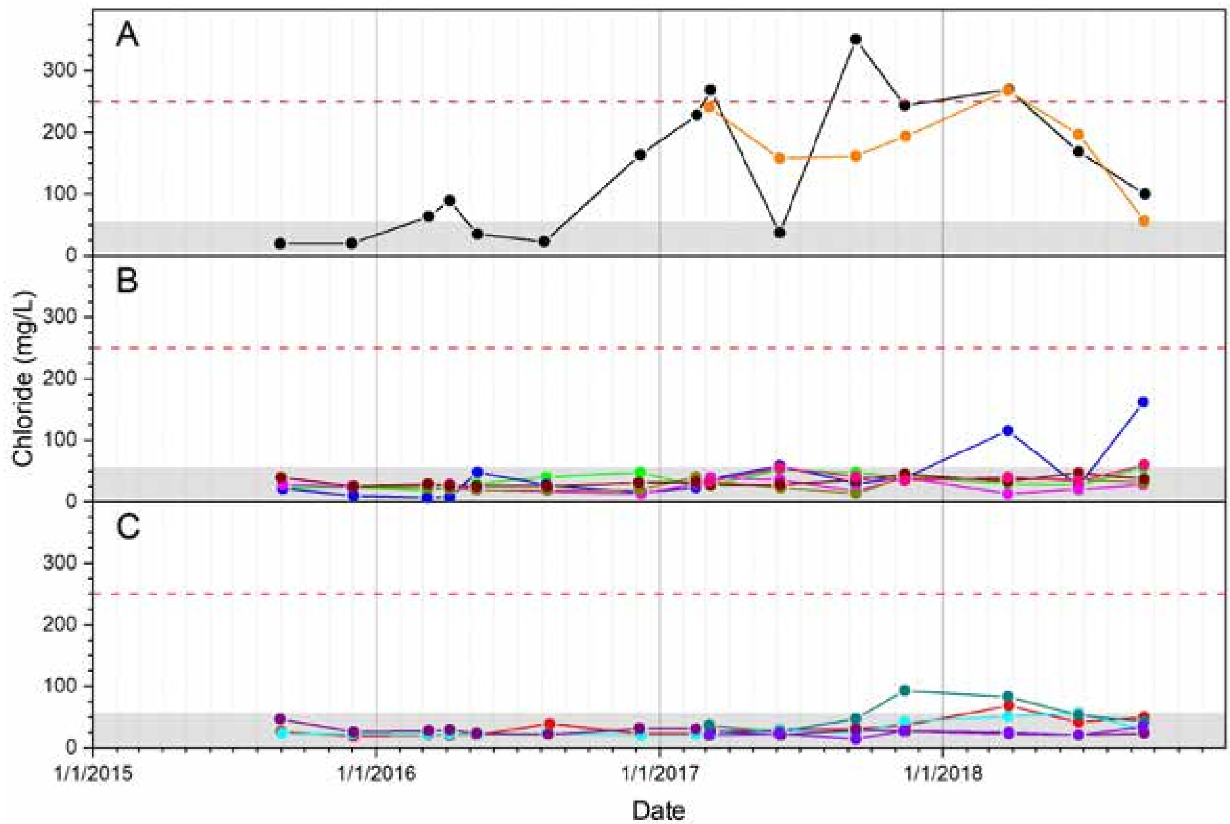

Figure D-39. Time series plots for chloride concentrations in A. Upgradient wells, B. Downgradient wells, and C. Background wells. The gray shaded regions represent the site-specific background range. Black circles and lines are FRGW01, red circles and lines are FRGW02, green circles and lines are FRGW03, blue circles and lines are FRGW04, cyan circles and lines are FRGW05, magenta circles and lines are FRGW06, dark yellow circles and lines are FRGW07, purple circles and lines are FRGW08, wine-colored circles and lines are FRGW09, dark cyan circles and lines are FRGW10, orange circles and lines are FRGW11, violet circles and lines are FRGW12, and pink circles and lines are FRGW13. The red dashed line represents the chloride sMCL of 250 mg/L.

5.3 Stormwater Contaminants

Table D-10. Summary of halogenated aliphatics and aromatics for Fort Riley groundwater samples.

	1,2,4-Trichlorobenzene	1,2-Dichlorobenzene	1,3-Dichlorobenzene	1,4-Dichlorobenzene	2,4,5-Trichlorophenol	2,4,6-Trichlorophenol	2,4-Dichlorophenol	2,4-Dinitrotoluene	2,6-Dinitrotoluene	Hexachlorobenzene
Units	**µg/L**	**µg/L**	**µg/L**	**µg/L**	**µg/L**	**µg/L**	**µg/L**	**µg/L**	**µg/L**	**µg/L**
Total Number of Analyses	53	53	53	53	44	44	44	9	9	53
Number of Detects	0	0	0	0	0	0	0	0	0	0
Percent Detects	0	0	0	0	0	0	0	0	0	0
Mean	-----	-----	-----	-----	-----	-----	-----	-----	-----	-----
Standard Deviation	-----	-----	-----	-----	-----	-----	-----	-----	-----	-----
Minimum	-----	-----	-----	-----	-----	-----	-----	-----	-----	-----
25th Percentile	-----	-----	-----	-----	-----	-----	-----	-----	-----	-----
Median	-----	-----	-----	-----	-----	-----	-----	-----	-----	-----
75th Percentile	-----	-----	-----	-----	-----	-----	-----	-----	-----	-----
Maximum	-----	-----	-----	-----	-----	-----	-----	-----	-----	-----

Table D-11. Summary of polycyclic aromatic hydrocarbons for the Fort Riley groundwater samples.

	Acenaphthene	Acenaphthylene	Anthracene	Benzo(a)anthracene	Benzo(a)pyrene	Benzo(b)fluoranthene	Benzo(g,h,i)perylene	Benzo(k)fluoranthene	Chrysene	Dibenz(a,h)anthracene	Fluoranthene	Fluorene	Indeno(1,2,3-cd)pyrene	Isophorone	Naphthalene	Phenanthrene	Pyrene
Units	**µg/L**	**µg/L**	**µg/L**	**µg/L**	**µg/L**	**µg/L**	**µg/L**	**µg/L**	**µg/L**	**µg/L**	**µg/L**	**µg/L**	**µg/L**	**µg/L**	**µg/L**	**µg/L**	**µg/L**
Total Number of Analyses	53	53	53	53	53	53	53	53	53	53	53	53	53	53	53	44	53
Number of Detects	0	0	0	0	0	0	0	4	0	0	0	0	0	0	0	0	0
Percent Detects	0	0	0	0	0	0	0	8	0	0	0	0	0	0	0	0	0
Mean	-----	-----	-----	-----	-----	-----	-----	0.02	-----	-----	-----	-----	-----	-----	-----	-----	-----
Standard Deviation	-----	-----	-----	-----	-----	-----	-----	0.00	-----	-----	-----	-----	-----	-----	-----	-----	-----
Minimum	-----	-----	-----	-----	-----	-----	-----	0.02	-----	-----	-----	-----	-----	-----	-----	-----	-----
25th Percentile	-----	-----	-----	-----	-----	-----	-----	0.02	-----	-----	-----	-----	-----	-----	-----	-----	-----
Median	-----	-----	-----	-----	-----	-----	-----	0.02	-----	-----	-----	-----	-----	-----	-----	-----	-----
75th Percentile	-----	-----	-----	-----	-----	-----	-----	0.02	-----	-----	-----	-----	-----	-----	-----	-----	-----
Maximum	-----	-----	-----	-----	-----	-----	-----	0.02	-----	-----	-----	-----	-----	-----	-----	-----	-----

Table D-12. Summary of pesticides for the Fort Riley groundwater samples.

	α-BHC	ß-BHC	Chlordane	δ-BHC	Dieldrin	Endosulfan I	Endosulfan II	Endosulfan Sulfate	Endrin	γ-BHC	Heptachlor	Heptachlor Epoxide	Isophorone	p,p'-DDD	p,p'-DDE	p,p'-DDT
Units	**µg/L**	**µg/L**	**µg/L**	**µg/L**	**µg/L**	**µg/L**	**µg/L**	**µg/L**	**µg/L**	**µg/L**	**µg/L**	**µg/L**	**µg/L**	**µg/L**	**µg/L**	**µg/L**
Total Number of Analyses	53	53	53	53	53	53	53	53	53	53	53	53	53	53	53	53
Number of Detects	0	0	0	0	0	0	0	0	0	0	0	0	0	0	0	0
Percent Detects	0	0	0	0	0	0	0	0	0	0	0	0	0	0	0	0
Mean	-----	-----	-----	-----	-----	-----	-----	-----	-----	-----	-----	-----	-----	-----	-----	-----
Standard Deviation	-----	-----	-----	-----	-----	-----	-----	-----	-----	-----	-----	-----	-----	-----	-----	-----
Minimum	-----	-----	-----	-----	-----	-----	-----	-----	-----	-----	-----	-----	-----	-----	-----	-----
25th Percentile	-----	-----	-----	-----	-----	-----	-----	-----	-----	-----	-----	-----	-----	-----	-----	-----
Median	-----	-----	-----	-----	-----	-----	-----	-----	-----	-----	-----	-----	-----	-----	-----	-----
75th Percentile	-----	-----	-----	-----	-----	-----	-----	-----	-----	-----	-----	-----	-----	-----	-----	-----
Maximum	-----	-----	-----	-----	-----	-----	-----	-----	-----	-----	-----	-----	-----	-----	-----	-----

Table D-13. Summary of phenols, ethers, and phthalates for the Fort Riley groundwater samples.

	2,4,5-Trichlorophenol	2,4,6-Trichlorophenol	2,4-Dichlorophenol	Pentachlorophenol	4-Bromophenyl-phenylether	4-Chlorophenyl-phenylether	Bis-(2-Ethylhexyl)phthalate	Butylbenzylphthalate	Diethylphthalate	Dimethylphthalate	Di-n-butylphthalate	Di-n-octylphthalate
Units	**µg/L**	**µg/L**	**µg/L**	**µg/L**	**µg/L**	**µg/L**	**µg/L**	**µg/L**	**µg/L**	**µg/L**	**µg/L**	**µg/L**
Total Number of Analyses	44	44	44	44	53	53	44	53	44	53	53	53
Number of Detects	0	0	0	0	0	0	0	0	0	0	17	1
Percent Detects	0	0	0	0	0	0	0	0	0	0	32	2
Mean	-----	-----	-----	-----	-----	-----	-----	-----	-----	-----	0.27	0.13
Standard Deviation	-----	-----	-----	-----	-----	-----	-----	-----	-----	-----	0.10	-----
Minimum	-----	-----	-----	-----	-----	-----	-----	-----	-----	-----	0.10	-----
25th Percentile	-----	-----	-----	-----	-----	-----	-----	-----	-----	-----	0.18	-----
Median	-----	-----	-----	-----	-----	-----	-----	-----	-----	-----	0.27	0.13
75th Percentile	-----	-----	-----	-----	-----	-----	-----	-----	-----	-----	0.35	-----
Maximum	-----	-----	-----	-----	-----	-----	-----	-----	-----	-----	0.47	-----

References

Kabata-Pendias, A. and Mukherjee, A.B. Chapter II-2, Trace Elements of Group 2. In: *Trace Elements from Soil to Human*. Springer-Verlag, Berlin. 2007a. pp 112-123.

Madejón, P. Chapter 19, Barium. In: *Heavy Metals in Soils: Trace Metals and Metalloids in Soils and their Bioavailability*, 3rd ed. Alloway, B.J., ed. Springer Science + Business Media Dordrecht. Heidelberg. 2013. pp 507-513.

SCIENCE

United States Environmental Protection Agency

Office of Research and Development
Washington, DC 20460